REFERENCE ONLY

UNIVERSITY OF LONDON THESIS

Degree PhD Year 2006 Name of Author HOPPER, R.A.

Nitric Oxide and Hippocampal Synaptic Plasticity

Rachel Anne Hopper

A thesis submitted for the degree of
Doctor of Philosophy

University College London

September 2005

ProQuest LLC
789 East Eisenhower Parkway
P.O. Box 1346
Ann Arbor, MI 48106-1346

Declaration

This thesis is submitted in part fulfilment of the requirements for the degree of Doctor of Philosophy at University College London and is my own composition. Unless otherwise stated, the work described was carried out by myself and is original. The contents of this thesis have not been previously submitted, in whole or part, for any degree at this or any other university.

Rachel Anne Hopper
University College London
September 2005

Acknowledgements

I would firstly like to thank my supervisors, Professor John Garthwaite and Dr. Peter Giese, for their support and guidance over the past three years. I am especially grateful to Barrie Lancaster for his invaluable electrophysiological expertise and instruction, without which this thesis would not have been possible. Thanks also to Barrie Gibb and Victoria Wykes for their assistance in transfections and cell culture, Charmaine Griffiths for her help in measuring NO concentrations, Giti Garthwaite for her knowledge of immunohistochemistry, Catherine Hall for her assistance with statistical analysis, and Elaine Mo for her insight into the world of molecular biology. Additional thanks are also due to the BBSRC and Merck Sharp & Dohme (Harlow, UK) for providing my funding.

A big thanks to all the members of the Neural Signalling group at the WIBR for their friendship and support. They have kept me sane through the seemingly endless LTP recordings and cGMP assays! I would especially like to say a big thanks to Catherine for always giving me a place to stay whenever it was needed, and Elaine and Gary for some great nights out.

Huge thanks go to all my family and friends for always being there, and for cheering me up when I was down. Finally I would like to say a special thank-you to Kirk for all his love and support, despite the hundreds of miles that existed between us for the majority of our studies.

Abstract

Nitric oxide (NO) functions widely as a signalling molecule in the brain and has been implicated in several types of synaptic plasticity, including NMDA receptor-dependent long-term potentiation (LTP) in the hippocampus. The precise role played by NO in this and related phenomena is uncertain and the aim of my research was to explore this question.

The principal receptor for NO possesses guanylyl cyclase activity, so that NO binding results in cGMP formation. NO has also been claimed to modify thiol residues (*S*-nitrosation) and, through this mechanism, exert a negative feedback on NMDA receptors. Tests of this hypothesis were conducted by recording NMDA receptor-mediated field excitatory postsynaptic potentials in the CA1 region of rat hippocampal slices. Neither manipulation of endogenous NO levels nor application of exogenous NO had any effect. The reported inhibition of synaptic NMDA receptor function when NO is released by UV light from a caged derivative was confirmed, but a similar result was obtained using a combination of exogenous NO and UV light, casting doubt on the physiological relevance this effect.

There has been debate over the isoform of NO synthase (endothelial, neuronal, or both) needed for hippocampal LTP and it has been suggested that LTP requires not only a phasic NO signal associated with tetanic stimulation but also a tonic level of NO. cGMP measurements in hippocampal slices indicated that endothelial NO synthase was largely responsible for the basal NO tone, and that T-type voltage-gated calcium channels may elicit the steady output of NO, presumably from endothelial cells. Electrophysiological tests conducted in CA1 found a deficit in LTP both in eNOS-deficient mice and in wild type mice subjected to selective nNOS inhibition. The results indicate that both isoforms of NO synthase participate in LTP but may perform distinct roles.

Table of Contents

List of Figures

List of Tables

List of Equations

List of Abbreviations

1400W	(+)cis-4-methyl-5-pentylpyrollidin-2-imine
6TM	6 transmembrane
7-NI	7-nitrindazole
AC	adenylyl cyclase
ACh	acetylcholine
ACSF	artificial cerebrospinal fluid
agatoxin	ω-agatovin IVA
AMPA	α-amino-3-hydroxy-5-methyl-4-isoxazoleproprionate
ANP	atrial natiuretic peptide
ARL-17477	α-fluoro-N-(3-(aminomethyl)-phenyl)-acetamide
ATP	adenosine triphosphate
BCA	bicinchoninic acid
BH_4	tetrahydrobiopterin
BDNF	brain-derived neurotrophic factor
Ca^{2+}	calcium
Caged NO	potassium pentachloronitrosylruthenate
CaM	calmodulin
CaM-KII	calmodulin II protein kinase
cAMP	cyclic adenosine monophosphate
cADPRT	cyclic adenosine diphosphate ribosyl transferase
CFTR	cystic fibrosis transmembrane conductor regulator
cGK	cGMP-dependent protein kinase
cGMP	cyclic guanosine 3'5'-monophosphate
CNG channel	cyclic nucleotide-gated ion channel

CNQX	6-cyano-7-nitroquinoxaline-2,3-dione
CNS	central nervous system
ω-CTx GVIA	ω-conotoxin GVIA
ω-CTx MVIIC	ω-conotoxin MVIIC
Cys	cysteine
D-AP5	D(-)-2-amino-5-phosphonopentanoate
DARPP-32	dopamine- and cAMP-reguated phosphoprotein of Mr 32,000
ddH_2O	double distilled water
DEA/NO	2-(N, N-diethylamino)-diazenolate-2-oxide
DG	dentate gyrus
DMEM	Dulbecco's modified eagles medium
DNA	deoxyribonucleic acid
EB	extraction buffer
EDRF	endothelium-derived relaxing factor
EHNA	erythro-9-(2-hydroxy-3-nonyl)-adenine hydrochloride
eNOS	endothelial nitric oxide synthase
EtOH	ethanol
FAD	flavin adenine dinucleotide
fEPSP	field excitatory postsynaptic potential
FHOD1	formin homology domain-containing protein
FMN	flavin mononucleotide
GABA	γ-aminobutyric acid
GC	guanylyl cyclase
GTP	guanosine 5'-triphosphate
HCN channel	hyperpolarisation-activated cyclic nucleotide-regulated non-selective cation channel

HEK-293 cell	human embryonic kidney cell
HFS	high frequency stimulation
His	histidine
HVA	high voltage activated
IBMX	3-isobutyl-1-methylxanthrine
ICAM-1	intracellular adhesion molecule-1
I_h	inward non-selective cation current
iNOS	inducible nitric oxide synthase
IP_3	inositol 1,3,4-triphosphate
K_d	dissociation constant
K_m	Michaelis constant
kDa	kilodaltons
KO	knockout
L-NAME	N^G-nitro-L-arginine methyl ester
L-NIO	L-N^5-(1-iminoethyl)-ornithine
L-NMMA	N-methyl-L-arginine
L-NNA	N-nitro-L-arginine
LTD	long term depression
LTP	long term potentiation
LVA	low voltage activated
L-VNIO	N^5-(1-imino-3-butenyl)-L-ornithine
MBI	mechanism based inhibitor
mGluR	metabotrophic glutamate receptor
mRNA	messenger ribonucleic acid
mtNOS	mitochondrial nitric oxide synthase

Na^+	sodium
NADPH	nicotinamide adenine dinucleotide phosphate hydrogen
Ni^{2+}	nickel
NGF	nerve growth factor
NMDA	N-methyl-D-aspartate
NO	nitric oxide
NOS	nitric oxide synthase
nNOS	neuronal nitric oxide synthase
NPA	N-propyl-L-arginine
ODQ	1-H-[1,2,4]-oxadiazolo-[4,3-a]-quinoxalin-1-one
PBS	phosphate buffered saline
PBST	phosphate buffered saline + Tween
PCR	polymerase chain reaction
PDE	phosphodiesterase
PDZ	PSD - 95, discs large and Zona occludens 1
pGC	particulate GC
PI3-K	phosphatidylinositol 3-kinase
PKA	protein kinase A
PKC	protein kinase C
PLC	phospholipase C
PMSF	phenylmethylsulphonyl fluoride
PSD-93	postsynaptic density 93
PSD-95	postsynaptic density 95
PVN	paraventricular nucleus
SDS	sodium dodecyl sulfate

SDS-PAGE	sodium dodecyl sulphate polyacrylamide gel electrophoresis
SIN-1	3 - morpholinosydnonimine hydrochloride
SNP	sodium nitroprusside
SOD	superoxide dismutase
TBS	Tris buffered saline
TBST	Tris buffered saline + Tween
tSXV	Ser/Thr-X-Val-COOH motif
TNF-α	tumour necrosis factor alpha
TRIM	trimethylphenylfluoroimidazole
UV	ultra violet
VASP	vasoldilator-stimulated protein
VCAM-1	vascular cell adhesion molecule-1
WT	wild type
YC-1	3-(5′-hydroxymethyl-2′-furyl)-1-benzyl indazole

Chapter 1

General Introduction

1.1 Historical background to nitric oxide

Nitric oxide (nitrogen monoxide radical; NO) is one of the smallest biologically active messenger molecules. It is also one of the first discovered gaseous biological messengers with a wide range of physiological and pathophysiological actions. NO is a colourless and odourless gas at standard temperature and pressure, with limited solubility in water (maximum concentration ~ 1 mM), but like CO_2 or O_2 it can cross cell membranes easily by diffusion, thereby obviating any direct control of its actions by release or uptake mechanisms.

NO first came to medical prominence as a poison when it almost brought an end to Sir Humphrey Davy (1778 – 1829). Davy was famous for his investigations into nitrous oxide as an anaesthetic agent. When he inhaled pure nitrous oxide he described *"losing connections with external things, trains of vivid visible images passed through my mind"*. He also noted that nitrous oxide relieved his toothache – *"as nitrous oxide in its extensive operation appears capable of destroying physical pain, it may probably be used with advantage during surgical operations in which no great effusion of blood takes place"*. The pioneering anaesthetist also tested other gases for comparison with nitrous oxide, one of which was NO. Upon the inspiration of NO he described *"a sense of burning in his tongue and his throat, and pain in his chest"*, and recorded he would *"never design again to attempt such a rash experiment"* (Davy, 1800).

Despite Davy's experience, and his warning that even low doses of NO as a contaminant of nitrous oxide had caused him to feel *"somewhat depressed and dilapidated"*, no steps were taken to monitor the NO content of nitrous oxide for many years. NO was rediscovered as a poison in 1966 at the Bristol Royal Infirmary when a contaminated stock of nitrous oxide killed one patient, and gravely injured a second. Post-mortem examination of this patient revealed excessive formation of

methaemoglobin leading to severe cyanosis, pulmonary oedema, and culminating in cardiac arrest (Clutton-Brock, 1967).

For the last two centuries NO has been viewed as a noxious, and generally troublesome, pollutant. It is a toxic gas that is a known constituent of car fumes, a component of cigarette smoke, and is widely believed to be involved in the depletion of ozone layer. NO is also a recognised by-product of microbial metabolism. In 1916 it was noted mammals excreted more nitrate than they consumed in their diet (Mitchell *et al.*, 1916), but it was not till the 1980s that nitrogen oxides were recognised as normal products of mammalian metabolism (Green *et al.*, 1981a,b). Interestingly, the use of organic nitrates such as nitro-glycerine has been advocated for the treatment of conditions such as angina and heart failure for over a century (Brunton, 1867). The first anti-anginal effect of nitro-glycerine was discovered in the late 1860s by Alfred Nobel (the founder of the Nobel Prize) who utilised nitro-glycerine in his factories to synthesise dynamite. It was here that Nobel made two very interesting observations regarding his factory workers. Firstly, many of his workers often complained of headaches on weekdays that appeared to disappear over the weekends. Secondly, workers which suffered from angina pectoris or heart failure often experienced relief from chest pain during the work week, but which recurred at weekends. Both effects were attributed to the vasodilatory action of nitro-glycerine, although the mechanism of action was not elucidated until the late 1970s and found to involve its metabolic conversion to NO (Arnold *et al.*, 1977; Katsuki *et al.*, 1977; Ignarro *et al.*, 1981).

In an apparently disparate field of research, the investigation into the role of acetylcholine (ACh) – induced relaxation of smooth muscle (Furchgott, 1980) led to the discovery of NO. In the late 1970s, Furchgott began to examine the effect of ACh on smooth muscle. At the time isolated arteries were cleared of endothelium in order to obtain a "pure" smooth muscle preparation, and ACh usually caused contraction. On one occasion Furchgott's technician, Zawadzki, did not remove the endothelium and ACh was found to induce a potent relaxation. It was quickly established that the relaxation only occurred if the endothelium was present, and that the observed relaxation was blocked by atropine, a muscarinic antagonist. The implication was that ACh was acting on endothelial cells to produce a substance able to diffuse to the smooth muscle and induce relaxation. This substance was termed endothelium-

derived relaxing factor (EDRF). In 1987, two separate laboratories published definitive evidence that NO was EDRF (Ignarro *et al.*, 1987; Palmer *et al.*, 1987).

The discovery that NO can also act as a neuronal messenger in the brain originated from studies in the Garthwaite laboratory. In the central nervous system (CNS), the ability of glutamate to evoke large increases in cyclic guanosine 3'5'-monophosphate (cGMP) concentration had been known for many years (Ferrendelli *et al.*, 1974). These increases were shown to be particularly prominent in the cerebellum, and were primarily mediated by specific populations of glutamate receptors (Garthwaite & Balazs, 1981). In 1987, it became apparent from investigations in the cerebellum that increases in cGMP did not occur in the cells that were stimulated by glutamate receptor agonists (Garthwaite & Garthwaite, 1987). Instead, N-methyl-D-aspartate (NMDA) receptor activation was found to induce the release of a diffusible intracellular messenger that bore a remarkable resemblance to EDRF (Dumuis *et al.*, 1988; Garthwaite *et al.*, 1988). Investigators subsequently appreciated that glutamate-stimulated cGMP formation in cerebellar tissues was due to the production of NO (Bredt & Snyder, 1989), thereby initiating investigations into the role of NO as a neural messenger molecule.

Parallel investigations in the immune system identified the ability of NO to serve a very different purpose from that of the signalling molecule in the vasculature and nervous system. As early as 1982, NO was implicated in the immune system as a marked increase in urinary nitrate excretion was observed in patients suffering from diarrhoea and fever (Hegesh & Shiloah, 1982; Wagner *et al.*, 1984). Further investigation revealed that activated macrophages exhibited increased nitrite and nitrate production *in vitro* (Stuehr & Marletta, 1985), however it was not until 1987 that a role for NO in macrophage cytotoxicity was first described (Hibbs *et al.*, 1987). Subsequently it has been realised that activated macrophages are capable of generating high levels of NO (Hibbs *et al.*, 1988), and that the NO-dependent mechanism of cytotoxicity is via a metabolic inhibition of DNA synthesis, mitochondrial respiration and aconitase activity (Granger *et al.*, 1980; Granger & Lehninger, 1982; Drapier & Hibbs, 1986, Stuehr & Nathan, 1989; MacMicking *et al.*, 1997) which culminates in the induction of apoptosis (Albina *et al.*, 1993). Furthermore, the cytotoxic action of NO appears to extend to the macrophages that produce it, because the activity of NO synthase in these cells correlates inversely with their life span in culture (Albina *et al.*, 1989).

Following these initial reports, NO has been the focus of much attention and research over the past two decades. It has attracted sufficient interest to be named molecule of the year in 1992 (by *Science*; Koshland, 1992) and go on to earn three scientists (Robert F. Furchgott, Louis J. Ignarro and Ferid Murad) the 1998 Nobel Prize for the discovery of NO as a signalling molecule in the cardiovascular system.

Although originally described in mammalian systems, NO has now been realised to be a ubiquitous signalling molecule across species. NO has been shown to act as a signalling molecule in fish (Saeij *et al.*, 2000), insects (Regulski *et al.*, 1995), marine sponges (Giovine *et al.*, 2001), myxomycetes (Golderer *et al.*, 2001) bacteria (Liu *et al.*, 2001), and even in plants (Durner *et al.*, 1999). The elucidation of the diverse roles of NO has revealed NO to be important in a number of surprising contexts. For example, NO has been found to be essential for the determination of firefly bioluminescent flashing (Trimmer *et al.*, 2001), and salivary NO has been demonstrated to act as a vasodilator in blood-sucking insects (Ribeiro & Nussenzveig, 1993). Novel NO-controlled physiological functions have also been uncovered, such as the contribution of NO signalling to olfactory-like feeding behaviour in *Hydra vulgaris* (Colasanti *et al.*, 1997), and a Ca^{2+}-sensitive NO synthase (NOS) has been implicated in melanin production in the ink-gland of *Sepia officinalis* (Palumbo *et al.*, 1997). These observations reveal NO to be a signalling molecule with a very ancient history, serving diverse biological functions in even the most primitive organisms.

1.2 Mechanism for nitric oxide generation: nitric oxide synthase

Subsequent to the discovery of NO as an important signalling molecule in the vasculature and nervous systems, a mechanism for its generation was rapidly sought. The family of enzymes responsible for the synthesis of NO in biological systems was first described in 1989 to be the Ca^{2+}/calmodulin-dependent NOS. These enzymes catalyse the production of NO and L-citrulline from the guanidine nitrogen of L-arginine, a process consuming five electrons.

Three distinct isoforms of NOS are present in mammalian systems, each of which have been purified and well characterised: endothelial NOS (eNOS; Palmer *et al.*, 1989), neuronal NOS (nNOS; Bredt *et al.*, 1991), and inducible NOS (iNOS; Hevel *et al.*, 1991). Recent studies have indicated that a fourth isoform of NOS may also exist: mitochondrial NOS (mtNOS; Lacza *et al.*, 2003). Since the first indication

of mitochondrial NO production in 1994 (Loesch *et al.*, 1994) the identity of this isoform has been subject to much controversy as to whether it is identical to one of the other known isoforms. Recent evidence however indicates that mtNOS may be a novel NOS isoform (Lacza *et al.*, 2003).

Two of the isoforms, eNOS and nNOS, are constitutively expressed throughout the brain, requiring Ca^{2+} and calmodulin (CaM) for their activation. eNOS is typically expressed in the endothelial cells of cerebral blood vessels, whereas nNOS tends to be localised to neuronal structures. In contrast, iNOS is not ordinarily found in any healthy cell. iNOS may be induced in a variety of cell types including macrophages, smooth muscle, cardiomyocytes and microglia, following activation of the cells with products of infection (including bacterial endotoxin or exotoxin), or certain inflammatory mediators (including the cytokines tumour necrosis factor or interleukin-1). Once induced, iNOS is constitutively active, leading to the long-term production of NO to cytotoxic levels that acts as a host defence mechanism.

The classification of the NOS family is summarised in table 1.1, and is based on their cellular location, in addition to their physical and biochemical characteristics. For completeness, the novel isoform mtNOS has been included.

	Neuronal NOS (nNOS)	Inducible NOS (iNOS)	Endothelial NOS (eNOS)	Mitochondrial NOS (mtNOS)
Other nomenclature	Type I	Type II	Type III	
Protein size (kDa)	160	130	135	125-130
Chromosomal location	12	17	7	?
Cellular Location	Neurones	Macrophages	Endothelial cells	Mitochondria
Subcellular location	Cytosolic/ particulate	Predominantly cytosolic	Predominantly particulate	
Expression	Constitutive	Inducible	Constitutive	Constitutive
Calcium dependence	Yes	No	Yes	Yes

Table 1.1: Characteristics of the NOS isoforms

Splice variants of the NOS isoforms have also been reported in various tissues, although the biological significance of these variants are poorly understood. To date, four nNOS splice variants have been detected (nNOSβ, nNOSγ, nNOSμ and nNOS-2). nNOSβ and nNOSγ were initially identified in the brain of nNOS-knockout mice (Huang *et al.*, 1993; Eliasson *et al.*, 1997) but have since been reported to also be present at low levels in the testes (Wang *et al.*, 1997). nNOSμ is selectively expressed in rat heart and skeletal muscle (Silvagno *et al.*, 1996), and in both rat and human penis and urethra (Magee *et al.*, 1996). Only mRNA has so far been detected for nNOS-2 (Ogura *et al.*, 1993).

Relatively little information exists on the iNOS splice variants, with alternatively spliced mRNA transcripts of iNOS detected in human epithelial and alveolar macrophages (Eissa *et al.*, 1996). No splice variants of eNOS have yet been reported.

1.2.1 Structure of nitric oxide synthase

The three main NOS isoforms share a common general structure, consisting of two subunits with molecular masses of approximately 130 kDa (iNOS), 135 kDa (eNOS) and 160 kDa (nNOS). All three isoforms require five bound co-factors and prosthetic groups for activity: flavin adenine dinucleotide (FAD), flavin mononucleotide (FMN), tetrahydrobiopterin (BH_4), iron protoporphyrin IX (haem) and CaM.

The active enzyme exists as a homodimer (Masters *et al.*, 1996; Stuehr, 1997), each monomer consisting of two major domains: an N-terminal oxygenase domain (homologous to haem-thiolate proteins) and a C-terminal reductase domain (homologous to the cytochrome P450s). The former contains binding sites for one molecule of nicotinamide adenine dinucleotide phosphate (NADPH), FAD and FMN, whereas the latter binds haem, BH_4 and L-arginine. An interlinker domain exists between the oxygenase and reductase domain which contains a CaM-binding sequence. The domain structure of the NOS isoforms is shown in figure 1.1.

Association of the monomers into active dimers creates an extensive interface between the oxygenase domains of the two subunits. Comparative analysis of NOS domain interactions using yeast two-hybrid systems reveal that subunit association of eNOS and nNOS involves both oxygenase and reductase domains, whereas for iNOS only the oxygenase domain is involved (Venema *et al.*, 1997). Haem, BH_4, and L-arginine all promote and/or stabilise the active dimeric form of all the NOS isoforms.

The presence of haem appears to be mandatory, with BH_4 and L-arginine acting to promote dimer formation and stabilisation (Klatt *et al.*, 1995, 1996).

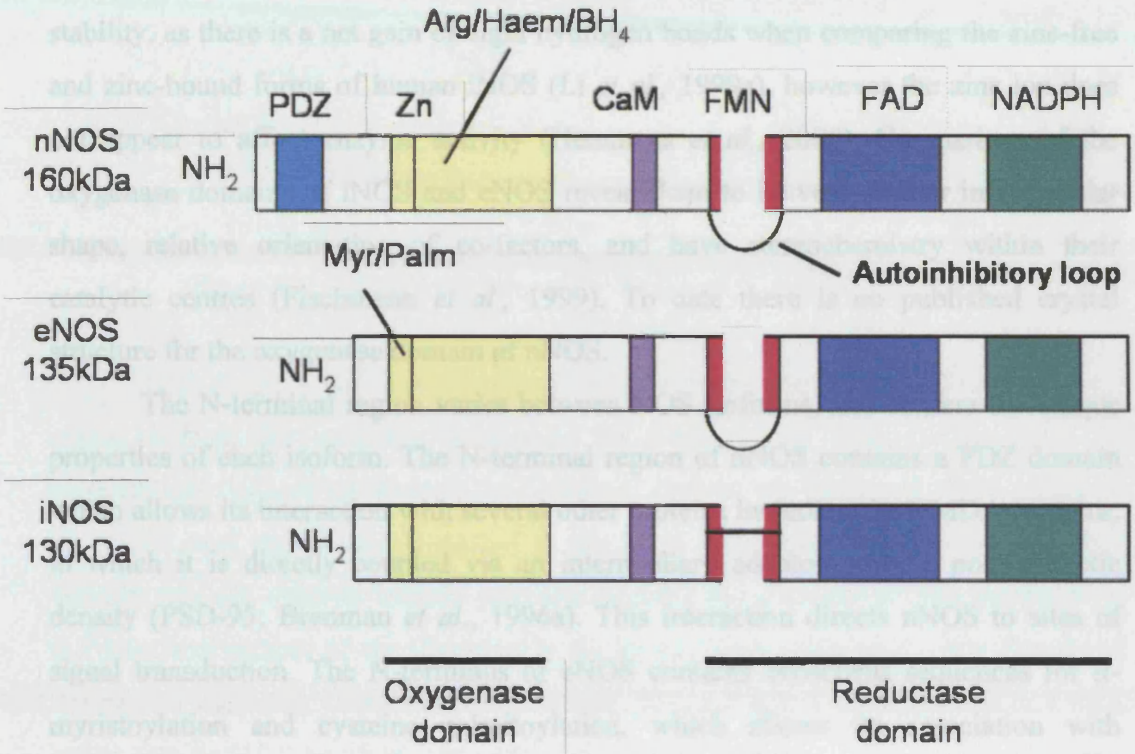

Figure 1.1: Domain structure of the three main NOS isoforms. *(adapted from Alderton et al., 2001). All three NOS isoforms exist as a homodimer, each monomer consisting of two major domains: an N-terminal oxygenase domain and a C-terminal reductase domain, with an interlinker domain between the oxygenase and reductase domain which contains a CaM-binding sequence. The autoinhibitory loop present in the middle of the FMN binding domains of nNOS and eNOS regulates the Ca^{2+} dependence of eNOS and nNOS, which is absent in the iNOS isoform.*

The crystal structure of the of iNOS (Crane *et al.*, 1997, 1998; Fischmann *et al.*, 1999; Li *et al.*, 1999a) and eNOS (Raman *et al.*, 1998) oxygenase domains have recently been elucidated, and reveal a structure considerably different from other haem-based oxygenases such as cytochrome P450s, peroxidases, and catalases. The NOS oxygenase domain is an elongated structure with a novel single-domain α-β fold that the authors describe as resembling "*a baseball catcher's mitt*" with the haem clasped in the webbed β-sheet palm of the mitt (Crane *et al.*, 1997). The NOS distal haem pocket differs from other haem-binding proteins as it is predominantly constructed from β structures, as opposed to α-helical.

Another notable feature of the oxygenase domain is the presence of a zinc ion tetrahedrally co-ordinated to two pairs of symmetry-related cysteine residues at the dimer interface (Raman *et al.*, 1998). The zinc ion appears to play a role in dimer stability, as there is a net gain of eight hydrogen bonds when comparing the zinc-free and zinc-bound forms of human iNOS (Li *et al.*, 1999a), however the zinc ion does not appear to affect enzyme activity (Hemmens *et al.*, 2000). Comparison of the oxygenase domains of iNOS and eNOS reveal them to be very similar in molecular shape, relative orientation of co-factors, and have stereochemistry within their catalytic centres (Fischmann *et al.*, 1999). To date there is no published crystal structure for the oxygenase domain of nNOS.

The N-terminal region varies between NOS isoforms, and confers the unique properties of each isoform. The N-terminal region of nNOS contains a PDZ domain which allows its interaction with several other proteins including the NMDA receptor, to which it is directly coupled via an intermediary adaptor protein, post synaptic density (PSD-95; Brenman *et al.*, 1996a). This interaction directs nNOS to sites of signal transduction. The N-terminus of eNOS contains consensus sequences for N-myristoylation and cysteine palmitoylation, which allows its association with membranes, hence localising the enzyme to sites of Ca^{2+} entry (Busconi & Michel, 1993, Liu *et al.*, 1995). In contrast, iNOS lacks these N-terminal consensus sequences and is therefore a cytosolic enzyme, usually found in glial cells, macrophages and neurones following damage and infection.

1.2.2 Catalytic mechanism

The biosynthesis of NO by NOS involves a two-step oxidation of L-arginine to L-citrulline, with the concomitant production of NO (figure 1.2). Arginine is derived primarily from dietary sources, but can also be synthesised in the kidney. The conversion of L-arginine to NO occurs at a catalytic site within the oxygenase domain which binds L-arginine in such an orientation so that the guanidine group of L-arginine is adjacent to the ferric iron of the haem prosthetic group.

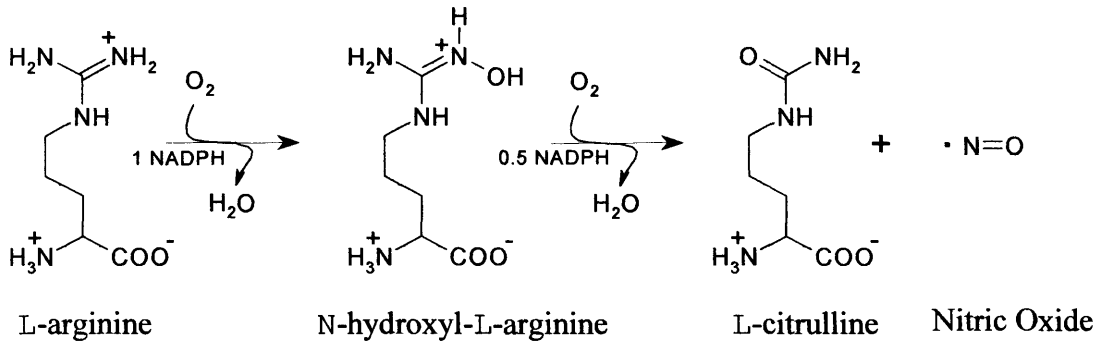

Figure 1.2: Catalytic mechanism for the two-step biosynthesis of NO.

Both steps in the biosynthesis of NO require the transfer of NADPH-derived electrons from the reductase domain to the haem group. Electrons provided by NADPH are transported through the reductase domain via FAD and FMN (Adak *et al.*, 1999), and are ultimately passed to the haem prosthetic group. Recent studies indicate that the electron transfer pathway between the domains is from the FMN in the reductase domain of one monomer to the haem bound in the oxygenase domain of the partner monomer (Siddhanta *et al.*, 1998). BH_4 has also been suggested to play a redox role in NOS catalysis, in which bound BH_5^+ donates one electron to haem, forming $BH_4^{\cdot +}$, which is then returned to a reduced state by accepting an electron from a flavin in the reductase domain (Bec *et al.*, 1998). The electron flow through the domains is summarised in figure 1.3.

Iron is initially reduced by the transfer of an electron from NADPH, which allows the haem iron to bind molecular oxygen, resulting in its cleavage. One oxygen atom is released as water, and the other is incorporated onto one of the terminal guanidine nitrogens of arginine to yield the intermediate N-hydroxyl-L-arginine. Subsequent activation of a further molecule of oxygen facilitates the subsequent oxidation of N-hydroxyl-L-arginine to produce water, NO, and L-citrulline.

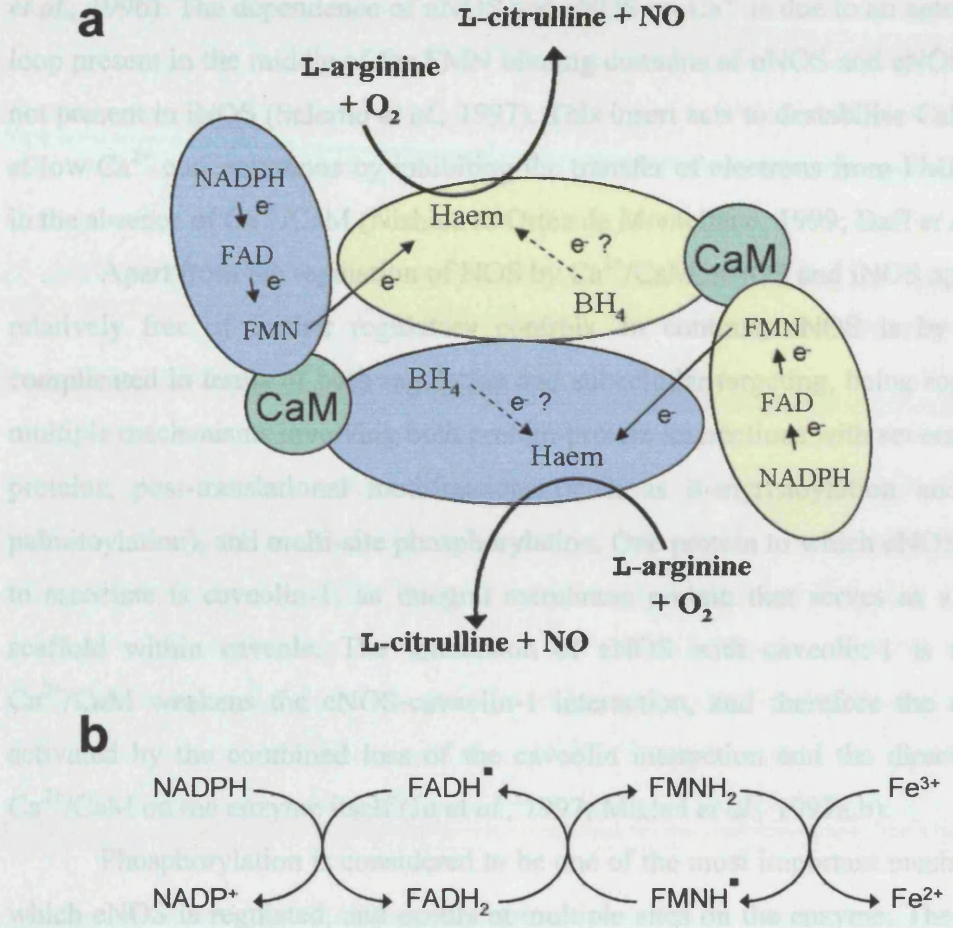

Figure 1.3: Electron flow within the NOS dimer.
(a) Schematic representation of the flow of electrons through the NOS homodimer
(b) Schematic representation of the electron transfer chain
(Adapted from Alderton et al., 2001).

1.2.3 Regulation of nitric oxide synthase

The binding of CaM is essential for NOS activity, and functions as a sensor of intracellular Ca^{2+} concentrations. CaM acts to induce a conformational change between the reductase and oxygenase domains in the dimer that regulates the electron transfer both within the reductase domain and the interdomain transfer of electrons between FMN and the haem prosthetic group (Panda *et al.*, 2001). For constitutive NOS isoforms, elevation of Ca^{2+} levels promotes the binding of CaM to NOS, whereas iNOS is unusual in that it binds CaM tightly even at low Ca^{2+} concentrations (Matsuda & Iyanagi, 1999). This has the effect of holding iNOS in an activated state that is largely independent of calcium, although a 2-fold increase in its activity is observed in the presence of 2.5 mM Ca^{2+} compared to that in 10 mM EGTA (Venema

et al., 1996). The dependence of nNOS and eNOS on Ca^{2+} is due to an autoinhibitory loop present in the middle of the FMN binding domains of nNOS and eNOS which is not present in iNOS (Salerno *et al.*, 1997). This insert acts to destabilise CaM binding at low Ca^{2+} concentrations by inhibiting the transfer of electrons from FMN to haem in the absence of Ca^{2+}/CaM (Nishida & Ortez de Montellano, 1999; Daff *et al.*, 1999).

Apart from the regulation of NOS by Ca^{2+}/CaM, nNOS and iNOS appear to be relatively free of further regulatory controls. In contrast, eNOS is by far more complicated in terms of both regulation and subcellular targeting, being regulated by multiple mechanisms involving both protein-protein interactions with several different proteins, post-translational modifications (such as N-myristoylation and cysteine palmitoylation), and multi-site phosphorylation. One protein to which eNOS is known to associate is caveolin-1, an integral membrane protein that serves as a structural scaffold within caveole. The interaction of eNOS with caveolin-1 is inhibitory: Ca^{2+}/CaM weakens the eNOS-caveolin-1 interaction, and therefore the enzyme is activated by the combined loss of the caveolin interaction and the direct effect of Ca^{2+}/CaM on the enzyme itself (Ju et *al.*, 1997; Michel *et al.*, 1997a,b).

Phosphorylation is considered to be one of the most important mechanisms by which eNOS is regulated, and occurs at multiple sites on the enzyme. The two most extensively studied phosphorylation sites on eNOS have been the activation site, human Ser 1177 (bovine Ser 1179) in the enzyme's C-terminal tail, and an inhibitory site, human Thr 495 (bovine Thr 497) located in the CaM-binding site sequence. Phosphorylation at Ser 1179 reduces the enzymes Ca^{2+}-dependence (Chen *et al.*, 1999), increases the rate of electron flux from the reductase domain to the oxygenase domain (McCabe, 2000), and increases the rate of NO production (Fulton *et al.*, 1999, Dimmeler *et al.*, 1999, Gallis *et al.*, 1999). In contrast, phosphorylation at Thr 497 decreases eNOS activity by increasing Ca^{2+}/CaM dependence (Chen *et al.*, 1999, Michell *et al.*, 2001, Fleming *et al.*, 2001).

Physiologically, the phosphorylation and dephosphorylation of these sites occurs in a highly co-ordinated manner. For example, application of bradykinin (a well-characterised activator of eNOS) to endothelial cells results in a transient dephosphorylation of the inhibitory site Thr 497, which is accompanied by phosphorylation of Ser 1179 (Fleming *et al.*, 2001, Harris *et al.*, 2001). Various studies propose a signal transduction pathway in which activation of phosphatidylinositol

3-kinase (PI3-K) and serine/threonine protein kinase Akt leads to the phosphorylation of eNOS (Igarashi and Michel, 2000). Akt has been found to activate the enzyme directly via phosphorylation of the Ser 1179 residue, whereas the mutant eNOS (S1179A) is resistant to phosphorylation and activation by Akt (Fulton *et al.*, 1999, Dimmeler *et al.*, 1999, Chen *et al.*, 1999). Ser 1179 is also the target of multiple protein kinases in addition to Akt, including protein kinase C (PKC), protein kinase A (PKA), cGMP-dependent protein kinase (cGK), and CaM II protein kinase (CaM-KII; Feron *et al.*, 1999; Butt *et al.*, 2000; Fleming *et al.*, 2001).

Other sites of phosphorylation of eNOS have also been reported, including Ser 116 in response to sheer stress (Gallis *et al.*, 1999), Ser 635 as a target of PKA and cGK *in vitro* (Butt *et al.*, 2000), and more recently Ser 617 in response to Akt and PKA (Michell *et al.*, 2002). Mimicking phosphorylation at Ser 635 (S635Asp) induces ~ 2-fold increase in activity of the purified protein, whereas mimicking phosphorylation at Ser 617 does not alter maximal activity but significantly increases Ca^{2+}/CaM sensitivity (Michell *et al.*, 2002). Figure 1.4 summarises the various phosphorylation sites and signal transduction pathways by which eNOS is regulated.

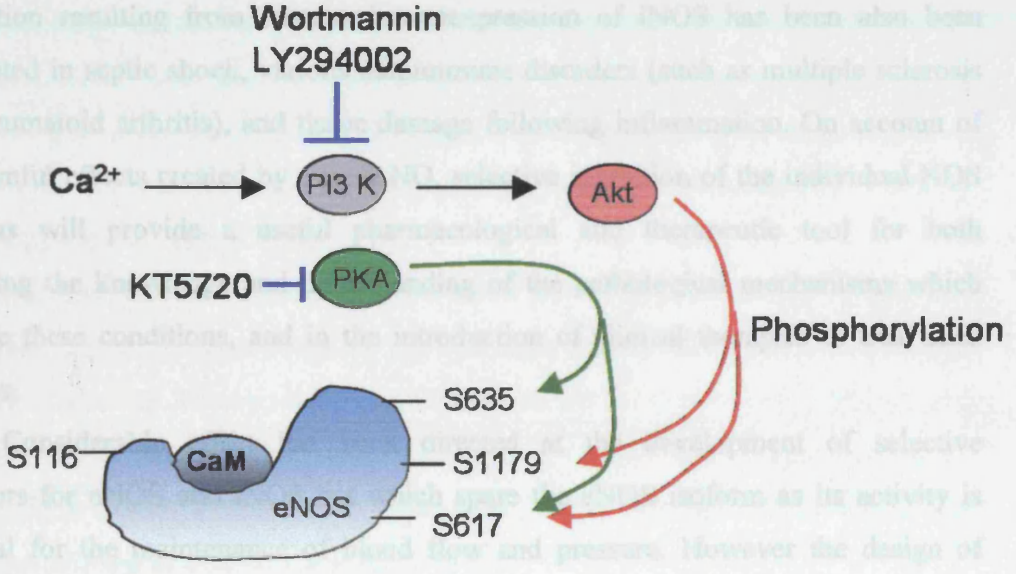

Figure 1.4: Phosphorylation pathways associated with eNOS. *eNOS contains multiple phosphorylation sites, the phosphorylation and dephosphorylation of which occurs in a highly co-ordinated manner. Pharmacological inhibition of PI3-K by wortmannin and LY294002; inhibition of PKA by KT5720.*

Phosphorylation has not been as extensively studied with either of the two alternative NOS isoforms, although there is evidence that nNOS may also be regulated by phosphorylation (Brune & Lapetina, 1991; Nakane *et al.*, 1991; Bredt *et al.*, 1992; Dinerman *et al.*, 1994b): CaM-kinase II (CaM-KII) has been found to induce phosphorylation of the Ser 847 residue, resulting in a reduction of nNOS activity which is thought to be partially due to the suppression of CaM binding (Hayashi *et al.*, 1999; Komeima *et al.*, 2000, 2001). More recently, the phosphorylation of Ser 741 has also been reported via CaM-KI (Song *et al.*, 2004), which again culminates in the inhibition of nNOS activity.

1.2.4 Pharmacological inhibition of nitric oxide synthase

Despite the importance of NO in many physiological processes, overproduction of NO can be detrimental, and has been implicated in a number of pathological conditions. Inappropriate activation of nNOS has been implicated in chronic visceral pain, migraine headaches, seizures, post-ischaemic stoke damage, long-term depression, as well as in various neurodegenerative diseases (such as Alzheimer's disease, Parkinson's disease, Schizophrenia, and AIDS dementia). Excess NO production resulting from sustained overexpression of iNOS has been also been implicated in septic shock, various autoimmune disorders (such as multiple sclerosis and rheumatoid arthritis), and tissue damage following inflammation. On account of the harmful effects created by excess NO, selective inhibition of the individual NOS isoforms will provide a useful pharmacological and therapeutic tool for both furthering the knowledge and understanding of the pathological mechanisms which underlie these conditions, and in the introduction of clinical therapies to treat such diseases.

Considerable effort has been directed at the development of selective inhibitors for nNOS and iNOS but which spare the eNOS isoform as its activity is essential for the maintenance of blood flow and pressure. However the design of isoform-specific inhibitors presents a challenging problem, in that the crystal structures reveal the active site residues for iNOS and eNOS to be nearly identical (Fischmann *et al.*, 1999; Li *et al.*, 1999a). Many different strategies have been developed in the search for isoform-specific NOS inhibitors, and can be divided into compounds which focus on the cofactor-binding sites, and those which target the L-arginine binding site. The inhibitors which target the cofactor-binding sites include

those which have actions on the haem binding site (such as 7-nitrindazole [7-NI] and trimethylphenylfluoroimidazole [TRIM]), those with actions on the BH_4 binding site, or those with effects on the flavoproteins (such as diphenyleneiodonium) or CaM (such as trifluoperazine). Although some of these compounds display some specificity and potency, they do not appear to be promising therapeutic NOS inhibitors as they may also interfere with the enzymatic activities of other enzymes which utilize similar cofactors.

The group of NOS inhibitors which target the L-arginine binding site have been more successful in the identification of isoform-selective NOS inhibitors. This group can be further divided into competitive inhibitors and mechanism based inhibitors (MBIs), which in addition to being competitive inhibitors of L-arginine binding are recognised by NOS enzymes as false substrates and are thereby metabolised during catalysis to products that irreversibly inactivate NOS.

The first series of competitive inhibitors created were analogues of the substrate L-arginine, the most commonly used being N-nitro-L-arginine (L-NNA) and N^G-nitro-L-arginine methyl ester (L-NAME). These compounds act as simple competitive inhibitors at the arginine binding site, have potencies in the low micromolar range (Alderton *et al.*, 2001), and show essentially no selectivity between isoforms. Despite their lack of specificity, these initial L-arginine analogues have proved to be of great value in the investigation of the physiological roles of NO, as well as in the treatment of clinical conditions associated with sustained iNOS activity such as septic shock (Petros *et al.*, 1991).

The first MBI to be identified that could function as an alternative substrate was N-methyl-L-arginine (L-NMMA), but again this compound did not possess a high degree of specificity between isoforms. The search for more selective inhibitors and L-arginine analogues revealed N-propyl-L-arginine (NPA) to be potent against the nNOS isoform (Zhang *et al.*, 1997; Cooper *et al.*, 2000), although this specificity has yet to be confirmed *in vivo* (Gowda *et al.*, 2004).

Since the initial series of L-arginine analogues, there have been a number of different inhibitors created which exhibit varying degrees of specificity. One group of MBIs which has recently been developed takes advantage of the inhibitory activity conferred by an amidine group. Compounds which contain an amidine group have been found to exhibit more selectivity and increased potency when compared to many

of the early compounds. Two promising compounds, α-fluoro-N-(3-(aminomethyl)-phenyl)-acetamidine [ARL-17477] and (+)cis-4-methyl-5-pentylpyrollidin-2-imine [1400W], have both been tested in intact tissue preparations, and share no structural homology with L-arginine or other amino acids although they are related to guanidine. ARL-17477 has been shown to exhibit at least a 100-fold selectivity for nNOS over eNOS and iNOS, whereas 1400W was found to be 5000-fold or 200-fold more selective for iNOS over eNOS or nNOS, respectively (Garvey *et al.*, 1997). Non L-arginine-based amino acid structural analogues which contain an amidine group also show promise as potent NOS inhibitors. Despite the initial compounds such as L-N^5-(1-iminoethyl)-ornithine [L-NIO] showing little inhibition specificity between NOS isoforms, recently N^5-(1-imino-3-butenyl)-L-ornithine (L-VNIO; Babu & Griffith, 1998) has been developed which is the most potent and nNOS-selective inhibitor to date. Table 1.2 compares the structures of the different generations of NOS inhibitors which target the L-arginine binding site.

It is clear that there is still much work remaining in the elucidation of the structure and mechanism of action of all three NOS isoforms. As the complete crystal structure becomes clear, this will assuredly aid both the understanding of NOS action and the discovery of new potent isoform-specific NOS inhibitors.

Mechanism Based Inhibitors (MBIs)			
	Competitive inhibitors	**N-nitro-L-arginine (L-NNA)** 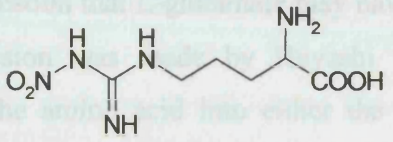	**N^G-nitro-L-arginine methyl ester (L-NAME)** 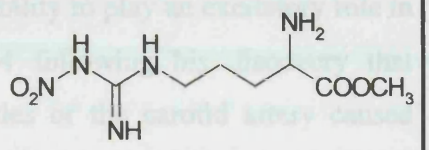
	L-arginine analogues	**N-methyl-L-arginine (L-NMMA)** 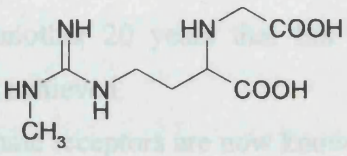	**N-propyl-L-arginine (NPA)** 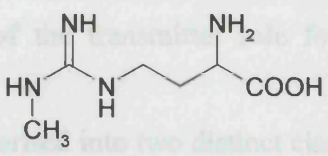
	Amino acid analogues	**L-N^5-(1-iminoethyl)-ornithine (L-NIO)** 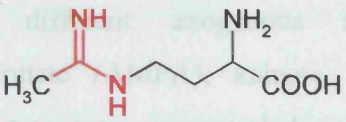	**N^5-(1-imino-3-butenyl)-L-ornithine (L-VNIO)** 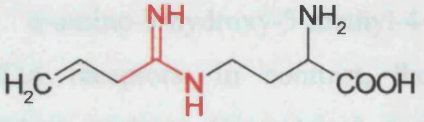
	Guanidine related compounds	**α-fluoro-N-(3-(aminomethyl)-phenyl)-acetamidine (ARL-17477)** 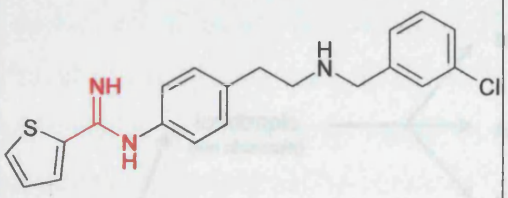	**cis-4-methyl-5-pentylpyrollidin-2-imine (1400W)** 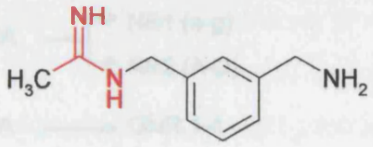

Table 1.2: Chemical structures of NOS inhibitors which target the L-arginine binding site. *L-arginine analogues act as simple competitive inhibitors at the L-arginine binding site. In addition to being competitive inhibitors of L-arginine binding mechanism based inhibitors are recognised by NOS as false substrates, and thereby are irreversibly metabolised during catalysis to inactive products. The amidine group which conferred an inhibitory activity is indicated in red.*

1.3 Interaction of glutamate and nitric oxide synthase in the CNS

L-glutamate is well known to be the principal excitatory neurotransmitter in the CNS. The first suggestion that L-glutamate may have the ability to play an excitatory role in neurotransmission was made by Hayashi in 1954 following his discovery that injection of the amino acid into either the ventricles or the carotid artery caused convulsions in dogs and monkeys (Hayashi, 1954). A few years later, in 1959, Curtis and colleagues went on to show that L-glutamate depolarised and excited individual spinal cord neurones in the cat (Curtis *et al.*, 1959). Despite these initial findings it was not for another 20 years that full acceptance of the transmitter role for L-glutamate was achieved.

Glutamate receptors are now known to be categorised into two distinct classes, ionotropic and metabotropic receptors. The ionotropic receptors contain cation-specific ion channels that can be further subdivided into three groups based on their affinity for different exogenous agonists: α-amino-3-hydroxy-5-methyl-4-isoxazolepropionate (AMPA), kainate and NMDA receptors. In contrast, the metabotropic receptors are coupled to GTP-binding proteins (G-proteins) and modulate the production of intracellular messengers. The current classification of glutamate receptors is summarised in figure 1.5.

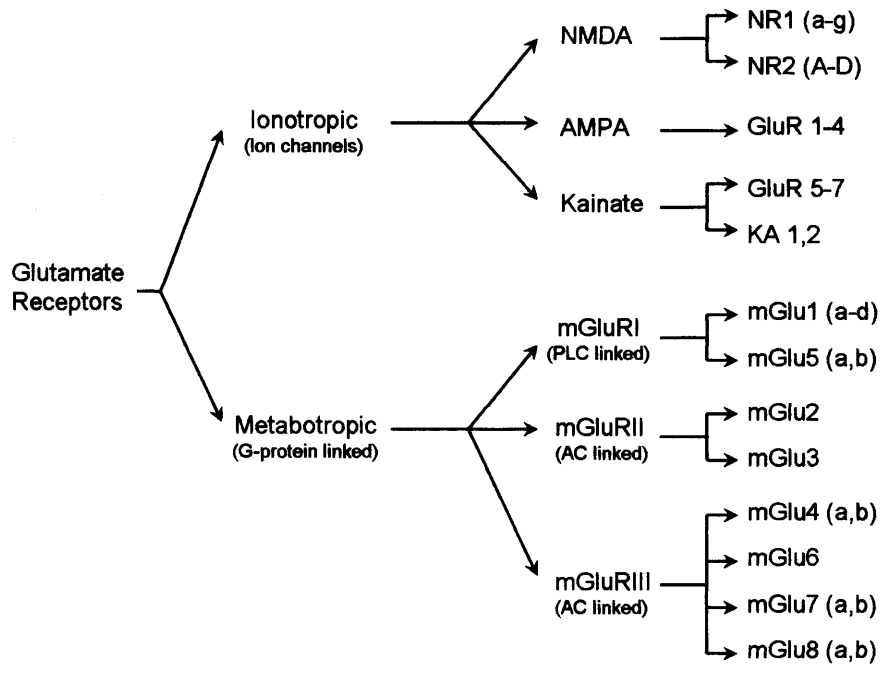

***Figure 1.5: Schematic representation of glutamate receptor subtypes, subunits and splice variants** (Adapted from Watkins, 2000).*

Glutamate receptors are now appreciated to underlie the majority of excitatory neurotransmission in the CNS. Glutamate typically mediates fast (millisecond) synaptic transmission through AMPA and kainate receptors, and a slightly slower (tens of milliseconds) excitation through NMDA receptors. The latter glutamate receptor usually participates only under depolarising conditions, due to blockade of the ionic channel by magnesium ions at resting membrane potential. Glutamate can also act on postsynaptically located metabotropic receptors to generate a slow (seconds) form of synaptic excitation (Batchelor & Garthwaite, 1997). Of particular importance for NO production is the NMDA receptor, where its activation leads to a transient influx of Ca^{2+} into the postsynaptic cell with the consequent activation of NOS (Garthwaite *et al.*, 1988); a process inhibited by D-AP5.

The predominant NOS isoform responsible for synthesising NO in the CNS under normal conditions is nNOS (Huang *et al.*, 1993). In 1996, the interesting observation was made that nNOS possesses an amino-terminal PDZ domain which interacts with PSD proteins such as PSD-95 and PSD-93 (Brenman *et al.*, 1996a,b). Furthermore, the NMDA receptor NR2 subunit (and certain NR1 splice forms) also contains a Ser/Thr-X-Val-COOH motif (tSXV) that enables its interaction with PSD-95 (Kornau *et al.*, 1995). By facilitating the proximity of NMDA receptors to the enzyme, the scaffolding protein directly exposes nNOS to the influx of Ca^{2+} entering the postsynaptic cell following the activation of NMDA receptors (Brenman *et al.*, 1996a). The nNOS splice variants, β and γ, both lack the PDZ domain and are therefore presumed to exist free in the cytoplasm, although their distribution generally follows that of nNOSα.

1.4 Guanylyl cyclase, the endogenous receptor for nitric oxide

A unique property of NO that sets it apart from other signalling molecules is its ability to diffuse freely and rapidly across cellular membranes. This gives NO the opportunity to spread three-dimensionally and act on neighbouring cellular elements in a non-synaptic fashion, irrespective of anatomical connectivity. It is predicted that the physiological sphere of influence of a single point source of NO has a diameter of approximately 200 microns, corresponding to a volume of brain enclosing around 2 million synapses (Wood & Garthwaite, 1994; Lancaster, 1997). However, despite NO being able to exert its influence on an extended area, NO is able to demonstrate relative selectivity of action due to the NO-receptor characteristics of the surrounding cells.

The only established physiological transduction pathway for NO involves the activation of guanylyl cyclase (GC). Given evidence that endogenously produced NO has effects independent of GC (Jacoby *et al.*, 2001; Lev-Ram *et al.*, 2002), it appears likely that other targets for NO exist which have not yet been identified. Guanylyl cyclases are a family of enzymes that catalyse the conversion of guanosine 5'-triphosphate (GTP) to the second messenger cGMP. Although cGMP-forming activity was first described to be present in mammalian tissues in 1969 (Hardman & Sutherland, 1969; Ishikawa *et al.*, 1969; Schultz *et al.*, 1969; White & Aurbach, 1969; Goldberg *et al.*, 1969), it took until the mid-1970s to determine that there were two different isoforms of GC (Garbers & Gray, 1974; Kimura & Murad, 1974; Chrisman *et al.*, 1975), which were consequently found to differ in their cellular location, structure and regulation (for review see Lucas *et al.*, 2000).

The two isoforms of GC which have been characterised include a membrane-bound isoform known as particulate GC (pGC) which is activated by natriuretic peptides or heat stable enterotoxins, and a soluble (or cytosolic) isoform which is activated by endogenous NO. The latter isoform was initially designated soluble GC to distinguish the enzyme from its membrane-bound counterpart, however recently one form of soluble GC was found to associate with the cell membrane (Russwurm *et al.*, 2001) and therefore this isoform (whether in solution or membrane bound) will be referred to as NO-activated GC. The following section focuses solely on the NO-activated GC.

1.4.1 Structure of guanylyl cyclase

NO-activated GC is a heterodimeric enzyme expressed in the cytoplasm of almost all mammalian cells and is composed of two different subunits, α and β, both of which are required for catalytic activity. Purification of the NO-activated GC was first achieved from rat and bovine lung (Koesling *et al.*, 1988, 1990; Nakane *et al.*, 1988, 1990), leading to the subsequent cloning and sequencing of the α_1 and β_1 subunits and were found to have molecular masses of 73 - 80 kDa and 70 kDa, respectively. The α_1 and β_1 subunits represent the most abundant forms of α and β subunits and have been determined to be widely distributed throughout the brain, although interestingly they are not necessarily expressed in a 1:1 ratio. The physiological relevance of the differing expression levels however remains unclear.

Homology screening has revealed the existence of alternative α and β subunits which include an α_2 subunit of ~ 82 kDa, and a β_2 subunit of ~ 76 kDa. The α_2 subunit was initially identified in human foetal brain (Harteneck *et al.*, 1991), and more recently has been found at a protein level in the placenta and uterus (Russwurm *et al.*, 1998; Budworth *et al.*, 1999). *In situ* hybridisation reveals α_2 mRNA to be widely expressed in the brain, with particular abundance in the cerebellum and the hippocampus (Gibb & Garthwaite, 2001). In contrast, mRNA of the β_2 subunit has been identified in the rat kidney, with lower expression levels present in the liver (Yuen *et al.*, 1990). The β_2 subunit however has yet to be found at the protein level. Furthermore, a frameshift has been found in the human gene of the β_2 subunit that is seemingly incompatible with the occurrence of a β_2 subunit on a protein level in humans (Behrends & Vehse, 2000), thereby questioning the physiological relevance of the β_2 subunit. Two additional subunits have been cloned, α_3 and β_3 (Giuili *et al.*, 1992), although these subunits have since been understood to represent human variants of the α_1 and β_1 subunits (Zabel *et al.*, 1998). Various splice variants of each subunit exist, however their physiological relevance is also unclear.

The two major types of α and β subunits so far identified permits four different heterodimeric possibilities: $\alpha_1\beta_1$, $\alpha_1\beta_2$, $\alpha_2\beta_1$, $\alpha_2\beta_2$. To date only two of the isoforms have been shown to exist at the protein level *in vivo*. The $\alpha_1\beta_1$ heterodimer represents the most abundant enzyme which exhibits widespread tissue distribution. The $\alpha_2\beta_1$ heterodimer was originally identified in human placenta (Russwurm *et al.*, 1998), but has since been found to also have a widespread distribution. Currently the highest

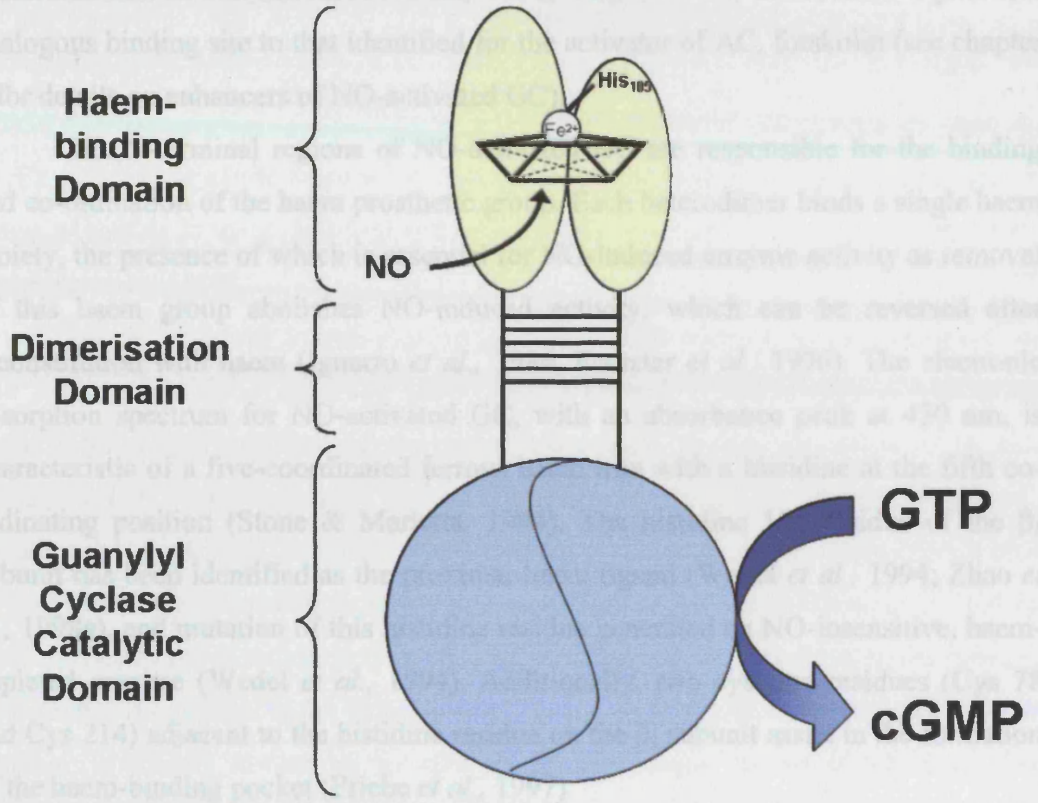

Figure 1.6: Domain structure of NO-activated GC.

concentration of the $\alpha_2\beta_1$ isoform has been found in the brain, where it is present in a comparable amount to the $\alpha_1\beta_1$ isoform (Mergia *et al.*, 2003) and has been shown to associate with the synaptic scaffolding protein, PSD-95 (Russwurm *et al.*, 2001). This isoform has been identified to be present at low levels in all other tissues tested so far.

The primary structure of each subunit of NO-activated GC can be divided up into three domains: a C-terminal catalytic domain, a dimerisation domain, and an N-terminal regulatory haem-binding domain (figure 1.6). The C-terminal catalytic domains are highly conserved among the subunits of NO-activated GC and show a high degree of homology to the respective regions of pGC and the adenylyl cyclases (AC). Analysis of N-terminally truncated mutants of NO-activated GC (which retain an intact dimerisation domain) reveal that the catalytic domains are sufficient for cGMP-forming activity, whereas NO stimulation requires the intact N-termini (Wedel *et al.*, 1995). Although NO-activated GC has not yet been crystallised it can be assumed from the high degree of sequence homology that the catalytic domain

resembles that of AC (Sunahara *et al.*, 1998; Tucker *et al.*, 1998) with a potential analogous binding site to that identified for the activator of AC, forskolin (see chapter 4 for details on enhancers of NO-activated GC).

The N-terminal regions of NO-activated GC are responsible for the binding and co-ordination of the haem prosthetic group. Each heterodimer binds a single haem moiety, the presence of which is essential for NO-induced enzyme activity as removal of this haem group abolishes NO-induced activity, which can be reversed after reconstitution with haem (Ignarro *et al.*, 1986, Foerster *et al.*, 1996). The electronic absorption spectrum for NO-activated GC, with an absorbance peak at 430 nm, is characteristic of a five-coordinated ferrous haem iron with a histidine at the fifth co-ordinating position (Stone & Marletta, 1994). The histidine 105 residue of the β_1 subunit has been identified as the proximal haem ligand (Wedel *et al.*, 1994; Zhao *et al.*, 1998a), and mutation of this histidine residue generated an NO-insensitive, haem-depleted enzyme (Wedel *et al.*, 1994). Additionally, two cysteine residues (Cys 78 and Cys 214) adjacent to the histidine residue on the β_1 subunit assist in the formation of the haem-binding pocket (Friebe *et al.*, 1997).

In contrast, the function of the N-terminal region of the α subunit remains unclear. The N-terminal region of the α subunits share approximately only 30% homology, with the histidine 105 residue not being conserved in either subunit. One study indicated that the N-terminal portion of the α_1 subunit may be required for haem binding (Wedel *et al.*, 1995), whereas a recent study claimed that deletion of the 259 N-terminal amino acids of the α_1 subunit had no effect on the properties of the enzyme at all (Koglin & Behrends, 2003). Interestingly it should be noted that despite the differences in the primary structure of the two α subunits, extensive analysis of the purified $\alpha_1\beta_1$ and $\alpha_2\beta_1$ isoforms did not reveal any functionally relevant differences with catalytic rates or sensitivity towards NO (Russwurm *et al.*, 1998).

An important feature of NO-activated GC is that, unlike other haemoproteins such as myoglobin and haemoglobin, the haem environment virtually excludes the binding of O_2 (Gerzer *et al.*, 1981). The consequence of which is that in the aerobic environment of the cell, NO-activated GC activity is not influenced by competition between NO and O_2. Furthermore, in contrast to other haemoproteins, the reaction of NO and O_2 resulting in the oxidation of the haem iron and the consequent formation of nitrate also will not occur, thereby allowing NO to freely associate and dissociate from the enzyme.

1.4.2 Activation of guanylyl cyclase

Among the three redox forms of NO (NO^-, $NO^\bullet$, and NO^+), only the uncharged NO radical has been shown to significantly activate NO-activated GC (Dierks & Burstyn, 1996). Activation of the enzyme is initiated by NO binding to the haem prosthetic group, resulting in up to 200-fold activation of the enzyme (Stone & Marletta, 1994; Humbert *et al.*, 1990).

Several different models exist to explain the activation of NO-activated GC by NO, the simplest involving a two-state model (figure 1.7): the binding of NO to the sixth coordinating position of the haem iron leads to the formation of a six-coordinated Fe^{2+}-haem complex with an absorption maximum of 420 nm (Zhao *et al.*, 1998b). The subsequent breakage of the histidine-iron bond yields a five-coordinated nitrosyl-haem complex with an absorption maximum at 399 nm (Makino *et al.*, 1999). The opening of the histidine-iron bond is believed to initiate a conformational change, presumably propagated to the enzyme's active site, resulting in a several hundred-fold increase in cGMP formation. In support of this simple model is evidence that protoporphyrin IX activates NO-activated GC independently of NO (Ignarro *et al.*, 1982), and that the six-coordinated haem intermediate does not activate the enzyme which supports the idea that breakage of the histidine-iron bond is a prerequisite for enzyme activity (Zhao *et al.*, 1998b).

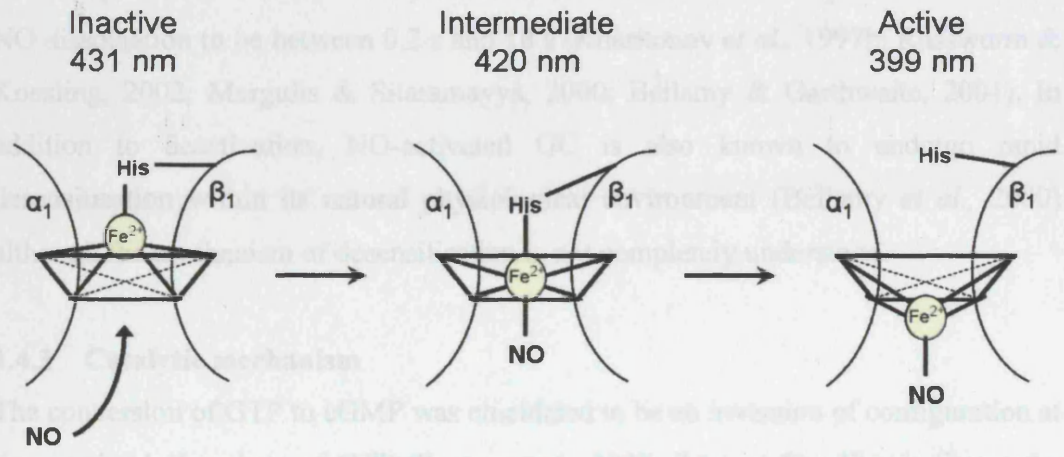

Figure 1.7: Two-state model of NO-activated GC activation.

Alternative models have also been suggested to explain the activation of NO-activated GC by NO. One model suggests that NO not only activates the enzyme by binding to the haem iron, but also regulates the velocity of activation via binding to a second non-haem binding site (Zhao *et al.*, 1999). However, this model is under dispute as the data has since been reinterpreted in favour of the two-state simple model (Bellamy *et al.*, 2002). A second alternative model has been suggested on the basis of comparison with microbial cytochrome *c'*, in that two molecules of NO bind to the haem-binding site (Sharma & Magde, 1999). Interestingly, a recent crystallographic study revealed that cytochrome *c'* binds NO on the proximal side of the haem-iron, rather than the distal side, a possibility that had never been observed or considered previously (Lawson *et al.*, 2000). Furthermore, cytochrome *c'* has been found to form a transient six-coordinated species analogous to NO-activated GC (Zhao *et al.*, 1999). The proposed mechanism based on these findings is that NO initially binds to the (cytochrome *c'* and NO-activated GC) haem iron in the distal position, and the subsequent displacement of the histidine and the distal NO by a second NO molecule, which forms a bond at the proximal side (Lawson *et al.*, 2003). However the haem environment differs between these enzymes and therefore the physiological relevance to this comparison remains to be seen.

Generally the dissociation of NO from the haem group is considered to trigger deactivation of NO-activated GC. Initial studies carried out on purified enzyme from bovine lung indicate that NO dissociates slowly, the half life being at least two minutes (Kharitonov *et al.*, 1997a). More recent studies however report the half life of NO dissociation to be between 0.2 s and 18 s (Kharitonov *et al.*, 1997b; Russwurm & Koesling, 2002; Margulis & Sitaramayya, 2000; Bellamy & Garthwaite, 2001). In addition to deactivation, NO-activated GC is also known to undergo rapid desensitisation within its natural physiological environment (Bellamy *et al.*, 2000) although the mechanism of desensitisation is not completely understood.

1.4.3 Catalytic mechanism

The conversion of GTP to cGMP was elucidated to be an inversion of configuration at the proximal phosphate of GTP (Senter *et al.*, 1983; figure 1.8). This indicates the catalytic mechanism to be a simple displacement reaction without the formation of a covalently bound enzyme-substrate intermediate, a mechanism common to the related ACs. A nucleophilic amino acid residue is required to accept a proton from the

hydroxyl group at position 5 of the ribose moiety of GTP, which allows the subsequent displacement of pyrophosphate and the formation of cGMP. The identity of this basic residue has not yet been determined, but it has been speculated that the histidine 105 residue (after bonding with the haem group) could provide the necessary base for catalysis (Sharma & Magda, 1999).

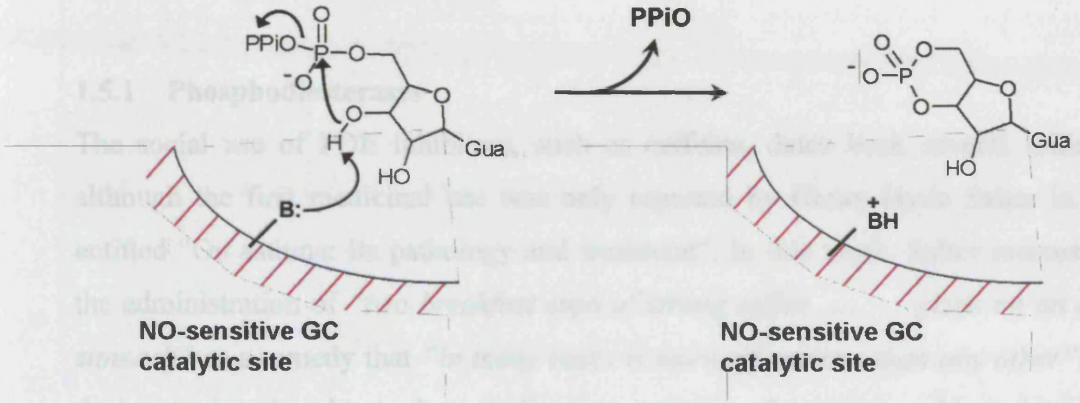

Figure 1.8: Proposed mechanism for catalysis of cGMP from GTP.
Nucleophilic residue designated B.
(Adapted from Senter et al., 1983)

1.4.4 Pharmacological inhibition of guanylyl cyclase

Several compounds have been developed to inhibit NO-activated GC. Early drugs such as methylene blue and LY83583 exhibit poor selectivity, and have been shown to interfere with NO synthesis (Mayer *et al.*, 1993a) and affect nucleotide-gated ion channels (Leinders-Zufall & Zufall, 1995a). The quinoxalin derivative, 1-*H*-[1,2,4]-oxadiazolo-[4,3-*a*]-quinoxalin-1-one (ODQ) was characterised in 1995 and found to be a potent and selective inhibitor of NO-activated GC in brain slices (Garthwaite *et al.*, 1995b). Studies on purified NO-activated GC reveal that ODQ competes with NO in a competitive manner and irreversibly inhibits NO-stimulated activity, leaving basal enzymatic activity unchanged. Spectral analysis suggests that ODQ acts by slow reversible oxidation of the haem iron (Schrammel *et al.*, 1996; Zhao *et al.*, 2000).

A number of compounds have also been developed which sensitize NO-activated GC towards NO. These will be discussed in chapter 4.

1.5 The cellular targets of cGMP

The cyclic nucleotide second messenger, cGMP, has been shown to regulate a wide variety of signal transduction pathways throughout the body. There are four well-established intracellular targets for cGMP: cGMP-regulated phosphodiesterases (PDEs), cGMP-dependent protein kinase (protein kinase G; PKG; cGK), cyclic nucleotide-gated (CNG) ion channels, and hyperpolarisation-activated cyclic nucleotide-regulated non-selective cation (HCN) channels.

1.5.1 Phosphodiesterases

The social use of PDE inhibitors, such as caffeine, dates back several millennia, although the first medicinal use was only reported by Henry Hyde Salter in 1860 entitled "On asthma: Its pathology and treatment". In this work, Salter recommends the administration of *"two breakfast cups of strong coffee ..... given on an empty stomach"* as a remedy that *"in many cases is more efficacious than any other"*. This dosing regime has been since realised to optimise absorption, achieve high peak serum levels, and specifically target the exaggerated diurnal variation in pulmonary function which is characteristic of asthma (Persson, 1985). However it was not until 1957 that the mechanistic understanding of cyclic nucleotides and PDEs began to evolve. In that year, Sutherland and Rall (Sutherland & Rall, 1957, 1958) first described the properties of a cyclic adenine ribonucleotide (now known as cAMP), and inhibition of its hydrolysis by sodium fluoride and caffeine. Over the ensuing decades, the importance of cyclic nucleotide second messengers in cellular signalling came to be appreciated and considerable effort has been directed towards the elucidation of PDEs and the pharmacological regulation of this pathway by PDE inhibitors.

The biological effects of cGMP are dependent on its intracellular concentration which is determined by the balance between its rate of synthesis and its rate of breakdown. PDEs are a superfamily of enzymes which catalyse the hydrolysis of cyclic nucleotides to the inactive 5'-nucleoside monophosphate (i.e. cAMP to 5'-AMP; cGMP to 5'-GMP), and therefore are responsible for the regulation of intracellular concentration of cyclic nucleotides. To date, PDEs have been categorised into 11 different families (PDE1 - PDE11) based on their substrate specificity and characteristic regulation by inhibitors and activators (table 1.3).

PDE isoform	Splice variants	Tissue distribution	Characteristics
1	3	Heart, brain, lung, smooth muscle	Ca^{2+}/CaM dependent
2	1	Adrenal gland, heart, lung, liver, platelets	cGMP-activated PDE
3	2	Heart, lung, liver, platelets, adipose tissue, immunocytes	cGMP-inhibited PDE
4	4	Sertoli cells, kidney, brain, liver, lung, immunocytes	cAMP-specific
5	1	Lung, platelets, smooth muscle	cGMP-specific
6	3	Photoreceptors	cGMP-specific
7	2	Skeletal muscle, heart, kidney, brain, pancreas, T lymphocytes	cAMP-specific
8	2	Testes, eye, liver, skeletal muscle, heart, kidney, ovary, brain, T-lymphocytes	cAMP-selective IBMX insensitive
9	1	Kidney, liver, lung, brain	cGMP-specific IBMX insensitive
10	1	Testes, brain	cAMP-selective cAMP-inhibited cGMP PDE
11	1	Skeletal muscle, prostate, kidney, liver, pituitary and salivary glands, testes	

Table 1.3: Classification of the PDE family

Additional heterogeneity within the PDE family is achieved through the presence of multiple splice variants which makes the total number of PDE isozymes currently recorded to exceed 30. Specific PDE isoforms display remarkably selective cellular and subcellular localisations (Bolger *et al.*, 1997; Jin *et al.*, 1998; Lobban *et al.*, 1994), and are therefore likely to participate in discrete signal transduction pathways in discrete physiological and pathophysiological processes.

Almost all PDEs exist as homodimers, with monomer molecular weights ranging from 50 to 135 kDa. They are composed of two broad functional domains: a catalytic C-terminal domain, and a regulatory N-terminal domain. The C-terminal catalytic domains are highly homologous across families (> 50 % sequence identity at the amino acid level), whereas the N-terminal domain contains one or more regulatory segments which impart specific subtypes and isoforms their unique functional fingerprints.

PDE families 2, 5, 6, 10, and 11 contain two non-catalytic allosteric sites in their N-terminal regions which were originally observed to bind cGMP (Charbonneau *et al.*, 1990). These sequences were later named "GAF domains" to reflect the names of the first three classes of proteins in which they were identified: cGMP-regulated

PDEs, the cyanobacterial *Anabaena* adenylate cyclase, and the *E.coli* transcription factor Fh1A (Aravind & Ponting, 1997). A molecular model of cGMP binding to the GAF domain is displayed in figure 1.9.

GAF domains represent one of the largest and most widespread of all the small molecule binding domains found in proteins involved with cyclic nucleotide signalling. The ligands for most GAF domains have yet to be identified, however cGMP is the only known ligand to bind to the GAF domain in PDEs (PDE 2, 5, 6, and 10). Interestingly, PDE11 exhibits a truncated GAF domain and neither cGMP nor cAMP binding to the domain has been reported to date. Crystallisation studies of the regulatory sequences have revealed that both the GAF-A and GAF-B domain are capable of cGMP-binding (cGMP binds to the GAF-B domain in mouse PDE2A, whilst cGMP binds to the GAF-A in bovine PDE5A), although what determines which domain binds cGMP is unclear. It is also currently not clear what the function is of the GAF domains which do not bind cGMP. In PDE2, the GAF-A domain may function as a dimer interface, although the role for the GAF-B domain in PDE5A is harder to predict.

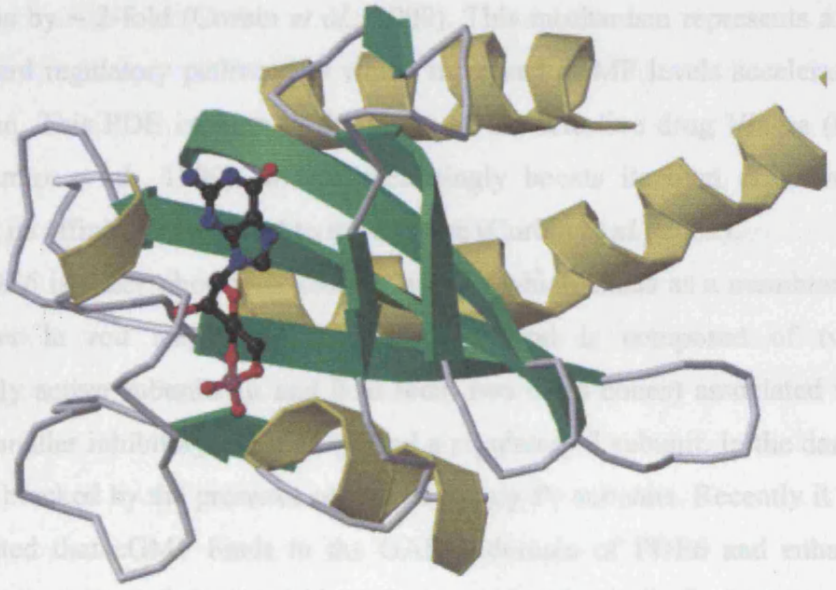

Figure 1.9: Molecular model of cGMP binding to the GAF domain.
(Martinez et al., 2002)

PDE2 is a homodimer consisting of two 100 - 150 kDa subunits, and catalyses the hydrolysis of both cGMP and cAMP (with a higher affinity for cGMP). This family was initially identified in the liver, heart and adrenal gland, but it is now known to be widely distributed. As described above, cGMP has been found to bind to a regulatory GAF sequence on the enzyme resulting in an enhancement of the rate of hydrolysis of both cGMP and cAMP. PDE2 is therefore also known by the alternative name of "cGMP-activated PDE" (Juilfs *et al.*, 1999). This modulatory effect by cGMP is an important mechanism by which cross-regulation may occur between cGMP and cAMP pathways.

PDE5 and PDE6 isoforms share a high degree of homology (45 – 48 % identity at the amino acid level) between catalytic domains, and are both highly selective for cGMP. PDE5 is a homodimer consisting of two 95 kDa subunits, and found abundantly in lung, platelet and smooth muscle. Binding of cGMP at the catalytic site of PDE5 stimulates cGMP to bind to the GAF-A domain, which in turn promotes the phosphorylation of the serine 93 residue by PKA or cGK (Thomas *et al.*, 1990; Turko *et al.*, 1998). It has been suggested recently that phosphorylation induces a conformational change which increases the affinity of the GAF-A domain for cGMP by ~ 10-fold (Francis *et al.*, 2002), and consequently increases the catalytic activity of the enzyme by ~ 2-fold (Corbin *et al.*, 2000). This mechanism represents a negative feed forward regulatory pathway by which increased cGMP levels accelerate cGMP degradation. This PDE isoform is the target of the selective drug Viagra (sildenafil citrate; Turko *et al.*, 1999), which interestingly boosts its own effectiveness by increasing its affinity once bound to the enzyme (Corbin *et al.*, 2002).

PDE6 is a key phototransduction enzyme which exists as a membrane-bound heterodimer in rod and cone photoreceptors, and is composed of two large catalytically active subunits (α and β in rods; two α' in cones) associated with two identical smaller inhibitory subunits (γ) and a regulatory δ subunit. In the dark, PDE6 activity is blocked by the presence of two inhibitory Pγ subunits. Recently it has been demonstrated that cGMP binds to the GAF-A domain of PDE6 and enhances the affinity between Pγ and the catalytic subunits, and reciprocally Pγ-binding enhances cGMP-binding to the GAF-A domain (Muradov *et al.*, 2004). Upon light stimulation, the enzyme is activated by GTP-bound transducin-α, which displaces Pγ from the catalytic core. cGMP hydrolysis results phototransduction by the closure of cGMP-gated channels and the consequent hyperpolarisation of the photoreceptor cell (Beavo,

1988). Most PDE5 inhibitors, including Viagra, inhibit PDE6 with similar potency due to the high homology between their catalytic domains.

PDE10 and PDE11 have only been recently described (Fujishige *et al.*, 1999a; Loughney *et al.*, 1999; Fawcett *et al.*, 2000; Soderling & Beavo, 2000), and have the capacity to hydrolyse both cGMP and cAMP. PDE10 binds cAMP with higher affinity than cGMP, although the enzyme hydrolyses cAMP five-fold less effectively than cGMP. *In vitro* analysis has revealed that cGMP hydrolysis is potently inhibited by cAMP, and it therefore been suggested that PDE10 may function as a cAMP-inhibited cGMP PDE *in vivo* (Fujishige *et al.*, 1999b). Preliminary studies indicate PDE10 contains a low-affinity cGMP-binding GAF domain, and *in vitro* binding studies indicate that the dissociation constant (K_d) for cGMP binding to the GAF domain is well above 9 μM (Soderling *et al.*, 1999). As *in vivo* cGMP concentrations are unlikely to reach such levels, it appears likely that either the affinity of PDE10 for cGMP is increased by some regulatory mechanism, or that the primary function of the GAF domain in PDE10 may be for something other than for cGMP-binding. PDE10 expression appears to be limited to the striatum and testes (Fujishige *et al.*, 1999b).

PDE11 also belongs to the GAF-containing PDEs although it has the unique structural feature of containing a truncated GAF domain in many of its splice variants. Preliminary studies indicate that neither cAMP nor cGMP act as allosteric effectors of this enzyme (Fawcett *et al.*, 2000). PDE11 is expressed at high levels in the prostate and skeletal muscle, but has also been identified in the kidney, liver, testes, and in the pituitary and salivary glands.

PDE1 is another dual-substrate PDE and is one of the key enzymes involved in the complex interactions between the cyclic nucleotides and Ca^{2+}-second messenger systems. The PDE1A and PDE1B isoforms hydrolyse cGMP more effectively than cAMP, whereas the PDE1C isoform hydrolyses cGMP and cAMP with equal efficiency (Beavo, 1995). Competitive inhibition of cGMP hydrolysis can be achieved via an elevation in cAMP levels, and vice versa. PDE1 is activated by the binding of CaM in the presence of Ca^{2+}, resulting in an increase in cyclic nucleotide hydrolysis. Enzyme activity is additionally regulated by phosphorylation, which is accompanied by an increase the binding affinity for CaM, effectively reducing the sensitivity of PDE1 to Ca^{2+} (Hashimoto *et al.*, 1989; Sharma & Wang, 1986). The role of this isoform is of particular interest in the NO-cGMP pathway due to its activation by Ca^{2+}/CaM (Kakkar *et al.*, 1999). It has been hypothesised that elevation in

intracellular Ca^{2+} levels simultaneously activates nNOS and PDE1 (Baltrons *et al.*, 1997), thereby accumulation of cGMP in stimulated cells are inhibited whilst neighbouring cells containing low cytosolic Ca^{2+} levels are free to respond (Mayer *et al.*, 1993b). PDE1 exhibits widespread distribution.

PDE3 can be distinguished from other PDEs by their high affinity for both cAMP and cGMP, and is often referred to as the cGMP-inhibited isoform. In contrast to PDE2, inhibition of the enzyme by cGMP is not achieved by cGMP binding to a non-catalytic site. Instead, cGMP is hydrolysed ten-times less effectively than cAMP and therefore when cGMP is bound to the catalytic site it acts as a competitive antagonist to cAMP degradation (Degerman *et al.*, 1997). PDE3 has been demonstrated to be activated two-fold by phosphorylation by either PKA or PI3-K (Manganiello & Degerman, 1999). Similar to other PDE isoforms, the N-terminal region also confers regulatory properties on the enzyme. Residues in the N-terminal region have been demonstrated to be important for membrane association (Shakur *et al.*, 2000) and are phosphorylated in response to insulin (Kitamura *et al.*, 1999). Therefore subcellular localisation could influence the specificity of protein kinase interactions with PDE3.

PDE9 reveals the highest affinity for cGMP so far recorded for any PDE isoform (K_m = 0.07 μM; Soderling *et al.*, 1998a), and is selective over cAMP by several hundred-fold (Soderling *et al.*, 1998a; Fisher *et al.*, 1998a). This high affinity for cGMP results in the cells that express PDE9 maintaining very low basal levels of cGMP, and therefore potentially is very important in cGMP signalling. PDE9 expresses wide tissue distribution and is widely expressed throughout the brain. The pattern of enzyme expression within the brain has been found to closely resemble that of NO-activated GC, suggesting a possible functional association or coupling of these two enzymes in the regulation of cGMP levels (Andreeva *et al.*, 2001). Interestingly, PDE9 is not effectively inhibited by the non-selective PDE inhibitor IBMX.

PDE4, PDE7, and PDE8 are all termed "cAMP-specific PDEs" and therefore these PDE families are not thought to play a role in cGMP signalling. PDE4 has been demonstrated in a number of vascular smooth muscle tissues, and has recently been discovered to play a critical role in cell homeostasis (Jin *et al.*, 1999). PDE7 and PDE8 appear primarily to be expressed at high levels in discrete cell types. PDE7 is expressed in lymphocytes and is involved in the regulation of cAMP-mediated immunosuppressive responses (Bloom & Beavo, 1996; Li *et al.*, 1999b), whereas

PDE8 is expressed at high levels in the testis, but is also present at lower levels in other tissues such as the liver, heart and ovaries (Soderling *et al.*, 1998b; Fisher *et al.*, 1998b). Like PDE9, PDE8 has been demonstrated to be unaffected by the PDE inhibitor IBMX. (Hayahashi *et al.*, 1998)

1.5.2 cGMP-stimulated protein kinases

The cGKs have emerged as important signal transduction mediators of the effects of certain hormones, inter/intracellular signals, toxins and drugs (Lohmann *et al.*, 1997). The first protein kinase to be selectively activated by cGMP was reported in lobster tail muscle extracts (Kuo & Greengard, 1970), but other similar kinases have subsequently been observed in a number of different tissues which will be described below.

There are two distinct forms of cGMP-dependent protein kinases: type I (cGKI) of which there are two splice variants, cGKIα and cGKIβ, and type II (cGKII). Recent investigations also reveal the presence of a splice variant of cGKII which appears to lack intrinsic protein kinase activity, instead functioning as an endogenous inhibitor of cGKI and cGKII (Gambaryan *et al.*, 2002). cGKI is a cytosolic 76 kDa homodimer widely expressed in mammalian tissues, with especially high levels in the cerebellum, platelets and in smooth muscle (Lohmann *et al.*, 1997). The two splice variants of cGKI differ only in their N-terminal domain, and confers different binding affinities for cGMP. cGKIα contains a high and a low affinity binding site for cGMP which display positive co-operative behaviour, whereas cGKIβ has two cGMP binding sites characterised by lower affinity and co-operability (Pfeifer *et al.*, 1999). In contrast, cGKII exists as an 86 kDa membrane-bound homodimer which is absent from the cardiovascular system but can be abundantly detected in the brain and intestine, with lower levels in lung, bone and kidney (Lohmann *et al.*, 1997). cGKII differs from cGKI primarily in the N-terminal region which confers subcellular localisation and substrate selectivity. Furthermore, cGKI and cGKII appear to be expressed in different cell types, with the exception of the growth plate in the tibia of newborn mice (Pfeifer *et al.*, 1996).

Each isoform of cGK exists as a dimer comprised of two identical monomers. Each monomer is composed of three functional domains: an N-terminal domain, a regulatory cyclic-nucleotide binding domain, and a C-terminal catalytic domain

(Lucas *et al.*, 2000). The N-terminal region contains four regulatory sites which include:

(a) Dimerisation site containing an α-helix with a conserved leucine/isoleucine heptad repeat, or "leucine zipper".
(b) Autoinhibitory site responsible for the inhibition of kinase activity in the absence of cGMP.
(c) Autophosphorylation site which increases the basal catalytic activity of the enzyme in the presence of cGMP.
(d) Intracellular localisation site including a myristoylation site in cGKII which determines its membrane association, and an acetylation site in cGKI.

The regulatory domain contains two homologous cyclic nucleotide-binding sites arranged in tandem that allow for full activation of the enzyme after the binding of two cGMP molecules, and a catalytic site which contains binding sites for Mg^{2+}/adenine triphosphate (ATP) and the target protein. When cGK is inactive, the regulatory and catalytic sites are covalently fused. Binding of two molecules of cGMP induces a conformational "elongation" in the enzyme that appears to distance the autoinhibitory region from the catalytic domain, resulting in the consequent activation of cGK (Wall *et al.*, 2003b). Additionally, activation can be achieved by autophosphorylation in the autoinhibitory domain.

The catalytic action of cGK is through the transfer of a γ-phosphate from a molecule of ATP to a serine or threonine residue on the target protein although the physiological substrates for cGKI and cGKII remain unclear. Probably the best characterised substrate for cGKI is the phosphatase inhibitor known as G-substrate, located primarily in cerebellar Purkinje cells (Endo *et al.*, 1999). Other target proteins of phosphorylation include inositol 1,3,4-triphosphate (IP_3) receptors which result in smooth muscle relaxation, vasodilator-stimulated protein (VASP) which results in platelet activation, and vimentin which results in neutrophil activation. DARPP-32, a phosphatase inhibitor sharing homology with G-substrate, has also been suggested as a target for cGKI (Tsou *et al.*, 1993). To date, the only recognised target substrate for cGKII is the cystic fibrosis transmembrane conductance regulator (CFTR) chloride channel which plays an important role as a mediator of salt and fluid transport across numerous epithelial tissues (Vaandrager *et al.*, 1998). Table 1.4 summarises the isoforms of cGK and their target substrates.

Isoform	Chromosomal location	Subcellular localisation	Tissue distribution	Substrate	Function
cGKIα	10	Cytoplasm	• Smooth muscle • Lung • Platelets •Brain / neurons	• G-substrate • IP_3 • VASP • Vimentin • DARPP-32 • Septin 3 • PDE5 • FHOD1	• Control of smooth muscle. • Regulation of smooth muscle migration, proliferation & differentiation. • Platelet aggregation.
cGKIβ	10	Cytoplasm			
cGKII	4	Membrane	• Brain • Intestine • Lung • Bone • Kidney	• CFTR	• Increased Cl^- secretion •Control of intestinal secretion • Inhibition of renin release • Promotion of bone growth

Table 1.4: Distribution and physiological functions of cGK.
(Formin homology domain-containing protein (FHOD1)).

Insight into the physiological roles of the cGMP-dependent protein kinases has been gained from the analysis of transgenic mice deficient in either cGKI or cGKII. Homozygous deletion of the cGKI gene in mice abolishes the NO/cGMP dependent relaxation of vascular, visceral, and penile smooth muscle (Hedlund *et al.*, 2000; Ny *et al.*, 2000; Pfeifer *et al.*, 1998), and results in severe vascular and intestinal dysfunction and death at an early age. In contrast, cGKII knockout mice exhibited a normal lifespan, although the mice did reveal decreased longnitudinal bone growth, decreased intestinal chloride secretion and altered renin secretion (Pfeifer *et al.*, 1996; Vaandrager *et al.*, 2000; Wagner *et al.*, 1998).

cGK signalling is also known to play an important role in the nervous system. cGKI is highly expressed in the cerebellar Purkinje cells where they are closely associated with NOS-containing granule and basket cells, throughout all the cellular layers in the hippocampus (Kleppisch *et al.*, 1999), and limited localisation elsewhere in the brain. Selective deletion of the cGKI gene results in impairment of long term potentiation (LTP) in the hippocampus, and reduced long term depression (LTD) in the cerebellum (Feil *et al.*, 2003; Kleppisch *et al.*, 2003). In contrast cGKII is widely distributed throughout the brain (de Vente *et al.*, 2001), and many regions expressing cGKII also contain or receive innervation from NO positive neurons.

1.5.3 Cyclic nucleotide gated ion channels

CNG channels are class of ion channels that are structurally related to voltage-gated ion channels, but have no apparent voltage sensitivity and additionally possess a cyclic nucleotide binding region. The first ion channels to be directly activated by cyclic nucleotides were discovered in the plasma membrane of retinal photoreceptors (Fesenko *et al.*, 1985), and have since been shown to play an essential role in visual and olfactory sensory signal transduction where they change sensory information into membrane potential (Zufall *et al.*, 1994; Finn *et al.*, 1996). CNG channels exhibit widespread distribution within the CNS, although their presence has additionally been demonstrated in a variety of non-sensory tissues such as the heart, testes and kidney (Biel *et al.*, 1996; Finn *et al.*, 1996).

Functional CNG channels exist as tetramers composed of three principal α-subunits which have the ability to form active channels when expressed alone, and one β-subunit which is unable to form an active channel by itself but appears to act to modulate the channel properties of the α-subunits (Bradley *et al.*, 1994; Liman & Buck, 1994; Zhong *et al.*, 2002). Properties controlled by the β-subunit include single-channel flickering, increased apparent affinity for cyclic nucleotides, and altered interaction with Ca^{2+}. To date, four distinct isoforms of the α-subunit have been cloned: CNGα1 from rod photoreceptors (Kaupp *et al.*, 1989), CNGα2 from cone photoreceptors (Bönigk *et al.*, 1993), and CNGα3 and α4 from olfactory neurons (Dhallan *et al.*, 1990, Kaupp, 1995). Additionally, three genes encoding β-subunits have also been identified: CNGβ1a in rod photoreceptors (Körschen *et al.*, 1995), CNGβ1b in olfactory neurons (Sautter *et al.*, 1998) and CNGβ3 in cone photoreceptors (Gerstner *et al.*, 2000)

All CNG channel subunits share a common modular architecture which includes a six transmembrane (6TM) domain homologous to that of the voltage-gated potassium channel family, consisting of six transmembrane segments (S1 – S6) with an ion conducting pore between S5 and S6 (figure 1.10). Additionally, CNG channels contain two interactive regulatory domains on the cytoplasmic side of the membrane which represent the N- and C-termini. A cyclic nucleotide binding domain homologous to that found in cGK is present on the C-terminus which consists of three α-helices and an eight-stranded antiparallel β-roll (Zagotta & Siegelbaum, 1996; Biel *et al.*, 1999). Two unconventional CaM binding sites have also been identified, one in each of the N- and C- termini of the β-subunit (Weitz *et al.*, 1998; Grunwald *et al.*,

1998). Zhong and colleagues have also recently identified a leucine zipper motif in the C-terminus of all α-subunits which appears to be involved in trimerisation of the α-subunits (Zhong *et al.*, 2002). This zipper motif is lacking in β-subunits.

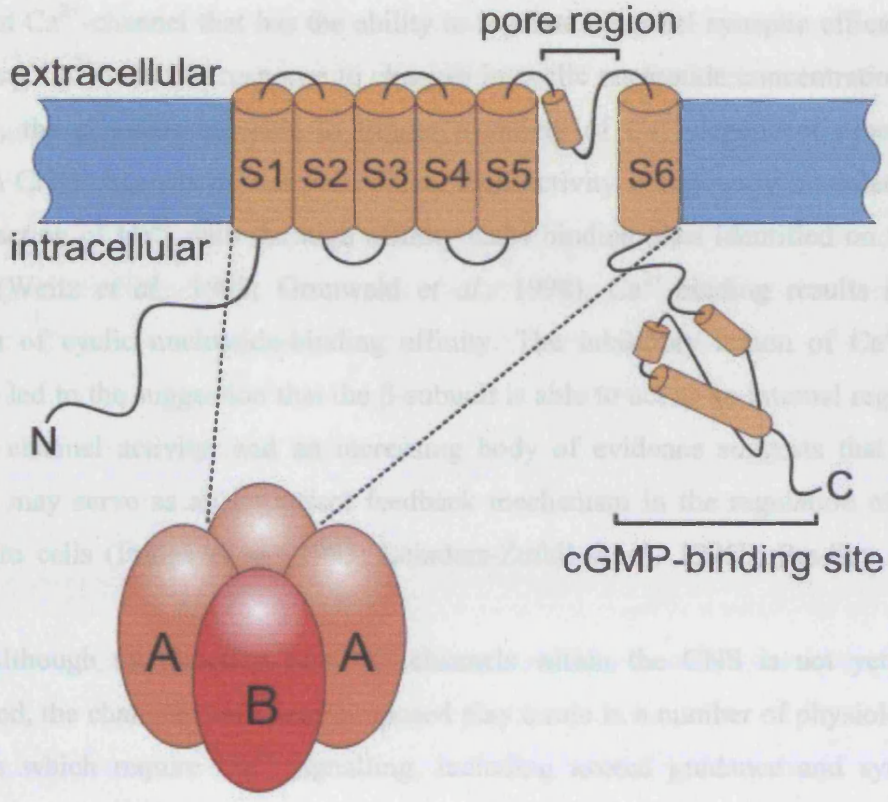

Figure 1.10: Transmembrane topology of a CNG channel subunit and the composition of the cone CNG channel.
(http://www.fz-juelich.de/ibi/ibi-1/Achromatopsia)

CNG channels are directly and co-operatively activated by the binding of intracellular cGMP and cAMP to the cyclic nucleotide binding site located in the C-terminal domain (Fesenko *et al.*, 1985; Nakamura & Gold, 1987), inducing a conformational change which culminates in the opening of an ion-conducting pore. Similar to cGK, the α-subunit is more sensitive to cGMP than cAMP (Zagotta & Siegelbaum, 1996), although the critical amino acids which confers this sensitivity differs between the two proteins. However, in contrast to most voltage-gated and

ligand-gated ion channels, CNG channels do not exhibit desensitisation, and instead remain open continuously in the presence of cyclic nucleotides.

All CNG channels have the ability to conduct both Na^+ and Ca^{2+} ions, but the channels are more permeable to Ca^{2+} than to Na^+ under physiological conditions (Frings *et al.*, 1995). Within the CNS, CNG channels appear to represent a cGMP-dependent Ca^{2+}-channel that has the ability to regulate neuronal synaptic efficacy by modulating Ca^{2+} levels in response to changes in cyclic nucleotide concentrations. In this way, the channels are able to trigger a variety of Ca^{2+}-dependent processes. Although CNG channels do not desensitize, their activity is indirectly modulated by the interaction of Ca^{2+} with the high affinity CaM binding sites identified on the β-subunit (Weitz *et al.*, 1998; Grunwald *et al.*, 1998). Ca^{2+}-binding results in the reduction of cyclic nucleotide-binding affinity. The inhibitory action of Ca^{2+} has therefore led to the suggestion that the β-subunit is able to act as an internal regulator of CNG channel activity, and an increasing body of evidence suggests that these channels may serve as an important feedback mechanism in the regulation of Ca^{2+} influx into cells (Frings *et al.*, 1995; Leinders-Zufall *et al.*, 1995b; Bradley *et al.*, 1997).

Although the function of CNG channels within the CNS is not yet fully understood, the channels have been proposed play a role in a number of physiological processes which require Ca^{2+} signalling, including axonal guidance and synaptic plasticity (Zufall *et al.*, 1997; Barnstable *et al.*, 2004). The spatial expression of CNG channels in mammalian CNS neurons reveals an interesting correlation to the elements of NO signal transduction pathways. Of particular relevance to the current work is the demonstration using *in situ* hybridisation and patch clamp recording techniques that CNG channels are present in the hippocampus. The channels were observed in the soma and proximal dendrites of pyramidal neurons, and in the granule cells of the dentate gyrus (Leinders-Zufall *et al.*, 1995b; Kingston *et al.*, 1996). This localisation places CNG channels in an ideal position to play a role in synaptic plasticity.

1.5.4 HCN channels

HCN channels are a specific subfamily of CNG channels which represent a potential, but as of yet unconfirmed, target for NO/cGMP signalling. Activation of HCN channels occurs upon hyperpolarisation of the membrane and leads to the slow onset of an inward non-selective cation current (I_h), and consequent membrane depolarisation. I_h currents were first described in the rabbit cardiac sino-atrial node (Noma & Irisawa, 1976), and shortly thereafter a similar hyperpolarisation-activated cation current was discovered in the brain (Bader *et al.*, 1979; Halliwell & Adams, 1982). I_h exhibits pacemaker activity in some cell types (such as in sino-atrial node cells and in thalamocortical relay neurons), being activated by the membrane hyperpolarisation following an action potential and acting to depolarize the membrane towards the threshold for firing a subsequent action potential. I_h is also known to play a significant role in determining the resting membrane potential of neurons (Pape, 1996; Robinson & Siegelbaum, 2003).

To date, four isoforms of HCN have been cloned in mammals (HCN1 - HCN4) which govern the kinetic and functional properties of the resultant channels. Consistent with CNG channels, all four HCN isoforms possess a structure similar to that of the voltage-gated potassium channel, and are highly conserved in their core transmembrane regions and cyclic nucleotide binding domains (80 – 90 % identical). Each subunit is composed of a 6TM domain (S1 – S6), a positively charged voltage sensor on the S4 segment, a pore forming region between S5 and S6, and cytosolic C- and N- termini. Additionally, the C-terminus contains a cyclic nucleotide-binding domain homologous to those found in cGKs and CNG channels.

Each HCN subunit however exhibits distinct, yet overlapping, patterns of mRNA expression within the brain. HCN1 is expressed predominantly in cortical structures, with high levels observed in the hippocampus, neocortex, and cerebellum, whereas HCN3 and HCN4 are almost exclusively expressed in subcortical regions mainly concentrated in the hypothalamus and thalamus, respectively (Notomi & Shiemoto, 2004). In contrast, HCN2 is widely distributed throughout the brain, with prominent expression in the hippocampus, thalamus and neocortex (Santoro *et al.*, 1998; Ludwig *et al.*, 1998). Furthermore, the HCN subtypes exhibit substantial differences in their biophysical properties, namely in terms of their kinetics and cyclic nucleotide sensitivity (Robinson & Siegelbaum, 2003). HCN1 homotetramers show fast activation kinetics but low cyclic nucleotide sensitivity; HCN2 are slower, but

exhibit greater cyclic nucleotide sensitivity, whilst HCN4 have the slowest activation kinetics and are strongly regulated by cyclic nucleotides. HCN channels are believed to exist as tetramers, although the presence of homomeric HCN channels is insufficient to explain the properties of physiological I_h currents. Instead native channels are best described by a combination of properties of the homomeric channels. For example hippocampal pyramidal neurons co-express HCN1 and HCN2, and the I_h current in these neurons exhibit activation kinetics intermediate between those exhibited by HCN1 and HCN2 homomers (Ulens & Tytgat, 2001).

One striking feature of HCN channels is that their activity can be potentiated by the direct binding of cyclic nucleotides. HCN channel regulation by cAMP has been described in several neuronal systems, and has been implicated to play a role in a number of physiological functions, including LTP and the modulation of membrane conductance (Cuttle *et al.*, 2001; Huang & Hsu, 2003). Recently, cGMP activation of HCN channels has also been demonstrated (Zagotta *et al.*, 2003), making HCN channels a putative targets for cGMP signalling, although direct evidence for this is lacking. Exogenously applied cGMP increases I_h in nodose and trigeminal neurons (Ingram & Williams, 1996) and in the calyx of Held (Cuttle *et al.*, 2001), whilst exogenous NO modulates I_h in thalamocortical relay neurons in a manner that is mimicked by the application of 8-Br-cGMP (Pape & Mager, 1992). However, a physiological link between NO synthesis and subsequent cGMP-mediated effects on I_h has yet to be uncovered.

1.6 Functions of nitric oxide in CNS physiology

Since its discovery as a signalling molecule within the CNS, NO has attracted a wealth of attention in an effort to understand its unorthodox role in CNS physiology. One of the most striking features of NO as a central messenger is that it does not mediate direct, classical neurotransmission – that is, it does not mediate a signal from one side of a single synaptic cleft to another and evoke excitatory or inhibitory changes in membrane potential. Rather, within the CNS, NO tends to play an ancillary role, instead modulating the properties of neural cells where synaptic signalling is mediated by neurotransmitters such as glutamate and γ-aminobutyric acid (GABA).

NO has been implicated in numerous physiological functions within the CNS, which appear to impinge on nearly every aspect of neural function and dysfunction (Garthwaite & Boulton, 1995a). Roles for NO have been ascribed in the visual system (Cudeiro & Rivadulla, 1999), central control of autonomic function (Paton *et al.*, 2002), monoaminergic projection systems (Kiss, 2000), neurotransmitter release (Prast & Philippu, 2001), Ca^{2+}-signalling (Clementi & Meldolesi, 1997), synaptic plasticity (Hölscher, 1997), development of the CNS (Moreno-Lopez *et al.*, 2004), behaviour (Nelson *et al.*, 1997), and in the regulation of blood flow (Mitchell & Tyml, 1996). However, this is by no means exhaustive of all the biological roles of NO within the CNS, new ones of which are constantly being discovered. The following section focuses on three areas of NO research which are attracting a lot of interest: CNS development, acute neuronal modulation and synaptic plasticity.

1.6.1 NO and development of the CNS

NO has been implicated in three chronologically distinct steps in the development of the CNS: inhibition of proliferation and promotion of differentiation, the directionality of neurite growth, and the refinement of topographical projections.

Accumulating evidence suggests that NO physiologically regulates neurogenesis by negatively controlling the proliferation rate of undifferentiated precursors, and by facilitating the neuronal differentiation process. Proliferation of cultured immature cortical neurons was enhanced by both NOS inhibition and the application of the NO scavenger, haemoglobin, whilst application of exogenous NO had the reverse effect (Cheng *et al.*, 2003). Furthermore, in several cell types there is evidence that endogenous NO produced in response to growth factors, such as nerve growth factor (NGF) and brain-derived neurotrophic factor (BDNF), may act as a

permissive agent to restrict cell cycle progression and promote differentiation (Peunova & Enikolopov, 1995; Phung *et al.*, 1999; Rialas *et al.*, 2000; Moreno-Lopez *et al.*, 2004). In this way it appears that NO acts in a paracrine fashion, being released from nearby differentiating neurons to stop neuronal precursors from proliferating and to induce a neuronal phenotype (Cheng *et al.*, 2003). Exogenous NO has also been demonstrated in *Drosophila* to modulate the balance between cell proliferation and differentiation in developing imaginal discs, and in the embryo (Kuzin *et al.*, 1996, 2000; Wingrove & O'Farrell, 1999).

There are also several lines of evidence which indicate that NO may control neurogenesis in the vertebrate brain. NO is produced abundantly in the developing brain, and the spatiotemporal pattern of NOS expression is compatible with the possibility that NO is an anti-proliferative agent. In the developing rodent brain and spinal cord, transient increases in NOS expression correlate with the cessation of proliferation and the beginning of differentiation, and in the adult brain, NOS-positive neurons lie adjacent to, but not within, areas of adult neurogenesis (Packer *et al.*, 2003; Moreno-Lopez *et al.*, 2000). Further evidence of NO as an anti-proliferative agent comes from mice lacking nNOS which exhibit an increased number of proliferating cells and a reduction in the complexity of neuronal dendrites (Inglis *et al.*, 1998), and from eNOS knockout animals which demonstrate thicker arterial walls than their wild type siblings (Rudic *et al.*, 1998). This indicates that NO derived from both eNOS and nNOS may contribute to the control of proliferation and differentiation in the CNS. The mechanism by which NO exerts these effects, however, remains unknown. No experiment appears to have directly tested the involvement of the NO-activated GC/cGMP pathway, however immunohistochemical studies detect only low levels of NO-activated GC and cGMP in neurons prior to differentiation, which opens up the possibility that an alternative signalling pathway may be involved (Arnhold *et al.*, 2002).

The proposed role for NO in controlling the direction of neurite outgrowth is more uncertain. Studies reveal contradictory results; some demonstrate NO-induced collapse and retraction of growth cones (Gallo *et al.*, 2002; He *et al.*, 2002), whereas other groups find NO and cGMP to be attractants and act protectively against growth cone collapse (Schmidt *et al.*, 2002; Steinbach *et al.*, 2002). These apparently opposing results may be explained by the concentration of NO donors: studies utilizing high non-physiological concentrations of NO tend to observe growth cone

collapse, whereas investigations using lower concentrations, or cGMP analogues, observe growth cone attraction and protection. Evidence therefore points to a role for NO in controlling neurite outgrowth, although the physiological relevance remains unclear as only one study to date has demonstrated that blockade of endogenous NO synthesis can block neurite outgrowth (Yamazaki *et al.*, 2001).

A role for NO in the refinement of topographical projections in specific brain areas has also been suggested. The spatial and temporal expression of NOS in the chick and rodent tectum and colliculus during the period of refinement is consistent with a role in refinement (Campello-Costa *et al.*, 2000; Wu *et al.*, 2001), and blockade of NO synthesis has been demonstrated to prevent the refinement of retinotectal projections (Wu *et al.*, 2001). Transgenic eNOS/nNOS double knockout mice reveal a more diffuse ipsilateral retinocollicular projection, which nevertheless becomes more refined with age (Wu *et al.*, 2000). The organisation of the other sensory projections appears to be independent of NO and lack the gross changes in neuroanatomy and behaviour following chronic *in vivo* NOS inhibition (Contestabile, 2000).

1.6.2 NO and acute neuronal modulation

NO can influence neuronal function in an acute manner by altering membrane excitability and neurotransmitter release. The molecule has been implicated to play a role in the release of the majority of neurotransmitters including ACh (Okada *et al.*, 2001), noradrenaline (Satoh *et al.*, 1996), dopamine (Hanbauer *et al.*, 1992), glutamate (Montague *et al.*, 1994), GABA (Segovia *et al.*, 1994), serotonin (Bogers *et al.*, 1991) and ATP (Olearczyk *et al.*, 2004). Additionally, in different brain regions the same receptor may be modulated by NO in different ways via different mechanisms, presumably due to the target proteins present in the specific area.

The ability of NO to inhibit neuronal activity has been demonstrated in a number of cell types. Exogenous NO decreases peak sodium currents in nodose ganglion neurones via the enhancement of the slow inactivation of voltage-dependent sodium channels (Bielefeldt *et al.*, 1999), whilst spinally-projecting paraventricular nucleus (PVN) neurones respond to exogenous NO or increased NO synthesis by enhanced GABA release (Li *et al.*, 2002). Furthermore, it has been recently determined that the subpopulation of PVN neurons in the hypothalamus which project to the rostral ventrolateral medulla are subject to a tonic inhibition by NO, and

therefore increase their discharge rate upon inhibition of endogenous NO synthesis (Stern *et al.*, 2003).

NO has also been demonstrated to induce disinhibition via the reduction of GABAergic transmission. In the cerebellum, Golgi cells are subject to a tonic NO-dependent hyperpolarisation, possibly via large conductance Ca^{2+}-activated K^+ channels, which results in a decreased rate of GABA release from these cells (Wall, 2003a). The net effect of NO is thereby a decrease in GABAergic transmission and a subsequent disinhibition of downstream granule cell activity. A similar effect has also been reported to occur in posterior pituitary nerve terminals (Ahern *et al.*, 1999) and in the rat hippocampus where inhibition was found to be partially through the NO/cGMP pathway, and partially via an NO-dependent, but cGMP-independent, pathway (Hada *et al.*, 2003).

NO may also have a more direct effect on excitability leading to increased glutamate release (Hirsch *et al.*, 1993; Montague *et al.*, 1994; Huang *et al.*, 2003), increased Na^+ currents in striatal interneurons, increased I_h in the thalamus (Pape & Mager, 1992) and increased tonic firing in Purkinje cells (Smith & Otis, 2003).

1.6.3 NO and synaptic plasticity

The function of NO that has been most extensively studied in the CNS is the molecule's involvement in the activity-dependent changes in synaptic signal strength, commonly referred to as synaptic plasticity. The first reproducible example of synaptic plasticity was the long-term enhancement of synaptic signal strength (long term potentiation; LTP) in the rabbit hippocampus following brief periods of high frequency stimulation (HFS; Bliss & Lømo, 1973). This long-lasting activity-dependent increase in the efficacy of synaptic transmission has since been demonstrated in numerous brain regions (Garthwaite *et al.*, 1995a), and can last for hours, days or even weeks. LTP has been best characterized in the hippocampus, where it is believed to be a cellular event involved in the acquisition and storage of information (Martin *et al.*, 2000).

Hippocampal LTP is dependent on the post-synaptic activation of one class of glutamate receptor, the NMDA receptor. The NMDA receptor is unusual as it combines elements of ligand- and voltage-gated receptors – it gates in response to glutamate binding, but membrane depolarization is required in order to expel the Mg^{2+} ion which blocks the pore in the resting state. This means that the NMDA receptor

acts as a coincidence detector: only being activated when glutamate is released into the synaptic cleft and the postsynaptic membrane is depolarized. Following the activation of the NMDA receptor, there is a subsequent entry of Ca^{2+} into the post-synaptic cell leading to a cascade of intracellular events culminating in the enhancement of synaptic strength (Madison & Malenka, 1991; Malenka, 1991; Chittajallu *et al.*, 1998).

LTP is a field that comprises of many controversies. One question that has attracted a lot of interest is the relative importance of presynaptic and postsynaptic mechanisms for enhancing the efficacy of synaptic transmission in LTP. Postsynaptic changes include increased receptor density and/or increased sensitivity to neurotransmission (Edwards, 1995), whereas evidence for a presynaptic change came from the finding that there was an enhanced release of transmitters from presynaptic terminals during LTP induction (Dolphin *et al.*, 1982; Williams *et al.*, 1989; Larkman *et al.*, 1995). Given the well-established postsynaptic involvement of the NMDA receptor in LTP induction, it therefore followed that a presynaptic modification would require a retrograde signalling system from the postsynaptic terminal to the presynaptic cell. Several molecules were suggested as candidates for diffusible messengers including arachidonic acid (Williams *et al.*, 1989), NO (Gally *et al.*, 1990), carbon monoxide (Zhuo *et al.*, 1993) and platelet-activating factor (Kato *et al.*, 1994). Amongst these candidates NO received the most attention, given that NO was synthesized in neurons following NMDA receptor activation and facilitated by the physical coupling of nNOS to the NMDA receptor. The first studies to implicate NO in the establishment of LTP appeared in 1991 (Böhme *et al.*, 1991; Schuman & Madison, 1991), although investigations carried out over the subsequent decade have yielded very controversial results. Some studies demonstrated a complete block of LTP in the hippocampus following application of NOS inhibitors (Böhme *et al.*, 1991; O'Dell *et al.*, 1991; Schuman & Madison, 1991; Bon *et al.*, 1992; Doyle *et al.*, 1996), other groups observed only a partial block of LTP (Hölscher *et al.*, 1999; Gribkoff & Lum-Ragan, 1992; Chetkovich *et al.*, 1993; Haley *et al.*, 1993; Iga *et al.*, 1993; Musleh *et al.*, 1993; Boulton *et al.*, 1995), whilst others found no effect at all of NOS inhibitors (Williams *et al.*, 1993a,b; Bannerman *et al.*, 1994; Cummings *et al.*, 1994,; Murphy *et al.*, 1994). Alternative studies additionally utilized an NO scavenger, haemoglobin, which also prevented the induction of LTP (Bon *et al.*, 1992; Haley *et al.*, 1992; Schuman & Madison, 1991).

As research has progressed it has become clear that LTP can be established by multiple, independent, effector mechanisms, some of which are NO-dependent and some of which are NO-independent. It also appears the stimulation protocol utilised is of utmost importance in determining the pathway by which LTP established. For example HFS that is usually subthreshold for LTP can enhance synaptic responses when combined with exogenously applied NO (Bon *et al.*, 1992), whilst stronger HFS is able to induce forms of LTP that are insensitive to NOS inhibitors (Chetkovich *et al.*, 1993). Interestingly, there are also observations that exogenous NO is able to inhibit synaptic transmission but goes on to induce a rebound potentiation that occludes LTP (Bon & Garthwaite, 2001a). The NO-dependence of LTP has additionally been demonstrated to be affected by various experimental conditions such as temperature, animal age, or even different strains of rat (Williams *et al.*, 1993a, Hölscher *et al.*, 2002).

The reciprocal phenomenon to LTP is long term depression (LTD) of synaptic strength. LTD has been best characterised in the cerebellum, where it occurs following co-activation of parallel fibre and climbing fibre inputs to a Purkinje cell by a prolonged low frequency stimulation. LTD has been implicated in particular forms of motor learning such as adaptation of the vestibulo-ocular reflex (Nagao & Ito, 1991; De Zeeuw *et al.*, 1998). Experimental evidence has identified three common requirements for the induction of cerebellar LTD; influx of Ca^{2+} through voltage-gated Ca^{2+} channels, activation of the metabotropic glutamate receptor mGluR1, and activation of AMPA receptors (Linden *et al.*, 1993).

The participation of NO in cerebellar LTD was first proposed in 1990 (Ito & Karachot, 1990; Crepel & Jaillard, 1990), although similar to LTP, its role has been a matter of controversy for many years. It has been demonstrated by a number of different groups that LTD can be blocked by NOS inhibition or application of haemoglobin (Crepel & Jaillard, 1990; Shibuki & Okada, 1991; Daniel *et al.*, 1993), whereas application of exogenous NO or a cGMP analogue induces an LTD-like phenomena that partially occludes LTD (Shibuki & Okada, 1991; Daniel *et al.*, 1993; Lev-Ram *et al.*, 1995: but see Linden & Connor, 1992). The role of NO in LTD has been most thoroughly investigated in the cerebellum and striatum, where NO appears to be generated presynaptically, or in interneurones, and has a postsynaptic action (Daniel *et al.*, 1998, Casado *et al.*, 2002, Centonze *et al.*, 1999).

The role of NO in both the LTP and LTD phenomena suggests that NO may be physiologically important in the regulation of metaplasticity within the brain, acting to fine tune synaptic responses to even subtle changes in external conditions.

1.7 Nitric oxide signalling in the hippocampus

The hippocampus is one of the most thoroughly studied regions of the mammalian CNS, named after its highly unusual and distinctive shape which resembles a seahorse (in Greek *hippo* means "horse" and *kampos* means "sea monster"; figure 1.11). The hippocampus is also sometimes referred to as the Ammon's horn due to its resemblance to a ram's horn (the Egyptian god, Ammon, had ram's horns).

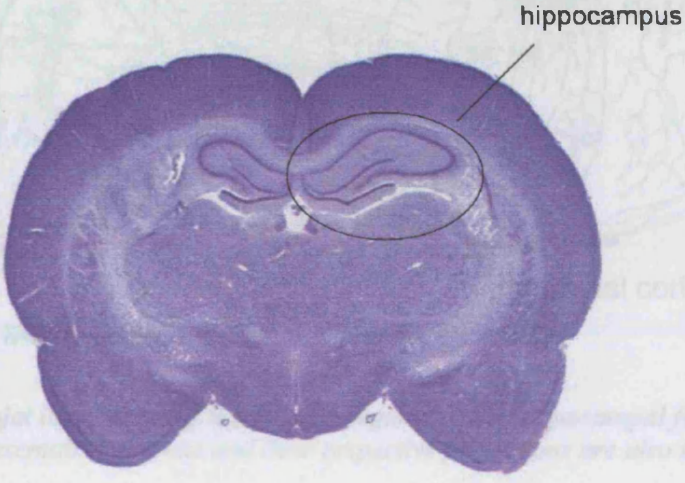

Figure 1.11 Nissl-stained transverse section through the rat brain.
The hippocampus can be observed below the cortex, with the dark layers containing stained cell bodies.

The hippocampus is one of a group of structures within the limbic system typically referred to as the hippocampal formation. This structure can be divided into the dentate gyrus, the hippocampus, the subiculum, presubiculum and parasubiculum, and the entorhinal cortex. The dentate gyrus, hippocampus and subiculum have a single cell layer with less cellular or acellular layers located above and below it. The other parts of the hippocampal formation have several layers to them. The hippocampus and dentate gyrus are highly laminated structures, with both the neuronal cell bodies and zones of connectivity arranged in orderly layers, and therefore have been the target of many neuroanatomical and electrophysiological studies. The various regions of the hippocampal formation are illustrated in figure 1.12.

The hippocampus is a region which has generated a lot of scientific interest over the years since it was recognised in the early 1950s to play a fundamental role in some forms of learning and memory. In a landmark paper by Scoville & Milner (1957), a patient known only by his initials, H.M., underwent bilateral hippocampal removal for treatment of intractable epilepsy. The result of the operation was alleviation of the epilepsy, however H.M. was additionally left with a permanent loss of the ability to form new long-term declarative memories.

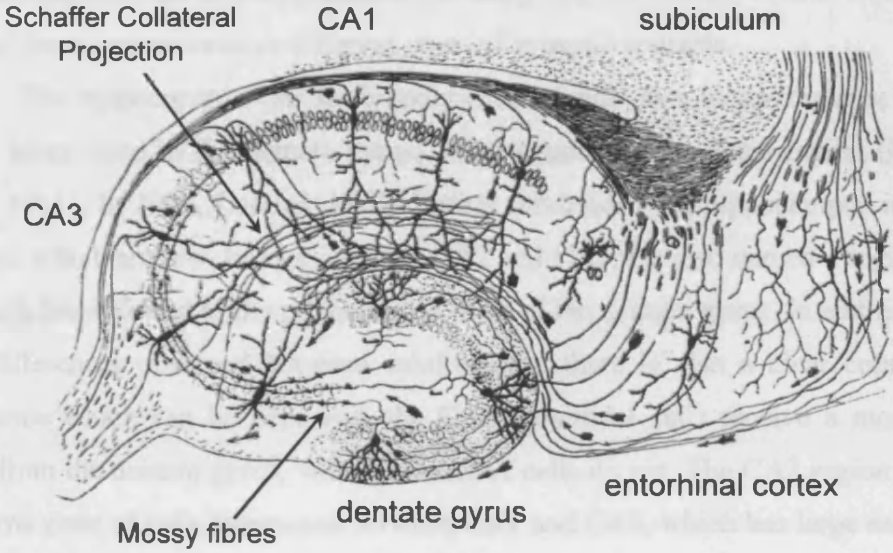

Figure 1.12: Cajal illustration of the various regions of the hippocampal formation (1901). *Representative neurons and their respective projections are also shown.*

1.7.1 Hippocampal anatomy

Dentate gyrus

The dentate gyrus consists of three layers: the principal (or granule) cell layer, the largely acellular molecular layer that is located above the granule cell layer, and the diffusely cellular polymorphic cell layer (or hilus) located below the granule cell layer. Granule cells are arranged 4 – 6 cells thick with dendrites extending perpendicularly into the molecular layer where they receive synaptic connections which will be discussed in 1.7.2. The axons of the granule cell are known as mossy fibres, and originate from the basal portion of the cell body extending into the polymorphic cell layer. The mossy fibres then synapse onto some of the neurons, such as mossy cells, in the polymorphic cell layer before coalescing into a bundle of fibres that enters the stratum lucidum of CA3. The polymorphic cells are of various types, but they only project to other regions of the dentate gyrus.

Hippocampus

The hippocampus also has a principle cell layer known as the pyramidal cell layer. Hippocampal pyramidal neurons are arranged 3 – 6 cells thick, with elaborate dendritic trees extending perpendicularly to the cell layer in both directions. The apical dendrites are longer than the basal dendrites, extending towards the centre of the hippocampus traversing three distinct regions: the stratum lucidum, the stratum radiatum, and the stratum lacunosum-moleculare (figure 1.13). The basal dendrites extend from the base of the pyramidal cell body into the stratum oriens. Dendrites in each of these regions receive different types of synaptic contacts.

The hippocampus can be broadly divided into two major regions; a large-celled layer close to the dentate gyrus, and a smaller-celled distal region (Ramon *y* Cajal, 1911). In 1934, Lorente de Nó further subdivided the hippocampus into three regions, which are now known as CA1, CA2 and CA3. He also named a region CA4, although this referred to the polymorphic layer of the dentate gyrus. In addition to the size differences observed between subdivisions, there is also a clear connectional difference which can be observed: the CA3 pyramidal cells receive a mossy fibre input from the dentate gyrus, whereas the CA1 cells do not. The CA2 region refers to a narrow zone of cells interposed between CA1 and CA3, which has large cell bodies like CA3, but does not receive mossy fibre innervation like CA1.

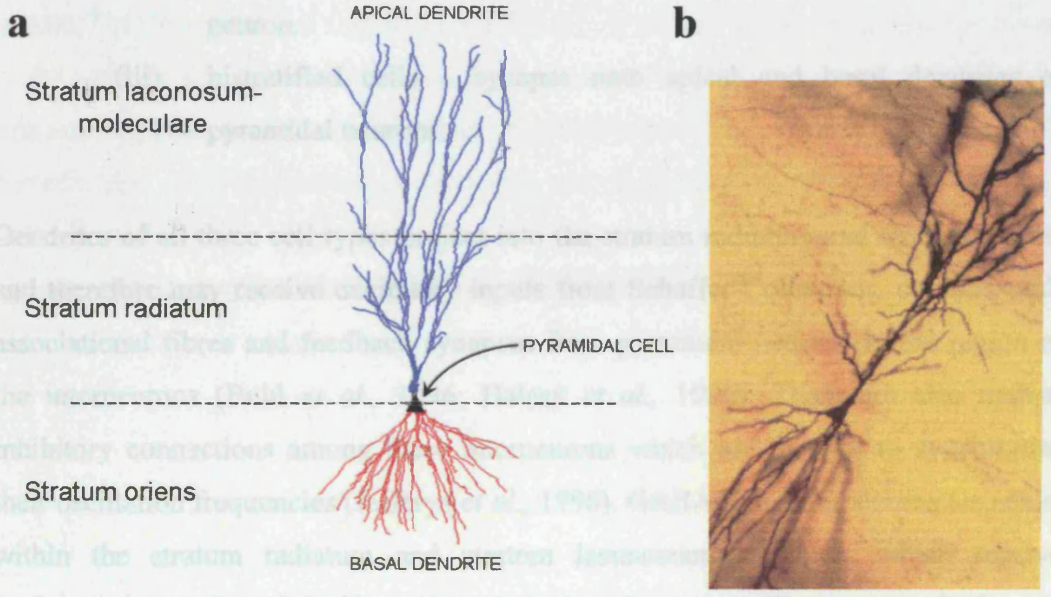

Figure 1.13: CA1 hippocampal neuron *(A) Optical trace of hippocampal CA1 neuron (adapted from www.krasnow.gmu.edu/alexei/cinema). (B) Golgi stain of hippocampal CA1 neuron (www. synapses.mcg.edu).*

Interneurons

The vast majority of interneurons within the dentate gyrus and hippocampus have local target regions, lack spines and are GABAergic. The most prominent interneuron in the dentate gyrus is the pyramidal basket cell, the cell bodies of which are typically located at the border between the granule cell layer and the polymorphic cell layer. There are at least five different types of basket cell (Ribak & Seress, 1983), and the axons from these neurons innervate the cell bodies of granule cells. Interneurons can also be found in the molecular layer and the polymorphic cell layer of the dentate gyrus. One interesting class of interneuron found in the polymorphic layer is called the mossy cell. These are excitatory neurons that project only to the molecular layers of the dentate gyrus both ipsilaterally and contralaterally, and tend to project to distant septotemporal levels of the dentate gyrus rather than locally.

Interneurons in the hippocampus have cell bodies in or near the pyramidal cell layer and can be classified into three groups on the basis of their synaptic targets:

(i) axo-axonic cells – synapse onto the initial segment of pyramidal neurons, thereby exerting a strong control over action potential initiation.

(ii) basket cells – synapse onto the somata of pyramidal neurons. One basket cell can make multiple contacts onto a single pyramidal neuron.

(iii) bistratified cells – synapse onto apical and basal dendrites of pyramidal neurons.

Dendrites of all three cell types project into the stratum radiatum and stratum oriens, and therefore may receive excitatory inputs from Schaffer-Collaterals, commissural-associational fibres and feedback synapses from pyramidal neurons in the region of the interneurons (Buhl *et al.*, 1996; Halasy *et al.*, 1996). There are also mutual inhibitory connections among these interneurons which are thought to synchronize their oscillation frequencies (Jefferys *et al.*, 1996). GABAergic interneurons also exist within the stratum radiatum and stratum lacunosum-moleculare which receive excitatory inputs from Schaffer collaterals and perforant path fibres, respectively, and synapse onto pyramidal neuron dendrites in various regions.

1.7.2 Synaptic connections within the hippocampal formation

Most sensory information reaches the hippocampus via the entorhinal cortex. Neurons located in layer II of the entorhinal cortex give rise to a pathway, the perforant path, which projects through the subiculum and terminates in a laminar pattern in both the dentate gyrus and in the CA3 region of the hippocampus. Neurons located in layer III of the entorhinal cortex do not project to the dentate gyrus or CA3, but instead project to CA1 and the subiculum. In this case, the projection is organised in a topographical fashion.

The dentate gyrus is the next step in the progression of connections through the hippocampal formation, and it gives rise to the mossy fibres that terminate on the proximal dendrites of the CA3 pyramidal cells. The granule cells also synapse onto cells of the polymorphic layer, which provides association connections to other levels of the dentate gyrus. The CA3 pyramidal cells, in turn, project heavily to other levels of CA3, as well as to the CA1. The projection from CA3 to CA1 is typically called the Schaffer Collateral projection. Each CA3 neuron is capable of making contact with numerous CA1 neurons (for example one CA1 neuron may be innervated by more than 5000 ipsilateral CA3 cells). CA1 pyramidal cells, unlike those from the CA3 make few connections within CA1, but instead give rise to connections which extend to both to the subiculum and to the deep layers of the entorhinal cortex. The subiculum additionally originates a projection to the deep layers of the entorhinal cortex. The deep layers of the entorhinal cortex, in turn, originate projections to many of the same cortical areas that originally projected to the entorhinal cortex. In this way information entering the entorhinal cortex from a particular cortical area is able to traverse the entire hippocampal circuitry, and ultimately be returned to the same cortical area from which it originated. Figure 1.14 summarises the synaptic connections made within the hippocampal formation.

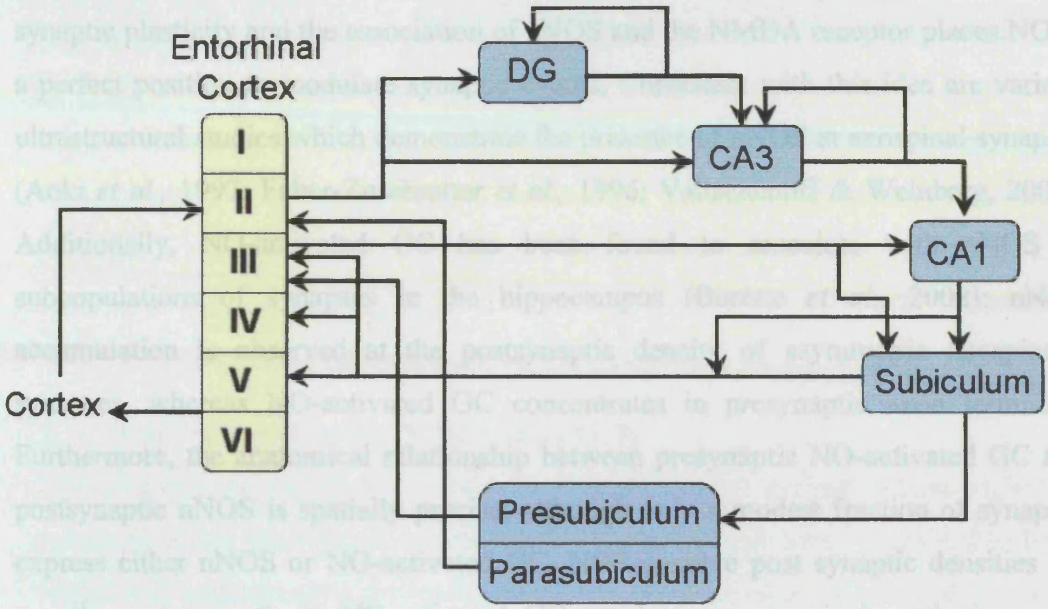

Figure 1.14: Major intrinsic connections in the hippocampal formation.
(Adapted from Johnston & Amaral, 1998)

1.7.3 Localisation of NO within the hippocampus.

Dramatic variations in immunoreactivity occur throughout the rat brain. In the adult hippocampus, nNOS staining was originally thought to be largely confined to a subpopulation of GABA-containing interneurons in the CA1 region (Bredt *et al.*, 1991; Valtschanoff *et al.*, 1993; Lumme *et al.*, 2000). Increasing evidence also describes limited nNOS expression in CA1 pyramidal cells (Endoh *et al.*, 1994; Wendland *et al.*, 1994; Blackshaw *et al.*, 2003), and dendritic spines (Burette *et al.*, 2002) when obtained by weak fixation. Some laboratories have failed to reproduce this finding, although this can likely be explained by the potential cross reactivity of the antibodies, the method of fixation, and the differing antibody incubation time required to stain interneurons and pyramidal cells. In order achieve optimal staining for interneurons, the reaction must be stopped before it would reveal any trace of nNOS in pyramidal cells. Therefore it is possible that the absence of nNOS staining observed by certain groups reflects lower levels of nNOS expression and insufficient time of incubation with antibodies, rather than complete lack of presence.

As discussed previously, biochemical investigations reveal an association of nNOS with PSD-95, together forming a complex with the NMDA receptor (Brenman

et al., 1996a; Christopherson *et al.*, 1999). The importance of the NMDA receptor in synaptic plasticity and the association of nNOS and the NMDA receptor places NO in a perfect position to modulate synaptic events. Consistent with this idea are various ultrastructural studies which demonstrate the presence of nNOS at axospinal synapses (Aoki *et al.*, 1997; Faber-Zuschratter *et al.*, 1996; Valtschanoff & Weinberg, 2001). Additionally, NO-activated GC has been found to associate with nNOS at subpopulations of synapses in the hippocampus (Burette *et al.*, 2002): nNOS accumulation is observed at the postsynaptic density of asymmetric axospinous synapses, whereas NO-activated GC concentrates in presynaptic axon terminals. Furthermore, the anatomical relationship between presynaptic NO-activated GC and postsynaptic nNOS is spatially precise; although only a modest fraction of synapses express either nNOS or NO-activated GC, NOS-positive post synaptic densities are usually post synaptic to NO-activated GC-positive axon terminals and vice versa (Burette *et al.*, 2002).

In contrast to nNOS, eNOS expression appears to be restricted to the vascular endothelium (Seidel *et al.*, 1997; Stanarius *et al.*, 1997; Töpel *et al.*, 1998), although there are a few reports that eNOS may also be present in CA1 pyramidal neurons (Dinerman *et al.*, 1994a; Doyle & Slater, 1997). Physiologically, NO produced from endothelial cells has been demonstrated to contribute to the maintenance of cerebral blood flow via the regulation of small artery and ateriolar tone (Umans & Levi, 1995; Wolf, 1997). However, capillaries lack smooth muscle cells (and therefore NO-activated GC). Instead in these blood vessels NO has been shown to attenuate the expression of intracellular adhesion molecule-1 (ICAM-1) and vascular cell adhesion molecule-1 (VCAM-1) *in vitro* (Biffl *et al.*, 1996; Takahashi *et al.*, 1996). It has therefore been suggested that NO has the ability to modify capillary blood flow by modulating local haemoconcentration and leukocyte adhesion, thereby increasing microvascular blood flow (Mitchell & Tyml, 1996). Additionally, NO has been demonstrated to alter the microvascular permeability in the intact and inflamed vasculature (Kubes, 1995), and consequently affect the blood brain barrier (Shukula *et al.*, 1996).

1.8 General aim of the study

NO is an important signalling molecule throughout the entire body, where the three 'classical' NO-mediated functions are smooth muscle relaxation, platelet aggregation and neurotransmission. Within the CNS, the function of NO that has been most extensively studied is the molecule's involvement in synaptic plasticity. The aim of my research was to further characterize the role that NO plays in hippocampal synaptic plasticity, focussing in particular on two important questions as described below:

i. Does NO regulate the NMDA receptor?

The principle physiological receptor for NO is guanylyl cyclase, whose activation results in cGMP formation. An alternative transduction pathway perceived to be of widespread importance is the modification of protein function by nitrosation of thiol groups. A prototypic protein that is considered to be regulated in this way is the NMDA receptor, the result of which is an inhibition of receptor function. Physiologically, this would represent an important negative feedback mechanism. However, despite extensive research, there is little direct evidence that NO regulates NMDA receptor function. The aim of this study was to directly investigate the effect of NO on native and cloned NMDA receptors in hippocampal slices and HEK-293 cells, respectively, using electrophysiological techniques.

ii. Which isoform of NOS is involved in hippocampal synaptic plasticity?

One form of synaptic plasticity that has attracted much attention over the past decade is LTP. NO has been implicated in LTP in the CA1 region of the hippocampus, although there is a longstanding debate as to which isoform of NOS is responsible. Both constitutive isoforms have been demonstrated to be present in the hippocampus, although due to the absence of selective NOS inhibitors pharmacological studies have not yet been able to resolve this issue. Genetic knockout studies of one or both of the NOS isoforms present in the hippocampus have been created, but have yielded contradictory results. The aim of this study was to further investigate which isoform of NOS mediates the involvement of NO in LTP using transgenic mice lacking eNOS using a combination of electrophysiological, biochemical, and molecular biological techniques.

Chapter 2

General Materials and Methods

2.1 Chemicals and reagents

Table 2.1 summarises the actions and source of all the pharmacological compounds utilised in the following chapters; all other standard chemicals were purchased from Sigma Aldrich unless otherwise stated.

Compound	Action	Source Company
1400W	iNOS inhibitor	Calbiochem
Acetylcholine	Cholinergic neurotransmitter	Sigma Aldrich
ω-Agatoxin IVA	P/Q Ca^{2+}-channel antagonist	Tocris Cookson
(+)-AJ 76	Dopamine antagonist	Tocris Cookson
AM 251	Cannabinoid antagonist	Tocris Cookson
L-arginine	NOS substrate	Sigma Aldrich
Atropine	Muscarinic antagonist	Sigma Aldrich
BAY 41-2272	Enhancer of NO-activated GC	Sigma Aldrich
Benzoquinonium	Nicotinic antagonist	Tocris Cookson
Bradykinin	eNOS stimulator	Sigma Aldrich
ω-Conotoxin GVIA	N-type Ca^{2+} channel antagonist	Tocris Cookson
ω-Conotoxin MVIIC	N/P/Q Ca^{2+}-channel antagonist	Tocris Cookson
CNQX	Kainate/AMPA antagonist	Tocris Cookson
D-AP5	NMDA antagonist	Tocris Cookson
DEA/NO	NO donor	Alexis Biochemicals
DPCPX	Adenosine antagonist	Tocris Cookson
EHNA	PDE2 antagonist	Sigma Aldrich
IBMX	General PDE antagonist	Sigma Aldrich
Ketamine	NMDA antagonist	Alexis Biochemicals
L-NIO	General NOS inhibitor	Alexis Biochemicals
L-NNA	General NOS inhibitor	Tocris Cookson

LY294002	PI3-K inhibitor	Sigma Aldrich
MCPG	mGluR antagonist	Tocris Cookson
Methysergide	5HT-antagonist	Tocris Cookson
Mibefradil	T-type Ca^{2+}-channel antagonist	Sigma Aldrich
Naloxone	Opioid antagonist	Tocris Cookson
NBQX	AMPA antagonist	Tocris Cookson
Nicergoline	General α agonist	Tocris Cookson
Nickel	R/T-type Ca^{2+} channel antagonist	Sigma Aldrich
Nifedipine	L-type Ca^{2+} channel antagonist	Sigma Aldrich
NMDA	NMDA receptor agonist	Sigma Aldrich
NPA	nNOS inhibitor	Alexis Biochemicals
ODQ	NO-activated GC inhibitor	Sigma Aldrich
Picrotoxin	$GABA_A$ antagonist	Sigma Aldrich
Potassium pentachloronitrosylruthenate	Caged NO donor	Alfa Aesar
Phenylmethylsulphonyl fluoride	Serine protease inhibitor	Roche
Raloxifene	eNOS stimulator	Sigma Aldrich
Scopolamine	General muscarinic antagonist	Tocris Cookson
SNX-482	R-type Ca^{2+} channel antagonist	Tocris Cookson
Sotalol	General β antagonist	Tocris Cookson
Superoxide dismutase (SOD)	Superoxide scavenger	Sigma Aldrich
Tumour Necrosis Factor alpha	eNOS stimulator	Promega
Tetrodotoxin (TTX)	Na^+ channel blocker	Sigma Aldrich
Urate	NO_2 scavenger	Sigma Aldrich
Vinyl L-NIO	nNOS inhibitor	Alexis Biochemicals
Wortmannin	PI3-K inhibitor	Sigma Aldrich

Table 2.1: Pharmacological compounds utilised, including their biological actions and source.

2.2 Hippocampal slice preparation

Hippocampal slices were prepared from 6 to 8-week-old male Sprague-Dawley rats (Charles River, Margate, UK). The animals were killed humanely according to the Scientific Procedures (1986) Act by way of stunning followed by cervical dislocation and decapitation. The brain was rapidly removed, the hippocampus dissected out (figure 2.1), and placed in cold (0 - 4 °C) artificial cerebrospinal fluid (ACSF) of the following composition (in mM): NaCl 124, KCl 3, NaH_2PO_4 1.25, $MgSO_4$ 1, $NaHCO_3$ 26, $CaCl_2$ 2, D-glucose 10, equilibrated with 95 % O_2 and 5 % CO_2. Transverse slices (400 μm thick) were cut using a Vibrotome ® Series 100 Sectioning system (Technical Products International Inc, St Louis, USA), and maintained in an interface holding chamber containing ACSF at room temperature (22 – 24 °C) for at least 1 h before use.

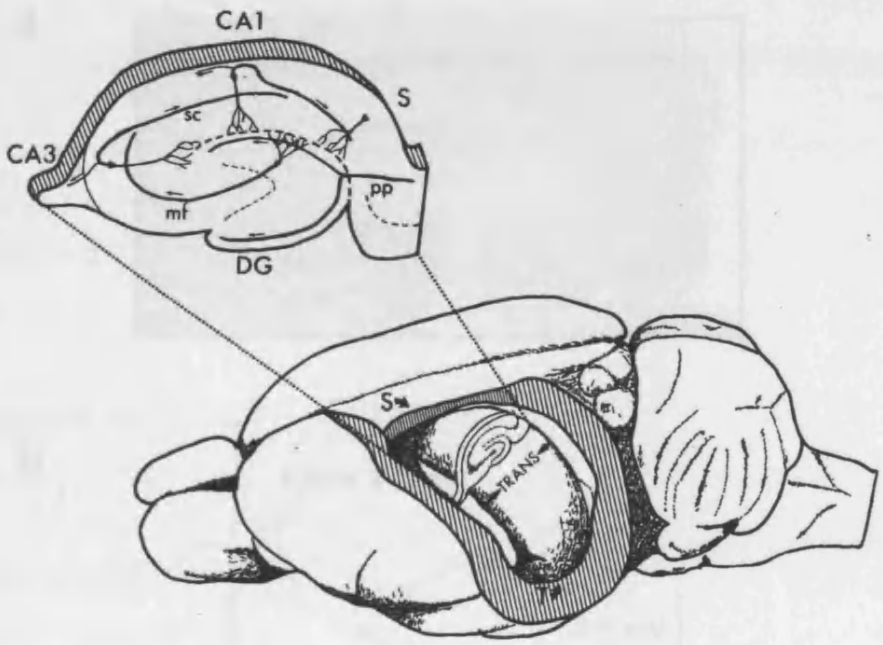

Figure 2.1: Line drawing illustrating the location of the hippocampus within the rat brain *(Johnson & Amaral, 1998).*

2.3 Electrophysiological recordings from hippocampal slices

Extracellular recordings of field excitatory postsynaptic potentials (fEPSPs) were made from the stratum radiatum of the CA1 area of the hippocampus following electrical stimulation (baseline frequency = 0.033 Hz) of the Schaffer Collateral-commissural pathway. Field EPSPs were made at either at room temperature or at 30 °C in a submerged recording chamber. Figure 2.2 illustrates (a) the position of the stimulating (Harvard apparatus Ltd, Kent, UK) and recording electrodes (typical pipette resistance 2 – 4 MΩ), and (b) the resultant synaptic response following stimulation. Slope measurements were made by linear regression (pClamp6/8) during the initial linear phase of each evoked fEPSP (20 – 50 % of the peak), and the values were normalized relative to the mean values obtained within the first 10 or 15 min of recording in the absence of any treatment.

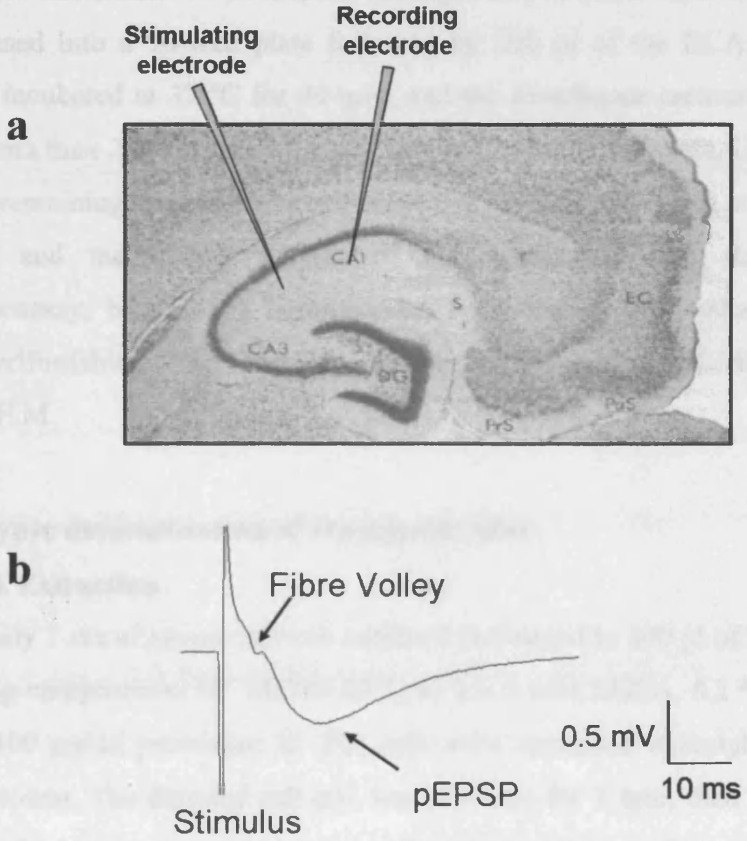

Figure 2.2: Stimulation and response of CA1 pyramidal neurons.
(a) Nissl-stained horizontal section through the rat hippocampus. The position of the recording and stimulating electrodes are indicated. The subiculum (S), presubiculum (PrS), parasubiculum (PaS) and entorhinal cortex (EC) are also illustrated (Adapted from Johnson & Amaral, 1998). (b) Synaptic response in the CA1 stratum radiatum in response to stimulation of the Schaffer collaterals. Population excitatory post synaptic potential (pEPSP).

2.4 cGMP measurement

Hippocampal slices were allowed to recover in carbogenated ACSF maintained in a shaking water bath for 1 - 2 h before use (at room temperature or 30 °C). The slices were then transferred to a fresh solution containing the non-specific PDE inhibitor 3-isobutyl-1-methylxanthine (IBMX; 1 mM) or the PDE2 inhibitor erythro-9-(2-hydroxy-3-nonyl)-adenine hydrochloride (EHNA; 300 μM) for 15 min. At the end of the exposure the slices were removed, inactivated by immersion in boiling hypotonic inactivation buffer (50 mM Tris, 4 mM EDTA, pH 7.4) for a minimum of 5 min, and homogenized by sonication.

The protein content of each sample was determined using the bicinchoninic acid (BCA) method (Pierce Rockford, IL, USA) with bovine serum albumin as standard. The assay is based on the reduction of Cu^{2+} to Cu^{+} in the presence of protein under alkaline conditions. 10 μl aliquots (in triplicate) of either standards or samples were dispensed into a 96-well plate followed by 200 μl of the BCA reagent. The plates were incubated at 37 °C for 30 min, and the absorbance measured at 562 nm using a Spectra max 250 spectrometer (Molecular Devices, California, USA).

The remaining samples were centrifuged at 10,000 g for 5 min at 4 °C to pellet the debris, and the cGMP content of the supernatant was determined by radioimmunoassay, based on a commercially available kit (Amersham Pharmacia Biotech, Hertfordshire, UK). Results are expressed as mean cGMP content/mg protein ± S.E.M.

2.5 Genotypic determination of transgenic mice

2.5.1 DNA Extraction

Approximately 1 cm of mouse tail was removed and added to 500 μl of lysis buffer of the following composition: 0.1 M Tris-HCl pH 8.5, 5 mM EDTA, 0.2 % SDS, 0.2 M NaCl, and 100 μg/ml proteinase K. The tails were incubated overnight at 55 °C to digest the protein. The digested tail mix was vortexed for 1 min, then centrifuged at 14,000 g for 10 min at room temperature. The supernatant was decanted into a fresh eppendorf, and 500 μl isopropenol was added. Each eppendorf was slowly inverted several times until a white precipitate was observed (deoxyribonucleic acid; DNA), then centrifuged for 2 min at 14,000 g. The supernatant was removed, and the pellet was washed twice with 500 μl 70 % EtOH. The pellet was left to dry at 37 °C

overnight, then re-suspended in 100 µl ddH_2O. The DNA was stored at - 20 °C until use.

2.5.2 Polymerase chain reaction (PCR)

The genotype of each sample was determined by the PCR technique of DNA amplification. PCR amplifications were carried out using the Promega PCR system according to the manufacturer's recommendations. In summary, 25 µl reactions were set up in 200 µl PCR tubes with 1 µl of each primer (Sigma Genosys; table 2.2), 200 µM PCR nucleotide mix (dNTPs; Promega), 0.75 U of *Taq* DNA Polymerase (Promega), 1 X PCR buffer (Promega) and 1 µl of mouse genomic DNA (purified as in 2.5.1). The optimum $MgCl_2$ concentration was determined using increasing $MgCl_2$ concentrations from 0 to 4 mM to be 1.5 mM.

PRIMER	Sequence 5'-3'	Concentration
eNOS-FOR	GGTGTTTGGCTGCCGATGC	2 pmol/µl
eNOS-REV	GCACAGCACACGGTGAACC	2 pmol/µl
NEO-FOR	GCATACGCTTGATCCGGCTACC	1.5 pmol/µl
NEO-REV	GAAGGCGATGCGCTGCGAATC	1.5 pmol/µl

Table 2.2: Primers used for PCR determination of mouse genotype.

Samples were briefly vortexed and PCR reactions were carried out in a thermocycler machine (MWG-Biotech Primus 96 plus). Samples were denatured at 94 °C for 5 min, followed by 35 cycles of PCR: melting the template at 94 °C for 1 min, annealing at 55 °C for 1 min and extending the DNA segment at 72 °C for 1 min. This was followed by 7 min at 72 °C in order to allow extension of DNA fragments to be completed. All runs included a negative control, where instead of mouse genomic DNA ddH_2O was used. Positive control DNA (wild type DNA) was also included in all PCR amplification runs. PCR products were stored at 4 °C until further use.

2.5.3 Agarose gel electrophoresis

DNA fragments were separated by electrophoresis on 1.5 % agarose gels. Agarose gels were prepared by melting 1.5 g of agrose (Invitrogen) in 100 ml of Tris-Acetate-EDTA (TAE) buffer (containing 0.8 mM Tris, 20 µM ethylenediaminetetraacetic acid (EDTA), pH 8.0, 1.1 % (v/v) glacial acetic acid) in a microwave until the agarose was melted. Ethidium bromide (2.5 µl/100 ml; Sigma Aldrich) was added to the molten gels and mixed. Gels were poured into the casting trays of a horizontal electrophoresis tank (Wide mini-sub ® cell GT; Bio-Rad) with the appropriate combs inserted. Gels were allowed to set and TAE buffer was added to cover the gel.

10 µl of 1 kb Plus DNA ladder (Invitrogen) was added to 16.7 µl gel loading dye (6 X concentrate; Type 1; Sigma Aldrich) and 72.3 µl ddH_2O. DNA ladder/dye mix (5 µl) was loaded into the first well in each gel using a micropipette. DNA samples (13.5 µl) were mixed with 1.5 µl of gel loading buffer (10 X loading dye; 0.42 % xylene cyanol FF (Sigma Aldrich), 50 % glycerol) and then loaded into the remaining wells. For each experiment, positive and negative controls were always run. Agarose gels were electrophoresed at a constant voltage of 100 V for 30 – 45 min. Gels were stopped when the bromophenol blue and the xylene cyanol dyes had separated ~ 1 – 2 cm. DNA bands were visualized under UV light using Chemi-imager 4400 v 5.1.

Chapter 3

Regulation of the NMDA receptor by nitric oxide

3.1 Introduction

The NMDA receptor has been extensively studies during the past decade because of its implication in many physiological processes. Physiological activation of NMDA receptors, and the subsequent Ca^{2+} entry into neurones, has been associated with critical processes as diverse as neuronal development, mediation of excitatory neurotransmission and synaptic plasticity. However, excessive activation of the NMDA receptor leads to altered Ca^{2+} homeostasis, and can be shown to contribute to neuronal cell death in a variety of acute and chronic neurological disorders including epilepsy, stroke and head trauma (Choi, 1988; Meldrum & Garthwaite, 1990; Köhr *et al.*, 1993). Precise regulation of NMDA receptor activity is therefore critical to normal brain function, as well as to the avoidance of neuronal damage and death; accordingly there are several endogenous mechanisms for receptor modulation (Dingledine *et al.*, 1999). Given the well-established involvement of the NMDA receptor in the generation of NO in response to activation of the NMDA receptor (as described in the general discussion; 1.3), it therefore followed that NO may be a potential contender for its modulation.

The best-known pathway for NO signal transduction is through NO–activated GC, whose activation results in the intracellular accumulation of cGMP (Denninger & Marletta, 1999; Friebe & Koesling, 2003). As described in the general introduction (section 1.5), subsequent binding of cGMP to protein kinases, ion channels, PDEs, and other proteins translates NO signals into long- and short-term functional alterations. Of these targets cGK provides the broadest means of controlling ion-channel function, with virtually every type of ion channel containing cGK consensus phosphorylation sites (White *et al.*, 1999).

An alternative route for NO signal transduction that has been perceived to be of widespread importance is the chemical modification of protein function by the transfer of the NO moiety to protein thiol groups (Ahern *et al.*, 2002, Stamler *et al.*, 2001). The NMDA receptor, present in most brain synapses, is a classical example of a protein allegedly regulated by *S*-nitrosation (Stamler *et al.*, 2001; Ahern *et al.*, 2002; Lipton *et al.*, 2002), the result of which being an inhibition of receptor function that reverses only slowly (Choi *et al.*, 2000), if at all (Murphy & Bliss, 1999). Figure 3.1 summarizes the actions of NO in the CNS.

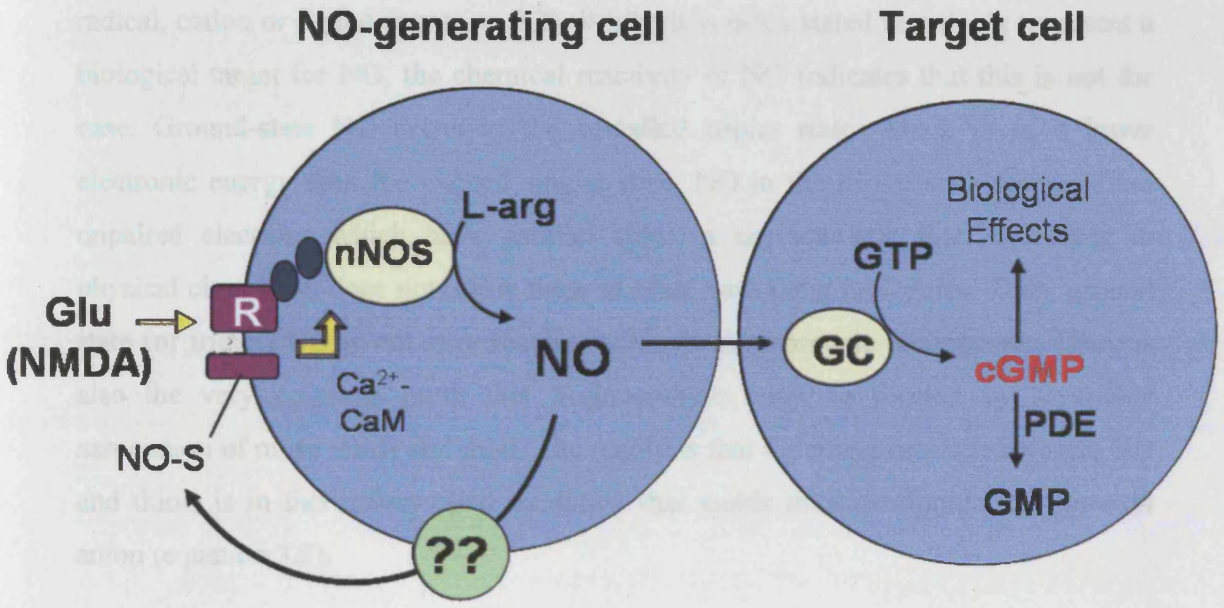

Figure 3.1: Actions of NO in the CNS.
The best-known pathway by which NO acts is via activation of NO-activated GC. An alternate pathway by which NO has been proposed to act is via the S-nitrosation of thiol groups at cysteine residues, however the mechanism by which this may occur is unclear.

Although the transfer of the NO-moiety to protein thiol groups is commonly referred to as *S*-nitros*yl*ation, the correct term for this process is *S*-nitrosation (Koppenol, 2002). Transnitrosation refers to the transfer of bound NO from one thiol group to another (including the reversible blockade of critical thiol groups in enzymes; equation 3.1).

S-nitrosation

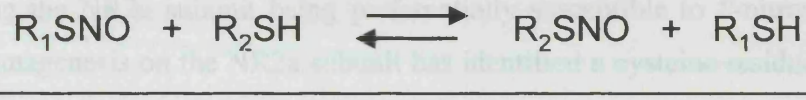

Equation 3.1: Mechanism for S-nitrosation.
Transfer of bound NO from one thiol group to another, with R being protein or peptide in nature.

In contrast, *S*-nitros*yl*ation refers to the direct action of NO that is either a radical, cation or ligand (equation 3.2). Whilst it is often stated that thiols represent a biological target for NO, the chemical reactivity of NO indicates that this is not the case. Ground-state NO exists in the so-called triplet state, which is of a lower electronic energy than the excited singlet state. NO in the triplet state contains two unpaired electrons which have parallel spins, a characteristic that, according to physical chemistry, does not allow them to react with most molecules. Thus, ground state (or triplet) NO is not very reactive towards most organic compounds. There is also the very common myth that *S*-nitrosothiols may be formed by reversible association of nitric oxide and thiol. The reality is that the direct reaction between NO and thiols is in fact a very slow oxidation that yields thiol disulphide and nitroxyl anion (equation 3.2).

S-nitrosylation

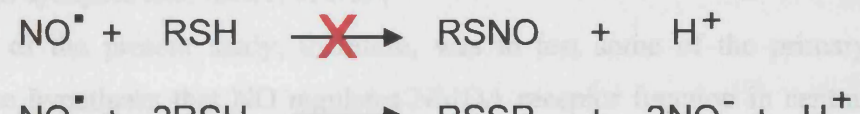

Equation 3.2: Mechanism for S-nitrosylation.
Direct reaction between NO and RSH is a very slow oxidation that yields thiol disulphide and the nitroxyl anion

NMDA receptors are composed of at least four subunits surrounding a central, water-filled pore. Functional NMDA receptors contain both NR1 and NR2 subunits, those containing the NR2a subunit being preferentially susceptible to *S*-nitrosation. Site-directed mutagenesis on the NR2a subunit has identified a cysteine residue (Cys 399) that is critical for this modification (Choi *et al.,* 2000). Functionally, the inhibitory effect of NO has been viewed either a negative feedback mechanism serving to protect against neuronal damage that can result from over-activation of NMDA receptors, or as a device that regulates the susceptibility of synapses to undergo plastic changes (Lei *et al.,* 1992; Manzoni *et al.,* 1992; Murphy & Bliss, 1999).

Despite the status accorded by some commentators to *S*-nitrosation as a physiological regulatory mechanism (Stamler *et al.,* 2001; Ahern *et al.,* 2002; Lipton *et al.,* 2002), numerous fundamental issues remain outstanding. For example, without a catalyst, NO cannot simply attach to thiol groups (Hogg, 2002), so it is unclear how such a chemical modification would occur. Also, many of the experiments leading to the idea that NMDA receptors are regulated by NO have relied on the indirect measurement of changes in cytosolic free Ca^{2+} (Lei *et al.,* 1992; Manzoni *et al.,* 1992; Tanaka *et al.,* 1993; Choi *et al.,* 2000), which could be affected by NO independently of any action on the NMDA receptor (Hoyt *et al.,* 1992). Finally, and most importantly, there have been very few studies that have examined the effect of NO on NMDA receptors in their normal synaptic location, the exception being those of Murphy *et al.* (1994) and Murphy & Bliss (1999) who found that photolysis of a caged NO derivative caused an enduring inhibition of NMDA receptor function in CA1 hippocampal synapses and, hence, of LTP.

The aim of the present study, therefore, was to test some of the primary predictions of the hypothesis that NO regulates NMDA receptor function in central synapses. The role of endogenous and exogenous NO in synaptic function will be investigated on native or cloned NMDA receptors, in acute rat hippocampal slices and HEK-293 cells respectively. This will then be discussed in relation to the potential physiological role of NO in the regulation of NMDA receptor function.

3.2 Methods

3.2.1 Tissue preparation

Hippocampal slices were prepared as described in chapter 2 (2.2).

3.2.2 Electrophysiological recordings

Extracellular recordings of field excitatory postsynaptic potentials (fEPSPs) were made from the stratum radiatum of the CA1 area of the hippocampus following electrical stimulation (baseline frequency = 0.033 Hz) of the Schaffer collateral-commissural pathway at room temperature (~ 24 °C). NMDA receptor-mediated responses were isolated pharmacologically using nominally Mg^{2+}-free ACSF containing 10 μM 6-cyano-7-nitroquinoxaline-2,3-dione (CNQX) to block AMPA receptors. D(-)-2-amino-5-phosphonopentanoate (D-AP5) was added to confirm that the responses were NMDA receptor-mediated. AMPA receptor-mediated responses were obtained in normal ACSF. Photolysis of caged NO (potassium pentachloronitrosylruthenate, $K_2Ru(NO)Cl_5$; Alfa Aesar, Karlsruhe, Germany) was performed using the 1 ms discharge from a xenon arc bulb (Zeiss) transmitted through a fibre optic, and filtered with a UG11 filter (270 – 370 nm). Stock solutions of the NONOate NO donor, diethylamine/NO adduct (DEA/NO) were made up in 10 mM NaOH and diluted at least 1:100 into the ACSF solution. Separate slices were used for each DEA/NO concentration tested. Slope measurements were made during the initial linear phase of each evoked potential (20 - 50% of the peak), and the values were normalised relative to the mean values obtained within the first 10 or 15 min of recording in the absence of any treatment.

Whole-cell current-clamp recordings were made from CA1 hippocampal cells at room temperature using an Axoclamp 2A (Axon Instrument, Foster city, CA). Typical pipette resistance was 2 - 4 MΩ. Pipette solutions contained (in mM): $KMeSO_4$ 150, KCl 10, HEPES 10, NaCl 4, Mg_2ATP 4. The pH was adjusted to 7.4 and the osmolarity to 280 - 290 mOsm/l. NMDA receptor-mediated responses were isolated using ACSF containing 10 μM CNQX and 50 μM picrotoxin. Some experiments (n = 2) were carried out in the nominal absence of extracellular Mg^{2+} with the membrane potential being held at -80 mV by current injection through the recording electrode; in others (n = 2) normal extracellular Mg^{2+} was used and the membrane potential was held at -60 mV. A short current pulse was included in every

trace to ensure correct adjustment of bridge balance. Slope measurements were made during the initial linear phase (20 – 50 %) of each evoked potential and the values were normalised relative to the mean values obtained within the first 10 min of recording in the absence of any treatment.

All data are presented as the means ± S.E.M.

3.2.3 cGMP measurement

cGMP accumulation was determined by radioimmunoassay as described in chapter 2 (2.4).

3.2.4 Cell Culture

Human embryonic kidney 293 cells (HEK–293 cells; European Collection of Cell Cultures, CAMR, Salisbury, ECACC No. 85120602) were grown in Dulbecco's modified eagles medium (DMEM), containing 10 % fetal bovine serum and 100 U/ml of both penicillin and streptomycin, at 37 °C in a 5 % CO_2 incubator. Exponentially growing cells were plated onto 9 mm diameter coverslips 24 h prior to transfection. HEK-293 cells were transfected with a mixture of plasmids containing the NR1 (provided by Dr. R. Shoepfer, University College London, UK) and NR2a (from Dr. P. Seeburg, Heidelberg, Germany) subunits of the NMDA receptor, and green fluorescent protein (Clontech, USA) to allow visualisation of the transfected cells. Transfections were performed using Effectene Transfection Reagent (Qiagen Ltd, UK) following the manufacturer's instructions. Approximately 76 % of cells expressing green fluorescent protein also expressed functional NMDA receptors. Following transfection, 500 μM ketamine was added to the DMEM culture medium to reduce glutamate-mediated cell toxicity. Studies on the recombinantly expressed receptors were performed two days after transfection, which gave optimal transient expression of the proteins.

3.2.5 Whole cell electrophysiology

Transfected HEK-293 cells were studied at room temperature. The recording chamber was mounted on an inverted microscope (Zeiss), and was continuously perfused with extracellular solution containing (in mM): NaCl 135, KCl 5.4, $CaCl_2$ 1.8, glycine 0.01, HEPES 5. The pH was adjusted to 7.25 with NaOH and osmolarity was maintained at 280 - 300 mOsm/l with sucrose. Whole-cell voltage clamp recordings were made from green fluorescent protein-positive cells using an Axopatch 1D (Axon Instrument, Foster city, CA) after capacitance and series resistance compensation. Typical pipette resistance was 3 - 6 MΩ. Patch pipette solutions contained (in mM): CsCl 140, $MgCl_2$ 1, EGTA 10, HEPES 10, Mg-ATP 4, pH 7.25 (CsOH) and osmolarity 280 – 300 mOsm/l (adjusted with sucrose).

Immediately after establishing the whole-cell configuration, short (100 ms) pressure pulses of glutamate (100 μM dissolved in external solution) were applied with a Picospritzer (Picospritzer IID, General Valve Corporation; New Jersey, USA) every 20 s. Glutamate was used at a concentration of 100 μM to ensure maximal activation of NMDA receptor, as the steady-state for glutamate binding to the NMDA receptor has an EC_{50} of 1.7 μM, and is saturated at 10 μM (Nahum-Levy *et al.*, 2001). Photolysis of caged NO was performed by illuminating a ~100 μm diameter circle surrounding the cell of interest using a mercury vapour 50 W bulb (Osram, UK) filtered with the UG11 filter used in the slice experiments (see above). Data acquisition and analysis were with pClamp6 or pClamp8 (Axon Instruments, CA, USA).

3.2.6 NO measurement

NO concentrations were measured using an electrochemical probe (ISO-NO; World Precision Instruments, Stevenage, UK) under the same experimental conditions used to record currents from the HEK-293 cells.

3.3 Results

3.3.1 Effect of endogenous NO on NMDA receptor-mediated synaptic transmission

Electrophysiological recordings of pharmacologically-isolated NMDA receptor-mediated fEPSPs were made from the CA1 region of adult rat hippocampal slices in order to test initially the prediction that manipulating the levels of endogenous NO influences synaptic NMDA receptor function. The excitatory synapses here express the NR2a receptor subunit (Steigerwald *et al.*, 2000) which is preferentially susceptible to *S*-nitrosation (Choi *et al.*, 2000) and the experiments were conducted at room temperature to be compatible with previous data (Lei *et al.*, 1992; Murphy *et al.*, 1994; Murphy & Bliss, 1999; Choi *et al.*, 2000). Under conditions of low frequency stimulation (0.033 Hz) the fEPSPs were reasonably stable (figure 3.4), indicating that repetitive NMDA receptor activation and the presumed accompanying NO formation did not cause the progressive rundown predicted for a slowly-reversible or irreversible inhibition of NMDA receptors (Lei *et al.*, 1992; Murphy *et al.*, 1994; Murphy & Bliss, 1999; Choi *et al.*, 2000). To boost the production of endogenous NO, the NO synthase substrate L-arginine was perfused in a concentration (100 μM) found to enhance NMDA receptor-evoked NO formation maximally in rat hippocampal slices (East & Garthwaite, 1991). The fEPSPs were not significantly reduced (figure 3.2). Maximal inhibition of NO synthase with the analogue L-NNA (100 μM; East & Garthwaite, 1991) also had no significant effect (figure 3.2).

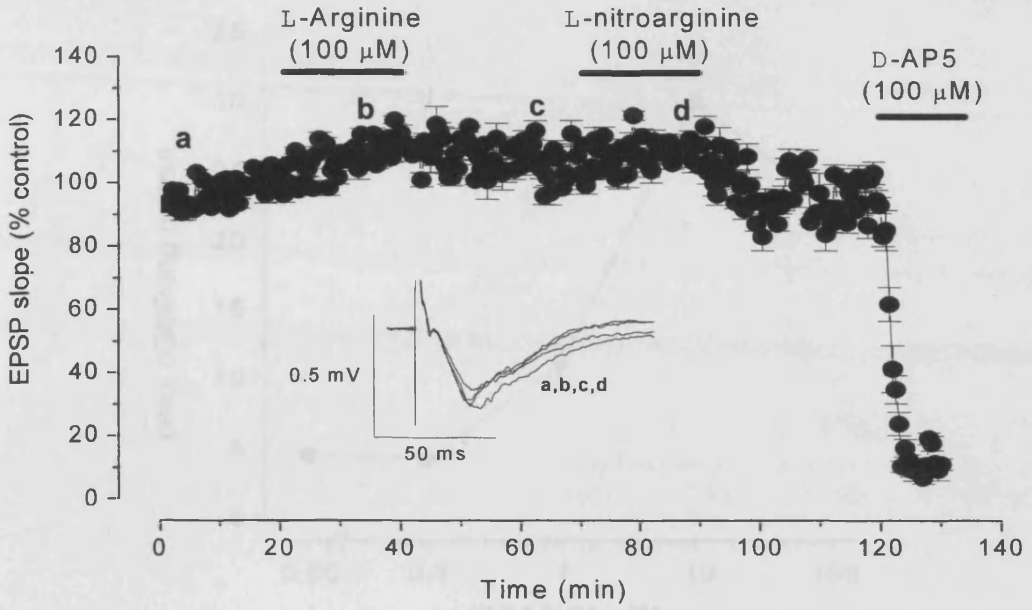

Figure 3.2: Effect of endogenous NO on NMDA-receptor-mediated synaptic transmission in the CA1 region of the hippocampus in vitro. *No significant change in the initial slope of the NMDA receptor-mediated fEPSPs was seen on application of 100 μM L-arginine or 100 μM L-NNA (20 min exposure; n = 4) in presence of 10 μM CNQX. Subsequent addition of 100 μM D-AP5 confirmed that the response was NMDA receptor-mediated. The inset shows representative traces taken at the times indicated by the letters.*

3.3.2 Effect of exogenous NO on hippocampal synaptic transmission

The negative results obtained on attempting to manipulate endogenous NO levels prompted tests of the effects of delivering NO exogenously. For this purpose, we used the NONOate DEA/NO, which releases authentic NO with predictable kinetics (Keefer *et al.*, 1996) and which has been shown to be able to substitute for endogenous NO in the induction of hippocampal synaptic plasticity (Bon & Garthwaite, 2001a; Bon & Garthwaite, 2003). To gauge the concentrations of DEA/NO that could be regarded as physiological, the range activating the NO-activated GC receptors in hippocampal slices was determined. Based on the ensuing accumulation of cGMP, the EC_{50} was 1.4 μM and maximal activation occurred at 10 μM DEA/NO (figure 3.3). These results are very similar to those obtained previously at 30 °C (Bon & Garthwaite, 2001a).

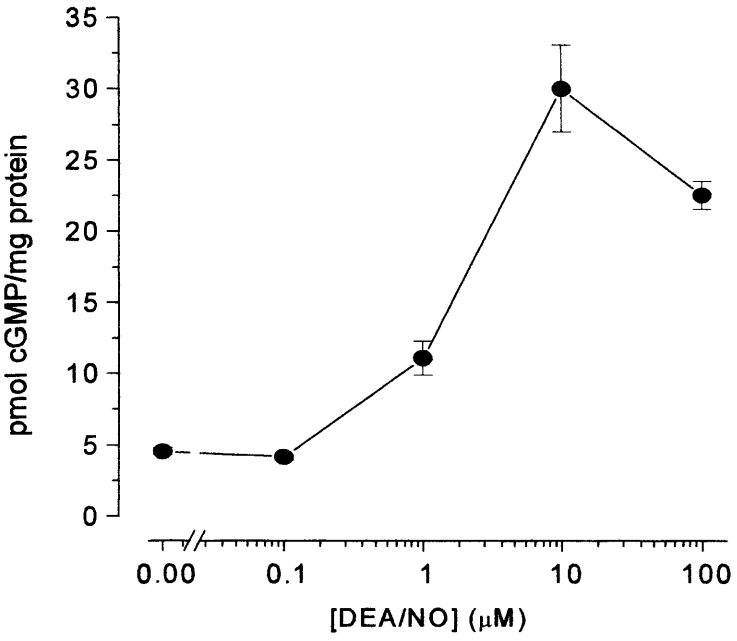

Figure 3.3: Concentration-response curve for DEA/NO on cGMP levels in adult rat hippocampal slices *(2 min exposure; n = 6).*

As NO-activated GC forms a complex with the NMDA receptor in the hippocampus (Russworm *et al.*, 2001), free NO should have access to the two proteins with equal ease. However in electrophysiological experiments, applications of up to 10 μM DEA/NO had no significant effect on NMDA receptor-mediated fEPSPs (data not shown). Even concentrations up to 300 μM produced no detectable change (figure 3.4). However, upon further increasing the concentration to 1 mM, the fEPSPs were significantly reduced but recovered fully on washout (figure 3.5b). The inhibition was non-specific, however, because the same DEA/NO concentration caused a similar depression of synaptic AMPA receptor-mediated fEPSPs (figure 3.5a). Such a depression has been observed previously in hippocampal slices and is attributable to the effects of metabolic stress caused by the inhibition of mitochondrial respiration by NO (Bon & Garthwaite, 2001a).

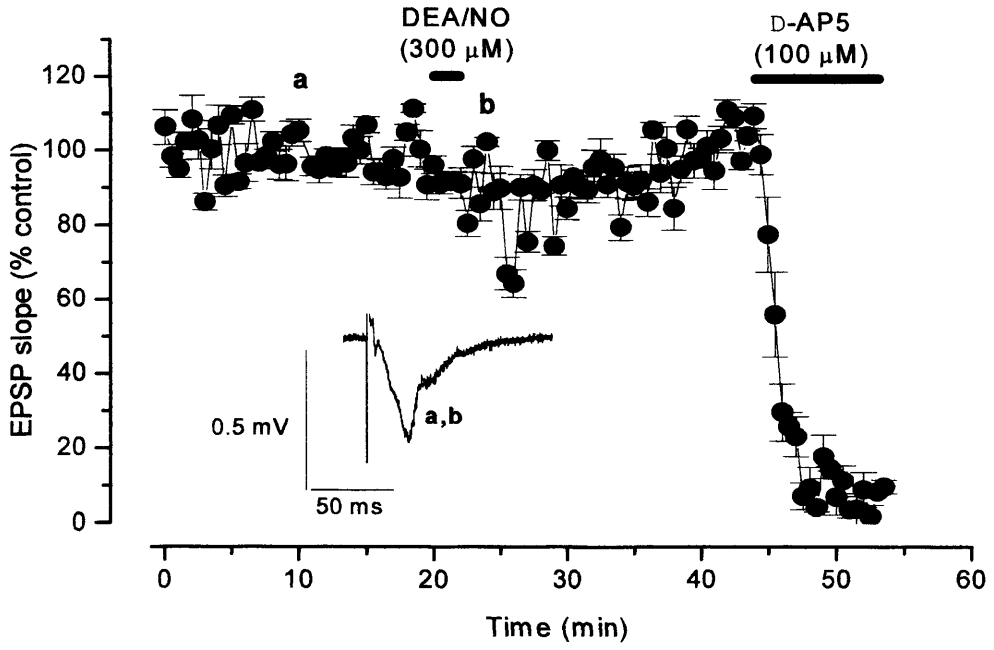

Figure 3.4: Effect of 2 minute application of 300μM DEA/NO on the NMDA receptor-mediated fEPSPs *(n = 4).*

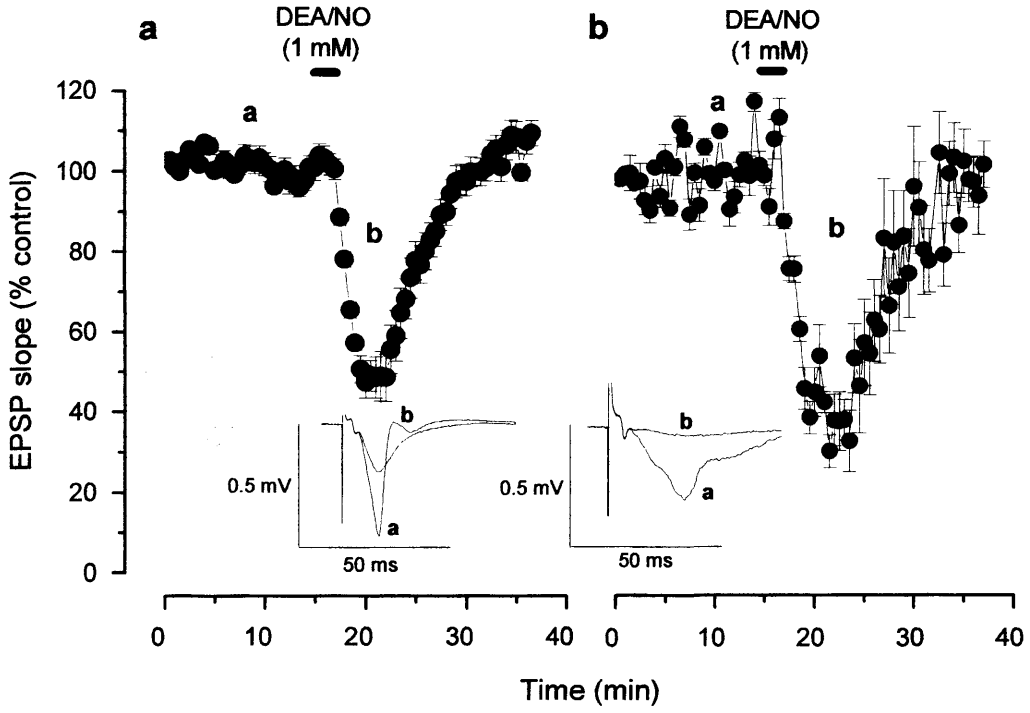

Figure 3.5: Comparison of the effects on AMPA- and NMDA-mediated synaptic responses following the application of 1 mM DEA/NO. *Non-specific depression of both (a) AMPA- and (b) NMDA-mediated fEPSPs following exposure to 1 mM DEA/NO in the same slice preparation (2 min DEA/NO application; n = 4).*

To check the validity of the field potential recordings, whole-cell recordings of the NMDA receptor-mediated EPSP were carried out. Addition of 300 μM DEA/NO had no significant effect (figure 3.6), confirming the initial findings.

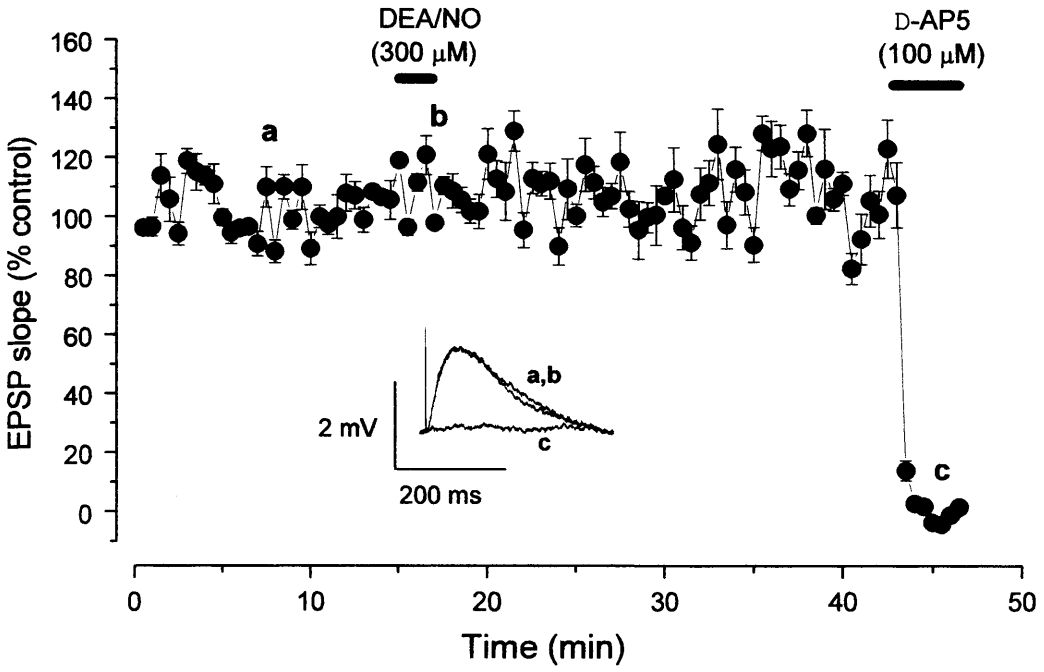

Figure 3.6: Action of 300 μM DEA/NO on NMDA receptor-mediated EPSPs recorded using the whole-cell technique *(n = 4). The insets show representative traces from an experiment carried out in the presence of 1 mM Mg^{2+} (membrane potential, -60 mV), taken at the times indicated by the letters.*

The lack of any selective effect of DEA/NO even in high concentration appears at odds with previous reports showing profound, selective, and apparently irreversible block of NMDA receptor function in the same synapses by release of NO from a caged derivative (potassium pentachloronitrosylruthenate) using a focused beam of UV light (Murphy *et al.*, 1994; Murphy & Bliss, 1999). On repeating this experiment, we confirmed the result: perfusion of 500 μM caged NO itself had no effect but a subsequent flash of UV light (also without effect on its own) caused an almost complete block of the fEPSPs within 2 min (94 ± 3 %; n = 4) that showed little sign of recovery during at least 10 min (figure 3.7).

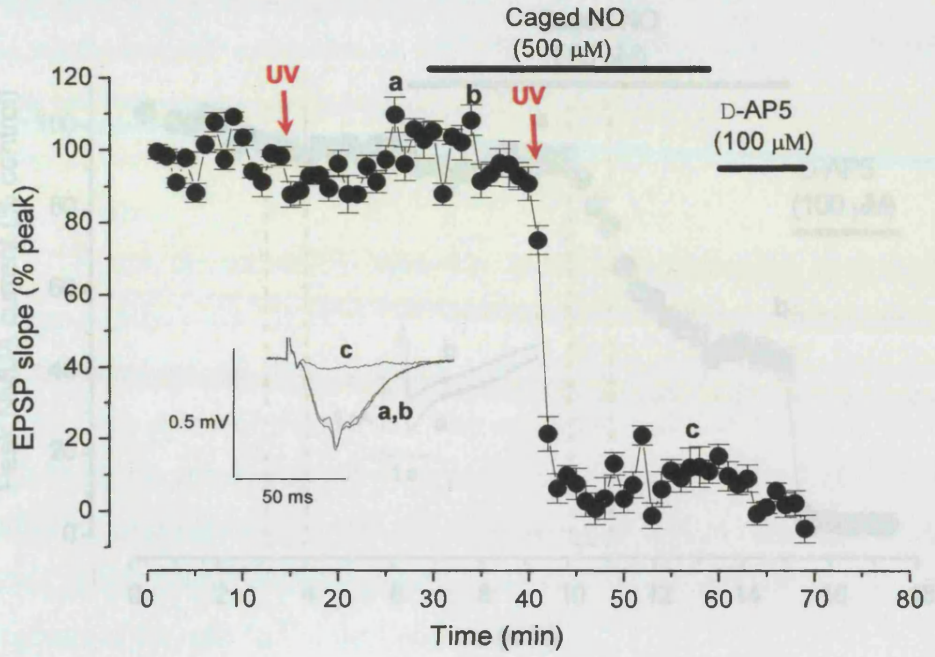

Figure 3.7:Effect of photolysis of caged NO on NMDA receptor-mediated synaptic transmission. *No significant change in the initial slope of the NMDA receptor-mediated fEPSPs was observed following either perfusion of 500 µM Caged NO alone or by a 1 ms UV flash. Application of the UV flash in the presence of 500 µM Caged NO depressed NMDA receptor-mediated fEPSP by 94 ± 3 % (mean ± S.E.M.; n = 4).The inset shows representative traces taken at the times indicated by the letters.*

3.3.3 Studies on heterologously expressed NMDA receptors

One explanation for the discrepant results obtained with the two different methods of applying NO could be that the NO needs to be delivered rapidly and in high concentrations in order to be able to influence the NMDA receptors, which would be the case with photolysis of the caged NO (Murphy *et al.*, 1994) but not with bath application of DEA/NO. To address this and other possibilities under more controlled conditions, whole-cell recordings were made from HEK-293 cells co-transfected with the NR1 and NR2a NMDA receptor subunits. When exposed to brief pulses of glutamate (100 µM, 100 ms) at regular 20 s intervals, current responses were reasonably stable for at least 20 min. For uncaging NO, space limitations of the recording apparatus precluded use of the flash gun used in the earlier slice experiments and so UV light from the microscope was used instead.

Similar to findings in slices, caged NO or UV light exposure on their own had no effect, but a combination of the two resulted in a slow-onset and apparently

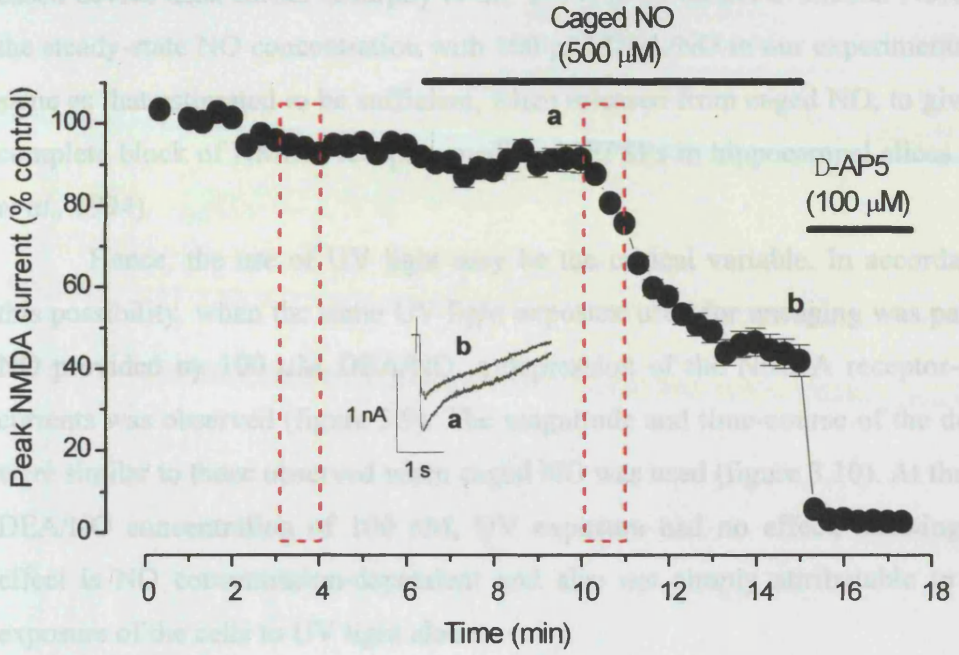

Figure 3.8: Effect of photolysis of 500 μM caged NO by exposure to UV light from the microscope on NMDA receptor currents. *No significant change on NMDA receptor currents was observed following individual exposure of HEK-293 cells transfected with NMDA receptor subunits to 500 μM caged NO or UV light. Application of UV light in the presence of 500 μM Caged NO depressed NMDA receptor currents by 53 ± 3 % (n = 5). Boxed region represents duration of UV light. The inset shows representative traces taken at the times indicated by the letters.*

irreversible depression of whole-cell currents (figure 3.8). A relatively prolonged light exposure (routinely 1 min) was needed to produce this effect and the amplitude of the depression (about 50 %) was less than found in slices (about 90 %), presumably because the UV light was of relatively low intensity and/or the released NO, or other substances, were being continuously washed out by the flow of the perfusing solution (2 chamber volumes/min).

In contrast to these findings, exposure to DEA/NO (100 nM or 100 μM for 9 min) had no significant effect (figure 3.9). The corresponding NO concentrations in the recording chamber were measured using an electrochemical probe. At 100 nM DEA/NO, NO rose gradually to reach 32 ± 5 nM (n = 3) after 9 min (see figure 3.10a for representative trace). With 100 μM DEA/NO, a plateau NO concentration of 5.1 ± 0.1 μM (n = 3) was achieved within 2 min (figure 3.10b). It was not possible to perform similar recordings in experiments with caged NO because the probe responded markedly to UV light alone (not illustrated) and, unfortunately, the carbon-

based device used earlier (Murphy *et al.*, 1994) is no longer available. Nevertheless, the steady-state NO concentration with 100 μM DEA/NO in our experiments was the same as that estimated to be sufficient, when released from caged NO, to give a near-complete block of NMDA receptor-mediated fEPSPs in hippocampal slices (Murphy *et al.*, 1994).

Hence, the use of UV light may be the critical variable. In accordance with this possibility, when the same UV light exposure used for uncaging was paired with NO provided by 100 μM DEA/NO, a depression of the NMDA receptor-mediated currents was observed (figure 3.9). The magnitude and time-course of the depression were similar to those observed when caged NO was used (figure 3.10). At the reduced DEA/NO concentration of 100 nM, UV exposure had no effect, showing that the effect is NO concentration-dependent and also not simply attributable to repeated exposure of the cells to UV light alone.

UV light can cause the production of many different types of reactive radicals in cells (Tyrrell & Keyse, 1990) some of which could combine with NO to form chemicals capable of yielding species able to nitrosate thiols. An obvious candidate was peroxynitrite, which is formed at diffusion-controlled rates from NO and superoxide ions, and which breaks down to yield NO_2 radicals that can act as nitrosating agents (Beckman & Koppenol, 1996; Hogg, 2002). A high concentration of superoxide dismutase (1000 U/ml; Beckman & Koppenol, 1996), however, did not prevent the inhibition of NMDA receptor currents brought about by the combination of UV light and caged NO (figure 3.11a). Further increasing the concentration of SOD to 10 000 U/ml had an adverse effect on the health of the HEK-293 cells. A powerful scavenger of NO_2, urate (300 μM; Ford *et al.*, 2002), also failed to prevent the depression of NMDA receptor currents (figure 3.11b).

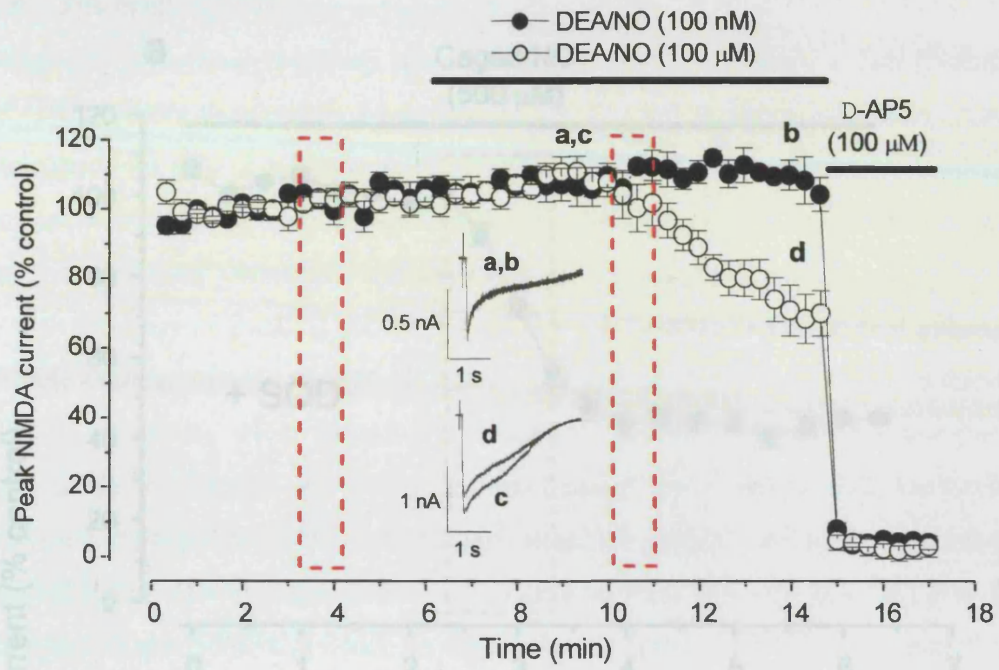

Figure 3.9: Combined effect of DEA/NO and UV light on NMDA receptor currents. *Application of DEA/NO (100 nM or 100 µM) on its own had no effect, whereas delivery of UV light in the presence of 100 µM DEA/NO, but not 100 nM DEA/NO, resulted in depression of NMDA receptor currents by 35 ± 7 % (mean ± S.E.M.; n = 4) in HEK-293 cells transfected with the NMDA receptor subunits. Boxed region represents duration of UV light. The inset shows representative traces taken at the times indicated by the letters.*

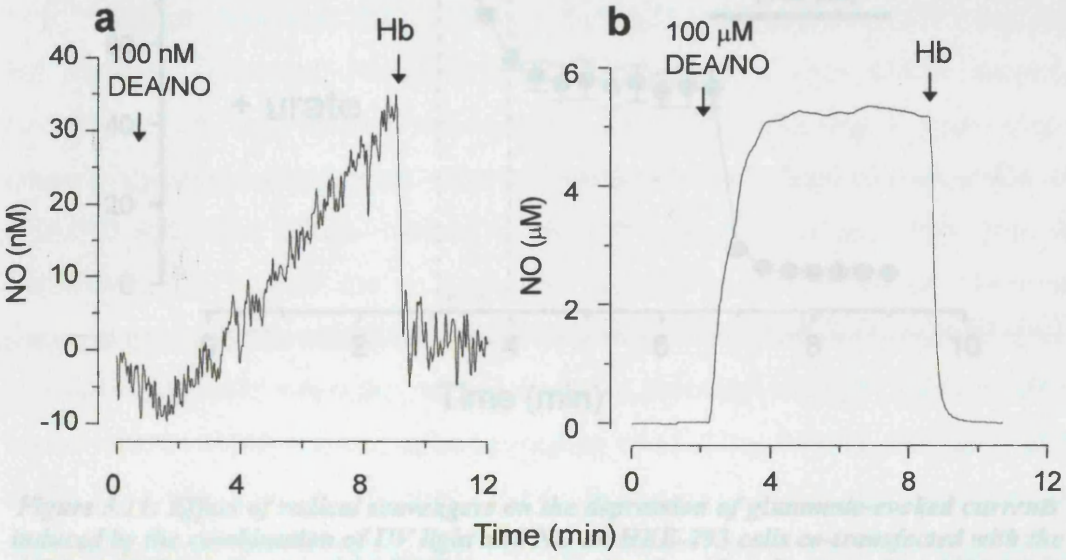

Figure 3.10: Representative recording of NO concentration profile on addition of (a) 100 nM or (b) 100 µM DEA/NO. *Oxyhaemoglobin (Hb; 50 µM) was added at the times indicated by the arrows to zero the NO concentration.*

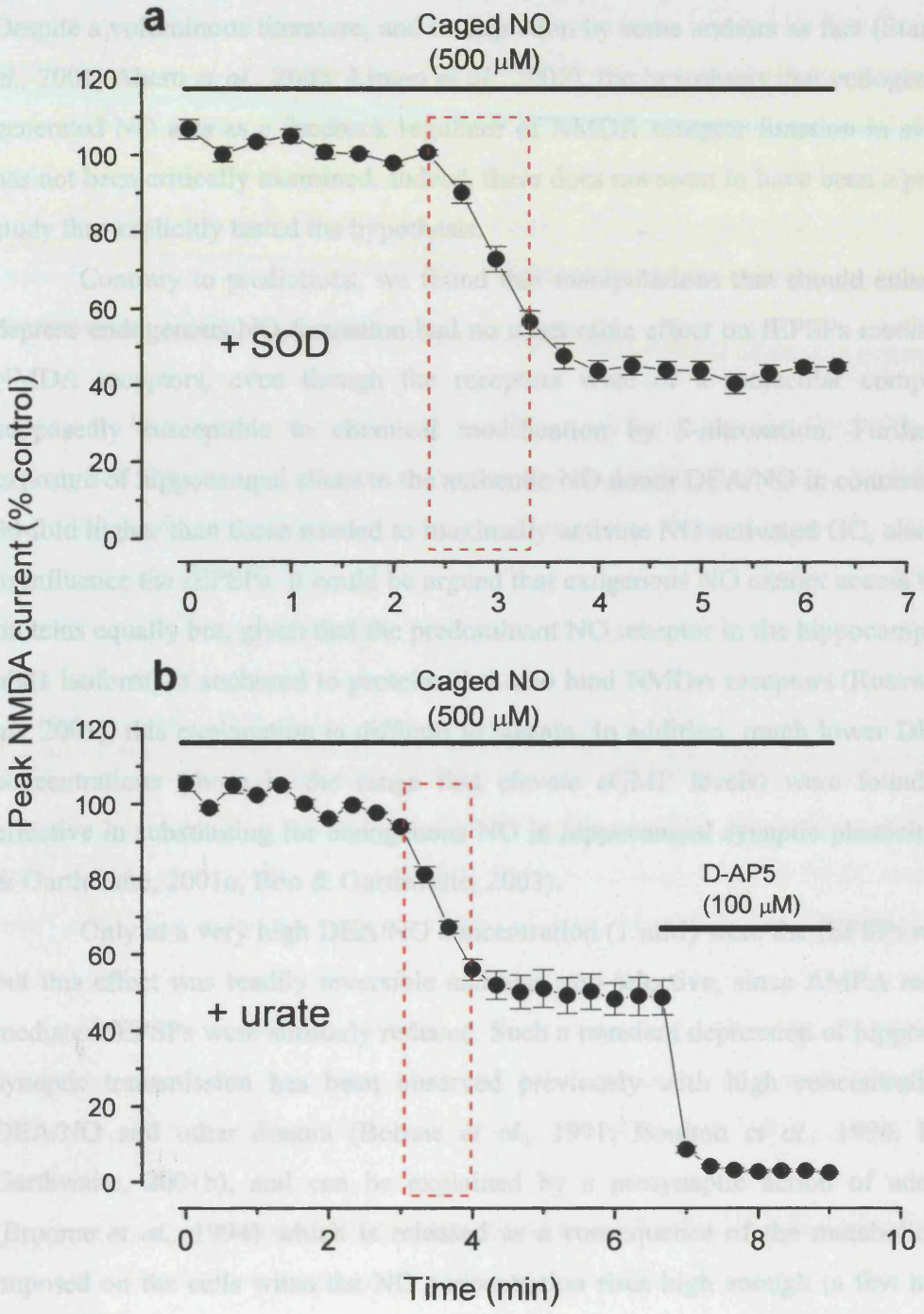

Figure 3.11: Effect of radical scavengers on the depression of glutamate-evoked currents induced by the combination of UV light and NO on HEK-293 cells co-transfected with the NR1 and NR2a subunits of the NMDA receptor. *No effect of application of (a) 1000 U/ml superoxide dismutase or (b) 300 μM urate on the inhibition of NMDA receptor currents by the delivery of UV light in the presence of 500 μM caged NO (n = 3 - 4). Dashed boxes indicate the duration of UV exposure.*

3.4 Discussion

Despite a voluminous literature, and its depiction by some authors as fact (Stamler *et al.*, 2001; Ahern *et al.*, 2002; Lipton *et al.*, 2002), the hypothesis that endogenously-generated NO acts as a feedback regulator of NMDA receptor function in synapses has not been critically examined. Indeed, there does not seem to have been a previous study that explicitly tested the hypothesis.

Contrary to predictions, we found that manipulations that should enhance or depress endogenous NO formation had no observable effect on fEPSPs mediated by NMDA receptors, even though the receptors were of a molecular composition supposedly susceptible to chemical modification by *S*-nitrosation. Furthermore, exposure of hippocampal slices to the authentic NO donor DEA/NO in concentrations 30-fold higher than those needed to maximally activate NO-activated GC, also failed to influence the fEPSPs. It could be argued that exogenous NO cannot access the two proteins equally but, given that the predominant NO receptor in the hippocampus (the α2β1 isoform) is anchored to proteins that also bind NMDA receptors (Russwurm *et al.*, 2001), this explanation is difficult to sustain. In addition, much lower DEA/NO concentrations (those in the range that elevate cGMP levels) were found to be effective in substituting for endogenous NO in hippocampal synaptic plasticity (Bon & Garthwaite, 2001a; Bon & Garthwaite, 2003).

Only at a very high DEA/NO concentration (1 mM) were the fEPSPs reduced but this effect was readily reversible and also non-selective, since AMPA receptor-mediated fEPSPs were similarly reduced. Such a transient depression of hippocampal synaptic transmission has been observed previously with high concentrations of DEA/NO and other donors (Bohme *et al.*, 1991; Boulton *et al.*, 1994; Bon & Garthwaite, 2001b), and can be explained by a presynaptic action of adenosine (Broome *et al.*, 1994) which is released as a consequence of the metabolic stress imposed on the cells when the NO concentration rises high enough (a few hundred nanomolar) to inhibit mitochondrial respiration (Bon & Garthwaite, 2001a). That a higher DEA/NO concentration than before was required for this effect (c.f. Bon & Garthwaite, 2001a) is explained by the rate of NO release from the donor (and therefore the resulting NO concentrations) being lower at the lower temperature used in the present experiments (Keefer *et al.*, 1996).

The only evidence that exogenous NO can inhibit synaptic NMDA receptors came from experiments in which NO was released from a caged derivative by UV light (Murphy *et al.*, 1994; Murphy & Bliss, 1999) and we were able to confirm this finding. On closer examination using transfected cells, however, it transpired that NO itself was not responsible but the combination of NO and UV light. Unfortunately the same experiment could not also be performed on slices with UV light from the flashlamp because the requisite NO concentrations (low micromolar) would inevitably have led to a profound non-specific synaptic depression through inhibition of mitochondrial respiration. Being of unlikely physiological significance, the mechanism of NMDA receptor block by NO and UV light was not pursued in detail, except that tests for an involvement of peroxynitrite proved to be negative. Nevertheless, the long duration of the resulting block of receptor activity would be consistent with NMDA receptor *S*-nitrosation (Lei *et al.*, 1992; Choi *et al.*, 2000) and there are a number of alternative ways through which this could be achieved. For example, light exposure similar to that used to uncage NO (namely UVA light of wavelength 300 - 350 nm) causes the formation of various reactive radicals and singlet oxygen which could result in the formation of thiyl radicals, to which NO can bind directly, forming a nitrosothiol (Tyrrell & Keyse, 1990; Beckman & Koppenol, 1996; Dillon *et al.*, 1999; Hogg, 2002). This could occur on the NMDA receptor itself, or on low molecular weight thiols (e.g. glutathione) that could then nitrosate thiol groups on the receptor by a transnitrosation reaction.

The negative findings with NO itself, together with the results indicating that the block of NMDA receptors resulting from uncaging NO with UV light is artifactual, demand an appraisal of the other evidence that NO regulates NMDA receptors.

First, *S*-nitrosated NMDA receptors and a collection of other proteins have been found in brain homogenates subjected to prolonged chemical treatment, the modification being reduced in tissue from animals lacking neuronal NO synthase (Jaffrey *at al.*, 2001). It is unclear if the proteins were *S*-nitrosated *in vivo*, however. Among other possible explanations of the result is that post-mortem acidosis leads to the formation of the *S*-nitroso compounds from the combination of nitrite (whose levels are expected to reflect NO synthase activity; Lauer *et al.*, 2001) and thiols (Tsikas *et al.*, 2001).

Second, in the earlier work (Lei *et al.*, 1992; Manzoni *et al.*, 1992; Choi *et al.*, 2000), administration of NO relied largely on the use of donors such as sodium nitroprusside, nitroglycerine, *S*-nitrosocysteine and 3-morpholino-sydnonimine (SIN-1), which are now considered problematic because of their intrinsic chemical reactivity and/or because they release reactive species in addition to NO (Feelisch, 1998).

Third, much of the data relied on the use of fluorescent Ca^{2+} imaging to monitor NMDA receptor function indirectly (Lei *et al.*, 1992; Manzoni *et al.*, 1992; Tanaka *et al.*, 1993; Choi *et al.*, 2000). Apart from cytosolic Ca^{2+} being susceptible to independent regulation by NO (Hoyt *et al.*, 1992) the fluorophore used in all cases was fura-2, whose use necessitates repeatedly exposing the cells to UVA light at similar wavelengths (340 - 380 nm) used to uncage NO. This raises the possibility that a similar artifactual block of NMDA receptors occurred in experiments of this type.

Finally, there have been direct patch electrode recordings of the effect of NO on NMDA receptor-mediated currents. The first of these (Manzoni *et al.*, 1992) used mainly the compound SIN-1 to deliver NO and found that, in contrast with the supposed *S*-nitrosation reaction (Lei *et al.*, 1992; Choi *et al.*, 2000), the block of NMDA-evoked currents in striatal neurones had a rapid onset and was readily reversible. The same result has recently been obtained using cell lines transfected with NR1/NR2A and exposed to SIN-1 (Gbadegesin *et al.*, 1999; Aizenman & Potthoff, 1999). Mutational analysis suggested a mechanism distinct from thiol modification (Aizenman & Potthoff, 1999), consistent with an interaction between NO and a metal binding site on the receptor (Fagni *et al.*, 1995). SIN-1 is problematic because it releases both NO and superoxide (leading to peroxynitrite formation; Feelisch, 1989, 1998) and when the experiments were repeated with NONOate donors, which release authentic NO, one study found that NMDA receptor-mediated currents were increased (Gbadegesin *et al.*, 1999) whereas another found that they were decreased (Aizenman & Potthoff, 1999). These opposite effects, together with the lack of significant change in either direction observed in our experiments, cannot readily be explained by differences in the applied NO concentration: direct measurement (present study and Gbadegesin *et al.*, 1999) or calculation from the half-

lives of the NONOates (Schmidt *et al.*, 1997; Aizenman & Potthoff, 1999) indicate that concentrations in the low micromolar range were applied in all cases.

Regardless of the reason for the variable effects of NONOates on heterologously-expressed receptors, the biological relevance of the resulting micromolar NO concentrations is highly questionable. These concentrations are about 1000-fold higher than are needed to activate NO-activated GC receptors half-maximally (Griffiths & Garthwaite, 2001; Bellamy *et al.*, 2002), they would cause almost complete inhibition of mitochondrial respiration *in vivo* (Brown, 1999; Bellamy *et al.*, 2002), and they are 100- to 1000-fold higher than the NO concentrations found following NMDA receptor activation in intact brain tissue (Lin *et al.*, 1996; Griffiths *et al.*, 2002).

Overall, the previous indirect evidence that NO affects NMDA receptor function is questionable and this, together with the additional direct evidence presented here, places the hypothesis that NO regulates the functioning of synaptic NMDA receptors in serious doubt.

Chapter 4

Mechanisms of basal NO synthesis in the hippocampus

4.1 Introduction

4.1.1 NO/cGMP signal transduction pathway

The NO/cGMP signal transduction pathway is thought to play an important role during synaptic plasticity, being involved in LTD in the cerebellum and striatum, and in LTP in the hippocampus and cerebral cortex (for more details see general introduction; 1.6.3). In cerebellar and striatal LTD, NO appears to be generated either presynaptically or in interneurons, and to exert its action postsynaptically. In contrast, NO is synthesised postsynaptically in cortical and hippocampal LTP, and is believed to act as a retrograde messenger on presynaptic terminals, although postsynaptic actions of NO in the hippocampus have also been reported (Ko & Kelly, 1999; Lu *et al.,* 1999).

In the CA1 region of the hippocampus, LTP is induced by brief tetanic stimulation of afferent glutamatergic fibers, and typically exhibits a form of LTP that critically depends on postsynaptic activation of the NMDA receptor (Bliss & Collingridge, 1993). As described in the general introduction (section 1.2), NMDA receptors are physically coupled to nNOS via PSD-95 (Brenman *et al.,* 1996a; Christopherson *et al.,* 1999), an arrangement that allows the influx of Ca^{2+} into the postsynaptic cell to couple to NO formation. In the previous chapter the proposed regulation of the NMDA receptor by NO was discussed, and determined to be of questionable physiological relevance.

The NMDA receptor/NO/cGMP pathway has been well-characterised in the cerebellum, where robust cGMP responses to excitatory amino acids and relatively low PDE activity facilitate the monitoring of cGMP production. However the pathway has not been as well-described in the hippocampus, which is surprising considering the importance of excitatory amino acid circuits in a number of physiological (learning and memory) and pathophysiological conditions (epilepsy, stroke, head trauma).

Localisation studies have revealed NMDA receptors to be abundantly expressed in the hippocampus, with particular prominence in the stratum radiatum (Monaghan *et al.*, 1984). nNOS staining is found to be largely confined to a subpopulation of GABA-containing interneurons in the stratum oriens and stratum radiatum (Bredt *et al.*, 1991; Valschanoff *et al.*, 1993; Lumme *et al.*, 2000), whereas when weak fixation protocols are followed staining can also be identified in CA1 pyramidal cells (Endoh *et al.*, 1994; Wendland *et al.*, 1994; Blackshaw *et al.*, 2003). In the case of NO-activated GC, the principal mediator of NO signal transduction, its distribution has been localised by *in situ* hybridisation to the pyramidal layers of CA1 - CA3 and to the granule layer of dentate gyrus (Matsuoka *et al.*, 1992; Burgunder & Cheung, 1994), whilst cGMP immunostaining can be detected uniformly throughout the hippocampus, with the pyramidal and granule cells exhibiting the most intense signal (Southam & Garthwaite, 1993). Interestingly, recent light and electron microscopy studies reveal NO-activated GC to associate with nNOS at subpopulations of synapses in the hippocampus (De Vente *et al.*, 1998; Burette *et al.*, 2002): nNOS accumulation is observed at the postsynaptic density of asymmetric axospinous synapses, whereas NO-activated GC concentrates close to the plasma membrane in presynaptic axon terminals. Furthermore, the anatomical relationship between presynaptic NO-activated GC and postsynaptic nNOS is spatially precise; although only a modest fraction of synapses express either nNOS or NO-activated GC, NOS-positive post synaptic densities are usually postsynaptic to NO-activated GC-positive axon terminals and vice versa (Burette *et al.*, 2002). These studies provide neuroanatomical support for the hypothesis that NO can act as a synapse-specific retrograde messenger in a subpopulation of synapses in the CA1 region of the hippocampus. However, it must also be noted that, in contrast to the above studies, a recent immunohistochemical study failed to find significant co-localization of nNOS and NO-activated GC in the hippocampus (Ding *et al.*, 2004).

Electrophysiological investigations additionally provide support for the retrograde messenger hypothesis: application of exogenous NO, timed to coincide with weak tetanic stimulation of afferent fibers, elicited an NMDA receptor-independent persistent potentiation of hippocampal synaptic transmission that occluded LTP (Zhuo *et al.*, 1993, 1994; Malen & Chapman, 1997; Bon & Garthwaite, 2003). Furthermore, recent observations by Bon & Garthwaite (2003) indicate that

LTP requires both a tonic NO level and a phasic NO signal arising from tetanic stimulation, and that the post-tetanus time window during which NO is required is ≤ 15 min (Haley *et al.,* 1992; Bon & Garthwaite, 2003). Figure 4.1 is a schematic diagram which illustrates the current understanding of the requirement for NO during LTP.

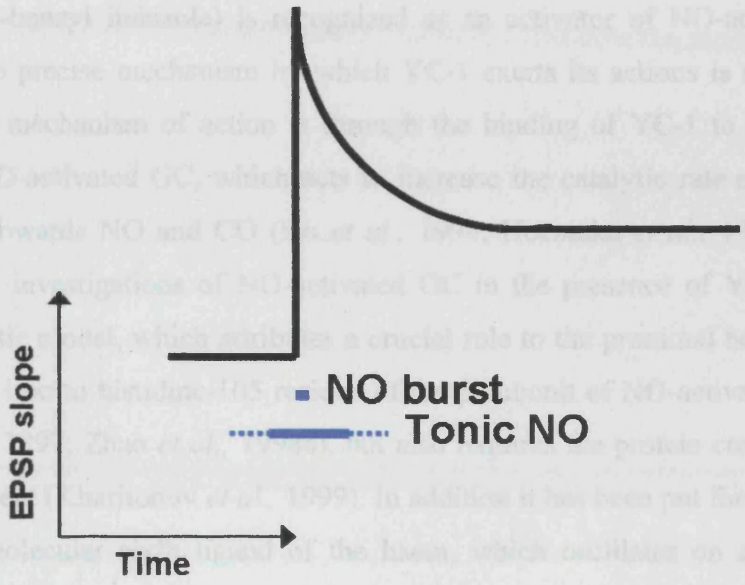

Figure 4.1 Schematic representation of the requirement for NO during LTP.

Despite the importance of both a tonic NO level at the time of LTP induction lasting for ≤ 15 min post LTP induction, and a phasic NO signal coinciding with LTP induction, the isoform of NOS responsible for NO production in the hippocampus has so far not been investigated. Measurements of cGMP reveal a biologically active level of NO to exist, even in unstimulated hippocampal slices, which is increased following tetanic stimulation (Chetkovich *et al.,* 1993). However, in contrast to the relatively high cGMP levels observed in the cerebellum, cGMP levels in the hippocampus are low, partially as a consequence of high PDE activity (DeVente & Steinbusch, 1992). Therefore, in order to study endogenous NO production in the hippocampus, using cGMP as an index, studies must be carried out in the presence of a PDE inhibitor such as IBMX, and an enhancer of NO-activated GC in order to sensitise NO-activated GC

towards NO, thereby increasing the cGMP accumulation resulting from any given stimulus.

4.1.2 Enhancers of NO-activated GC

The main mechanism of physiological activation and pharmacological inhibition of NO-activated GC is via changes in the state of the enzyme's haem-moiety; however, other regulatory mechanisms are also known to exist. YC-1 (3-(5'-hydroxymethyl-2'furyl)-1-benzyl indazole) is recognized as an activator of NO-activated GC, and whilst the precise mechanism by which YC-1 exerts its actions is not yet clear, the proposed mechanism of action is through the binding of YC-1 to an allosteric site within NO-activated GC, which acts to increase the catalytic rate and sensitises the enzyme towards NO and CO (Ko *et al.*, 1994; Hoenicka *et al.*, 1999). Kinetic and equilibria investigations of NO-activated GC in the presence of YC-1 has led to a mechanistic model, which attributes a crucial role to the proximal bond that connects the haem iron to histidine-105 residue of the β-subunit of NO-activated GC (Zhao & Marletta, 1997; Zhao *et al.*, 1998a), but also requires the protein control of the distal environment (Kharitonov *et al.*, 1999). In addition it has been put forward that there is an intramolecular sixth ligand of the haem, which oscillates on and off the sixth coordinate, thereby conferring a certain degree of ligand specificity (Hobbs, 1997). The direct binding of NO-activated GC activators to this site has been proposed to block this intramolecular binding site, and thereby strengthen the binding of NO to the enzyme. YC-1 has been shown to inhibit platelet aggregation via the elevation of cGMP levels leading to VASP phosphorylation (Wu *et al.*, 1995, 1997; Friebe *et al.* 1998; Becker *et al.*, 2000), and to relax pre-contracted aortic rings (Mülsch *et al.*, 1997).

Recently a new allosteric compound, BAY 41–2272, has been described which is a pyrazolopyridine derivative able to stimulate NO-activated GC directly via an NO-independent, but a haem-dependent mechanism, and affects the activity of NO-activated GC in a manner similar to YC-1 (Straub *et al.*, 2001; Stasch *et al.*, 2001). However, in contrast to YC-1, BAY 41-2272 exhibits a distinctly higher potency, of about two orders of magnitude, and does not appear to inhibit PDE activity in concentrations up to 10^{-5} M (Stasch *et al.*, 2001), thereby offering significantly greater selectivity. BAY 41-2272 has been found to be a potent vasodilator of aortic rings *in vitro*, and *in vivo* exhibits antiplatelet activity, reduces

mean arterial blood pressure in normal and hypertensive rats, and increases survival rates in a low-NO rat model of hypertension (Stasch *et al.*, 2001; Straub *et al.*, 2001). Figure 4.2 compares the structure of YC-1 and BAY 41-2272, highlighting the similarities in their structures.

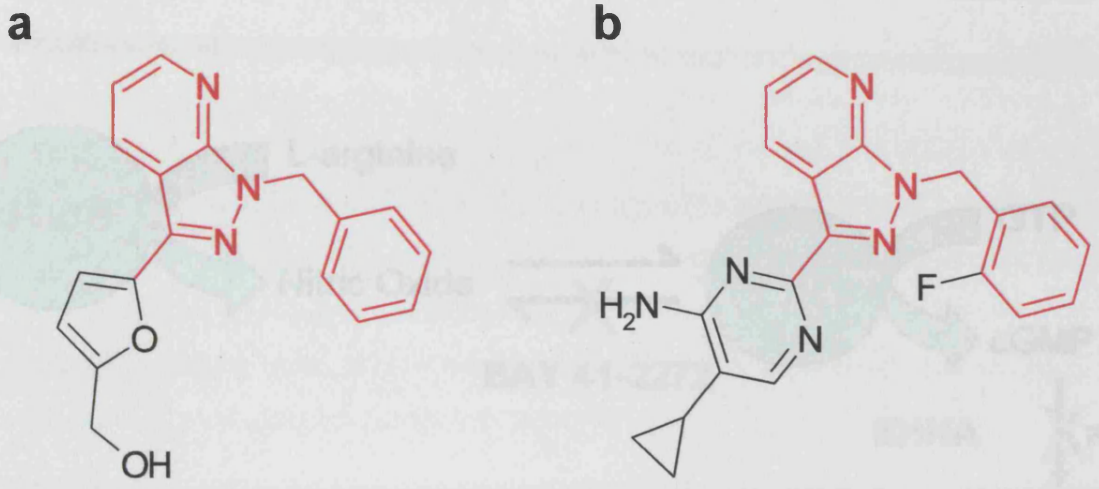

Figure 4.2: Structure of (a) YC-1 and (b) BAY 41-2272. *The common backbone between the compounds is highlighted in red.*

Photoaffinity labeling studies reveal that both compounds bind to the N-terminal region of the α-subunit in close proximity to two cysteine residues (αCys 238 and αCys 243), which highlights a unique, allosteric regulatory site on NO-activated GC distinct from the NO-binding site (Stasch *et al.*, 2001; Becker *et al.*, 2001).

4.1.3 Aim

The aim of the present study was to investigate the endogenous production of NO in the hippocampus. Initially the isoform of NOS responsible for the basal levels of NO was studied by examination of cGMP accumulation in adult hippocampal slices in the presence of a PDE inhibitor to prevent the breakdown of cGMP, and BAY 41-2272 to sensitize the enzyme towards NO (as depicted in figure 4.3).

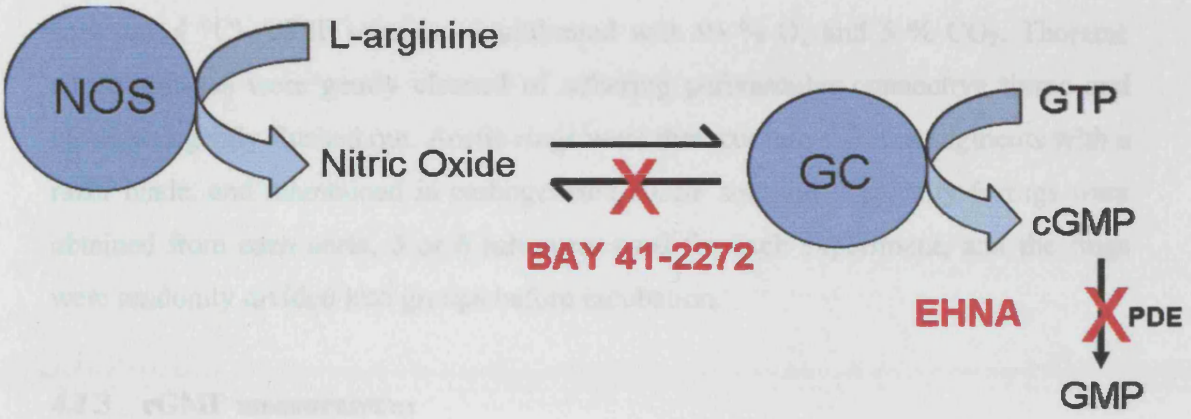

Figure 4.3: NO synthesis and breakdown in the CNS.
Points of pharmacological regulation of this pathway are marked.

4.2 Methods

4.2.1 Hippocampal tissue preparation

Hippocampal slices were prepared as described in chapter 2 (2.2).

4.2.2 Aortic ring preparation

Aortic rings were prepared from 6 to 8-week-old male Sprague-Dawley rats (Charles River, Margate, UK). The animals were killed humanely according to Home Office regulations by way of stunning followed by cervical dislocation. The thoracic portions of rat aortas were rapidly removed from the animals and immediately immersed in cold (0 - 4 °C) ACSF solution, equilibrated with 95 % O_2 and 5 % CO_2. Thoracic aortic portions were gently cleaned of adhering perivascular connective tissue and blood was gently flushed out. Aortic rings were then cut into ~ 3 mm segments with a razor blade, and maintained in carbogenated ACSF solution. Typically 6 rings were obtained from each aorta, 5 or 6 rats were used for each experiment, and the rings were randomly divided into groups before incubation.

4.2.3 cGMP measurement

Hippocampal slices or aortic rings were allowed to recover in carbogenated ACSF maintained in a shaking water bath at 30 °C for at least 1 - 2 h before use. Hippocampal slices or aortic rings were then transferred to a fresh solution containing the general PDE inhibitor 3-isobutyl-1-methylxanthine (IBMX; 1 mM) or the PDE2 inhibitor erythro-9-(2-hydroxy-3-nonyl)-adenine hydrochloride (EHNA; 300 μM) for 15 min, before being exposed to either the enhancer of NO-activated GC, BAY 41-2272 for 5 min, or to NMDA for 2 min. All pharmacological agonists/antagonists were present for the same period as the PDE inhibitor except for wortmannin, raloxifene and LY294002, in which the slices were pre-incubated for 30 min, 15 min, and 10 min respectively, prior to PDE inhibition in accordance with previous studies (Simoncini *et al.*, 2000; Simoncini *et al.*, 2002a; Isenovic *et al.*, 2002). At the end of the exposure the hippocampal slices or aortic rings were removed, inactivated by immersion in boiling hypotonic inactivation buffer for a minimum of 5 min, and homogenized by sonication.

The protein content and cGMP accumulation were determined as described in chapter 2 (2.4).

4.2.4 Western blotting

Mouse DNA was prepared as described in chapter 2 (2.5.1), of which 15 µl was combined with 5 µl loading dye of the following composition: 100 mM Tris-HCl (pH 6.8), 4 % (w/v) SDS, 0.2 % (w/v) bromophenol blue, 20 % (v/v) glycerol, and 10 % (v/v) β-mercaptoethanol. Samples were heated to 100 °C for 5 min, and then separated by electrophoresis on a 10 % SDS-PAGE gel at 200 mV for 45 min. Proteins were then transferred to nitrocellulose membrane (Hybond ECL; Amersham Biosciences, Buckinghamshire, UK) and blocked for 2 h at room temperature in 5 % (w/v) non-fat milk made up in PBST buffer of the following composition: 80 mM Na_2HPO_4, 20 mM NaH_2PO_4, 100 mM NaCl, and 0.1 % (v/v) Tween 20. Membranes were incubated with the primary anti-eNOS antibody (1:2000 dilution made up in PBST; BD Biosciences, Oxford, UK) overnight at 4 °C. The membranes were washed 3 times in PBST to remove unbound antibodies before being incubated in the anti-mouse-horseradish peroxidase-conjugated secondary antibody (1:4000 dilution made up in PBST; DAKO, Ely, Cambridgeshire, UK) for 1 hr at room temperature. A final triplicate wash was performed in PBST to remove unbound secondary antibody, and then protein bands were visualised using an enhanced chemiluminescence kit (ECL Plus; Amersham Biosciences, Buckinghamshire, UK) according to the manufacturer's protocol.

4.2.5 Resin preparation

The amino acids arginine and citrulline can be separated according to their different charges. The resin AG 50W X8 resin (Biorad) binds positively charged species, including arginine. The resin was fully hydrated by washing 4 times with an excess of 1 M NaOH, and then washing in distilled water until the effluent pH was < 8. The resin was made up to a 50 % (v/v) packed resin slurry with 1 mM EDTA in 20 mM pH 7.2 HEPES buffer by 'eye'. This resin was kept stirring prior to the addition to samples to ensure that a constant volume of buffer and resin was added. The efficiency of arginine binding to the resin was tested by counting the radioactive content of the ^{14}C-arginine standards before and after incubation with the resin slurry.

4.2.6 NOS homogenate assay

Hippocampal tissue was added to extraction buffer (EB buffer), maintained at 4 °C, of the following composition: 20 mM HEPES, 1 mM EDTA, 320 mM sucrose, and in the presence of a protease inhibitor cocktail (Roche 1 873 580). 10 mg/ml phenylmethylsulphonyl fluoride (PMSF) was then added, the mixture sonicated, and the homogenate protein content determined as described in chapter 2 (2.4).

The NOS activity of each enzyme extract was determined by the conversion of radiolabelled arginine to citrulline (Knowles & Salter, 1998). Briefly, 20 µl of enzyme extract was added to 230 µl 20 mM HEPES, pH 7.4 containing 50 mM valine, 1 mM DTT, 0.2 mM $CaCl_2$, 1 mM $MgCl_2$, 1 mM L-citrulline, 100 µM NADPH, 10 µM BH_4, 80 U/ml CaM, 1 µM FAD, 1 µM FMN and 19 µM L-arginine, 0.1 µM ^{14}C-arginine. Valine is included in this mixture at such high concentrations to limit arginase activity in the absence of more selective inhibitors. In control reactions 1 mM EGTA was also included. The incubation mix was kept at 37 °C for 20 minutes, and then the reaction terminated by the addition of 750 µl resin slurry and mixing thoroughly. After the resin had settled, 300 µl of the supernatant was taken and added to scintillant, and the radioactive content was determined. The arginine content was expressed as pmol arginine/mg protein.

4.2.7 Data Analysis

All data are presented as the mean ± S.E.M; concentration response data were fitted with the logistic function on Origin 6.1 (equation 4.1). Differences between experimental results were analysed using SPSS and GraphPad Instat software utilizing a one-way or two-way ANOVA with Tukey's post-hoc test; P values of < 0.05 were regarded as significant.

$$y = \frac{A_1 - A_2}{1 + \left(\frac{x}{x_0}\right)^p} + A_2$$

Equation 4.1: Origin logistic function. *Where x = concentration of drug; x_0 = centre point on curve; p = power; A_1 = initial y value; A_2 = final y value; y = cGMP level.*

4.3 Results

4.3.1 Pharmacological discrimination between eNOS and nNOS activity

4.3.1.1 nNOS inhibition

Although there are numerous estimations in the literature regarding the potency of the various NOS inhibitors, a direct comparison is difficult owing to the use of various assay systems, assay conditions and species. As nNOS forms a complex with the NMDA receptor in the hippocampus (Brenman *et al.*, 1996a), NMDA was used as a positive control for nNOS-induced NO production (and thereby nNOS-induced cGMP accumulation) in hippocampal slices. Incubation of slices with increasing concentrations of NMDA resulted in a concentration-dependent increase in cGMP levels which was maximal at 100 μM, with an EC_{50} of 10 μM NMDA (figure 4.4). These results are very similar to those obtained previously (East & Garthwaite, 1991).

Incubation of slices with 100 μM NMDA in the presence of increasing concentrations of three different nNOS inhibitors, L-VNIO, NPA or 1400W, resulted in a concentration-dependent decrease in cGMP levels with IC_{50} values of 0.003 μM (figure 4.5a), 0.03 μM (figure 4.5b), and 0.03 μM (figure 4.5c) respectively. It must be noted that for the purpose of fitting the data in figure 4.5 with the logistic function, the control cGMP level (i.e. cGMP level with no antagonist present) is shown as $1e^{-8}$ μM. These results reveal the nNOS inhibitors to be more potent than observed in previous studies (Table 4.2; Boer *et al.*, 2000; Cooper *et al.*, 2000).

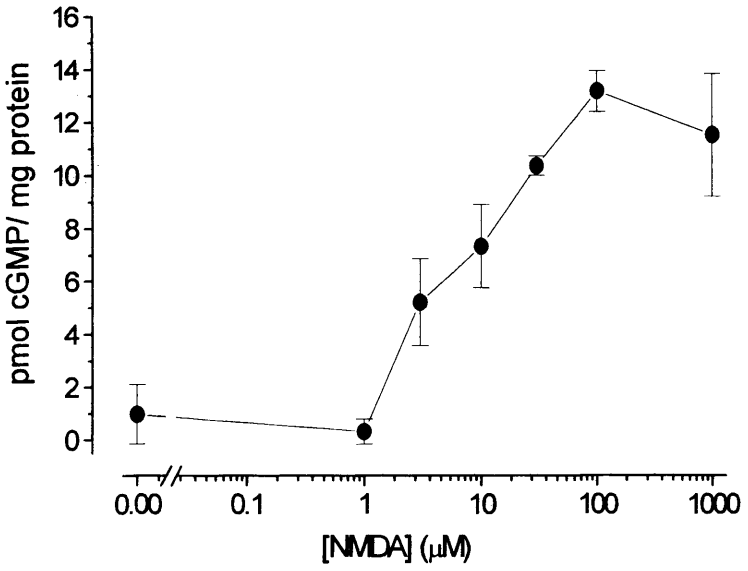

Figure 4.4: Concentration-response curve for NMDA on cGMP levels in adult rat hippocampal slices *(2 min exposure; n = 5).*

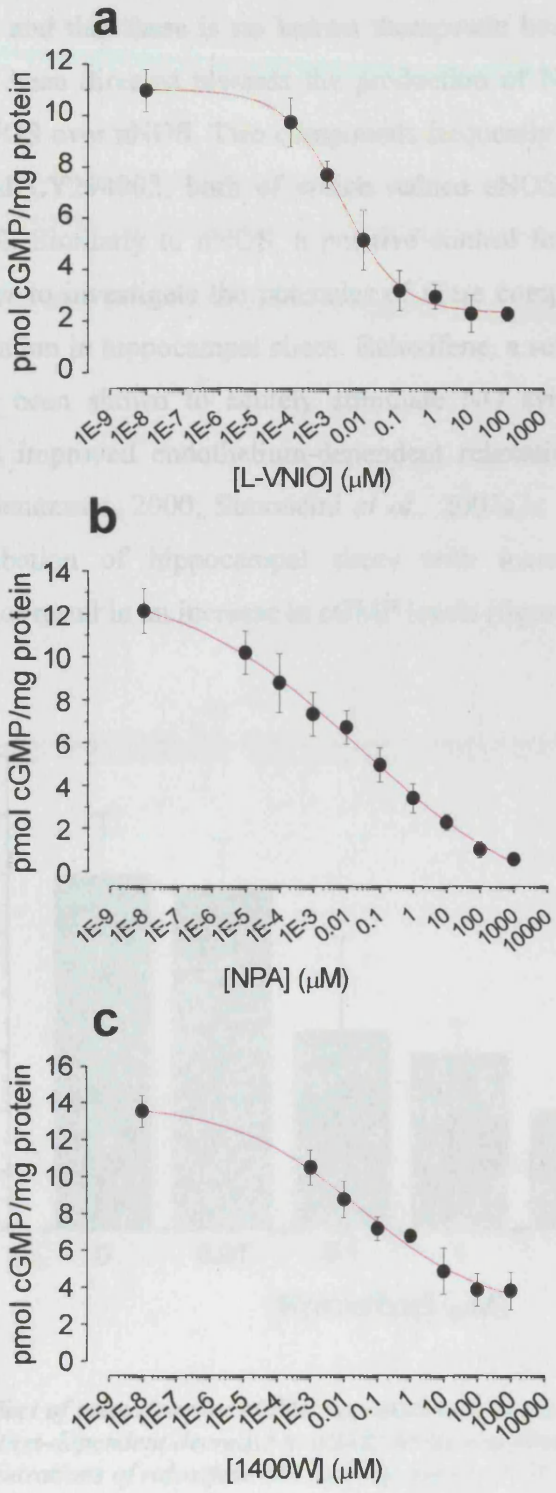

Figure 4.5: Effect of nNOS inhibitors on NMDA-stimulated cGMP levels in adult rat hippocampal slices in presence of IBMX.

A concentration dependent decrease in cGMP levels was observed in the presence of increasing concentrations of (a) L-VNIO, (b) NPA, and (c) 1400W (n = 5).

4.3.1.2 eNOS inhibition

Due to the fact that eNOS activity is essential for the maintenance of blood flow and blood pressure, and that there is no known therapeutic benefit of eNOS inhibition, little effort has been directed towards the production of NOS inhibitors which are selective for eNOS over nNOS. Two compounds frequently used to inhibit eNOS are wortmannin and LY294002, both of which reduce eNOS activity via an indirect action on PI3-K. Similarly to nNOS, a positive control for eNOS-generated NO is required in order to investigate the potencies of these compounds on eNOS-induced cGMP accumulation in hippocampal slices. Raloxifene, a selective oestrogen receptor modulator, has been shown to acutely stimulate NO synthesis, an effect that is associated with improved endothelium-dependent relaxation (Figtree *et al.*, 1999; Simoncini & Genazzani, 2000; Simoncini *et al.*, 2002a,b; Wassmann *et al.*, 2002). However, incubation of hippocampal slices with increasing concentrations of raloxifene did not result in an increase in cGMP levels (figure 4.6).

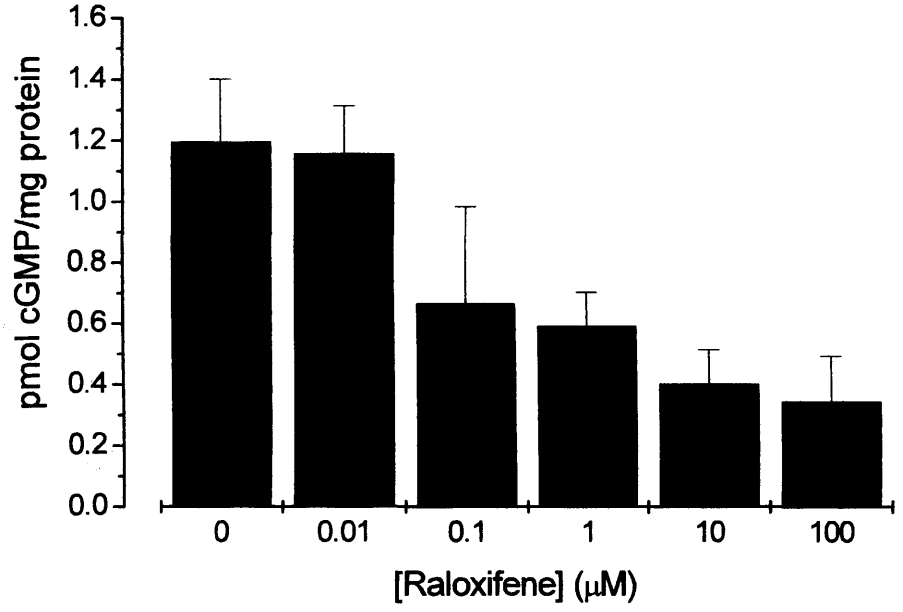

Figure 4.6: Effect of raloxifene on cGMP accumulation in adult rat hippocampal slices. *A concentration-dependent decrease in cGMP levels was observed in the presence of increasing concentrations of raloxifene (30 min exposure; n = 5). 1 mM IBMX was applied to the slices for the final 15 min of incubation with raloxifene.*

In a further attempt to find a positive control for the actions of wortmannin and LY294002, slices were incubated with two alternative compounds at a concentration previously found to stimulate eNOS activity: tumour necrosis factor alpha (TNFα; Barsacchi *et al.*, 2003) and bradykinin (Harris *et al.*, 2001). However, no significant change in cGMP accumulation was observed when hippocampal slices were exposed to either TNFα (figure 4.7a) or bradykinin (figure 4.7b). Furthermore, no significant change in cGMP levels was observed in the presence of wortmannin or LY294002 and TNFα, whereas wortmannin was found to significantly inhibit basal cGMP accumulation in the presence of bradykinin.

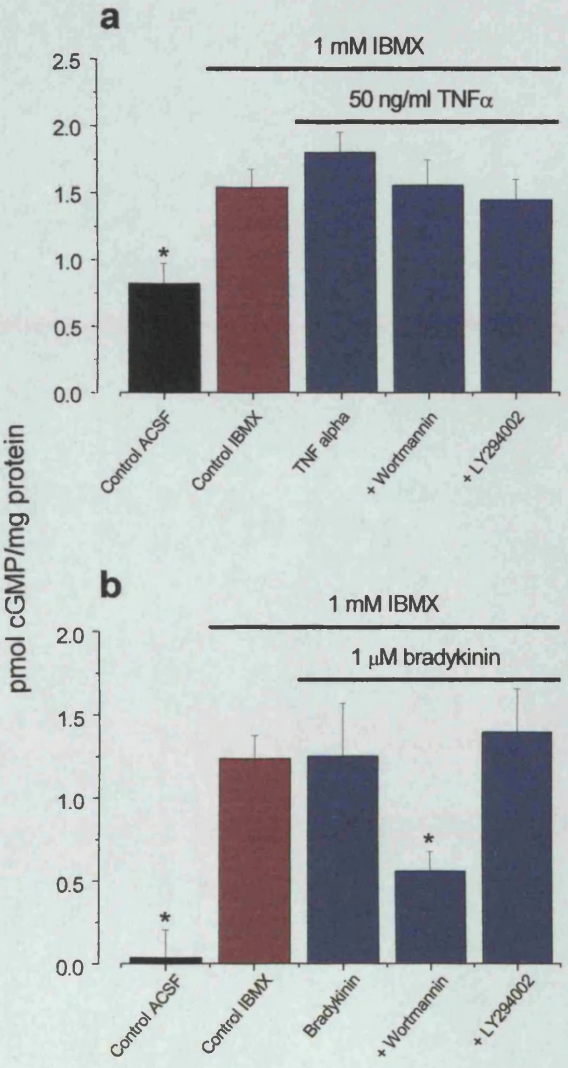

Figure 4.7: Effect of TNFα and bradykinin on cGMP accumulation in adult rat hippocampal slices. *No significant change in cGMP accumulation was seen on application of (a) 50 ng/ml TNFα or (b) 1 μM bradykinin (15 min exposure; n = 5). *P < 0.05 vs. IBMX control; one-way ANOVA with Tukey's post-hoc test.*

When interpreting the results with raloxifene, TNFα, and bradykinin, it must be taken into account that the cGMP levels involved are at the boundary of detection and therefore absolute values are unlikely to be trustworthy. It must also be noted that they are the result of single experiments which were not investigated further given that no significant difference in cGMP accumulation was noted in their presence.

4.3.2 Effect of NOS inhibition on cGMP accumulation in presence of IBMX

4.3.2.1 Measurement of BAY 41-2272-stimulated cGMP production

The effect of BAY 41-2272 on cGMP levels in rat hippocampal slices was measured in the presence of the general PDE inhibitor, IBMX (figure 4.8). In the absence of BAY 41-2272, the cGMP content of the hippocampal slice was determined to be 2.9 ± 0.7 pmol cGMP/mg protein. Incubation of slices with increasing concentrations of BAY 41-2272 resulted in a concentration-dependent increase of cGMP levels. Based on the ensuing accumulation of cGMP, the EC_{50} for BAY 41-2272 was 10 μM (figure 4.8). To gauge the proportion of the cGMP response that could be regarded as NO-dependent, slices were incubated with increasing concentrations of BAY 41-2272 in the presence of the general NOS inhibitor, L-NNA (100 μM). Incubation with L-NNA prevented the increase in cGMP levels produced by BAY 41-2272, although a residual increase in NOS-insensitive cGMP levels can be observed at the highest concentration of BAY 41-2272. This residual increase is presumably attributable to the direct activation of NO-activated GC by BAY 41-2272. 30 μM BAY 41-2272 resulted in almost maximal stimulation of NO-activated GC whilst having a relatively small NO-insensitive component, and therefore this concentration was used in all subsequent experiments.

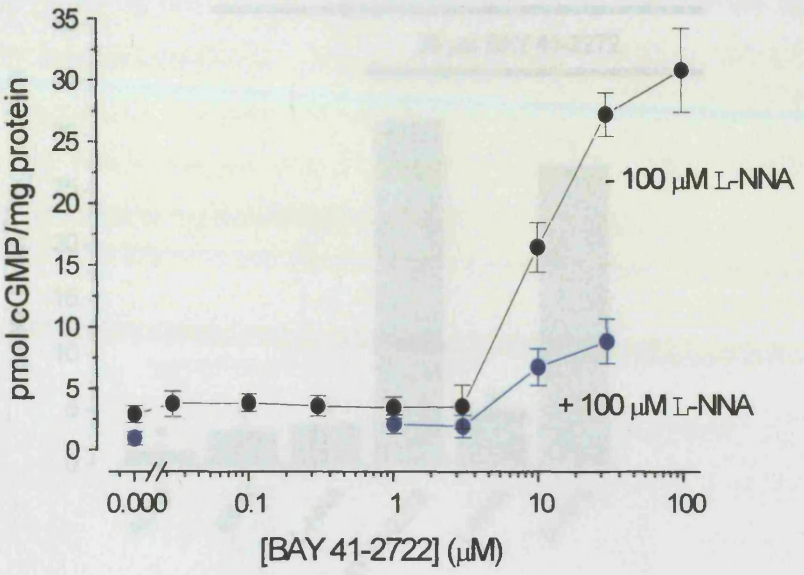

Figure 4.8: Concentration-response curve for BAY 41-2272 on cGMP levels in adult rat hippocampal slices. *A concentration- dependent increase in cGMP levels was observed on application of BAY 41-2272 (5 min exposure) which was significantly inhibited in the presence of 100 µM L-NNA (n = 6).*

4.3.2.2 Effect of different NOS inhibitors in rat hippocampal slices

No significant difference in basal cGMP levels was observed in the presence or absence of the general NOS inhibitor, L-NNA (100 µM). However, incubation with 30 µM BAY 41-2272, a concentration of BAY 41-2272 previously found to enhance NO-dependent cGMP formation, resulted in a ~ 10-fold increase in cGMP levels (figure 4.9). This increase was inhibited by 100 µM L-NNA to a cGMP level not significantly different to that obtained following incubation with L-NNA in the absence of BAY 41-2272, confirming that endogenous NO production was responsible for the increased level of cGMP. In contrast, no significant effect on NO-dependent cGMP production was observed by the application of the NMDA antagonist, D-AP5 (100 µM). This suggests that endogenous NO production in the hippocampus is NOS-dependent, but NMDA receptor-independent.

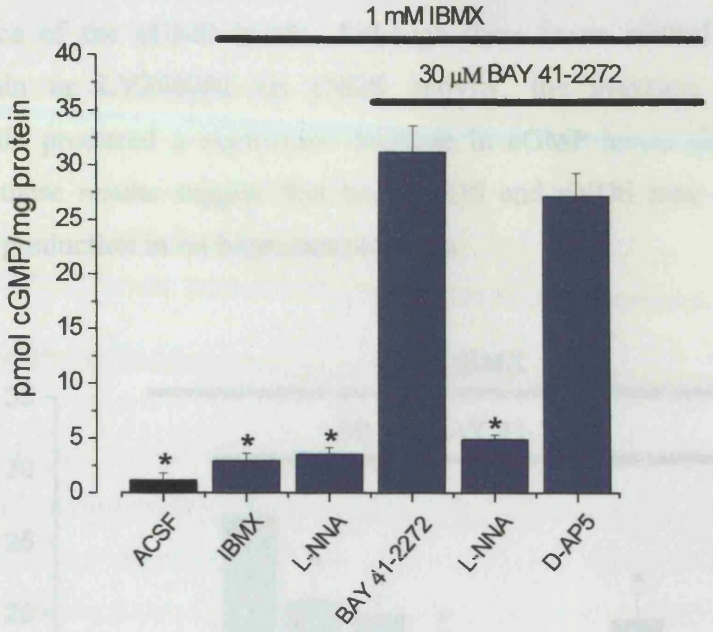

Figure 4.9: Endogenous NOS activity in adult rat hippocampal slices.
*Slices were incubated in the presence of 1 mM IBMX for 15 min; no significant change in cGMP levels was observed in the presence of L-NNA (100 µM). Incubation with BAY 41-2272 (5 min exposure 30 µM) resulted in an increase of cGMP accumulation which was inhibited by L-NNA (100 µM), but was unaffected by D-AP5 (100 µM; n = 5). *P < 0.05 vs. BAY 41-2272- treated slices; one-way ANOVA with Tukey's post-hoc test.*

The finding that basal NO-dependent cGMP levels were NMDA receptor-independent indicates that the nNOS isoform may play little or no role in basal NO production in the hippocampus. In order to investigate this matter further, and to determine which isoform of NOS may be responsible, hippocampal slices were exposed to different NOS inhibitors in the presence of BAY 41-2272. In accordance with previous observations, application of 30 µM BAY 41-2272 resulted in an increase in cGMP accumulation. This increase was significantly reduced by ~ 25 % following incubation with L-VNIO (0.1 µM), 1400W (1 µM), or NPA (1 µM; figure 4.10). Concentrations of L-VNIO, 1400W and NPA were chosen that produced ≥ 80 % inhibition of nNOS activity, but that were not supramaximal so as to avoid potential inhibition of eNOS activity since all three compounds are also known to inhibit eNOS activity, albeit with a lower potency (Boer *et al.*, 2000; Zhang *et al.*, 1997). As 1400W is a more potent inhibitor of iNOS than nNOS (Boer *et al.*, 2000; Young *et al.*, 2000), application of 1400W is additionally a control for the contribution of iNOS to endogenous NO levels. Two different general NOS inhibitors

(L-NIO and L-NNA) significantly inhibited cGMP accumulation, confirming the NO-dependence of the cGMP levels. Although there is no control for the action of wortmannin or LY294002 on eNOS activity, the presence of LY294002 or wortmannin produced a significant decrease in cGMP levels (figure 4.10). Taken together, these results suggest that both eNOS and nNOS may contribute towards basal NO production in rat hippocampal slices.

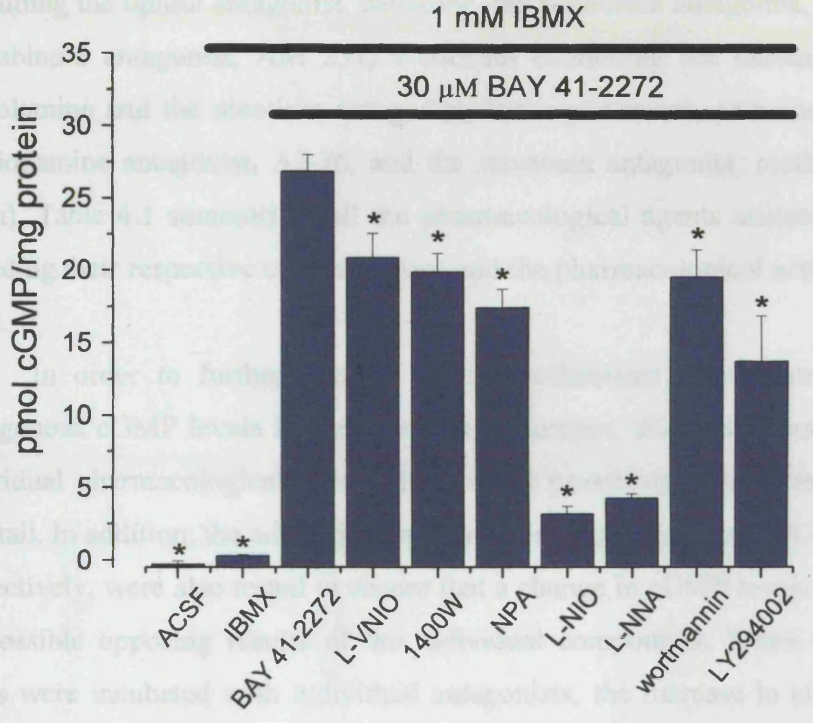

Figure 4.10: Effect of different NOS inhibitors on cGMP levels in adult rat hippocampal slices. *Incubation of slices with nNOS inhibitors (L-VNIO, 0.1μM; 1400W, 1 μM; NPA, 1 μM) resulted in the reduction of cGMP levels by ~ 25 %. Application of 100 μM L-NNA or 100 L-NIO almost completely inhibited cGMP accumulation, whereas 1 μM wortmannin and 50 μM LY294002 reduced cGMP levels by up to 50 % (n = 5). *P < 0.05 vs. BAY 41-2272 treated slices; one-way ANOVA with Tukey's post-hoc test.*

4.3.3 Effect of neurotransmitter inhibitors on cGMP accumulation in rat hippocampal slices

Pharmacological agents were used to investigate potential mechanisms which may contribute to changes in cGMP levels in hippocampal slices under resting conditions. Slices were incubated in ACSF containing 1 mM IBMX for 15 min in the presence or absence of a cocktail containing 2 - 3 pharmacological antagonists. Initially, various antagonist cocktails were used in order to detect any mechanisms worthy of further

study. The increase in cGMP production observed following 5 min exposure to BAY 41-2272 was reduced by the AMPA antagonists, CNQX and NBQX, the voltage-gated Na^+ channel inhibitor, tetrodotoxin (TTX), a cocktail of the α and β adrenoreceptor antagonists, nicergoline and sotalol, and by the NO-activated GC inhibitor, ODQ (figure 4.11a). No significant effect on cGMP accumulation was observed upon incubation with the mGluR antagonist, MCPG, a cocktail containing the $GABA_A$ antagonist, picrotoxin and the muscarinic antagonist, atropine, a cocktail containing the opioid antagonist, naloxone, the adenosine antagonist, DPCPX and the cannabinoid antagonist, AM 251, a cocktail containing the muscarinic antagonist, scopolamine and the nicotinic antagonist, benzoquinonium, or a cocktail containing the dopamine antagonist, AJ-76, and the serotonin antagonist, methysergide (figure 4.11a). Table 4.1 summarises all the pharmacological agents utilised in figure 4.11, including their respective concentrations and the pharmacological actions attributed to them.

In order to further explore which mechanisms may contribute to resting endogenous cGMP levels in the rodent hippocampus, slices were incubated with the individual pharmacological agents that looked promising when present as part of a cocktail. In addition, the adenosine and cannabinoid antagonists, DPCPX and AM 251 respectively, were also tested to ensure that a change in cGMP levels was not masked by possible opposing results of the individual compounds. When rat hippocampal slices were incubated with individual antagonists, the increase in cGMP production induced by 5 min exposure to BAY 41-2272 was reduced by incubation with TTX, CNQX, AM 251, DPCPX, sotalol or in the absence of external Ca^{2+} (Ca^{2+}-free ACSF containing the Ca^{2+} chelator, EGTA (1 mM; figure 4.11b). No significant effect on cGMP accumulation was observed in the presence of nicergoline. These results suggest that resting cGMP levels in the hippocampus may be influenced by Na^+ channels, AMPA receptors, cannabinoid receptors, adenosine receptors, β adrenoreceptors, and is partially dependent on external Ca^{2+}.

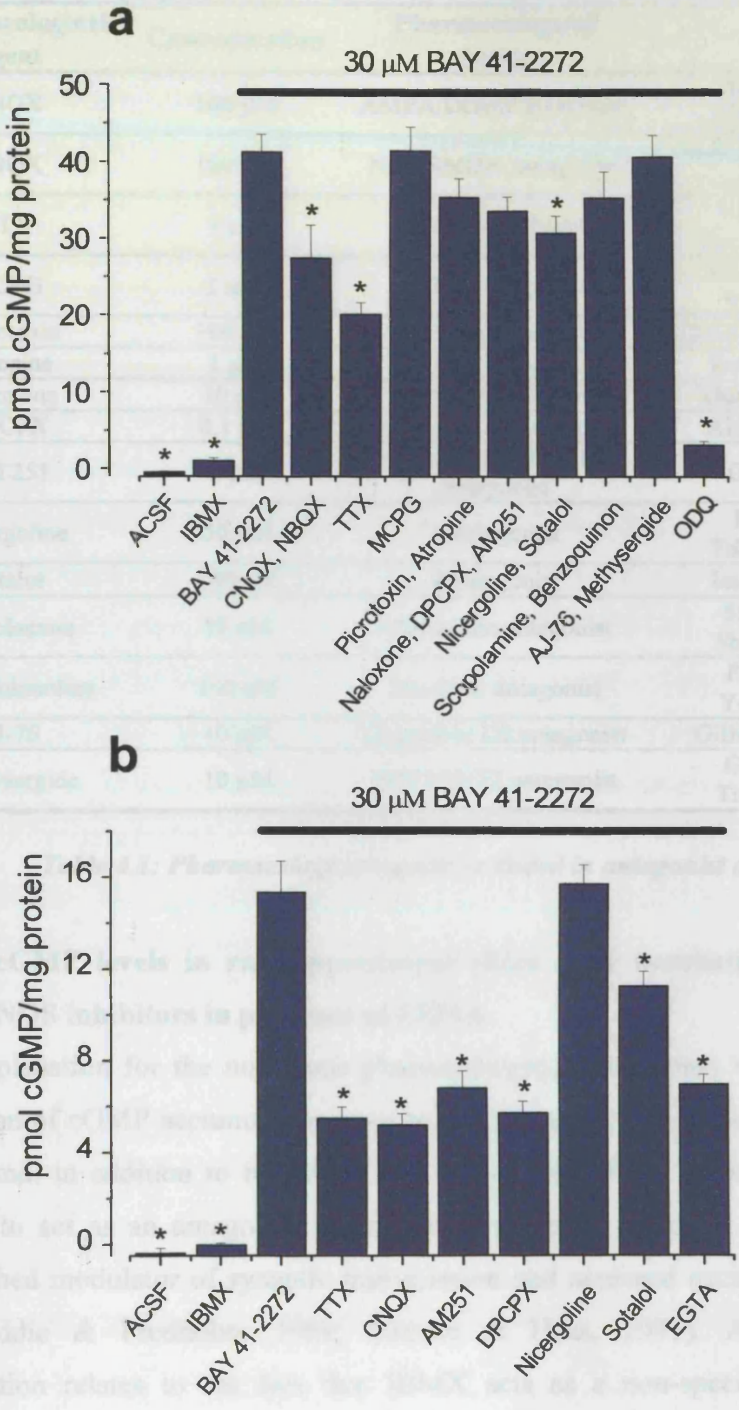

Figure 4.11: Effect of pharmacological agents on cGMP levels in adult rat hippocampal slices. *Incubation of slices in ACSF containing IBMX (1mM) and BAY 41-2272 (30 μM) in the absence or presence of a variety of pharmacological agents: CNQX (100 μM), NBQX (100 μM), TTX (1 μM), MCPG (1 mM), picrotoxin (100 μM), atropine (1 μM), naloxone (10 μM), DPCPX (0.1 μM), AM251 (2 μM), nicergoline (50 μM), sotalol (100 nM), scopolamine (50 μM), benzoquinonium (100 nM), AJ-76 (10 μM), methysergide (100 nM), ODQ (1 μM) and EGTA (1 mM). *P < 0.05 vs. BAY 41-2272 treated slices; one-way ANOVA with Tukey's post-hoc test.*

Pharmacological Agent	Concentration	Pharmacological Action	Reference
CNQX	100 µM	AMPA/kainate antagonist	Blake *et al.*, 1989 Yamada *et al.*, 1989
NBQX	100 µM	Non-NMDA antagonist	Goldstein & Litwin, 1993 Cronberg *et al.*, 2004
TTX	1 µM	Na channel blocker	Kaneda *et al.*, 1989 Kononenko *et al.*, 2004
MCPG	1 mM	mGluR antagonist	Frenguelli *et al.*, 1993 Davies *et al.*, 1995
Picrotoxin	100 µM	GABA A antagonist	Chevaleyre & Castillo, 2004
Atropine	1 µM	mAChR antagonist	Imbrogno *et al.*, 2003
Naloxone	10 µM	Opioid antagonist	Dunwiddie *et al.*, 1982
DPCPX	0.1 µM	Adenosine A1 antagonist	Alzheimer *et al.*, 1991
AM 251	2 µM	Cannabinoid CB1 antagonist	Gately *et al.*, 1996
Nicergoline	50 µM	α antagonist	Heitz *et al.*, 1986 Takahashi *et al.*, 1990
Sotalol	100 nM	β antagonist	Imbrogno *et al.*, 2003
Scopolamine	50 µM	Muscarinic antagonist	Shibata *et al.*, 1992 Shinoura *et al.*, 2002
Benzoquinonium	100 nM	Nicotinic antagonist	Pereira *et al.*, 1993 Yeoman *et al.*, 1993
AJ-76	10 µM	Dopamine D2 antagonist	Gifford & Johnson, 1993
Methysergide	10 µM	5HT1/5HT2 antagonist	Ge & Barnes, 1996 Tuladhar *et al.*, 1996

Table 4.1: Pharmacological agents included in antagonist cocktails.

4.3.4 cGMP levels in rat hippocampal slices after incubation with different NOS inhibitors in presence of EHNA

One explanation for the numerous pharmacological antagonists which result in the inhibition of cGMP accumulation may be due to the fact that IBMX is not a "clean" compound: in addition to its action as a non-specific PDE inhibitor, IBMX is also known to act as an antagonist of adenosine receptors (Choi *et al.*, 1988), a well-established modulator of synaptic transmission and neuronal excitability in the CNS (Dunwiddie & Fredholm, 1989; Greene & Haas, 1991). A second possible explanation relates to the fact that IBMX acts as a non-specific PDE inhibitor, preventing the breakdown of cAMP as well as cGMP. Various studies find that cross-talk arises between the cAMP and cGMP signalling pathways capable of cross-modulation of each other's synthesis, degradation and actions (Vigne *et al.*, 1994; Suvarna & O'Donnell, 2002). Therefore the fact that IBMX inhibits the breakdown of both cAMP and cGMP may also potentially complicate the interpretation of biochemical results.

In order to address this possibility, cGMP accumulation experiments were repeated using the selective PDE2 inhibitor, EHNA. PDE2 exhibits strong expression in neurons of the hippocampus (Repaske *et al.*, 1993), and although it is able to degrade both cAMP and cGMP with similar K_m and K_d *in vitro* (Martins *et al.*, 1982), studies carried out on cortical neurons and hippocampal slices indicate that PDE2 inhibition selectively increases only cGMP levels (Suvarna & O'Donnell, 2002; Boess *et al.*, 2004).

4.3.4.1 Optimisation of EHNA concentration in presence of BAY 41-2272

In order to determine the optimum concentration of EHNA required for PDE2 inhibition, cGMP accumulation was determined in hippocampal slices following exposure to BAY 41-2272. Exposure of hippocampal slices to 30 μM BAY 41-2272 (5 min) in the presence of increasing concentrations of EHNA resulted in a concentration dependent increase in cGMP levels (figure 4.12). Over the concentration range investigated, the increase in cGMP accumulation did not reach a maximum, an observation consistent with previous findings (van Staveren *et al.*, 2001). A concentration of 300 μM EHNA produced roughly equivalent cGMP accumulation to that observed with IBMX (figure 4.4), and therefore this concentration was used in all subsequent experiments.

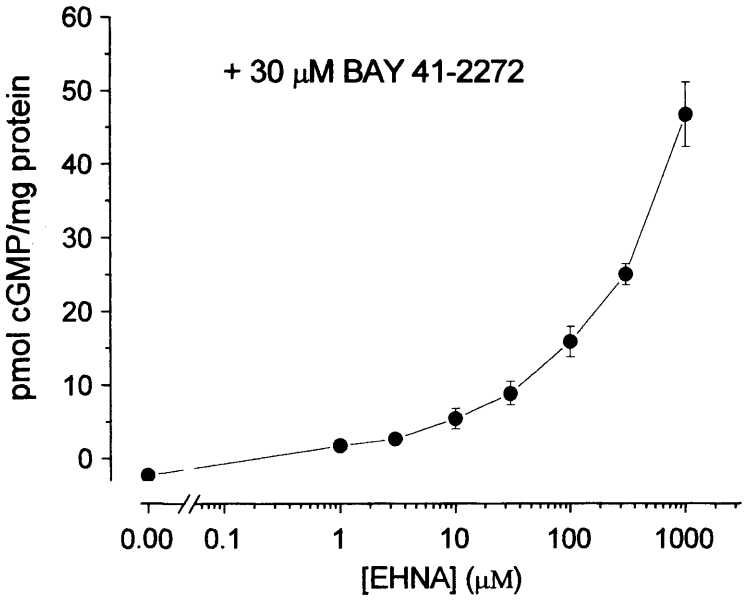

Figure 4.12: Concentration-response curve for EHNA on cGMP levels in adult rat hippocampal slices. *(15 min exposure; n = 5).*

4.3.4.2 Selectivity of nNOS inhibitors on cGMP accumulation

To check the validity of the control experiments obtained in the presence of IBMX, cGMP accumulation was measured in response to 2 min exposure to NMDA in the presence of EHNA (300 μM). Similar to observations in the presence of IBMX, incubation of slices with increasing concentrations of NMDA resulted in a concentration-dependent increase of cGMP levels which was maximal at 100 μM, with an EC_{50} of ~ 10 μM NMDA (figure 4.13).

As previous estimations for the nNOS inhibitor IC_{50} values were obtained in the presence of IBMX, the potencies of the nNOS inhibitors in the presence of EHNA were tested. Incubation of slices with 100 μM NMDA in the presence of increasing concentrations of L-VNIO and 1400W, resulted in a concentration-dependent decrease in cGMP levels with IC_{50} values of 0.01 μM (figure 4.14a), and 0.01 μM (figure 4.14b), respectively. Similarly to results obtained in the presence of IBMX, for the purpose of fitting the data in figure 4.14 with the logistic function, the control cGMP level (i.e. cGMP level with no antagonist present) is shown as $1e^{-9}$ μM. These results reveal the potencies of L-VNIO and 1400W for nNOS inhibition to be very similar whether in the presence of IBMX or EHNA.

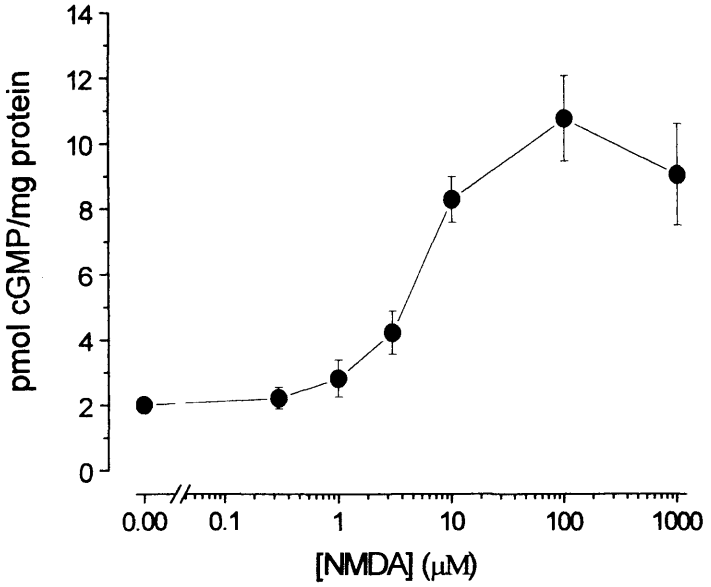

Figure 4.13: Concentration-response curve for NMDA-stimulated cGMP levels in adult rat hippocampal slices in presence of EHNA *(2 min exposure to NMDA; n = 5).*

In order to test the selectivity of the inhibitors for nNOS over eNOS at the concentrations used in all subsequent experiments, their action on cGMP accumulation was observed in rat hippocampal slices following NMDA activation (nNOS), and in aortic rings following ACh stimulation (eNOS). Incubation of hippocampal slices with 100 μM NMDA resulted in a ~ 10-fold increase in cGMP levels, which was inhibited by the presence of 1 μM 1400W, 1 μM NPA or 0.1 μM L-VNIO (figure 4.15a). This confirms that NO-generation from nNOS is predominantly inhibited at these concentrations.

In contrast, incubation of aortic rings with 10 μM ACh resulted in a ~ 12-fold increase in cGMP levels which was not significantly affected by the presence of 1 μM 1400W, 1 μM NPA or 0.1 μM L-VNIO (Figure 4.15b). However, this increase was prevented by 100 μM L-NNA, confirming that endogenous NO production was responsible for the increased level of cGMP. Therefore these results indicate that at the concentrations applied, 1400W, NPA and L-VNIO are all selective inhibitors for the nNOS over the eNOS isoform.

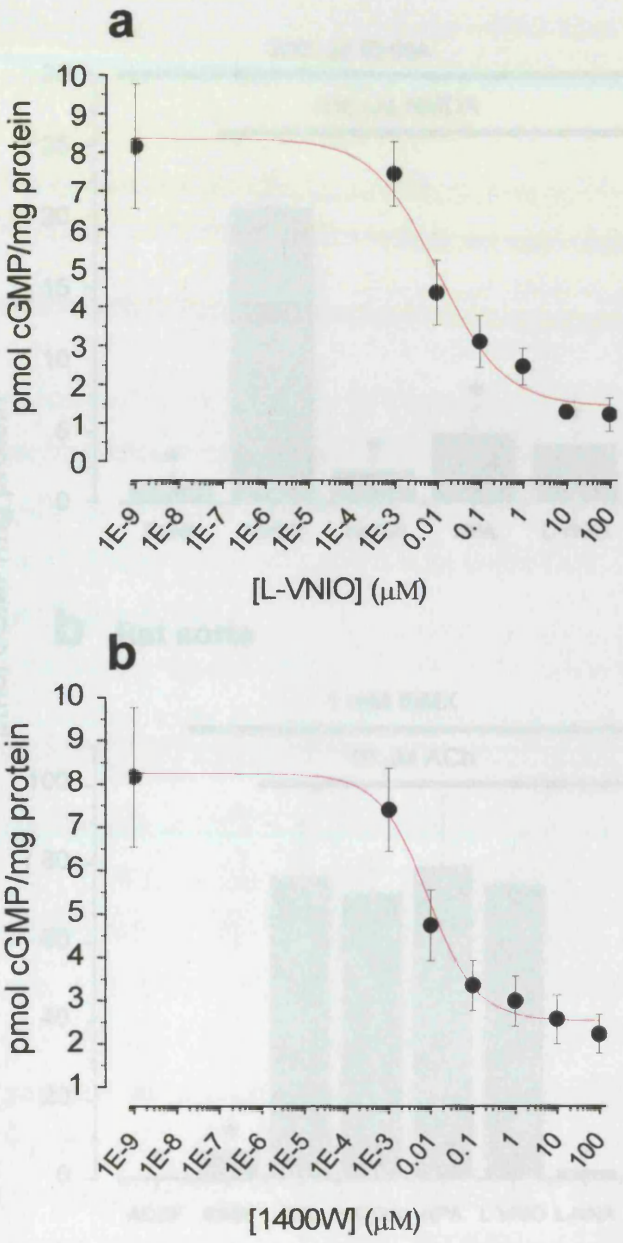

Figure 4.14: Effect of nNOS inhibitors on NMDA-stimulated cGMP levels in adult rat hippocampal slices in presence of EHNA.
A concentration dependent decrease in cGMP levels was observed in the presence of increasing concentrations of (a) L-VNIO, and (b) 1400W (n = 5).

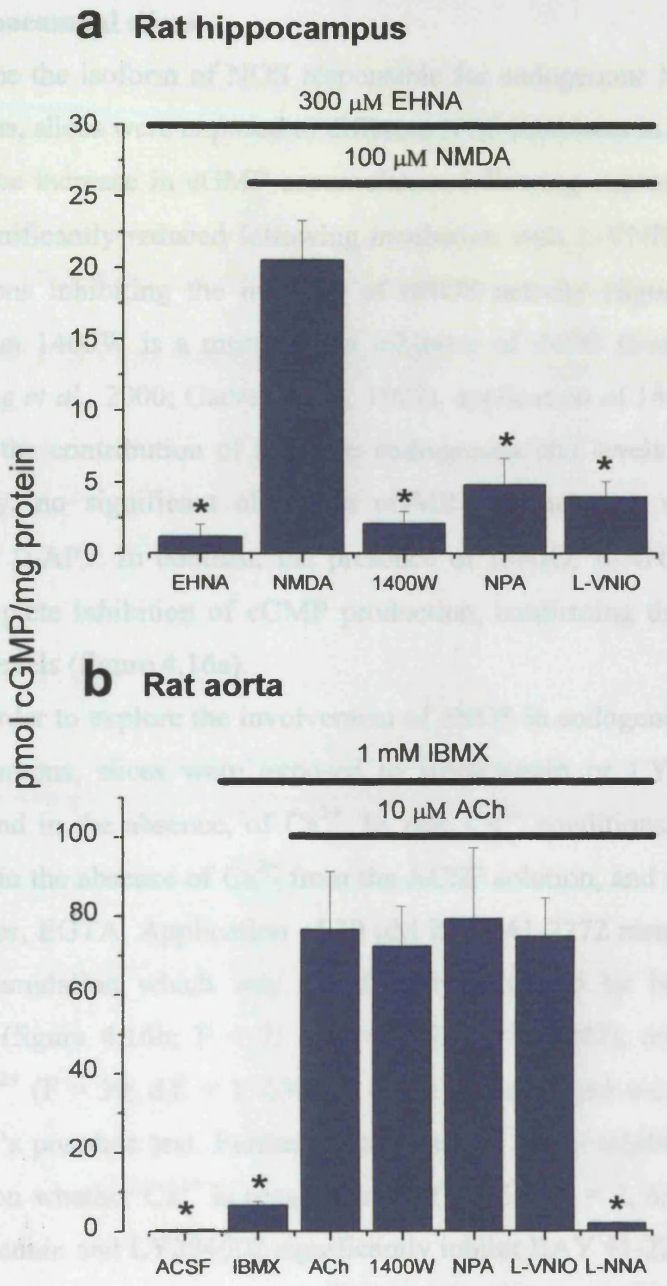

Figure 4.15: Selectivity of nNOS inhibitors.

*(a) Adult rat hippocampal slices were incubated in the presence of 300 μM EHNA for 15 min. Application of BAY 41-2272 (30 μM; 5 min exposure) resulted in an increase in cGMP accumulation which was inhibited by 1400W (1 μM), NPA (1 μM) or L-VNIO (0.1 μM). (b) Adult rat aortic rings were incubated in the presence of 1 mM IBMX for 15 min. ACh (10 μM; 1 min exposure) resulted in an increase in cGMP accumulation which was prevented by L-NNA (100 μM). No significant change in cGMP levels was observed in the presence of 1400W (1 μM), NPA (1 μM) or L-VNIO (0.1 μM). *P < 0.05 vs. NMDA or ACh treated slices (n = 5); one-way ANOVA with Tukey's post-hoc test.*

4.3.4.3 Effect of different NOS inhibitors on cGMP accumulation in rat hippocampal slices

To determine the isoform of NOS responsible for endogenous NO production in the hippocampus, slices were exposed to different NOS inhibitors in the presence of BAY 41-2272. The increase in cGMP accumulation following exposure to BAY 41-2272 was not significantly reduced following incubation with L-VNIO, 1400W or NPA at concentrations inhibiting the majority of nNOS activity (figure 4.16a). Given the evidence that 1400W is a more potent inhibitor of iNOS than nNOS (Boer *et al.*, 2000; Young *et al.*, 2000; Garvey *et al.*, 1997), application of 1400W is additionally a control for the contribution of iNOS to endogenous NO levels in the hippocampus. Additionally, no significant effect on cGMP accumulation was observed in the presence of D-AP5. In contrast, the presence of L-NIO, L-NNA or ODQ produced almost complete inhibition of cGMP production, confirming the NO-dependence of the cGMP levels (figure 4.16a).

In order to explore the involvement of eNOS in endogenous NO production in the hippocampus, slices were exposed to wortmannin or LY294002, both in the presence, and in the absence, of Ca^{2+}. In zero Ca^{2+} conditions, the experiment was carried out in the absence of Ca^{2+} from the ACSF solution, and in the presence of the Ca^{2+}-chelator, EGTA. Application of 30 μM BAY 41-2272 resulted in an increase in cGMP accumulation which was significantly inhibited by both wortmannin and LY294002 (figure 4.16b; $F = 7$; d.f. = 2, 63; $P = 0.002$), and by the absence of external Ca^{2+} ($F = 39$; d.f. = 1, 63; $P < 0.001$), as analysed using two-way ANOVA with Tukey's post-hoc test. Furthermore the effect of the inhibitors was found to be dependent on whether Ca^{2+} is present or not ($F = 5$; d.f. = 2, 63; $P = 0.011$): that is, both wortmannin and LY294002 significantly inhibit BAY 41-2272-stimulated cGMP accumulation in the presence of Ca^{2+}, whereas they have no significant effect on cGMP levels when compared to the zero Ca^{2+} BAY 41-2272 control (figure 4.16b).

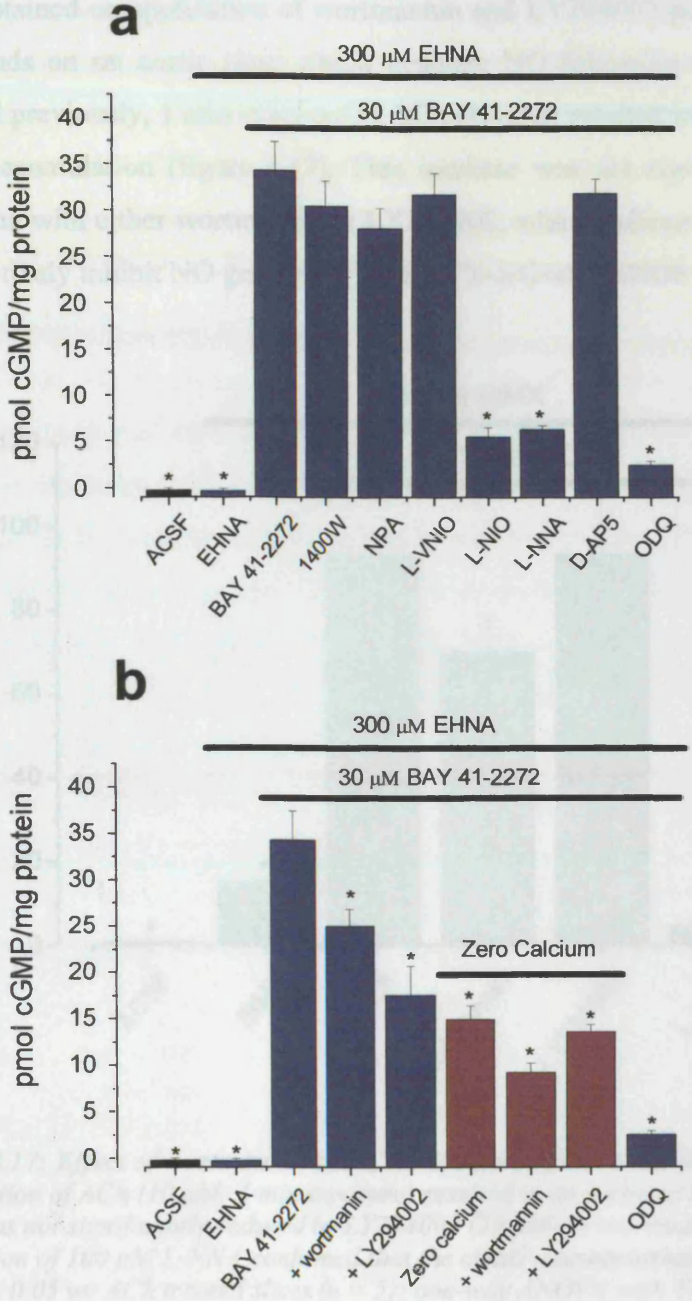

Figure 4.16: Effect of different NOS inhibitors on cGMP levels in adult rat hippocampal slices. *Application of BAY 41-2272 (30 μM; 5 min exposure) resulted in an increase in cGMP accumulation which was (a) not significantly inhibited by the presence of nNOS inhibitors (L-VNIO, 0.1 μM; 1400W, 1 μM; NPA, 1 μM) or D-AP5, but was significantly decreased by application of 100 μM L-NNA or 100 μM L-NIO. *P < 0.05 BAY 41-2272 treated slices (n = 5); one-way ANOVA with Tukey's post-hoc test. (b) Incubation with wortmannin (1 μM; 45 min exposure) or LY294002 (20 μM; 25 min exposure) significantly reduced BAY 41-2272-stimulated cGMP accumulation, both in the presence and absence of external Ca^{2+}, when compared with BAY 41-2272 treated slices in the presence of Ca^{2+}. *P < 0.05 BAY 41-2272 treated slices (n = 8 - 14); one-way ANOVA with Tukey's post-hoc test.*

The inconclusive results for the involvement of eNOS in endogenous NO levels obtained on application of wortmannin and LY294002 prompted tests of these compounds on rat aortic rings which generate NO following eNOS activation. As observed previously, 1 min exposure to ACh (10 μM) resulted in ~ 10-fold increase in cGMP accumulation (figure 4.17). This increase was not significantly changed by incubation with either wortmannin or LY294002, which indicates both compounds do not effectively inhibit NO generation from ACh-activated eNOS in rat aorta.

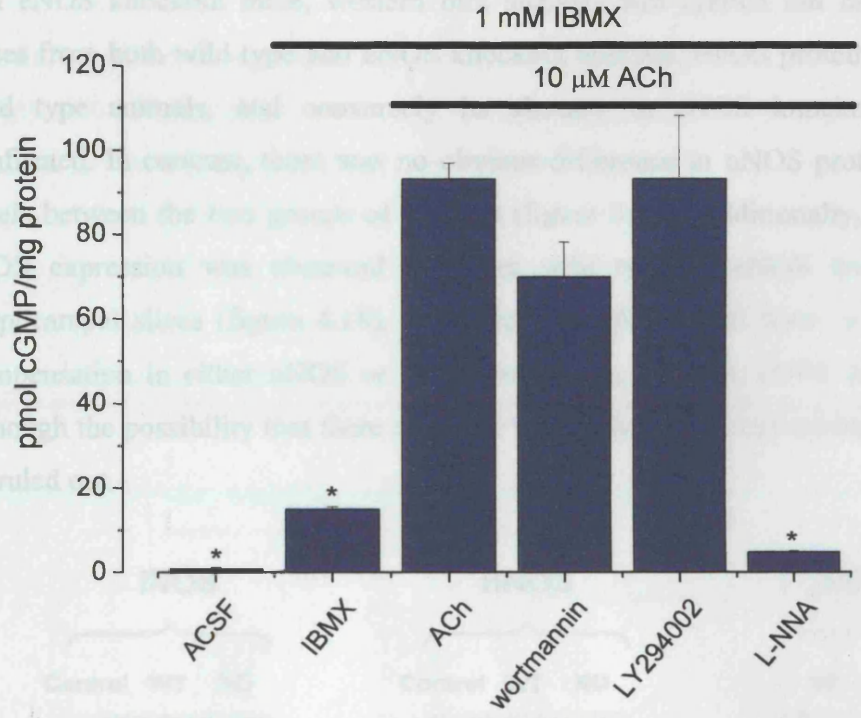

Figure 4.17: Effect of wortmannin and LY294002 on cGMP levels in adult rat aortic rings. *Application of ACh (10 μM; 1 min exposure) resulted in an increase in cGMP accumulation which was not significantly reduced by LY294002 (20 μM) or wortmannin (1 μM). Subsequent addition of 100 μM L-NNA confirmed that the cGMP accumulation was NOS-mediated. *P < 0.05 vs. ACh treated slices (n = 5); one-way ANOVA with Tukey's post-hoc test.*

4.3.4.4 Effect of different NOS inhibitors on cGMP accumulation in mouse hippocampal slices

The absence of selective eNOS inhibitors prevents the direct testing of the contribution that eNOS plays in generating endogenous cGMP production in the rat hippocampus. Therefore, in order to explore the contribution of eNOS towards tonic levels of NO in the hippocampus, cGMP levels were analysed in hippocampal slices obtained from 8 - 12 week old eNOS knockout (Huang *et al.,* 1995a) or wild type (129SV/C57BL/6) mice. In order to check NOS isoform expression in the wild type and eNOS knockout mice, western blot analysis was carried out on hippocampal slices from both wild type and eNOS knockout animals. eNOS protein expression in wild type animals, and conversely its absence in eNOS knockout mice, was confirmed. In contrast, there was no obvious difference in nNOS protein expression levels between the two groups of animals (figure 4.18). Additionally, no significant iNOS expression was observed in either wild type or eNOS knockout mouse hippocampal slices (figure 4.18). These results indicate that there is no significant compensation in either nNOS or iNOS expression levels in eNOS knockout mice, although the possibility that there might be subtle changes in expression levels cannot be ruled out.

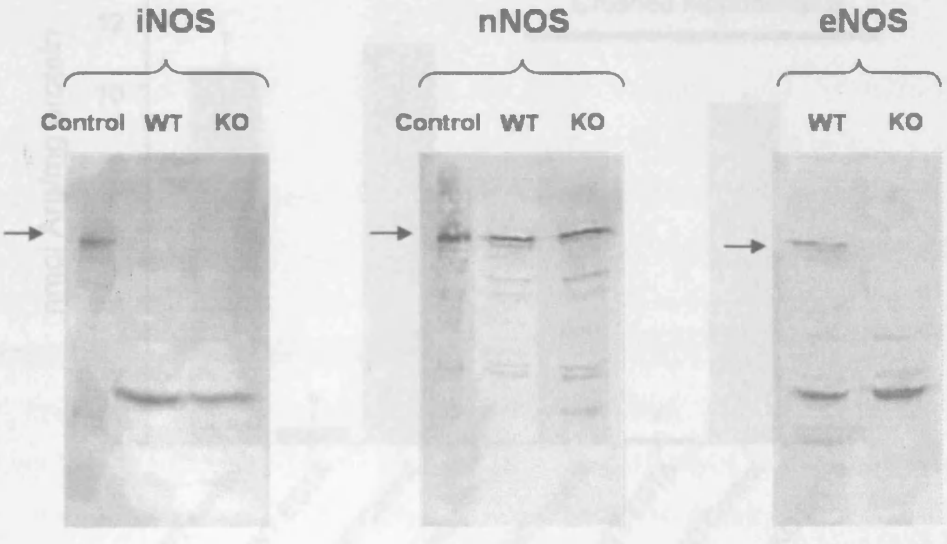

Figure 4.18: Western blot analysis of NOS protein in wild type and eNOS knockout mouse hippocampus.

No difference in iNOS or nNOS expression was observed between wild type (WT) and eNOS knockout (KO) hippocampal slices. The absence of eNOS expression in eNOS knockout animals was also confirmed. Arrows indicate position of NOS protein.

In order to investigate the possibility that iNOS is up-regulated within eNOS knockout mice, functional NOS activity within the mouse hippocampus was determined by means of the conversion of radio-labelled arginine to citrulline. Comparison of wild type and eNOS knockout hippocampal slices by means of two-way ANOVA analysis with a Tukey's post-hoc test, however, revealed no significant difference in NOS activity ($F = 0.02$; d.f. = 1, 79; $P = 0.885$; figure 4.19). Slices were incubated in carbogenated ACSF for 1 – 2 hr in a shaking waterbath at 30 °C to be consistent with the biochemical studies. No significant difference was also observed when the hippocampus was removed, the two ends removed, and then immediately frozen, crushed and sonicated without any incubation ($F = 4$; d.f. = 1, 79; $P = 0.06$; figure 4.19). In contrast, when nNOS and eNOS activity was prevented by the removal of Ca^{2+} (which is obligatory for eNOS and nNOS activity) using the Ca^{2+} chelator, EGTA, the conversion of arginine to citrulline was almost completely inhibited ($F = 227$; d.f. = 1, 79; $P < 0.001$). This condition presumably reflects no significant change in iNOS activity between wild type and eNOS knockout hippocampi, since iNOS activity is Ca^{2+}-independent.

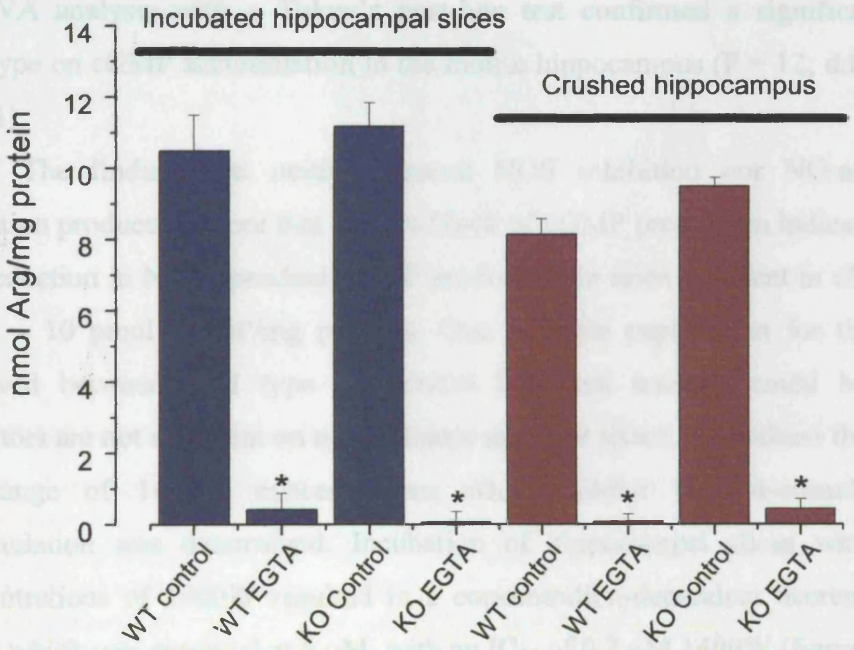

Figure 4.19: NOS activity in wild type and eNOS knockout mouse hippocampus. *No significant difference in NOS activity was observed between wild type (WT) and eNOS knockout (KO) hippocampi (n = 5). Incubated slices: 400 μm hippocampal slices incubated for 1 - 2 hr at 30 °C in a shaking waterbath, frozen, crushed and sonicated. Crushed hippocampus: fresh hippocampi were frozen immediately, crushed and sonicated. *P < 0.05 vs. WT controls; one-way ANOVA with Tukey's post-hoc test.*

Following validation of the eNOS knockout model, the contribution of eNOS towards basal NO production was explored by analysis of cGMP levels in hippocampal slices obtained from eNOS knockout or wild type mice in the presence of EHNA. Both experiments were run side-by-side and using the same solutions to ensure directly comparable results. Similar to the findings in the rat hippocampus, 5 min exposure to BAY 41-2272 resulted in an increase in cGMP production in the mouse hippocampus (figure 4.20). In wild type mice the increase in cGMP accumulation was not significantly changed by nNOS inhibition (1400W, NPA, and L-VNIO) or NMDA receptor inhibition (D-AP5), whereas incubation with general NOS inhibitors (L-NNA and L-NIO) or ODQ resulted in significant reduction in cGMP levels (figure 4.20a).

The increase in cGMP accumulation observed in eNOS knockout mice following 5 min exposure to BAY 41-2272 was not significantly changed by incubation with 1400W, NPA, L-VNIO, L-NIO, L-NNA or D-AP5 (figure 4.20b). However, the increase in cGMP level was significantly decreased by the application of ODQ, although to a lesser degree than observed in wild type animals. Comparison of cGMP levels between eNOS knockout and wild type animals by means of two-way ANOVA analysis with a Tukey's post-hoc test confirmed a significant effect of genotype on cGMP accumulation in the mouse hippocampus ($F = 12$; d.f. = 1, 264; $P = 0.01$).

The finding that neither general NOS inhibition nor NO-activated GC inhibition produces a more that a 50 % block of cGMP production indicates that there is a reduction in NO-dependent cGMP production in mice deficient in eNOS (from ~ 20 to ~ 10 pmol cGMP/mg protein). One possible explanation for the difference observed between wild type and eNOS knockout animals could be that NOS inhibitors are not as potent on mouse tissue as on rat tissue. To address this possibility the range of 1400W concentrations which inhibit NMDA-stimulated cGMP accumulation was determined. Incubation of hippocampal slices with increasing concentrations of 1400W resulted in a concentration-dependent decrease in cGMP levels which was maximal at 5 μM, with an IC_{50} of 0.2 μM 1400W (figure 4.21a).

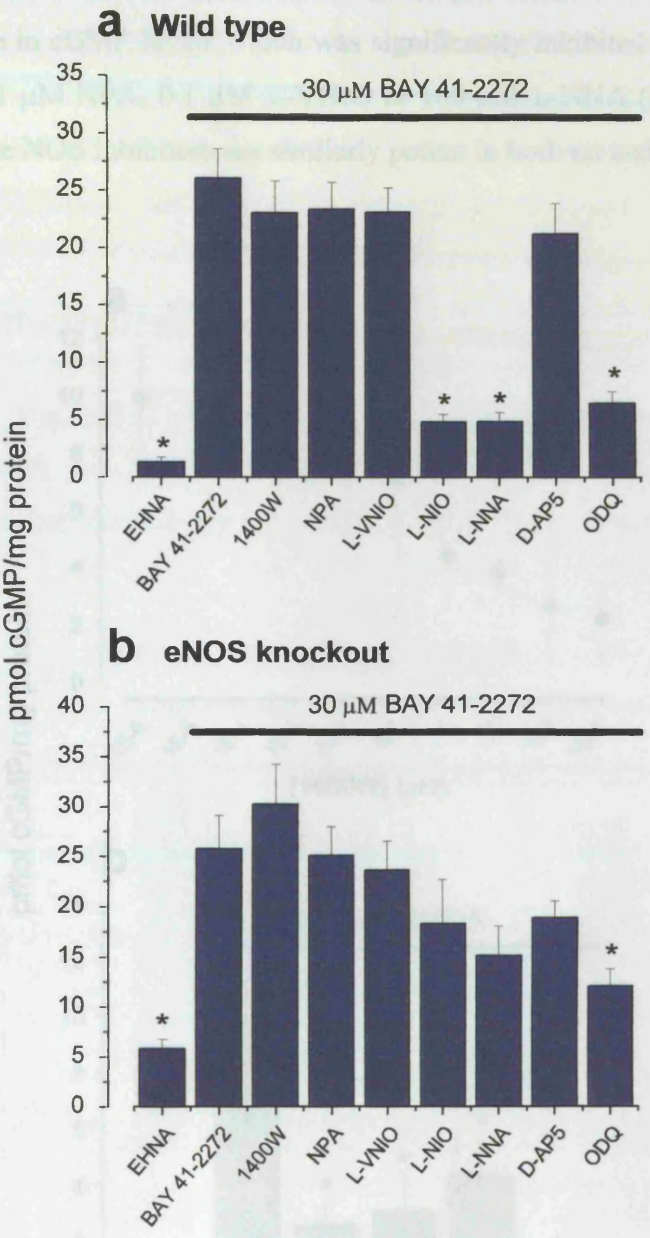

Figure 4.20: Effect of NOS inhibition on cGMP levels in adult mouse hippocampal slices in the presence of EHNA. *Incubation of slices with nNOS inhibitors (1400W, 1 μM; NPA, 1 μM; L-VNIO, 1 μM), or D-AP5 (100 μM) had no significant effect on cGMP accumulation in (a) wild type and (b) eNOS knockout animals. General NOS inhibitors (L-NNA, L-NIO; 100 μM) significantly reduced cGMP levels in wild type animals, but had no significant effect in eNOS knockout animals. Incubation with ODQ resulted in a significant reduction in cGMP levels in both wild type and eNOS knockout mice. *P < 0.05 vs. BAY 41-2272 treated slices (n = 15); one-way ANOVA with Tukey's post-hoc test.*

In order to investigate the potencies of the remaining nNOS inhibitors, wild type hippocampal slices were incubated with 100 μM NMDA which resulted in a ~ 10-fold increase in cGMP levels which was significantly inhibited by the presence of 1 μM 1400W, 1 μM NPA, 0.1 μM L-VNIO or 100 μM L-NNA (figure 4.21b). This indicates that the NOS inhibitors are similarly potent in both rat and mouse tissue.

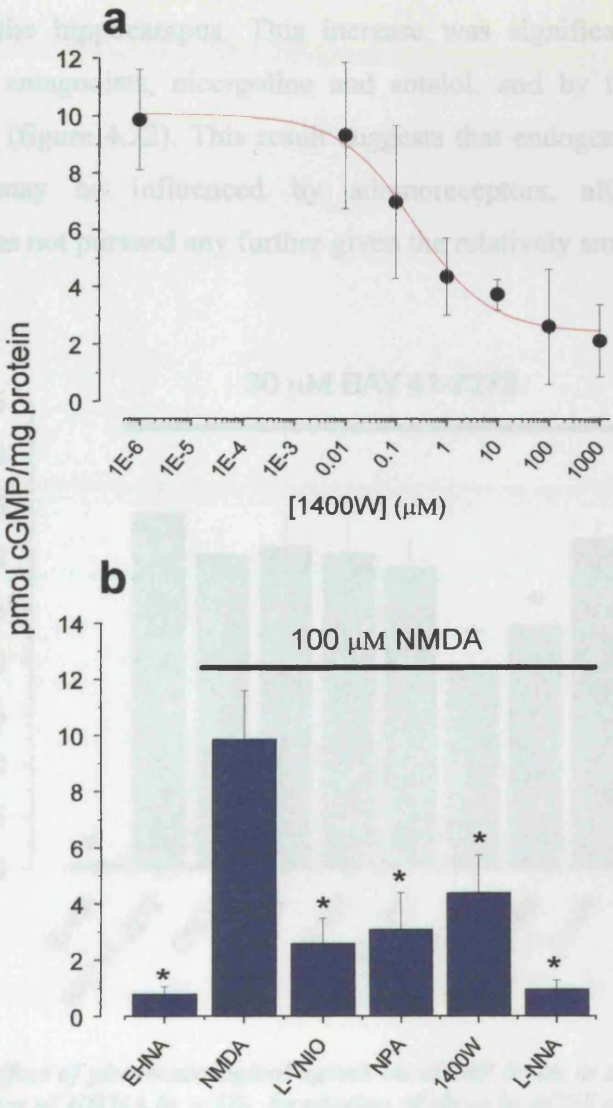

Figure 4.21: Effect of nNOS inhibitors on cGMP accumulation in adult mouse hippocampal slices in presence of EHNA. *(a) A concentration dependent decrease in cGMP levels was observed in the presence of increasing concentrations of 1400W. (b) Application of NMDA (100 μM; 2 min exposure) resulted in an increase in cGMP accumulation which was inhibited by incubation with L-VNIO (0.1 μM), NPA (1 μM), 1400W (1 μM) or L-NNA (100 μM). *P < 0.05 vs. NMDA treated slices (n = 5); one-way ANOVA with Tukey's post-hoc test.*

4.3.5 Effect of neurotransmitter inhibitors on cGMP accumulation in rat hippocampal slices in presence of EHNA

In order to investigate the validity of the numerous pharmacological compounds which resulted in a reduction in cGMP accumulation when incubated in the presence of IBMX, hippocampal slices were incubated in ACSF containing 300 μM EHNA for 15 min in the presence or absence of the following compounds. As observed previously, 5 min exposure to BAY 41-2272 resulted in an increase in cGMP production in the hippocampus. This increase was significantly reduced by the adrenoreceptor antagonists, nicergoline and sotalol, and by the NO-activated GC inhibitor, ODQ (figure 4.22). This result suggests that endogenous NO levels in the hippocampus may be influenced by adrenoreceptors, although this line of investigation was not pursued any further given the relatively small effects

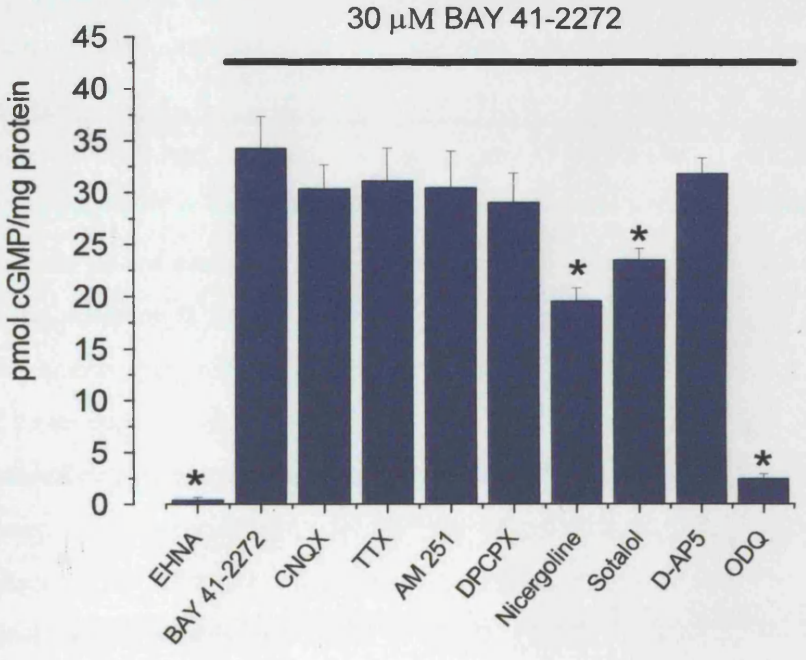

Figure 4.22: Effect of pharmacological agents on cGMP levels in adult rat hippocampal slices in presence of EHNA *(n = 10). Incubation of slices in ACSF containing EHNA (300 μM) and BAY 41-2272 (30 μM) in the absence (control) or presence of a variety of pharmacological agents: CNQX (100 μM), TTX (1 μM), AM251 (2 μM), DPCPX (0.1 μM), Nicergoline (50 μM), Sotalol (100 nM), D-AP5 (100 μM), and ODQ (1 μM). *P < 0.05 vs. BAY 41-2272 treated slices; one-way ANOVA with Tukey's post-hoc test.*

In contrast to the results obtained in the presence of IBMX, no effect on cGMP accumulation was noted following incubation with CNQX, TTX, AM 251, or DPCPX in the presence of EHNA (figure 4.22). The much "cleaner" result profile obtained in the presence of EHNA suggest that the numerous pharmacological antagonists which resulted in the inhibition of cGMP accumulation in the presence of IBMX may have been down to non-specific effects influenced by either the inhibition of cAMP breakdown or by the action of IBMX on adenosine receptors.

4.4 Discussion

Given the importance of the NO/cGMP pathway in hippocampal synaptic plasticity, it is surprising that the isoform of NOS responsible for tonic NO production in the hippocampus has so far not been investigated. The object of the present study was therefore to investigate the basal production of NO in the hippocampus using cGMP levels as an indicator.

Potency and selectivity of NOS inhibitors

Several studies have measured the potency and selectivity of various nNOS inhibitors, however, a direct comparison is difficult due to the use of various assay systems, assay conditions and species (Nakane *et al.*, 1995; Wolff *et al.*, 1998). For example different groups utilised different concentrations of arginine in their assay systems: 10 μM (Cowart *et al.*, 1998); 70 μM (Hagen *et al.*, 1998); 0.1 μM (Wolff *et al.*, 1998). As a great proportion of the NOS inhibitors are arginine-competitive, the resultant IC_{50} values are directly dependent on the arginine concentration used in the respective assay system. Table 4.2 summarises the reported potencies of two general NOS inhibitors (L-NNA and L-NIO), and three nNOS inhibitors (L-VNIO, 1400W and NPA).

As an added complication, the majority of investigations into the potency of these compounds on different NOS isoforms have so far been carried out on isolated enzymes, which may not reflect their potencies at the cellular level. Therefore we decided to re-evaluate the inhibitory potencies of three reported nNOS inhibitors on hippocampal slice tissue. A lower potency for nNOS inhibition was predicted in tissue as opposed to isolated enzyme as a result of cell permeability and/or intracellular metabolism of the inhibitor. However, IC_{50} values of approximately 0.003 μM, 0.03 μM, and 0.03 μM were obtained for L-VNIO, 1400W, and NPA, respectively, in the presence of IBMX. Very similar IC_{50} values of approximately 0.01 μM and 0.01 μM were also determined for L-VNIO and 1400W, respectively, in the presence of EHNA.

	IC_{50} (μM)			selectivity	
Compound	**nNOS**	**eNOS**	**iNOS**	**eNOS/nNOS**	**Reference**
L-NNA	0.03	0.08	1.5	3	Boer *et al.*, 2000
	0.02	0.03	13	1.5	Cooper *et al.*, 2000
L-NIO	0.5	0.63	0.25	1	Boer *et al.*, 2000
	1.7	3.9	3.9	2	Rees *et al.*, 1990
L-VNIO	0.5	1.4	0.7	3	Boer *et al.*, 2000
	0.1	12	60	120	Babu & Griffith, 1998
1400W	2.5	2.5	0.13	10	Boer *et al.*, 2000
	7.3	1000	0.23	130	Young *et al.*, 2000
	2	50	0.007	25	Garvey *et al.*, 1997
NPA	0.085	2	209	24	Cooper *et al.*, 2000
	0.057	8.5	180	149	Zhang *et al.*, 1997

Table 4.2: Potency and selectivity of NOS inhibitors on the purified enzymes.

Surprisingly these results reveal all three nNOS inhibitors to be more potent in hippocampal tissue than in isolated enzymes, indicating that the compounds appear to have no difficulty in permeating the cell membrane and acting on intracellular NOS. The explanation for the apparent increased potency compared to the literature data, however, is unclear. One possibility relates to the concentration of arginine present in the assay system, since most of the compounds are arginine-competitive, and IC_{50} values are directly dependent on the arginine concentration used in the respective assay system.

Additionally, it must also be noted that the concentration-response curves observed for 1400W and NPA are very shallow (i.e. inhibition occurring over ~ 6 log units) in the presence of IBMX, although, again, the explanation for this is unclear. It is possible that this reflects a permeability problem across the cell membrane,

especially given that NPA and 1400W do not appear to completely inhibit cGMP accumulation, even at the highest concentration applied. However, this scenario seems unlikely as a more 'normal-shaped' concentration-response curve was obtained for 1400W in the presence of EHNA. Interestingly, the concentration-response curve for L-VNIO was found to be consistent between the IBMX and EHNA conditions, and also to be very similar between 1400W and L-VNIO in the presence of EHNA. This finding implies that the shallow concentration-response curves observed in the presence of IBMX may be more likely to be related to the presence of IBMX, as opposed to a characteristic trait of the respective inhibitor.

Overall, all three inhibitors were determined to be selective for the nNOS isoform over the eNOS isoform, as concentrations which inhibit the majority of nNOS activity resulted in no significant change in cGMP accumulation in rat aortic rings (which generate NO from the eNOS isoform). Unfortunately, a positive control for the action of these inhibitors on eNOS-induced cGMP accumulation in hippocampal slices was not attained. Three compounds previously found to stimulate eNOS activity (raloxifene, TNFα, and bradykinin; Harris *et al.,* 2001; Simoncini *et al.,* 2002a,b; Barsacchi *et al.,* 2003) were found to have no significant effect on basal cGMP levels in the hippocampal slice preparation, although it must be noted that the cGMP levels involved are at the boundary of detection and therefore absolute values are unlikely to be trustworthy. Taken together, these data identify three selective nNOS inhibitors that are able to inhibit the bulk of nNOS activity at concentrations which spare the eNOS isoform.

Effect of NOS inhibition in the hippocampus

The isoform of NOS responsible for basal levels of NO in the hippocampus was studied by examination of the cGMP accumulation in adult hippocampal slices following incubation with a PDE inhibitor to prevent breakdown of cGMP, and BAY 41-2272 to inhibit the dissociation of NO from NO-activated GC. To our knowledge, this is the first study to investigate the specific isoform of NOS involved in the tonic production of NO in the hippocampus. Selective inhibition of nNOS was found to have little or no effect on cGMP accumulation, either in the presence of IBMX or EHNA. As 1400W is considered to have a higher potency for iNOS than nNOS (Boer *et al.,* 2000; Young *et al.,* 2000), incubation with 1400W additionally acts as a control for the contribution of iNOS to endogenous NO levels. In contrast, general NOS

inhibition almost completely abolished cGMP accumulation confirming the NO-dependence of the cGMP levels. Therefore the assumption from these results, by process of elimination, is that eNOS is likely to be responsible for tonic NO production in the hippocampus. Unfortunately, this hypothesis cannot be tested pharmacologically as, to date, there are no selective eNOS inhibitors.

Control experiments carried out on rat aortic rings (which generate NO from eNOS) demonstrate very little inhibition of ACh-induced cGMP accumulation following exposure to either LY294002 or wortmannin. This finding is consistent with the observation by Kobayashi and colleagues (2004) that pre-treatment of aortic strips with LY294002, or an Akt inhibitor, had no significant effect on ACh-induced cGMP accumulation. The explanation for this result relates to the mechanism of ACh-induced NO generation in the aorta. It has been demonstrated that activation of eNOS by various agonists, including ACh and bradykinin, is mediated primarily by elevation in intracellular free Ca^{2+} concentration (Forstermann *et al.*, 1991; Knowles & Moncada, 1994; Moncada *et al.*, 1991). However, several stimuli, such as shear stress and PI3-K, have also been found to activate NO production in a Ca^{2+}-independent manner (section 1.2.3). As well as activating of the PI3-K/Akt pathway (Kitayama *et al.*, 2000), tyrosine kinase has also recently been shown to modulate ACh-induced dilation of the rat basilar artery *in-vivo* (Kitazono *et al.*, 1998). Tyrosine kinase exerts its effects via IP_3 receptors (Jayaraman *et al.*, 1996) with the consequent release of Ca^{2+} from intracellular stores. Given that both LY294002 and wortmannin are inhibitors of PI3-K, (with little or no inhibitory effects on phosphatidylinositol-4-kinase, PKC, or tyrosine kinase: Powis *et al.*, 1994; Vlahos *et al.*, 1994) it is likely that the lack of inhibitory action of these two compounds on ACh-induced cGMP accumulation may be a reflection of their lack of inhibition of intracellular free Ca^{2+} levels, and their lack of inhibition of eNOS.

The specificity of LY294002 and wortmannin as PI3-K inhibitors may also go some way towards explaining the minimal inhibition of cGMP accumulation in the presence of these compounds on BAY 41-2272-stimulated hippocampal slices. That is, if basal production of NO in the hippocampus is regulated by a combination of intracellular Ca^{2+} levels and phosphorylation, then inhibition of PI3-K by LY294004 or wortmannin would only remove one regulatory pathway, leaving the others intact to stimulate eNOS activation. Therefore inhibition of PI3-K would not be expected to

completely inhibit eNOS activity. Furthermore, of particular relevance to this current study, is a recent report by Kitayama and colleagues (2000) which suggested that PI3-K may not be involved in the basal production of NO *in-vivo*, despite its potential action in ACh-induced NO production.

Given the fact that there are no selective eNOS inhibitors available, the isoform of NOS responsible for basal NO levels was then explored in a different way, by investigation of cGMP levels in hippocampal slices obtained from mice deficient in eNOS. It would be predicted that if eNOS was responsible for tonic NO production in the hippocampus, basal cGMP production would be either reduced or non-existent in eNOS knockout mice. However, surprisingly, basal cGMP production was found to be similar between wild type and eNOS knockout hippocampal slices. This finding is also in contrast to various studies which report higher cGMP content in vessels from wild type mice when compared to their eNOS knockout counterparts (Brandes *et al.*, 2000; Hussain *et al.*, 2001; Li *et al.*, 2001). One possible explanation for this observation may be tissue-specific variation in cGMP levels, especially given that PDE expression varies between tissues, and that none of the previous studies were carried out in the hippocampus. Another potential explanation could be that as basal cGMP levels are so low in the hippocampus without sensitising NO-activated GC to NO, the previously reported differences between the two groups of mice may reflect natural variation within a population, as opposed to any real difference. By inhibiting the dissociation of NO from NO-activated GC with BAY 41-2272, the effect is an increased sensitivity of the enzyme to NO which allows small changes in endogenous NO production to be reflected by larger differences in cGMP accumulation.

Predictably, wild type hippocampal slices were found to exhibit very similar BAY 41-2272-stimulated cGMP responses following NOS inhibition to those observed in the rat: no effect upon nNOS or iNOS inhibition, and almost complete inhibition of cGMP accumulation in the presence of general NOS inhibitors. In contrast, in the presence of EHNA there was a marked reduction in NOS-dependent cGMP production in eNOS-deficient mice. The lack of effect of L-NNA and L-NIO argues against a role for other NOS isoforms in the production of cGMP, instead suggesting an alternative compensatory mechanism for the absence of eNOS in mutant mice. Consistent with this idea is the demonstration of cross-talk between NO-activated GC and pGC systems (Hussain *et al.*, 2001). NO-deficient vessels (human internal mammary artery; wild type aorta in presence of NOS inhibitors;

eNOS knockout aorta) have been demonstrated to exhibit increased sensitivity to atrial natriuretic peptide (ANP); conversely pre-treatment of vessels with an excess of NO reduces their responsiveness to ANP. Additionally, treatment of rat renal glomeruli with L-NAME leads to an increase in the activity and sensitivity of the ANP-dependent pGC system (Lewko *et al.*, 1997). Evidence for compensatory mechanisms other than NOS upregulation also arises from studies exploring cardiac function. Cardiac cGMP levels were found to be the same in eNOS knockout and wild type mice (Gyurko *et al.*, 2000). However, higher expression levels of ANP are observed in eNOS-deficient animals which appear to provide a mechanism capable of maintaining basal cGMP levels in the absence of eNOS. This is consistent with the finding that ANP injected intravenously into L-NNA-treated wild type mice is also found to restore ventricular relaxation (Gyurko *et al.*, 2000).

Given that ODQ is selective for NO-activated GC over pGC (Garthwaite *et al.*, 1995b), it would therefore be predicted that if pGC activity could account for the cGMP accumulation observed in eNOS knockout mice, ODQ would have no effect on cGMP accumulation in these animals. However, in apparent contrast to this supposition, ODQ still produced significant inhibition (~ 50 %) of BAY 41-2272-stimulated cGMP production in the absence of eNOS. This finding implies that there is an NO-activated GC component of cGMP accumulation that remains in eNOS knockout animals, although the origin of these levels is a mystery, especially given that general NOS inhibitors have no significant effect on cGMP accumulation in these animals. The most likely explanation is that there is a minor contribution from nNOS to tonic NO levels in the hippocampus that is too small (with the current n values) to be registered as significant with nNOS inhibitors, especially when used at sub maximal concentrations, as is the case in the present study. In support of this there are various reports which find that eNOS-deficient mice exhibit an increased sensitivity towards exogenous NO (Hussain *et al.*, 1999, 2001; Waldron *et al.*, 1999; Brandes *et al.*, 2000), indicating that if nNOS does make a small contribution to tonic NO levels, the relevant contribution would be amplified in the knockout animal. A second possibility is that in the presence of BAY 41-2272, the endogenous level of CO may be sufficient to give a small degree of GC activation in eNOS knockout animals (given that BAY 41-2272 has been reported to sensitise NO-activated GC towards CO; Martin *et al.*, 2005). A third possibility, although unlikely, is that there may be

another, currently undiscovered, source of NO in the hippocampus (distinct from eNOS, nNOS, and iNOS) capable of activating NO-activated GC in the hippocampus.

It is also important to note another unexpected observation made in eNOS knockout mice: BAY 41-2272 retained its activity in the hippocampus of eNOS-deficient animals. Consistent with this Hussain and colleagues (1999) found YC-1 to be equipotent between wild type and eNOS knockout animals. At first glance these finding appears to imply that a source of basal NO is present in the hippocampus in the absence of eNOS, although the origin of this source is unclear. It is more probable, however, that the explanation for this activity lies in a combination of different factors. One possibility, as mentioned previously, is that nNOS may play a minor role in tonic NO production that is too small to be registered as significant in the current study. A second possibility is that iNOS may be upregulated in eNOS knockout animals as previously reported by Li and colleagues (Li *et al.*, 2001). However, no obvious compensation in either iNOS or nNOS protein expression was observed between wild type and eNOS knockout hippocampal slices, although subtle changes in expression levels cannot be ruled out. Additionally no significant change in iNOS activity was noted between the two groups of animals. These findings are consistent with the lack of effect of iNOS and nNOS inhibitors in eNOS-deficient hippocampal slices. Another possibility is that a proportion of the cGMP accumulation may be NO-independent, especially given that BAY 41-2272 can exert a small NO-independent increase in NO-activated GC activity at the concentration of BAY 41-2272 used in the current study. Other potential explanations also include upregulation of NO-activated GC, and/or altered PDE activity in eNOS-deficient mice (Hussain *et al.*, 1999, 2001).

Taken together, these findings support the hypothesis that eNOS is responsible for the basal levels of NO in the hippocampus, and that in eNOS-deficient mice there may be an increased importance of pGC in the maintenance of cGMP levels, which may be able to compensate, at least in part, for the absence of eNOS. In support of this proposal is the recent demonstration that basal cGMP-staining appears to be restricted to astrocytes in the presence (and absence) of EHNA, although it must also be noted that this astrocytic staining was only observed in the mouse, and that it was not inhibited by NOS or NO-activated GC inhibitors indicating that this staining may be non-specific. Following incubation with BAY 41-2272, there was an increase in staining of astrocytes, blood vessel walls and in varicose fibres (van Staveren *et al.*,

2004), although the relevance of the astrocytic staining is uncertain given that it was not inhibited by a NOS inhibitor.

Possible mechanism underlying endogenous NO production

The complementary question addressed in the present study concerned the mechanism responsible for maintaining basal NO production in the hippocampus. Exposure to the NMDA receptor antagonist D-AP5 was observed to have no effect on cGMP accumulation, indicating that tonic NO production in the hippocampus is independent of the NMDA receptor. This finding is consistent with the assumption that basal levels of NO result from eNOS activation, which is most likely present in endothelial cells as opposed to neurons (where the NMDA receptors are located). Evidence for tonic NO generated independently of NMDA receptors additionally comes from data on hippocampal and striatal slices demonstrating that most of the basal cGMP (augmented by a PDE inhibitor) was sustained by NOS but not by NMDA receptors (Chetkovich *et al.*, 1993; Griffiths *et al.*, 2002).

Investigation of the potential mechanisms contributing to endogenous NO production revealed a discrepancy between the results achieved with IBMX and EHNA. In the presence of IBMX a decrease in cGMP accumulation was observed following exposure to the voltage-gated Na^+ channel inhibitor TTX, the AMPA antagonist CNQX, the cannabinoid antagonist AM 251, the adenosine antagonist DPCPX, and the β adrenergic antagonist sotalol. These data is in partial agreement with a previous study, also carried out in the presence of IBMX, which observed an inhibition of cGMP accumulation in the striatum by TTX, but not by the AMPA antagonist NBQX (Griffiths *et al.*, 2002). In contrast, when hippocampal slices were incubated with EHNA, the only significant reduction in cGMP levels was observed with α (nicergoline) and β (sotalol) adrenoreceptor antagonists. This result indicates that endogenous NO levels in the hippocampus may be influenced by adrenoreceptors, although this line of investigation was not pursued any further given the relatively small effect.

This experiment highlights a distinct difference in cGMP accumulation between that observed in the presence of IBMX or EHNA. One feasible explanation for this difference may be due to the fact that IBMX is not a "clean" compound: in addition to its action as a non-specific PDE inhibitor, IBMX is also known to act as an antagonist of adenosine receptors (Choi *et al.*, 1988). Adenosine is a well-established

modulator of synaptic transmission and neuronal excitability in the CNS (Dunwiddie & Fredholm, 1989; Greene & Haas, 1991), typically acting through the presynaptic A1 receptor to decrease neuronal firing via suppression of glutamate release (Fowler *et al.*, 1999; Mitchell *et al.*, 1993, Wu & Saggau, 1994). Given that adenosine release results in the decrease of neuronal excitability, conversely the presence of IBMX (which inhibits the adenosine receptor) leads to an increase in neuronal firing. It is also relevant to note that EHNA is an inhibitor of adenosine deaminase (Sattin & Rall, 1970), and therefore potentially may also influence adenosine levels in the hippocampus. However, a recent study by Suvarna & O'Donnell (2002) demonstrated that neither adenosine nor an adenosine deaminase inhibitor mimicked the effect of EHNA on cGMP accumulation, therefore indicating that EHNA's inhibition of PDE2, and not its effects on adenosine metabolism, mediates its effects on cGMP concentration in the hippocampus.

A second possible explanation for the difference in cGMP accumulation relates to the PDE isoform inhibited: IBMX is a general PDE inhibitor, whereas EHNA is a selective PDE2 inhibitor. To date, several PDE isoforms have been localised in the rat hippocampus. *In situ* hybridisation and immunohistochemical studies demonstrate the presence of PDE1, PDE2, PDE3, and PDE4 in this brain region of the rat (Furuyama *et al.*, 1994; Ludvig *et al.*, 1991; Reinhardt & Bondy, 1996; Repaske *et al.*, 1993), although recent studies indicate that other PDE isoforms may also be present (such as PDE5 and PDE9; van Staveren et al., 2004). Recent evidence finds no effect of PDE1 or PDE3 inhibition on cGMP accumulation in the hippocampus (van Staveren *et al.*, 2001; Suvarna & O'Donnell, 2002), whereas PDE4 is a cAMP-specific PDE (general introduction; 1.5.1) and therefore inhibition of this isoform is of little benefit to the current study. In contrast, PDE2 is a cGMP-activated PDE which is able to degrade both cGMP and cAMP with similar K_m and V_{max} *in vitro* (Martins *et al.*, 1982), although studies carried out on cortical neurons and hippocampal slices indicate that PDE2 inhibition selectively increases only cGMP levels (Suvarna & O'Donnell, 2002; Boess *et al.*, 2004). The rationale for this is most likely due to the presence of several other cAMP metabolising enzymes, including PDE4, in these cells. Therefore in the presence of EHNA it is likely that cGMP breakdown would be inhibited, whilst leaving cAMP levels relatively free to vary as per usual. However in contrast, IBMX would prevent the breakdown of both cAMP and cGMP. Various studies have found that cross-talk arises between the cAMP and

cGMP signalling pathways capable of modulation of each other's synthesis, degradation and actions (Vigne *et al.,* 1994; Suvarna & O'Donnell, 2002). Furthermore, a recent study by Lu and colleagues (Lu *et al.,* 2004) demonstrated that increased levels of cAMP leads to increased glutamate release, and the homeostatic release of adenosine. The authors postulated that this may provide an important negative feedback modulation of neuronal excitability, by which increases of neuronal activity are dampened by the release of adenosine following activation of glutamate receptors.

Overall, it seems likely that the interpretation of biochemical results obtained in the presence of IBMX may be complicated by effects of adenosine release and/or increased levels of both cGMP and cAMP. This indicates that the results obtained in the presence of EHNA may provide a more accurate reflection of cGMP responses. This finding highlights the importance of the choice of PDE inhibitor when cyclic nucleotide levels are studied in complex tissues.

Chapter 5

Involvement of calcium channels in basal NO production in the hippocampus

5.1 Introduction

As described in the general introduction (section 1.2), both constitutive isoforms of NOS have an absolute requirement for Ca^{2+} for their activation. Whilst Ca^{2+} entry via the NMDA receptor following synaptic activation may be sufficient to activate nNOS phasically, it cannot account for the continued presence of Ca^{2+} required to sustain tonic NO production in the hippocampus. The majority of Ca^{2+} entry into the cell is mediated by voltage-gated Ca^{2+} channels, whose entry then triggers a range of cellular responses such as the regulation of Ca^{2+}-dependent second messenger cascades, Ca^{2+} release from cytoplasmic stores, and gene expression (Dolmetsch *et al.*, 2001).

Excitable tissues express a multitude of voltage-gated Ca^{2+} channels, each of which are associated with specialized physiological roles. Based on both their pharmacological and biophysical profiles, voltage-dependent Ca^{2+} channels can be classified into T-, L-, N-, P-, Q-, and R- types. Both structurally and functionally the primary division is between low voltage-activated (LVA) T-type Ca^{2+} channels which typically activate at fairly negative potentials (-70 mV to -50 mV), and high voltage-activated (HVA) channels which activate at more positive membrane potentials and include L-, N-, P-, Q-, and R-types. HVA Ca^{2+} channels are crucial for muscle contraction and neurotransmitter release, whereas LVA tend to be involved in the generation of repetitive electrical activity.

In the CNS, different types of HVA Ca^{2+} channels serve specialized cellular functions, and exhibit varying subcellular distributions. For example, L-type Ca^{2+} channels are typically confined to cell bodies (Hell *et al.*, 1993) where they are likely to regulate Ca^{2+}-dependent enzymes and gene expression. N- and P/Q- type calcium channels show highest expression levels at presynaptic terminals and are directly coupled to neurotransmitter release (Wheeler *et al.*, 1994; Westenbroek *et al.*, 1992, 1995). R-type Ca^{2+} channels are expressed on proximal dendrites and may, in some neurons, participate in neurotransmitter release (Hanson & Smith, 2002). T-type Ca^{2+}

channels are expressed in a variety of different cell types where they are typically involved in shaping the action potential, and in controlling patterns of repetitive firing (Ertel *et al.*, 2000). Table 5.1 summarises the various voltage-gated Ca^{2+} channels, their tissue localization, and their respective inhibitors.

α subunit	Alternative Name/ Splice variants	Channel type	Primary tissue	Inhibitor
1A	$Ca_v2.1a$ $Ca_v2.1b$	P- and/or Q- (purkinje)	Brain, cochlea, pituitary	ω-aga IVA, ω-CTx MVIIC
1B	$Ca_v2.2a$ $Ca_v2.2b$	N- (neuron)	Brain, nervous system	ω-CTx GVIA, ω-CTx MVIIC
1C	$Ca_v1.2a$ $Ca_v1.2b$ $Ca_v1.2c$	L- (large)	Heart Smooth muscle Brain, heart, pituitary, adrenal	Nifedipine
1D	$Ca_v1.3$	L-	Brain, pancreas, kidney, ovary, cochlea	Nifedipine
1E	$Ca_v2.3a$ $Ca_v2.3b$	R- (resistant)	Brain, cochlea, retina, heart, pituitary Brain, cochlea, retina	SNX-482, Nickel
1F	$Ca_v1.4$	?	Retina	?
1G	$Ca_v3.1$	T- (transient)	Brain, Nervous system	Mibefradil, Nickel
1H	$Ca_v3.2$	T-	Brain, heart, kidney, liver	Mibefradil, Nickel
1I	$Ca_v3.3$	T-	Brain	Mibefradil, Nickel
1S	$Ca_v1.1$	L-	Skeletal muscle	Nifedipine

Table 5.1: Classification of voltage-gated Ca^{2+} channels:
channel type, primary localization and their respective inhibitors.

Given the diverse roles of voltage-gated Ca^{2+} channels in synaptic function, and the fact that Ca^{2+} influx as a result of NMDA receptor activation cannot account for sustained Ca^{2+} levels required for tonic NO production, it seems conceivable that voltage-gated Ca^{2+} channels may play an important role in basal NO production in the hippocampus. The aim of the current study was to investigate the role of voltage-gated Ca^{2+} channels in maintaining the Ca^{2+} levels required for NOS activity.

5.2 Methods

5.2.1 Hippocampal tissue preparation

Hippocampal slices were prepared as described in chapter 2 (2.2).

5.2.2 cGMP measurement

Hippocampal slices were allowed to recover in carbogenated ACSF maintained in a shaking water bath at 30 °C for at least 1 - 2 h before use. Hippocampal slices were then transferred to a fresh solution containing the general PDE inhibitor 3-isobutyl-1-methylxanthine (IBMX; 1 mM) or the PDE2 inhibitor erythro-9-(2-hydroxy-3-nonyl)-adenine hydrochloride (EHNA; 300 μM) for 15 min, before being exposed to the enhancer of NO-activated GC, BAY 41-2272 for 5 min. At the end of the exposure the hippocampal slices were removed, inactivated by immersion in boiling hypotonic inactivation buffer for a minimum of 5 min, and homogenized by sonication.

The protein content and cGMP accumulation were determined as described in chapter 2 (2.4).

5.2.3 Data Analysis

All data are presented as the mean ± S.E.M; differences between experimental results were analysed using SPSS and/or GraphPad Instat software by way of a one-way or two-way ANOVA with Tukey's post-hoc test; P values of < 0.05 were regarded as significant.

5.3 Results

5.3.1 Effect of calcium channel inhibitors on cGMP accumulation in rat hippocampal slices in presence of EHNA

As discussed in the general introduction (section 1.2), both constitutive isoforms of NOS exhibit Ca^{2+}-dependence. To investigate the Ca^{2+}-dependence of cGMP accumulation, hippocampal slices were initially incubated with the general Ca^{2+} channel inhibitor, cadmium. The increase in cGMP accumulation observed following 5 min exposure to BAY 41-2272 was significantly reduced by the presence of cadmium (figure 5.1).

To determine which subtype of voltage-gated Ca^{2+} channel may contribute to basal endogenous cGMP production in the rodent hippocampus, slices were incubated with the Ca^{2+} channel inhibitors for each of the subtypes. The increase in cGMP accumulation observed following 5 min exposure to BAY 41-2272 was significantly reduced by incubation with nickel (Ni^{2+}; R-/T-type Ca^{2+} channel inhibitor; Soong *et al.*, 1993), mibefradil (T-type Ca^{2+} channel inhibitor; Martin *et al.*, 2000), and to a lesser degree ω-conotoxin GVIA (ω-CTx-GVIA; N-type Ca^{2+} channel inhibitor; Wheeler *et al.*, 1994) (figure 5.1). No significant effect on cGMP levels was observed in the presence of nifedipine (L-type Ca^{2+} channel inhibitor; Creba & Karobath, 1986), ω-conotoxin MVIIC (ω-CTx-MVIIC; N-/P/Q-type Ca^{2+} channel inhibitor; Wheeler *et al.*, 1994), ω-agatoxin IVA (P/Q-type Ca^{2+} channel inhibitor; Randall & Tsien, 1995) or SNX-482 (R-type Ca^{2+} channel inhibitor; Newcomb *et al.*, 1998) (figure 5.1).

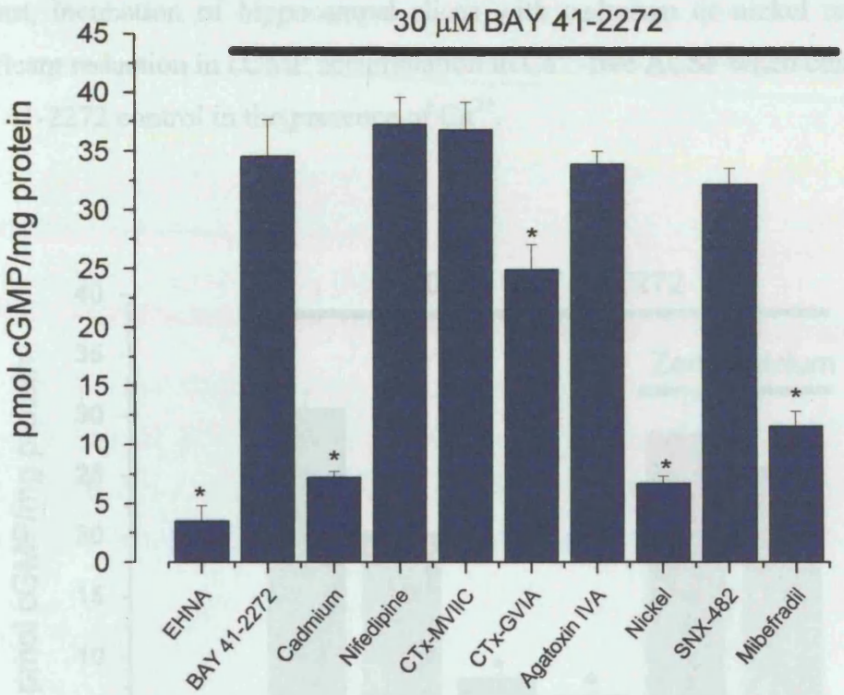

Figure 5.1: Effect of subtype-selective Ca^{2+}-channel inhibitors on cGMP levels in rat hippocampal slices. *Incubation of hippocampal slices in cadmium (200 μM), nickel (50 μM), mibefradil (3 μM) and CTx-GVIA (1 μM) resulted in a significant inhibition of cGMP accumulation. No significant change in cGMP level was observed in the presence of nifedipine (20 μM), CTx-MVIIC (500 nM), ω- agatoxin (100 nM) or SNX-482 (100 nM.). *P < 0.05 vs. BAY 41-2272 treated slices (n = 5 - 10); one-way ANOVA with Tukey's post-hoc test.*

5.3.2 Effect of zero calcium on cGMP accumulation in rat hippocampal slices in presence of EHNA

The almost complete inhibition of cGMP production in the presence of cadmium (~ 90 %) appears at odds with only ~ 50 % reduction observed in Ca^{2+}-free ACSF (chapter 4; figure 4.16b). One explanation could be that as NO-activated GC usually exists in a state of inhibition by Ca^{2+} (Kazerounian *et al.*, 2002), Ca^{2+}-free ACSF may result in disinhibition of the cyclase as internal Ca^{2+} would be reduced, which would not be the case for cadmium as internal Ca^{2+} would remain untouched and only Ca^{2+} uptake would be prevented. To address this possibility hippocampal slices were incubated in nickel and cadmium both in the presence, and absence, of Ca^{2+} in the external ACSF medium. In accordance with results obtained previously, incubation in nickel, cadmium or Ca^{2+}-free ACSF all produced a significant reduction in cGMP accumulation (figure 5.2). Additionally the presence of nickel and cadmium resulted

in a significant reduction in cGMP levels to that observed in Ca^{2+}-free ACSF. In contrast, incubation of hippocampal slices with cadmium or nickel resulted in no significant reduction in cGMP accumulation in Ca^{2+}-free ACSF when compared to the BAY 41-2272 control in the presence of Ca^{2+}.

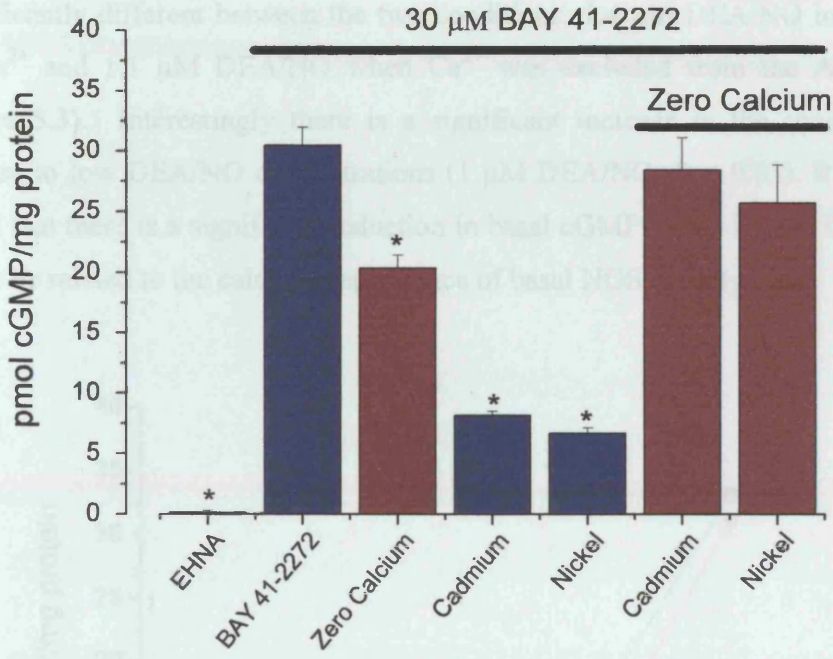

Figure 5.2: Effect of zero calcium on cGMP accumulation in rat hippocampal slices. *Incubation of slices in zero calcium (1 mM EGTA), cadmium (200 μM) or nickel (50 μM) significantly reduced cGMP accumulation. Application of cadmium or nickel in the absence of calcium prevented this reduction. .*P < 0.05 vs. BAY 41-2272 treated slices (n = 5); one-way ANOVA with Tukey's post-hoc test.*

Comparison of cGMP levels by means of two-way ANOVA analysis with a Tukey's post-hoc test confirmed cadmium and nickel significantly inhibit cGMP levels ($F = 20$; d.f. = 2, 30; $P < 0.001$), and also reveal a significant interaction to exist between the presence or absence of external Ca^{2+} and the effect of cadmium and nickel ($F = 64$; d.f. = 2, 30; $P < 0.001$). That is, both cadmium and nickel significantly inhibited BAY 41-2272-stimulated cGMP accumulation in the presence of Ca^{2+}, whereas they had no significant effect on cGMP levels in the absence of external Ca^{2+}.

These results indicate that the discrepancy observed between Ca^{2+}-free ACSF and incubation with cadmium could be explained by disinhibition of the cyclase. In order to test this hypothesis a concentration-response curve was carried out in Ca^{2+}-free ACSF, the prediction being that there would be an enhancement of the cGMP response to DEA/NO in the absence of Ca^{2+} in the external medium if the cyclase was disinhibited. However, the EC_{50} for cGMP accumulation was not found to be significantly different between the two conditions: 1.4 μM DEA/NO in the presence of Ca^{2+} and 1.1 μM DEA/NO when Ca^{2+} was excluded from the ACSF solution (figure 5.3). Interestingly there is a significant increase in the sensitivity of the cyclase to low DEA/NO concentrations (1 μM DEA/NO; $P < 0.05$). It must also be noted that there is a significant reduction in basal cGMP levels in zero Ca^{2+}, which is likely be related to the calcium dependence of basal NOS activity.

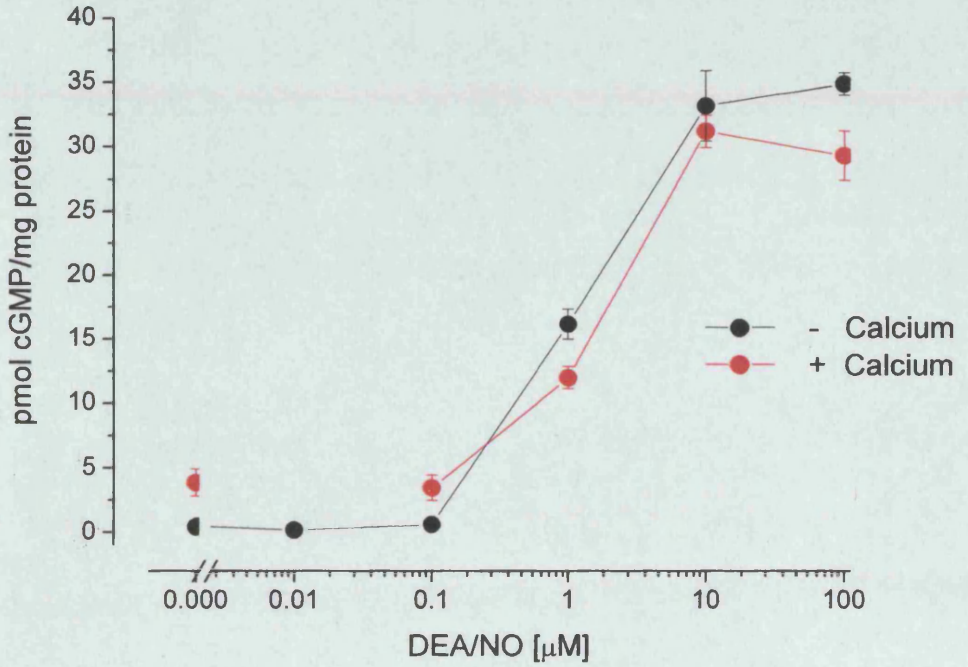

Figure 5.3: Concentration-response curve for DEA/NO on cGMP levels in adult rat hippocampal slices in presence and absence of Ca^{2+} *(2 min exposure; n = 5).Experiments carried out in presence of EHNA.*

5.4 Discussion

The current study addressed a complementary question to that investigated in chapter 4; given the absolute requirement for Ca^{2+} of both the constitutive forms of NOS, what is the involvement of voltage-gated Ca^{2+} channels in the basal production of NO in the hippocampus?

Firstly we investigated the effect of selective inhibition of individual subtypes of voltage-gated Ca^{2+} channel on basal cGMP production in the hippocampus. Inhibition of L-type, P/Q-type and R-type Ca^{2+} channels were found to have no effect on cGMP accumulation, and only a small inhibition resulted from N-type Ca^{2+} channels inhibition. In contrast, basal cGMP levels were significantly inhibited by nickel (50 μM) or mibefradil (3 μM). At this concentration nickel is known to inhibit both R-type and T-type Ca^{2+} channels (Zamponi *et al.*, 1996; Tottene *et al.*, 1996), although at higher concentrations (such as in the hundred micromolar range), nickel additionally blocks transiently expressed N-type, L-type and P/Q-type Ca^{2+} channels (Zamponi *et al.*, 1996) and capacitative Ca^{2+} channels (Zweifach & Lewis, 1993, 1996). Mibefradil on the other hand is an L-type and T-type antagonist (Massie, 1997), although an effect mediated via L-type Ca^{2+} channels can be discounted since a selective L-type antagonist, nifedipine, had no effect on cGMP accumulation. There is also evidence that mibefradil is an N-type antagonist (Bezprozvanny & Tsien, 1995; Göthert & Molderings, 1997; Van der Lee *et al.*, 2000), R-type antagonist (Randall & Tsien, 1997) and that it can inhibit neuronal Na^{+} channels (Eller *et al.*, 2000). However, these effects can also be excluded since both the Na^{+} channel inhibitor TTX, and selective R- and N-type Ca^{2+} channel inhibitors had little or no effect. Our findings therefore suggest that the majority of basal NO production in the hippocampus is likely to be mediated via T-type Ca^{2+} channels.

T-type Ca^{2+} channels are expressed throughout the body, including in nervous tissue, heart, kidney, smooth muscle, sperm, and in many endocrine organs (for review see Perez-Reyes, 2003). To date, three different isoforms of T-type Ca^{2+} channels have been shown to exist, each of which exhibits a distinct tissue distribution. Many regions of the brain have been found to express more than one of these isoforms; interestingly all three isoforms are present in hippocampal pyramidal neurons (Talley *et al.*, 1999). Of particular relevance to the current study is the demonstration of T-type Ca^{2+} channels on microvascular endothelial cells of the

bovine adrenal medulla (Bossu *et al.*, 1989; Vinet & Vargas, 1999) and from rat brain (Delpiano & Altura, 1996). Furthermore, these channels exhibit a window current; that is they display a large overlap between the curves describing their inactivation and activation which effectively allows them to support a maintained current under steady state conditions (Hughes *et al.*, 1999; Jones, 2003). Sustained Ca^{2+} entry through T-type channels has been implicated in secretion from adrenal glomerulosa cells (Cohen *et al.*, 1988), and pacemaker potentials in sino-atrial node cells (Hagiwara *et al.*, 1988; Nilius, 1986).

These findings represent an plausible mechanism by which sustained Ca^{2+} entry may occur into the cell under resting conditions, which would then be available to activate the endothelial isoform of NOS (presumably present in endothelial cells) and consequently generate tonic NO levels. Consistent with this idea are studies which find mice lacking in T-type Ca^{2+} channels to exhibit constitutively constricted coronary arterioles and focal myocardial fibrosis (Chen *et al.*, 2003). These mice demonstrate a normal contractile response; however, their NO-mediated relaxation appears to be defective. Also of possible relevance is the observation that a low concentration of nickel is able to prevent the relaxation of coronary arteries (Chen *et al.*, 2003), as well as inhibit the induction of LTP in the hippocampal CA1 pyramidal cells (Magee & Johnston, 1997).

It is important to note that a second putative mechanism of Ca^{2+} entry into endothelial cells has also been suggested in the literature: via transient receptor potential (TRP) channels. Although not investigated in this study, one member of the TRP family (TRPV4) has been found to be highly expressed in endothelial cells (Wissenbach *et al.*, 2000) and are thought to be constitutively open in endothelial cells at body temperature, thereby potentially contributing to the maintenance of a steady-state Ca^{2+} concentration (Güler *et al.*, 2002; Nilius *et al.*, 2003). Furthermore, mice lacking TRPV4 exhibit an inhibition of endothelium NO-dependent vasorelaxation (Freichel *et al.*, 2001). However, given that 50 μM nickel resulted in an inhibition of basal cGMP production, and that this concentration of nickel is not thought to inhibit TRPV4 channels (Golovina *et al.*, 2001), our findings indicate that TRPV4 channels do not contribute to any great extent towards basal NO production in the hippocampus. Nevertheless, it would be interesting to explore the relative concentrations of Ca^{2+} entry mediated by T-type Ca^{2+} channels as opposed to TRPV4 channels.

The second part of the study investigated the surprising observation that cGMP accumulation was almost completely inhibited by the general voltage-gated Ca^{2+}-channel inhibitor, cadmium, whilst only ~ 50 % reduction in cGMP levels was observed in Ca^{2+}-free ACSF. The most likely explanation for this discrepancy relates to the discovery that NO-activated GC usually exists in a state of inhibition by Ca^{2+} (Kazerounian *et al.*, 2002). In the Ca^{2+}-free ACSF condition, the internal Ca^{2+} available in the cell would be reduced, thereby disinhibiting the cyclase, whereas in the case of cadmium only Ca^{2+} uptake would be prevented, with internal Ca^{2+} levels remaining intact. Therefore, in contrast to Ca^{2+}-free ACSF, exposure to cadmium would leave the state of the cyclase unchanged. Consistent with this idea is the observation that incubation of hippocampal slices with cadmium or nickel significantly inhibited BAY 41-2272-stimulated cGMP accumulation in the presence of Ca^{2+}, whereas they had no significant effect on cGMP levels in the absence of external Ca^{2+}. The latter condition is likely to represent the lowest concentration of internal Ca^{2+} of all the conditions tested, given that Ca^{2+} uptake would be prevented in addition to initially reduced levels of internal Ca^{2+}. Therefore maximal disinihibition of the cyclase would be predicted in the latter condition when compared with either Ca^{2+}-free ACSF, cadmium or nickel alone. Our results also demonstrated that, although the cGMP concentration-response curve was not significantly changed by the presence or absence of Ca^{2+} in the external ACSF solution, there was a significant increase in sensitivity of the cyclase to low DEA/NO concentrations (1 μM DEA/NO; $P < 0.05$). Additionally, there was a significant reduction in basal cGMP levels in zero Ca^{2+} conditions, which is likely to reflect the calcium dependence of basal NOS activity.

Overall, the data here indicates that T-type Ca^{2+} channels may play an important role in maintaining a steady influx of Ca^{2+} into the cell which is capable of sustaining eNOS activation.

Chapter 6

Involvement of NO in long term potentiation

6.1 Introduction

LTP is a form of synaptic plasticity in which synaptic transmission is enhanced for hours, days or even weeks, and is widely considered to be the cellular correlate for learning and memory. In the CA1 region of the hippocampus LTP is induced by brief tetanic stimulation of afferent glutamatergic fibres, and typically exhibits a form of LTP that critically depends on postsynaptic activation of the NMDA receptor with the consequent influx of Ca^{2+} into the postsynaptic cell (Bliss & Collingridge, 1993). With the exception of mossy fiber-CA3 synapses, LTP induction is NMDA receptor dependent in all regions of the hippocampus, although one form of LTP has also been reported in CA1 that can be induced without activation of the NMDA receptor (Grover & Teyler, 1990). In this instance, exposure to high external Ca^{2+} concentrations induced a NMDA receptor-independent LTP, presumably facilitated by Ca^{2+} influx through voltage-gated Ca^{2+} channels. In both situations, Ca^{2+} entry into the post-synaptic cell results in a cascade of intracellular events culminating in the enhancement of synaptic transmission (Madison & Malenka, 1991; Malenka *et al.*, 1991; Chittajallu *et al.*, 1998).

LTP is conventionally separated into two distinct phases: induction and expression. The induction of LTP relates to the sequence of events taking place during and shortly following a brief period of high frequency stimulation (HFS). This phase generally lasts for ~ 1 min following tetanus (Bortolotto *et al.*, 2001), and is widely thought to reflect NMDA receptor activation, and the consequent influx of Ca^{2+} into the postsynaptic cell. The expression of LTP can be further subdivided into early-LTP and late-LTP, based on their sensitivity to protein synthesis inhibitors. Early-LTP lasts ~ 1 hr, and is generally considered to be resistant to protein synthesis. In contrast, late-LTP lasts for > 3 hr, and is dependent on protein and mRNA synthesis (Frey *et al.*, 1993; Huang & Kandel, 1994; Abel *et al.*, 1997).

Several theories exist as to how specific synapses are strengthened and weakened following activity, although it now seems clear that both pre- and postsynaptic changes contribute to hippocampal LTP. Postsynaptic changes include increased AMPA receptor density (Edwards, 1995), whereas evidence for a presynaptic change came from the finding that there was an enhanced release of glutamate from presynaptic terminals, correlating with LTP (Dolphin *et al.*, 1982; Williams *et al.*, 1989; Larkman *et al.*, 1995). Given the well-established postsynaptic involvement of the NMDA receptor in LTP induction, it therefore followed that a presynaptic modification would require a retrograde signalling system from the postsynaptic terminal to the presynaptic cell. Several molecules were suggested as candidates for diffusible messengers including arachidonic acid (Williams *et al.*, 1989), NO (Gally *et al.*, 1990), carbon monoxide (Zhuo *et al.*, 1993) and platelet-activating factor (Kato *et al.*, 1994).

Amongst these candidates NO received the most attention, given that NO was synthesized in neurons following NMDA receptor activation, facilitated by the physical coupling of nNOS to the NMDA receptor via PSD-95 (Brenman *et al.*, 1996a; Christopherson *et al.*, 1999), an arrangement that allows the influx of Ca^{2+} in the post-synaptic cell to couple to NO formation. The first studies to implicate NO in the establishment of LTP appeared in 1991 (Böhme *et al.*, 1991; Schuman & Madison, 1991), although subsequent experiments designed to test this hypothesis have yielded very controversial results. Table 6.1 summarises the major studies investigating the effect of NOS inhibition on hippocampal LTP: some authors demonstrate either a partial or complete block of LTP, whereas other groups report no effect at all of NOS inhibition. Various groups also report that agents which bind NO, such as haemoglobin (to absorb NO in the extracellular space), prevent the induction of LTP (O'Dell *et al.*, 1991; Schuman & Madison, 1991; Bon *et al.*, 1992; Haley *et al.*, 1992), indicating that NO must leave the postsynaptic cell to function.

Study	LTP protocol	Basal Stimulation	Temp	Species	Time of recording	Age of animal
Complete Inhibition						
Böhme *et al.*, 1991	2 x 100 Hz	0.2 Hz	32 °C	Rat	60 min	140-200 g
O'Dell *et al.*, 1991	2 x 100 Hz	0.02 Hz	24 °C	Guinea Pig	75 min	-
Schuman & Madison, 1991	4-5 x 100 Hz	0.033 Hz	22 °C	Rat	70 min	-
Bon *et al.*, 1992	2 x 100 Hz	0.2 Hz	32 °C	Rat	60 min	150-200 g
Haley *et al.*, 1992	10 x 100 Hz	0.067 Hz	22 °C	Rat	60 min	-
Doyle *et al.*, 1996	1-3 x 100 Hz	0.033 Hz	In vivo	Rat	60 min	250-350 g
Zhuo *et al.*, 1999	1 x 100 Hz	0.02 Hz	30 °C	Rat	60 min	4-6 weeks
Partial Inhibition						
Chetkovich *et al.*, 1993	3 x 100 Hz	0.1 Hz	32 °C	Rat	60 min	~ 125 g
Musleh *et al.*, 1993	Theta burst	0.067 Hz	35 °C	Rat	40 min	150-200 g
Boulton *et al.*, 1995	1 x 100 Hz	0.033 Hz	24 or 29 °C	Rat	60 min	4-6 weeks
Kleppisch *et al.*, 1999	Theta Burst	0.067 Hz	27.5 °C	Mouse	60 min	-
No inhibition						
Bannerman *et al.*, 1994	3 x 100 Hz	0.1 Hz	In vivo	Rat	60 min	250-450 g
Cummings *et al.*, 1994	4 x 100 Hz	0.1 Hz	25-29 °C	Rat	50 min	12-18 days
Inhibition under certain conditions						
Gribkoff & Lum-Ragan, 1992	Various	0.016 Hz	32 °C	Rat	60 min	1-3 months
Chetkovich *et al.*, 1993	Various	0.1 Hz	32 °C	Rat	60 min	~ 125 g
Haley *et al.*, 1993	Various	0.033 Hz	31 °C	Rat	60 min	100-200 g
Williams *et al.*, 1993a,b	6 x 100 Hz	0.033 Hz	24 or 29 °C	Rat	60 min	Young (5-7 weeks) or old (4-6 months)
Lum-Ragan & Gribkoff, 1993	Various	0.02 Hz	32-34 °C	Rat	60 min	75-100 g

Table 6.1: Effect of NOS inhibition on hippocampal LTP.
'-' indicates age of animal unknown

As research has progressed it has become clear that LTP can be established by multiple independent effector mechanisms, some of which are NO-dependent and some of which are NO-independent. It also appears the stimulation protocol utilized is of utmost importance in determining the pathway by which LTP is established. For example, a weak tetanic stimulation that is alone insufficient to induce LTP can enhance synaptic responses when timed to coincide with direct application of NO (Bon *et al.*, 1992; Zhuo *et al.*, 1993; Bon & Garthwaite, 2003), whilst stronger HFS is able to induce forms of LTP that are insensitive to NOS inhibitors (Chetkovich *et al.*, 1993; Haley *et al.*, 1993; O'Dell *et al.*, 1994). Furthermore, in contrast to the inhibitory effect of NOS inhibition, exposure of hippocampal slices to NO donors (such as sodium nitroprusside (SNP), hydroxylamine or DEA/NO) result in a long-lasting enhancement of excitatory synaptic transmission that occludes LTP (Böhme *et*

al., 1991; Bon *et al.*, 1992; Bon & Garthwaite, 2001a,b). The NO-dependence of LTP has additionally been shown to be affected by various experimental conditions such as temperature, animal age, or even the particular strain of rat or mouse used in the study (Williams *et al.*, 1993a; Hölscher *et al.*, 2002; Blackshaw *et al.*, 2003). It must, however, be noted that Boulton and colleagues (1995) failed to find a temperature-dependence of NO-dependent LTP.

Another point of controversy concerns the isoform of NOS which mediates the involvement of NO in LTP. Although both constitutive NOS isoforms are present in the hippocampus, their cellular locations are found to differ. In the adult hippocampus nNOS staining was originally thought to be largely confined to a subpopulation of GABA-containing interneurons in the stratum oriens and stratum radiatum (Bredt *et al.*, 1991; Valschanoff *et al.*, 1993; Lumme *et al.*, 2000; Seress *et al.*, 2002). However it is increasingly becoming clear that nNOS expression is also present in CA1-CA3 pyramidal cells (Endoh *et al.*, 1994; Wendland *et al.*, 1994; Doyle & Slater, 1997; Blackshaw *et al.*, 2003), and in dendritic spines (Burette *et al.*, 2002) when obtained by weak fixation protocols. Some laboratories have failed to reproduce this finding, although this can likely be explained by the potential cross reactivity of the antibodies, the method of fixation, and the differing antibody incubation time required to stain interneurons and pyramidal cells (see general introduction, 1.7.3, for more details).

In contrast, the majority of studies observe eNOS expression to be restricted to the vascular endothelium (Seidel *et al.*, 1997; Stanarius *et al.*, 1997; Töpel *et al.*, 1998), although there are a couple of reports that eNOS may also be present in CA1 pyramidal neurons and/or in astroglia-like cells (Dinerman *et al.*, 1994; Doyle & Slater, 1997). One explanation for the difference in eNOS localisation may be the species in which the study was carried out on: Doyle and Slater carried out their study on human tissue, whereas the majority of the remaining studies were carried out on rat tissue (with the exception of Blackshaw et al., (2003) who performed *in situ* hybridization for eNOS in both mouse and human). It is also possible that some of the astroglial eNOS visualised by Doyle and Slater may have been induced post mortem, although there is other evidence that some astroglia may display both constitutive and inducible forms of NOS (Murphy *et al.*, 1993). Murphy and colleagues do not distinguish whether the constitutive form of NOS in astrocytes is eNOS or nNOS. With respect to the reported eNOS expression in pyramidal cells, the investigators

demonstrated elimination of staining with preabsorption using the peptide, and the absence of staining with pre-immune serum (Dinerman *et al.*, 1994; O'Dell *et al.*, 1994). However, these types of controls do not rule out cross-reactivity with other proteins. More recent studies from the same group observe eNOS immunoreactivity and mRNA to be restricted to blood vessels in the brain (Demas *et al.*, 1999), which is in agreement with other immunohistochemical evidence utilising a number of selective eNOS antibodies (Seidel et al., 1997; Stanarius et al., 1997; Topel et al., 1998). Taken together, these findings indicate that the observations of eNOS expression in pyramidal cells are likely to be artifactual.

Ideally the isoform of NOS which mediates the involvement of NO in LTP would be investigated using selective inhibitors of nNOS and eNOS, however, as discussed in chapter 4, a selective eNOS inhibitor does not yet exist. Genetic NOS knockout models have therefore been exploited as the next best alternative. The nNOS knockout (-/-) mouse model was first reported in 1993 (Huang *et al.*, 1993), created by homologous recombination in embryonic stem cells by deletion of the first protein coding exon of nNOS. The deleted section of the codon contained the PDZ domain necessary for the association of nNOS to the NMDA receptor. Disruption of the nNOS gene resulted in elimination of 95 – 98 % of nNOS activity in the hippocampus in these mice, leaving only variant transcripts that lack the first exon and that are present at extremely low levels. The first study investigating LTP in these animals observed that nNOS -/- mice exhibited normal LTP (O'Dell *et al.*, 1994), which was reduced by general NOS inhibition. This finding led the authors to suggest that another isoform of NOS may participate in LTP.

A couple of years later an eNOS knockout model was produced, where a mutation was targeted to the NADPH ribose and adenine-binding sites of eNOS. Enzymatic assay confirmed a lack of eNOS activity in these mice, and immunohistochemistry found lack of eNOS expression in all tissues examined. LTP was found to be normal in these mutant mice, although targeted deletion of both nNOS and eNOS was demonstrated to result in the loss of LTP (Son *et al.*, 1996). In contrast, an independent group found that eNOS -/- mice lack NOS-inhibitor-sensitive LTP, but exhibit NOS-inhibitor-insensitive LTP (Wilson *et al.*, 1999). Both groups used the same mouse construct (129SV/C57BL/6), the same targeting strategy, and tested the mice at the same age so the explanation for the discrepancy is not immediately apparent. However, one plausible explanation may be the stimulation

protocol used to induce LTP: Son *et al.* used 2 trains of 100 Hz at 1 s duration whereas Wilson *et al.* used 3 trains of 100 Hz at 0.1 s duration to induce LTP. This possibility will be addressed in the current work

A second strategy was also developed to target eNOS in the adult animal, adding support for the case that eNOS activity is important in LTP. Adult hippocampal slices infected with recombinant adenovirus vectors containing either a truncated eNOS (which lacks catalytic activity yet retains the NH_2-terminal sequence required for myristoylation) or an eNOS fused to a transmembrane protein (CD8), demonstrated that membrane-targeted eNOS is required for LTP, and its function cannot be compensated by nNOS (Kantor *et al.*, 1996).

Although the evidence from the genetic models appears to indicate that the eNOS isoform mediates the majority of the involvement of NO in LTP, it is by no means conclusive. It is possible that genetic knockout animals are able to compensate with another subtype, whereas adult wild type animals could not. Another possibility that has so far also not been addressed is that nNOS and eNOS may both be required for differential functions in the induction and maintenance phases of LTP. In addition to being involved in the induction phase of LTP as a retrograde messenger, NO is also thought to contribute to the expression phase of LTP in the hippocampus which is dependent on protein and mRNA synthesis (Frey *et al.*, 1993; Huang & Kandel, 1994; Nguyen *et al.*, 1994). Accordingly, recent studies have demonstrated that NO contributes to late-phase LTP through the stimulation of postsynaptic NO-sensitive GC and cGK, which may act in parallel with the cAMP/PKA pathway to increase phosphorylation of the transcription factor CREB (Lu *et al.*, 1999, 2002).

The aim of the present study was to investigate the requirement for NO in hippocampal LTP, focussing in particular on the isoform of NOS responsible. Initially we set out to investigate the effect of exogenous NO on synaptic transmission, however, we were unable to reproduce the previously reported rebound potentiation following bath application of DEA/NO. Subsequently the isoform of NOS which mediates the involvement of NO in LTP was explored using a combination of genetic and pharmacological techniques. In particular, the explanation for the apparent discrepancy between different laboratories in analogous studies on the deficit of LTP in eNOS-deficient mice will be discussed.

6.2 Methods

6.2.1 Endothelial NOS deficient mice

Mice homozygous for a mutation in eNOS (Huang *et al.,* 1995) were crossed with wild type 129SV/C57BL/6 mice (Charles River, Margate, UK) to generate heterozygous mutant mice. Heterozygous mice from different litters were then mated, and the genotype of their offspring was determined as described below. Homozygous eNOS knockout mice and their control homozygous wild type littermates were selected for the study. Mice deficient in eNOS were viable, fertile, and indistinguishable from their wild type and heterozygous littermates in gross physical appearance.

6.2.2 Genotypic determination of transgenic mice

Mice from each litter were genotyped by PCR as described in chapter 2 (2.5) to confirm the presence or absence of the eNOS or NEO gene. The amplified products were electrophoresed in 1.5 % agrose gel with 2.5 µl/100 ml ethidium bromide, and DNA bands were visualised under UV light. Figure 6.1a demonstrates a representative agarose gel as visualised under UV light; figure 6.1b shows the same agarose gel as viewed under phase contrast to enhance the DNA bands. Heterozygotes were distinguished from their homozygote littermates by the presence of two DNA bands; homozygotes exhibited only one band. Positive and negative samples were always run on each gel.

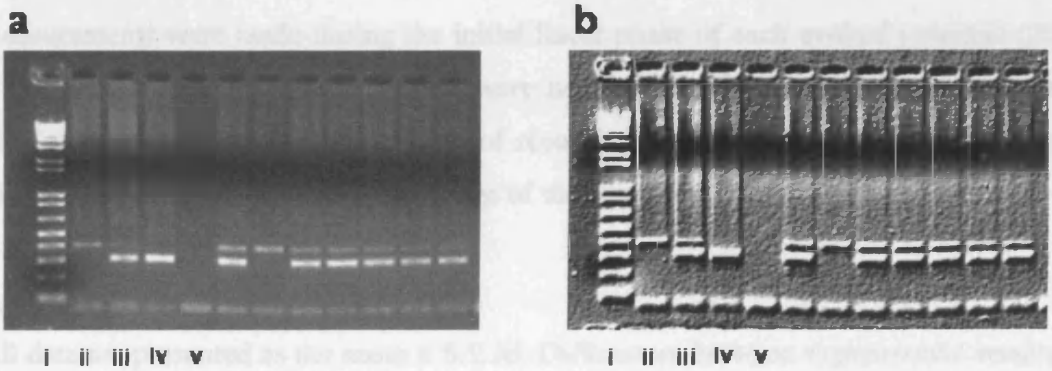

Figure 6.1: Genotyping of wild type and eNOS knockout mice.
(a) Agarose gel as visualised under UV light; (b) same agarose gel as viewed by phase-contrast. The columns in both represent: (i) DNA ladder; (ii) homozygous eNOS knockout mice; (iii) heterozygous mice; (iv) homozygous wild type mice; (v) negative control.

6.2.3 Tissue preparation

Hippocampal slices were prepared from either 6 to 8 week-old male Sprague-Dawley rats (Charles River, Margate, UK) or 8 - 12 week old male eNOS knockout (Huang *et al.*, 1995) or male wild type mice (Charles River, Margate, UK or Harlan, Bicester, UK) as described in chapter 2 (2.2).

6.2.4 Electrophysiological recordings

Extracellular recordings of field excitatory postsynaptic potentials (fEPSPs) were made from the stratum radiatum of the CA1 area of the hippocampus following electrical stimulation (baseline frequency 0.033 Hz or 0.2 Hz) of the Schaffer collateral pathway at 30 °C. The strength of presynaptic stimulation was adjusted to evoke fEPSPs that were ~ 30 % of the maximum fEPSP slope. After recording stable baseline synaptic responses for at least 20 min, LTP was induced by either one train of 100 Hz stimulation (1 s duration), or by three trains of 100 Hz stimulation (0.1 s duration) delivered 20 s apart at the test stimulation intensity. Stock solutions of the NONOate NO donor, diethylamine/NO adduct (DEA/NO) were made up in 10 mM NaOH and diluted at least 1:100 into the ACSF solution. Hippocampal slices to be tested in the presence of DEA/NO were incubated with DEA/NO for 5 min prior to and 10 min post tetanic stimulation. Both 1400W and L-VNIO were perfused for 15 min prior to and 15 min post tetanic stimulation to be consistent with biochemical results obtained in chapter 4. L-NNA was present for the duration of the respective experiment. Experiments were carried out blind to the origin of the tissue. Slope measurements were made during the initial linear phase of each evoked potential (20 – 50 % of the peak) and the values were normalised relative to the mean values obtained within the first 10 or 15 min of recording in the absence of any treatment. The fEPSPs are presented as a percentage of the baseline.

6.2.5 Data Analysis

All data are presented as the mean ± S.E.M. Differences between experimental results were analysed using a one-way ANOVA with Tukey's post-hoc test; P values of < 0.05 were regarded as significant.

6.3 Results

6.3.1 Effect of NO donors on synaptic transmission

The effect of NO donors on synaptic transmission has been investigated by a number of different groups, although the majority of studies (Böhme *et al.*, 1991; Bon *et al.*, 1992; Boulton *et al.*, 1994) have utilised NO donors such as SNP, hydroxylamine, or various nitrosothiols, all of which are now considered to be problematic because of their intrinsic chemical reactivity and/or because they release reactive species in addition to NO (Feelisch, 1998). More recently the effect of authentic NO (released from the NONOate DEA/NO) on synaptic transmission has been examined, and found to elicit an enduring potentiation of CA1 hippocampal neurotransmission that occludes tetanus-induced LTP (Bon & Garthwaite, 2001a,b; Bon & Garthwaite, 2002). This effect was found to be critically dependent on the frequency of synaptic transmission, occurring at 0.2 Hz but not at 0.033 Hz. However, on repetition of this experiment we could not reproduce all the findings obtained previously. In accordance with Bon & Garthwaite, 10 min perfusion of 300 μM DEA/NO resulted in a depression of synaptic transmission at 0.2 Hz that was reversible upon washout of NO. However, in contrast to the robust rebound potentiation observed by Bon & Garthwaite, the depression was followed by only minimal rebound potentiation (figure 6.2a). Subsequent tetanus-induced LTP (one train of 100 Hz; 1s) however was found to be normal.

The explanation for this discrepancy is unclear. Checks were made by the authors in the previous study that NO was responsible for the effects observed; degraded DEA/NO had no effect on synaptic transmission, and a second NONOate, PAPA/NO, had the same effect as DEA/NO, albeit to a lesser degree (Bon & Garthwaite, 2001b). The same frequency of synaptic transmission (0.2 Hz), the same strength of presynaptic stimulation (~ 30 % of maximum fEPSP slope), and the same source of DEA/NO (Alexis Biochemicals), were used in both the current study and in previous reports. The source of DEA/NO was additionally tested from an alternative company (Sigma) with the same result. Similar observations were also made in both the rat (figure 6.2a) and the mouse (figure 6.2b) hippocampus, giving additional support to the validity of our results. Furthermore, various experiments carried out on the same electrophysiological set-up used to obtain the previous findings again resulted in only minimal rebound potentiation. Given that the explanation for the

discrepancy still remained uncertain, the decision was made not to pursue this method of investigation any further.

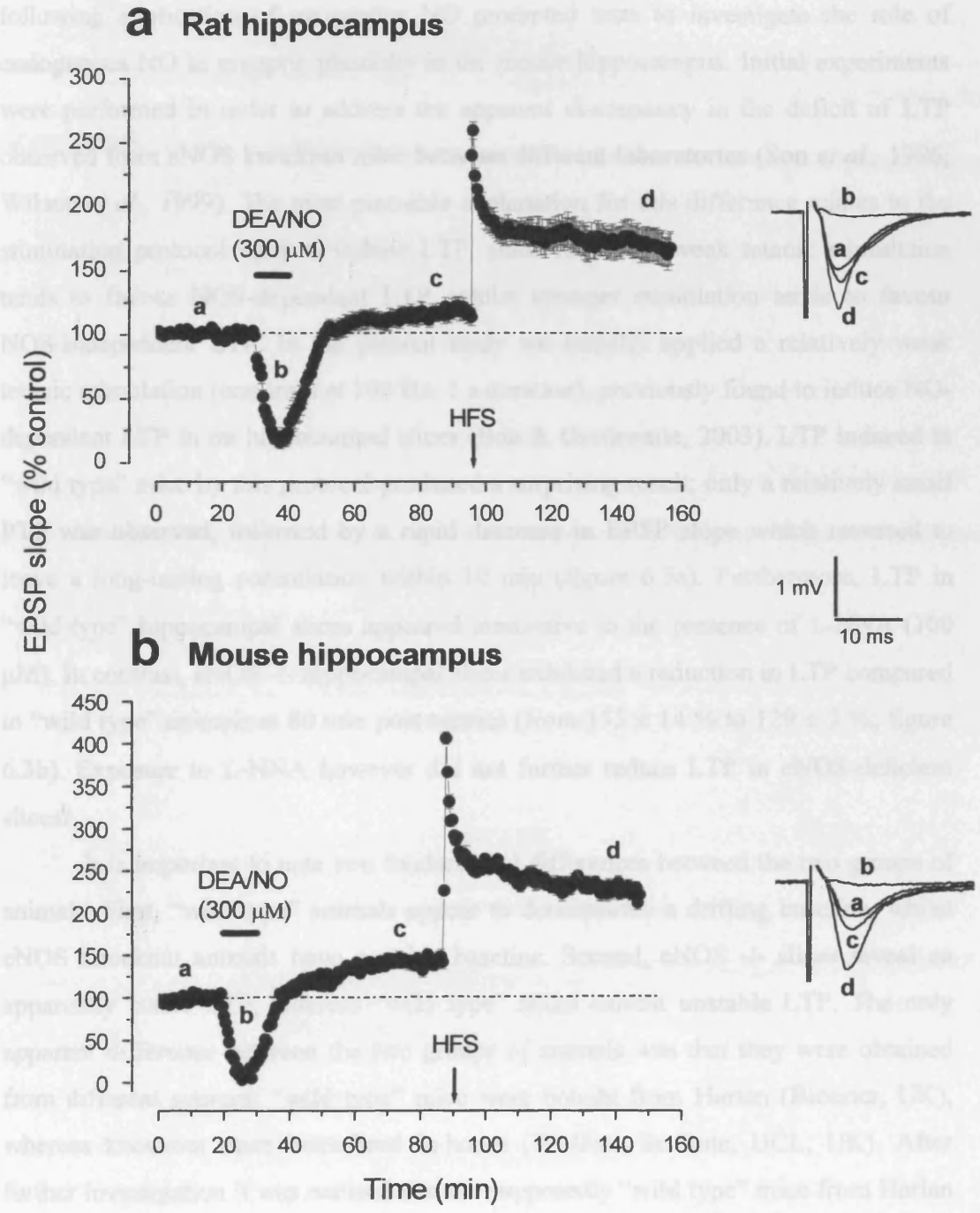

Figure 6.2: Effect of DEA/NO on synaptic transmission at a basal frequency of 0.2 Hz. *Comparison of effect of DEA/NO (300 μM; 10 min exposure) on (a) rat and (b) mouse synaptic transmission (n = 4). LTP was induced by one train of 100 Hz (1-s duration) at the time indicated by the arrow. Insets show representative traces taken at the times indicated by the letters.*

6.3.2 Effect of weak tetanic stimulation on LTP in eNOS knockout mouse hippocampal slices at 0.2 Hz baseline stimulation frequency

The inconclusive results obtained on attempting to induce rebound potentiation following application of exogenous NO prompted tests to investigate the role of endogenous NO in synaptic plasticity in the mouse hippocampus. Initial experiments were performed in order to address the apparent discrepancy in the deficit of LTP observed from eNOS knockout mice between different laboratories (Son *et al.*, 1996; Wilson *et al.*, 1999). The most plausible explanation for this difference relates to the stimulation protocol used to induce LTP, since relatively weak tetanic stimulation tends to favour NOS-dependent LTP, whilst stronger stimulation tends to favour NOS-independent LTP. In the present study we initially applied a relatively weak tetanic stimulation (one train at 100 Hz; 1 s duration), previously found to induce NO-dependent LTP in rat hippocampal slices (Bon & Garthwaite, 2003). LTP induced in "wild type" mice by this protocol produced a surprising result; only a relatively small PTP was observed, followed by a rapid decrease in EPSP slope which reversed to leave a long-lasting potentiation within 10 min (figure 6.3a). Furthermore, LTP in "wild type" hippocampal slices appeared insensitive to the presence of L-NNA (100 μM). In contrast, eNOS -/- hippocampal slices exhibited a reduction in LTP compared to "wild type" animals at 80 min post tetanus (from 155 ± 14 % to 129 ± 3 %; figure 6.3b). Exposure to L-NNA however did not further reduce LTP in eNOS-deficient slices.

It is important to note two fundamental differences between the two groups of animals. First, "wild type" animals appear to demonstrate a drifting baseline, whilst eNOS knockout animals have a stable baseline. Second, eNOS -/- slices reveal an apparently stable LTP, whereas "wild type" slices exhibit unstable LTP. The only apparent difference between the two groups of animals was that they were obtained from different sources: "wild type" mice were bought from Harlan (Bicester, UK), whereas knockout mice were bred in-house (Wolfson Institute, UCL, UK). After further investigation it was realised that the supposedly "wild type" mice from Harlan contained a chromosomal deletion of the α-synuclein locus (Specht & Schoepfer, 2001), an abundant presynaptic protein important in regulating presynaptic vesicular pools (Cabin *et al.*, 2002), and in augmenting neurotransmitter release (Liu *et al.*, 2004). Harlan subsequently removed these mice from sale.

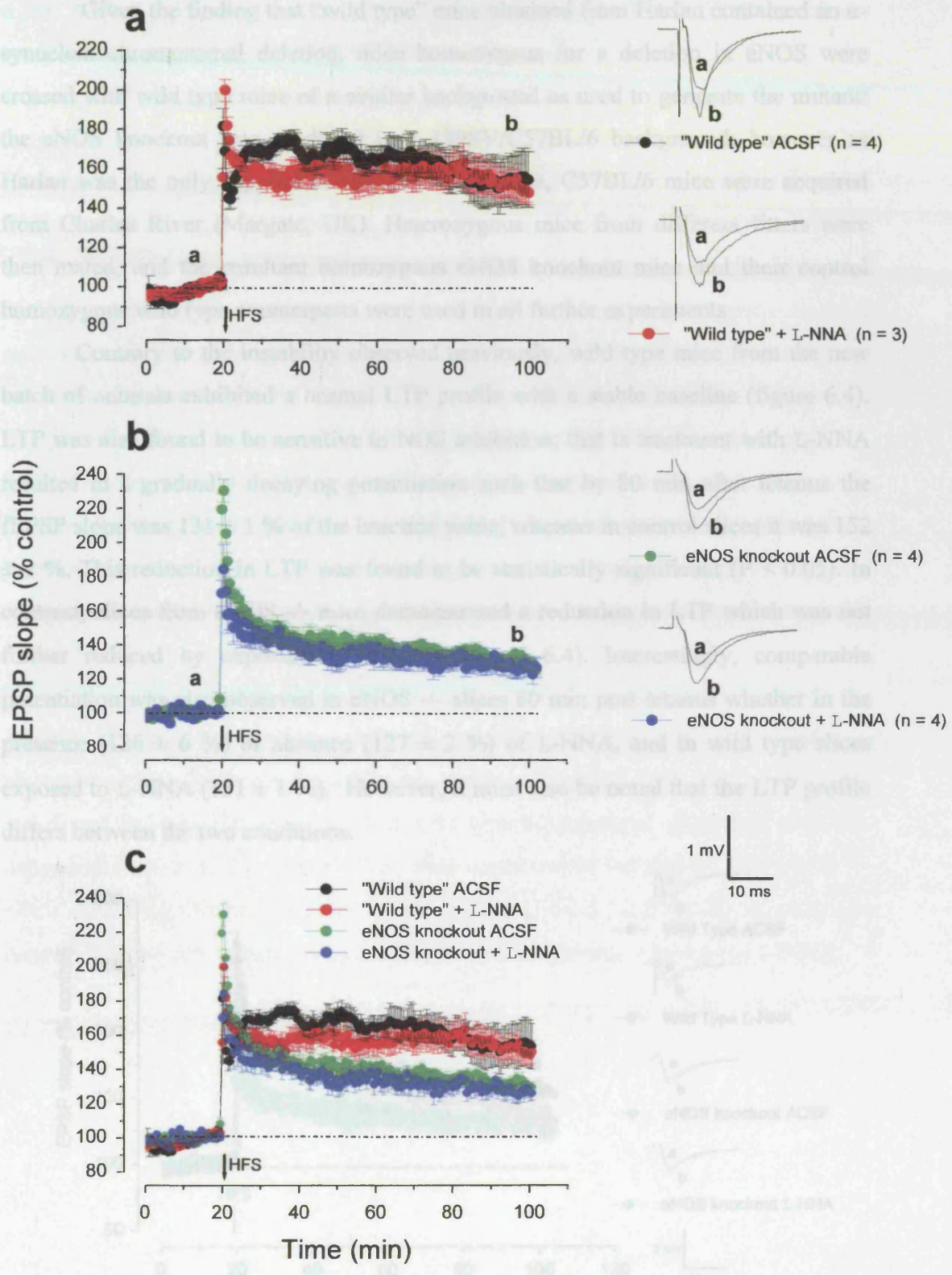

Figure 6.3: LTP in CA1 region of the hippocampus in wild type and eNOS-deficient mice at 0.2 Hz baseline frequency. *LTP was induced by one train of 100 Hz (1 s duration) at the time indicated by the arrow. Insets show representative traces taken at the times indicated by the letters.*

Given the finding that "wild type" mice obtained from Harlan contained an α-synuclein chromosomal deletion, mice homozygous for a deletion in eNOS were crossed with wild type mice of a similar background as used to generate the mutant: the eNOS knockout was produced in a 129SV/C57BL/6 background; however as Harlan was the only supplier of this particular cross, C57BL/6 mice were acquired from Charles River (Margate, UK). Heterozygous mice from different litters were then mated, and the resultant homozygous eNOS knockout mice and their control homozygous wild type counterparts were used in all further experiments.

Contrary to the instability observed previously, wild type mice from the new batch of animals exhibited a normal LTP profile with a stable baseline (figure 6.4). LTP was also found to be sensitive to NOS inhibition: that is treatment with L-NNA resulted in a gradually decaying potentiation such that by 80 min after tetanus the fEPSP slope was 131 ± 1 % of the baseline value, whereas in control slices it was 152 ± 2 %. This reduction in LTP was found to be statistically significant ($P < 0.05$). In contrast, slices from eNOS -/- mice demonstrated a reduction in LTP which was not further reduced by exposure to L-NNA (figure 6.4). Interestingly, comparable potentiation was also observed in eNOS -/- slices 80 min post tetanus whether in the presence (126 ± 6 %) or absence (127 ± 2 %) of L-NNA, and in wild type slices exposed to L-NNA (131 ± 1 %). However, it must also be noted that the LTP profile differs between the two conditions.

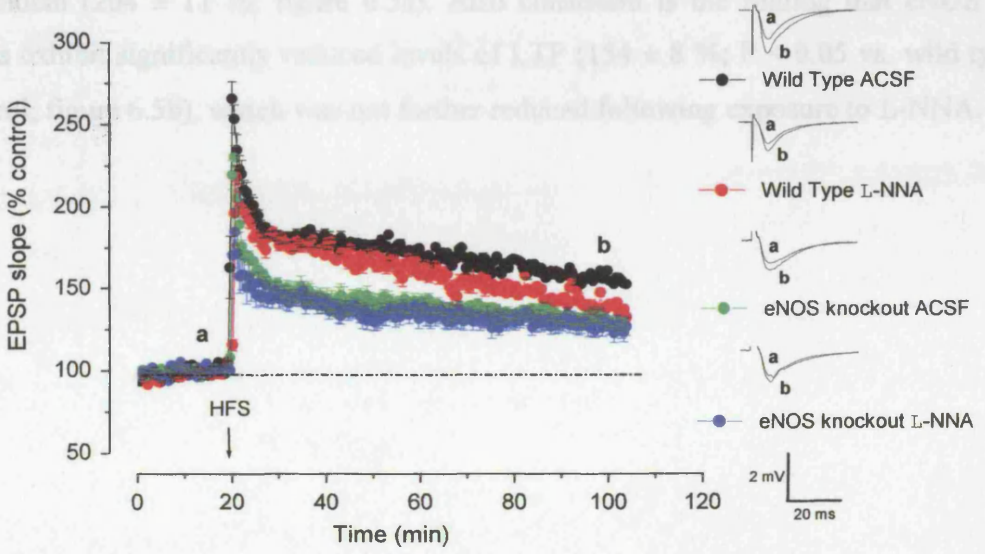

Figure 6.4: LTP in control littermates of wild type and eNOS deficient mice at 0.2 Hz baseline frequency. *LTP was induced by one train of 100 Hz (1 s duration) at the time indicated by the arrow (n = 5). Insets show representative traces taken at the times indicated by the letters.*

6.3.3 Effect of tetanic stimulation on LTP in endothelial NOS knockout hippocampal slices at 0.033 Hz

It is widely recognised that the frequency at which electrophysiological experiments are undertaken is of great importance. Typically frequencies in the range of 1 – 3 Hz give rise to LTD, whereas stimulation in the 30 - 100 Hz range is required for LTP (Bliss & Collingridge, 1993). Varying stimulation frequencies have also been used in the literature to evoke baseline fEPSPs, the highest of which being 0.2 Hz (Böhme *et al.*, 1991, 1993). However, recent studies indicate that long lasting plastic changes may occur in central synapses in normal animals at stimulation frequencies as low as 0.2 Hz that do not occur at 0.033 Hz, such that potentiation results from exogenous NO paired with a weak tetanus at 0.2 Hz, but not at 0.033 Hz (Bon & Garthwaite, 2001b). Furthermore this NO-triggered potentiation appears to share mechanisms in common with normal HFS-induced LTP; LTP was progressively occluded in proportion with the degree of prior NO-triggered potentiation, and the NO-triggered potentiation could be inhibited by NMDA receptor antagonists similar to HFS-induced LTP (Bon & Garthwaite, 2001a).

In order to explore the possibility that this phenomenon may be influencing the results obtained so far, the experiments were repeated at 0.033 Hz. Similar to observations at 0.2 Hz, a relatively weak tetanic stimulation (100 Hz; 1 s duration) was found to induce a robust LTP in wild type hippocampal slices that was NO-dependent (204 ± 11 %; figure 6.5a). Also consistent is the finding that eNOS -/- slices exhibit significantly reduced levels of LTP (154 ± 8 %; $P < 0.05$ vs. wild type control; figure 6.5b), which was not further reduced following exposure to L-NNA.

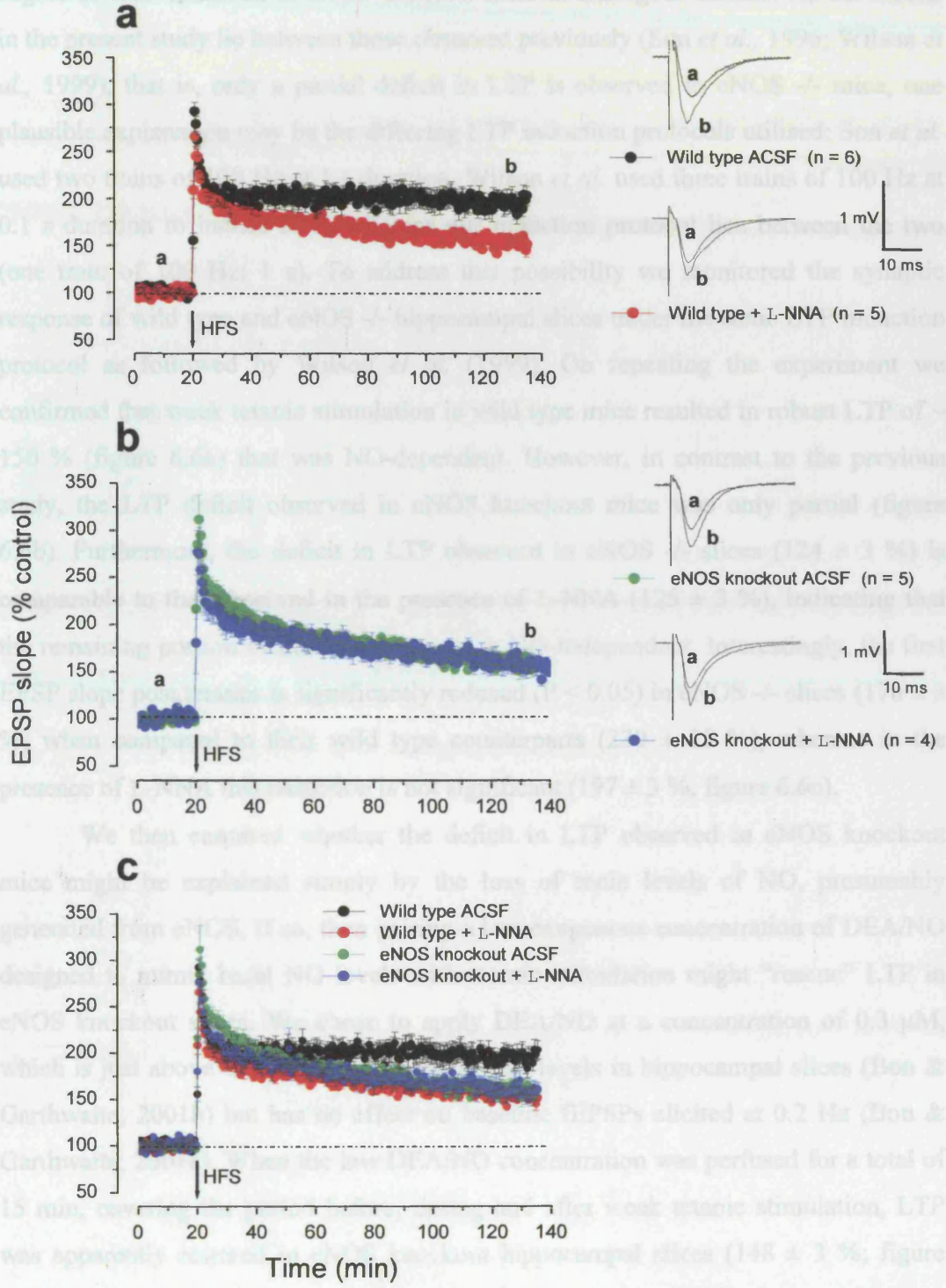

Figure 6.5: LTP in CA1 region of the hippocampus in wild type and eNOS-deficient mice at 0.033 Hz baseline frequency. *LTP was induced by one train of 100 Hz (1 s duration) at the time indicated by the arrow. Insets show representative traces taken at the times indicated by the letters.*

We then addressed why there is a discrepancy in the literature between the degree of LTP observed in eNOS-deficient mice in analogous studies. As the results in the present study lie between those observed previously (Son *et al.*, 1996; Wilson *et al.*, 1999), that is, only a partial deficit in LTP is observed in eNOS -/- mice, one plausible explanation may be the differing LTP induction protocols utilised: Son *et al.* used two trains of 100 Hz at 1 s duration, Wilson *et al.* used three trains of 100 Hz at 0.1 s duration to induce LTP, whereas our induction protocol lies between the two (one train of 100 Hz; 1 s). To address this possibility we monitored the synaptic response of wild type and eNOS -/- hippocampal slices under the same LTP induction protocol as followed by Wilson *et al.* (1999). On repeating the experiment we confirmed that weak tetanic stimulation in wild type mice resulted in robust LTP of ~ 150 % (figure 6.6a) that was NO-dependent. However, in contrast to the previous study, the LTP deficit observed in eNOS knockout mice was only partial (figure 6.6b). Furthermore, the deficit in LTP observed in eNOS -/- slices (124 ± 3 %) is comparable to that observed in the presence of L-NNA (125 ± 3 %), indicating that the remaining portion of the LTP response is NO-independent. Interestingly, the first EPSP slope post tetanus is significantly reduced ($P < 0.05$) in eNOS -/- slices (170 ± 3 %) when compared to their wild type counterparts (230 ± 15 %), whereas in the presence of L-NNA this reduction is not significant (197 ± 3 %; figure 6.6c).

We then enquired whether the deficit in LTP observed in eNOS knockout mice might be explained simply by the loss of tonic levels of NO, presumably generated from eNOS. If so, then pairing a low exogenous concentration of DEA/NO designed to mimic basal NO levels with tetanic stimulation might "rescue" LTP in eNOS knockout slices. We chose to apply DEA/NO at a concentration of 0.3 μM, which is just above threshold for raising cGMP levels in hippocampal slices (Bon & Garthwaite, 2001b) but has no effect on baseline fEPSPs elicited at 0.2 Hz (Bon & Garthwaite, 2001a). When the low DEA/NO concentration was perfused for a total of 15 min, covering the period before, during and after weak tetanic stimulation, LTP was apparently restored in eNOS knockout hippocampal slices (148 ± 3 %; figure 6.7). It must be noted, however, that although the degree of LTP observed in these slices did not significantly differ from the wild type (145 ± 6 %), the initial transient phase of LTP was not fully restored. Figure 6.8 confirms that 0.3 μM DEA/NO alone has no effect on LTP.

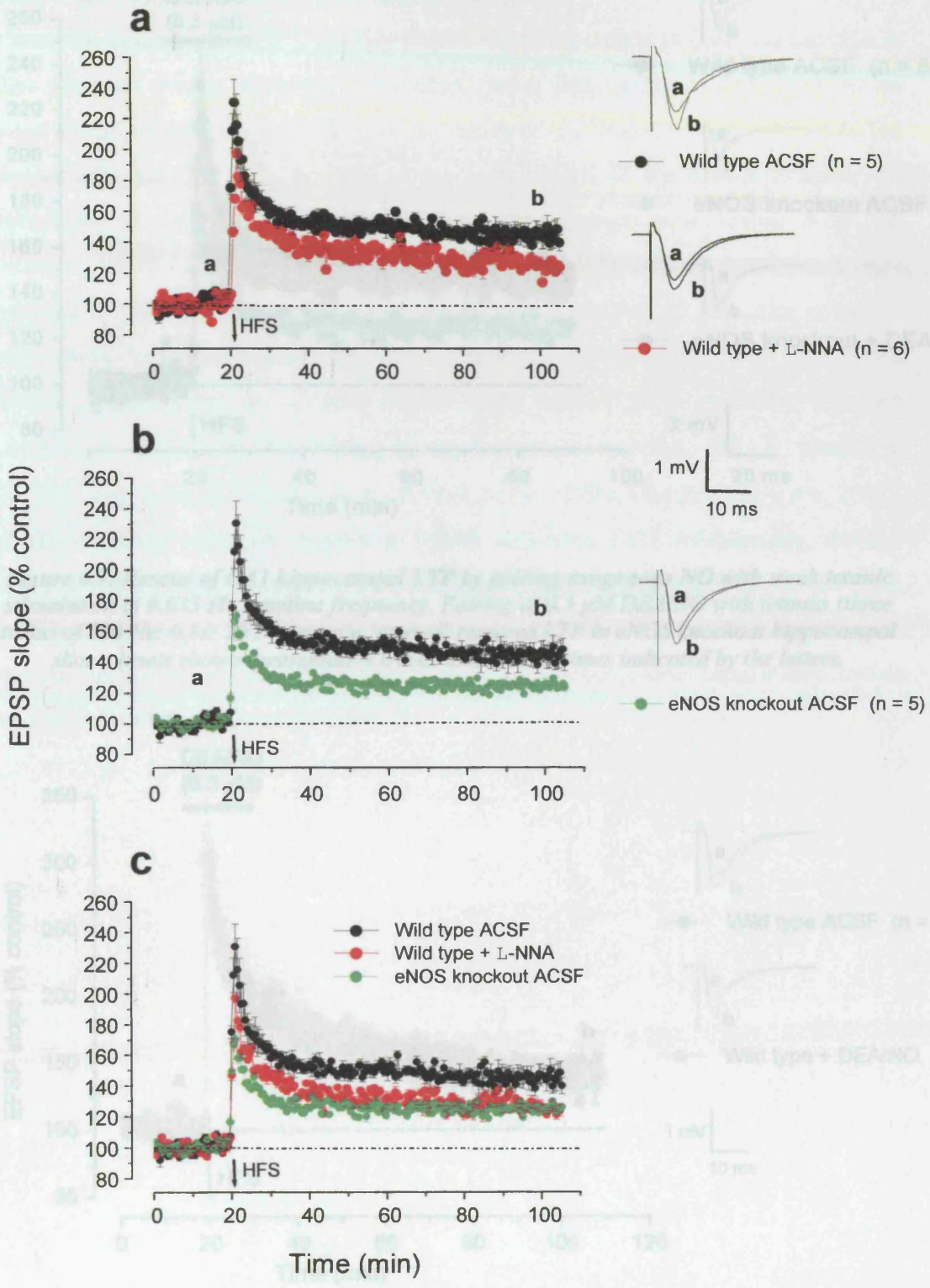

Figure 6.6: LTP induced by three trains of 100 Hz; 0.1s; 20 s intertrain interval at 0.033 Hz baseline frequency. *The tetanic stimulation was applied at the time indicated by the arrow. Insets show representative traces taken at the times indicated by the letters.*

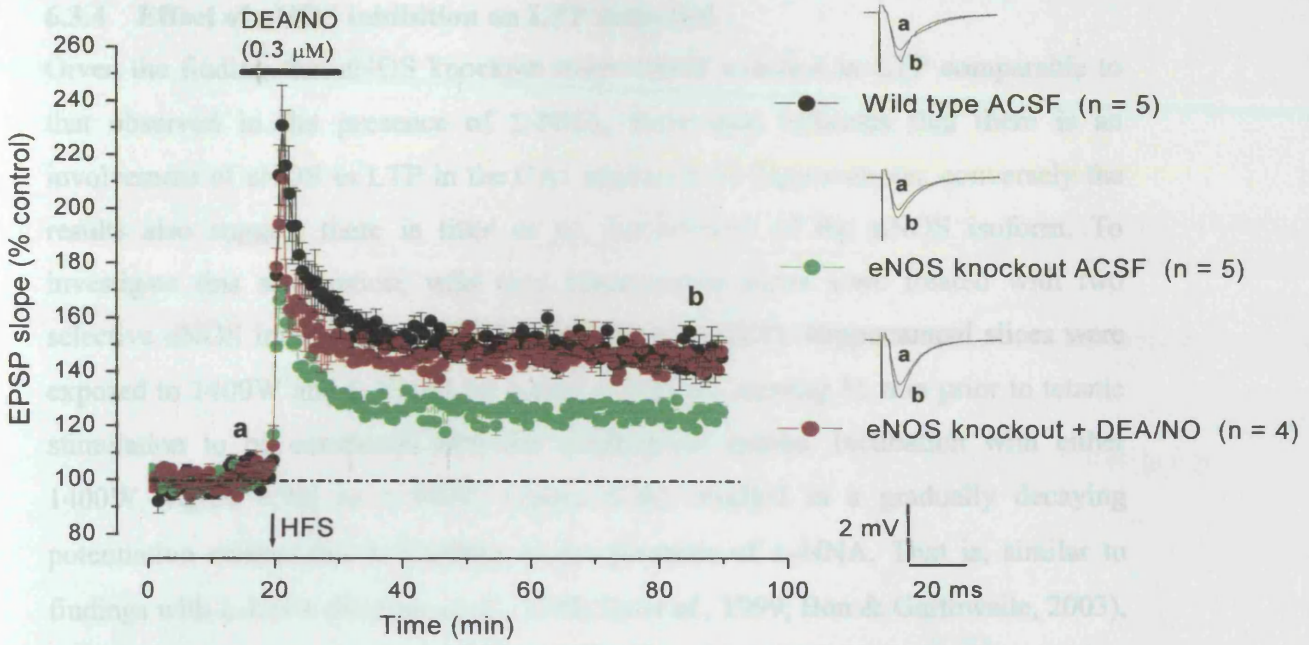

Figure 6.7: Rescue of CA1 hippocampal LTP by pairing exogenous NO with weak tetanic stimulation at 0.033 Hz baseline frequency. *Pairing of 0.3 μM DEA/NO with tetanus (three trains of 100 Hz; 0.1s; 20 s intertrain interval) restored LTP in eNOS knockout hippocampal slices. Insets show representative traces taken at the times indicated by the letters.*

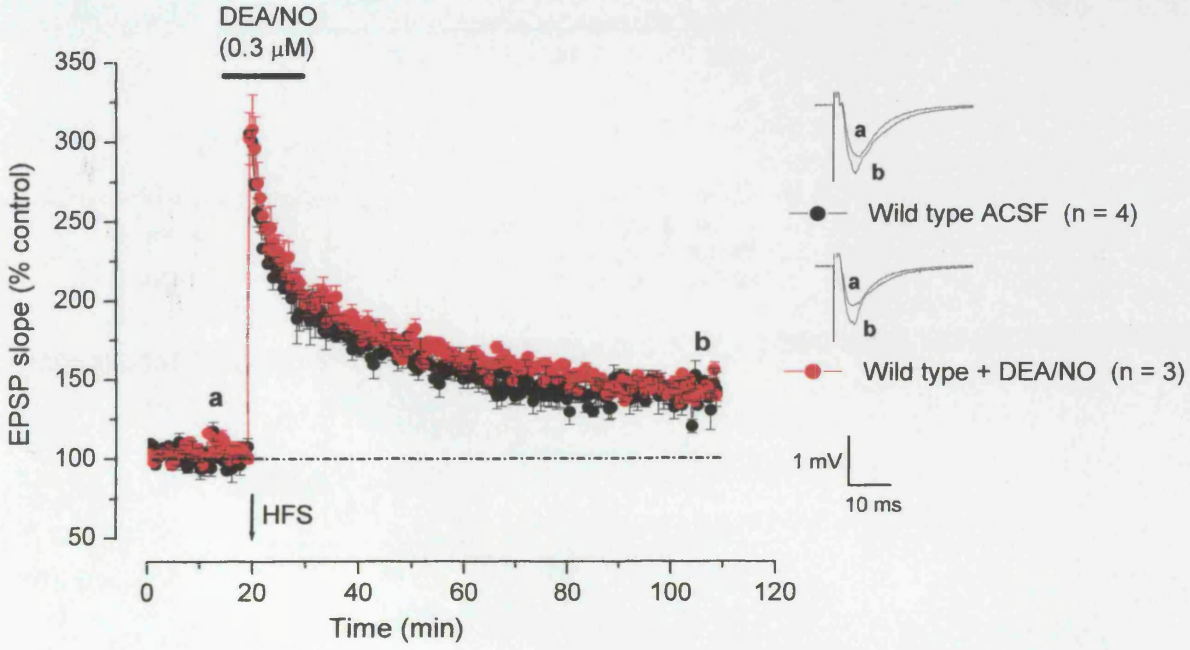

Figure 6.8: Effect of 0.3 μM DEA/NO on hippocampal LTP with weak tetanic stimulation at 0.033 Hz baseline frequency. *LTP was induced at the time indicated by the arrow. Insets show representative traces taken at the times indicated by the letters.*

6.3.4 Effect of nNOS inhibition on LTP induction

Given the finding that eNOS knockout mice exhibit a deficit in LTP comparable to that observed in the presence of L-NNA, these data indicates that there is an involvement of eNOS in LTP in the CA1 region of the hippocampus; conversely the results also suggest there is little or no involvement of the nNOS isoform. To investigate this assumption, wild type hippocampal slices were treated with two selective nNOS inhibitors identified in chapter 4 (4.3.1.1). Hippocampal slices were exposed to 1400W and L-VNIO for a total of 30 min, starting 15 min prior to tetanic stimulation to be consistent with the biochemical results. Incubation with either 1400W (figure 6.9a) or L-VNIO (figure 6.9b) resulted in a gradually decaying potentiation comparable to findings in the presence of L-NNA. That is, similar to findings with L-NNA (Boulton *et al.*, 1995; Lu *et al.*, 1999; Bon & Garthwaite, 2003), nNOS inhibition primarily appears to inhibit late-phase LTP. Additionally, the fact that two different nNOS inhibitors resulted in the same inhibition of late-phase LTP, indicates that the effect observed is attributable to their action on NO formation as opposed to any direct effect on protein synthesis or transcriptional/translational events associated with the maintenance of LTP.

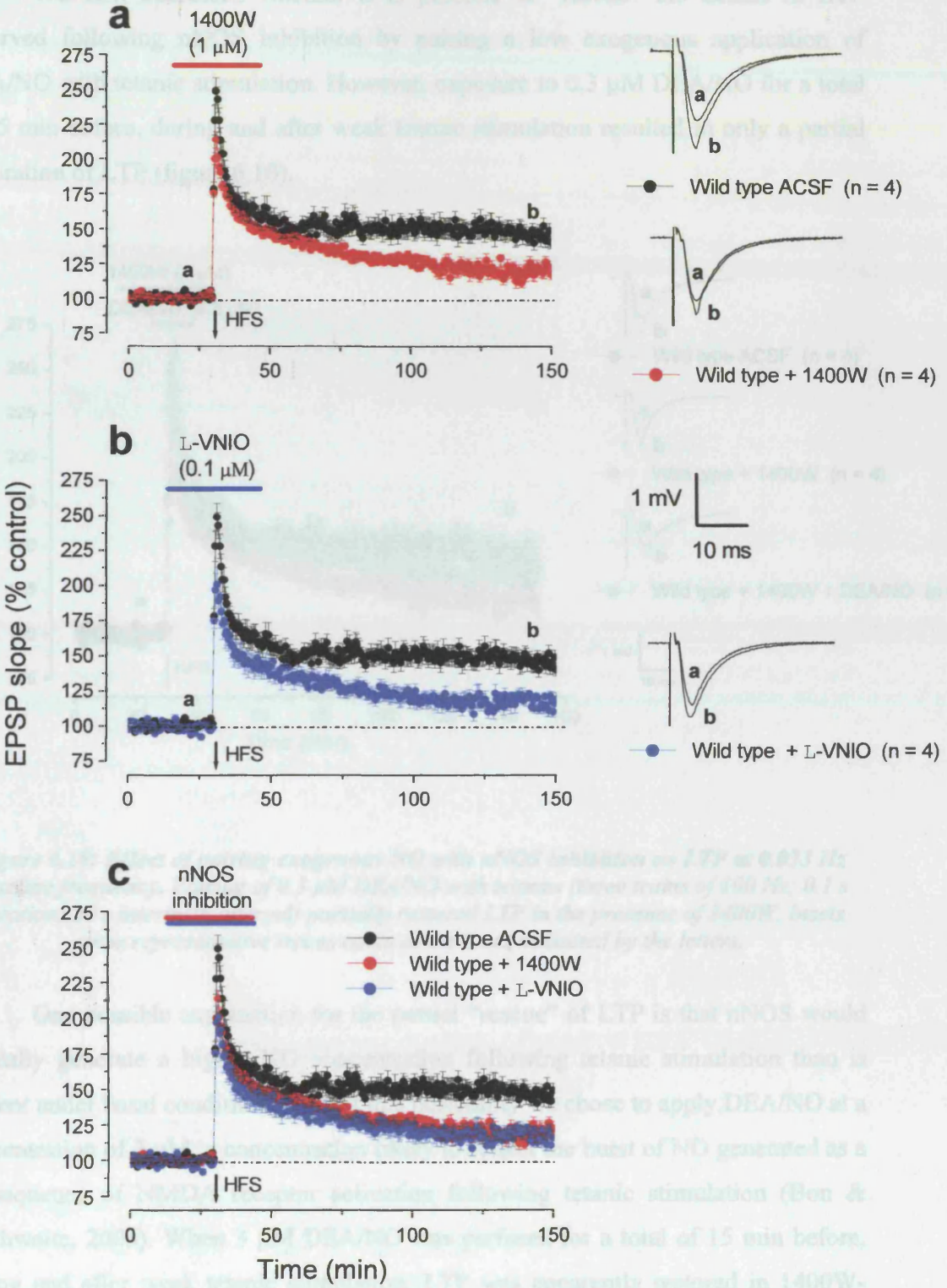

Figure 6.9: Effect of nNOS inhibition on LTP in wild type mouse hippocampal slices at 0.033 Hz baseline frequency. *Incubation with either (a) 1400W or (b) L-VNIO resulted in a reduction in LTP in wild type slices. LTP was induced by three trains of 100 Hz (0.1s duration; 20 s intertrain interval) at the time indicated by the arrow (n = 4).*

We then addressed whether it is possible to "rescue" the deficit in LTP observed following nNOS inhibition by pairing a low exogenous application of DEA/NO with tetanic stimulation. However, exposure to 0.3 μM DEA/NO for a total of 15 min before, during and after weak tetanic stimulation resulted in only a partial restoration of LTP (figure 6.10).

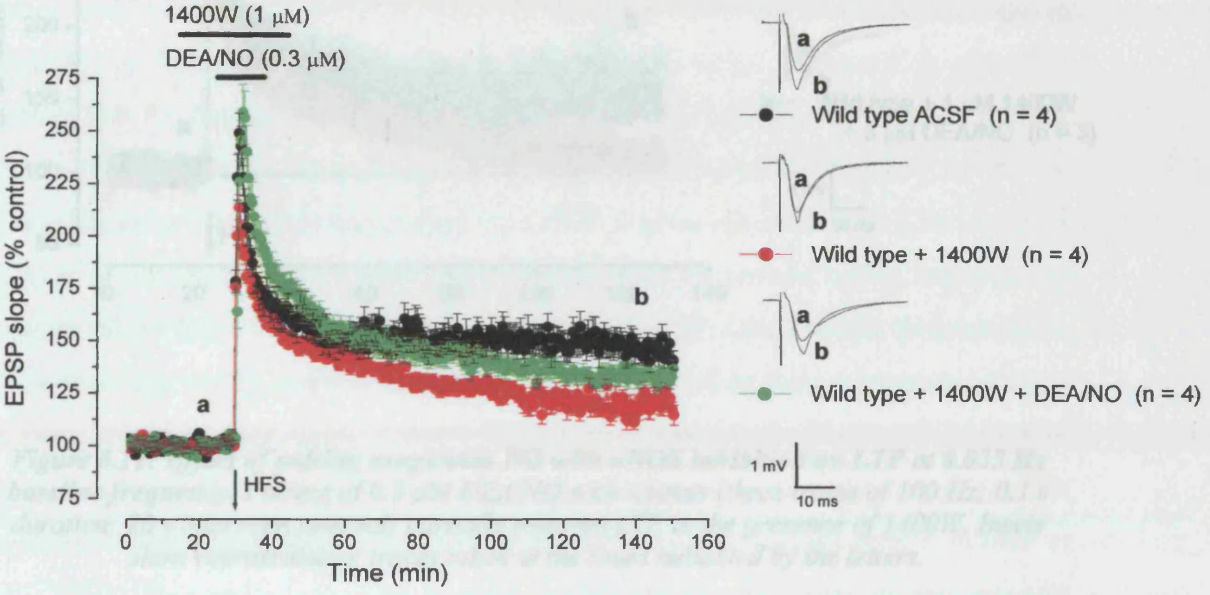

Figure 6.10: Effect of pairing exogenous NO with nNOS inhibition on LTP at 0.033 Hz baseline frequency. *Pairing of 0.3 μM DEA/NO with tetanus (three trains of 100 Hz; 0.1 s duration; 20 s intertrain interval) partially restored LTP in the presence of 1400W. Insets show representative traces taken at the times indicated by the letters.*

One possible explanation for the partial "rescue" of LTP is that nNOS would typically generate a higher NO concentration following tetanic stimulation than is present under basal conditions. To test this possibility we chose to apply DEA/NO at a concentration of 3 μM, a concentration likely to reflect the burst of NO generated as a consequence of NMDA receptor activation following tetanic stimulation (Bon & Garthwaite, 2003). When 3 μM DEA/NO was perfused for a total of 15 min before, during and after weak tetanic stimulation, LTP was apparently restored in 1400W-treated hippocampal slices (figure 6.11). The degree of LTP observed under these conditions was not significantly different from untreated wild type hippocampal slices. Furthermore, the initial transient phase of LTP was fully restored. Figure 6.12 confirms that 3 μM DEA/NO alone has no effect on LTP.

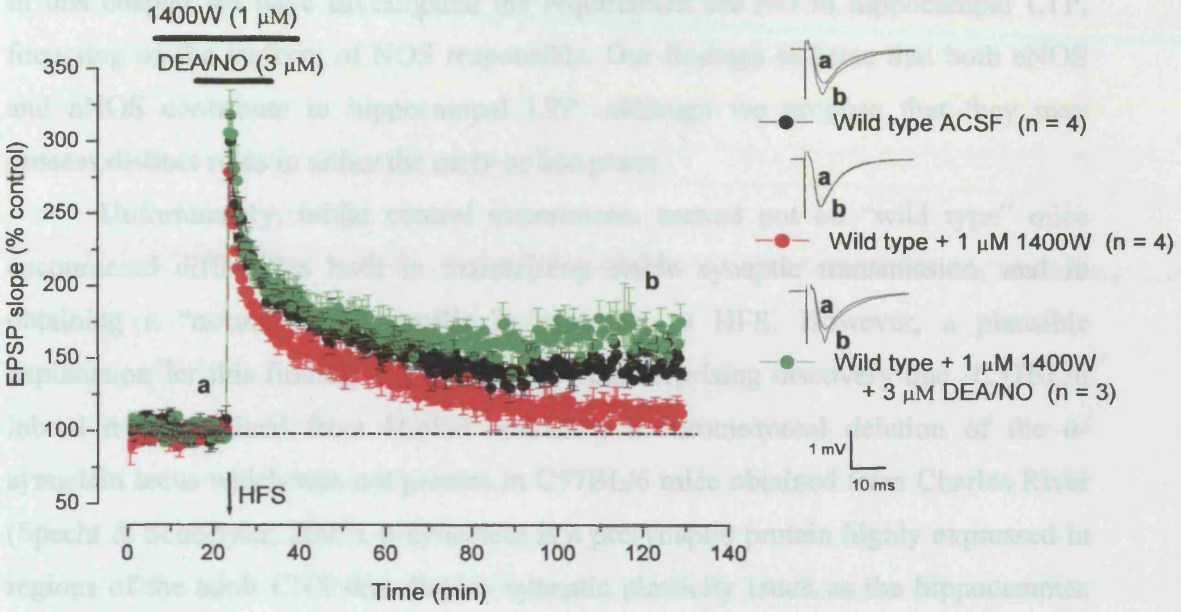

Figure 6.11: Effect of pairing exogenous NO with nNOS inhibition on LTP at 0.033 Hz baseline frequency. *Pairing of 0.3 μM DEA/NO with tetanus (three trains of 100 Hz; 0.1 s duration; 20 s intertrain interval) partially restored LTP in the presence of 1400W. Insets show representative traces taken at the times indicated by the letters.*

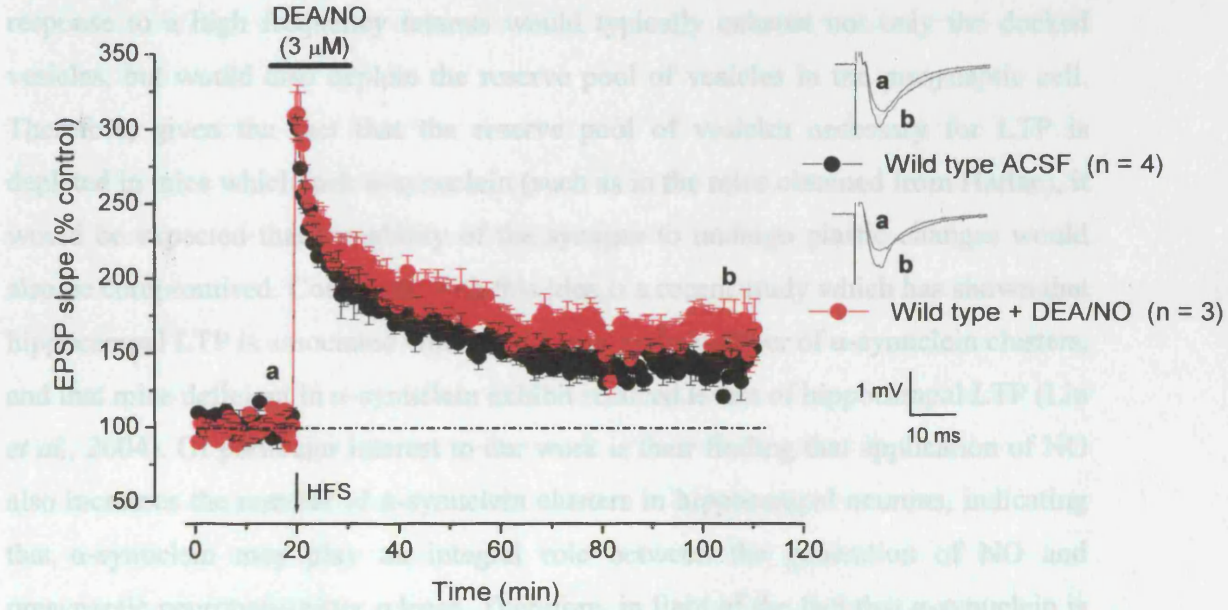

Figure 6.12: Effect of 3 μM DEA/NO on hippocampal LTP with weak tetanic stimulation at 0.033 Hz baseline frequency. *LTP was induced at the time indicated by the arrow. Insets show representative traces taken at the times indicated by the letters.*

6.4 Discussion

In this chapter we have investigated the requirement for NO in hippocampal LTP, focussing on the isoform of NOS responsible. Our findings indicate that both eNOS and nNOS contribute to hippocampal LTP, although we propose that they may possess distinct roles in either the early or late phase.

Unfortunately, initial control experiments carried out on "wild type" mice encountered difficulties both in maintaining stable synaptic transmission, and in obtaining a "normal" LTP profile in response to HFS. However, a plausible explanation for this finding was provided by the surprising discovery that C57BL/6 inbred mice obtained from Harlan contained a chromosomal deletion of the α-synuclein locus which was not present in C57BL/6 mice obtained from Charles River (Specht & Schoepfer, 2001). α-synuclein is a presynaptic protein highly expressed in regions of the adult CNS that display synaptic plasticity (such as the hippocampus; Petersen *et al.*, 1999), and has been found to be localised in the presynaptic terminal in close proximity to synaptic vesicles (Iwai *et al.*, 1995). Analysis of mice lacking α-synuclein revealed a marked decrease in the pool of resting-reserve synaptic vesicles in these animals, although the quantity of docked vesicles appears normal (Cabin *et al.*, 2002). This realisation was of vital importance to my work, as the synaptic response to a high frequency tetanus would typically exhaust not only the docked vesicles, but would also deplete the reserve pool of vesicles in the presynaptic cell. Therefore, given the fact that the reserve pool of vesicles necessary for LTP is depleted in mice which lack α-synuclein (such as in the mice obtained from Harlan), it would be expected that the ability of the synapse to undergo plastic changes would also be compromised. Consistent with this idea is a recent study which has shown that hippocampal LTP is associated with an increase in the number of α-synuclein clusters, and that mice deficient in α-synuclein exhibit reduced levels of hippocampal LTP (Liu *et al.*, 2004). Of particular interest to our work is their finding that application of NO also increases the number of α-synuclein clusters in hippocampal neurons, indicating that α-synuclein may play an integral role between the generation of NO and presynaptic neurotransmitter release. Therefore, in light of the fact that α-synuclein is likely to play an important role in synaptic plasticity, and that "wild type" C57BL/6 mice from Harlan are deficient in α-synuclein, we crossed eNOS knockout mice with

C57BL/6 mice from another source (Charles River, UK) to generate eNOS mutant and wild type littermates which do not contain this deletion.

Attempts made to address the relative contribution of the nNOS and eNOS isoforms to hippocampal LTP via genetic manipulations have so far proved unsuccessful in clarifying the situation. Initial studies found that mice lacking both eNOS and nNOS demonstrated reduced LTP in the stratum radiatum of the hippocampus (Son *et al.,* 1996), whereas animals which were mutant for only nNOS or eNOS exhibited normal or nearly normal LTP which was still sensitive to NOS inhibition (O'Dell *et al.,* 1994; Son *et al.,* 1996). In contrast, Wilson *et al.,* (1999) observed that LTP induced by a weak tetanus was completely absent in both eNOS knockout mice and in the presence of L-NNA in wild type animals, whilst LTP induced by a stronger tetanus was unaffected. Furthermore, LTP induced by the stronger tetanus was found to be NO-independent, that is it was insensitive to NOS inhibition. Since the authors of the latter study observed a complete absence of LTP in eNOS knockout animals they concluded that NO-dependent LTP is mediated by eNOS alone, with little or no contribution to nNOS, although this prediction was not explicitly tested. Also consistent with their conclusion is a report from Kantor *et al.* (1996), which found that transfection of hippocampal slices with a recombinant retrovirus carrying a dominant-negative truncated non-functional eNOS blocked LTP in the stratum radiatum.

The results obtained in the present chapter allow us to address four important questions regarding the contribution of the nNOS and eNOS isoforms to the induction and expression of LTP in the rodent hippocampus. The first issue we addressed was whether eNOS or nNOS generates the NO required for LTP. In our experiments we found that, although mice deficient in eNOS exhibited a significant deficit in LTP as reported previously (Wilson *et al.,* 1999), there was also a significant amount of residual LTP. However, no further reduction in LTP was observed in the presence of L-NNA, indicating that the residual component is NO-independent. Interestingly, it is the early phase of LTP that appears to be most affected in eNOS -/- slices when compared to their wild type counterparts (figure 6.13), although this does not seem to hinder the capacity of the hippocampus to maintain stable LTP, albeit to a lesser degree than in wild type animals.

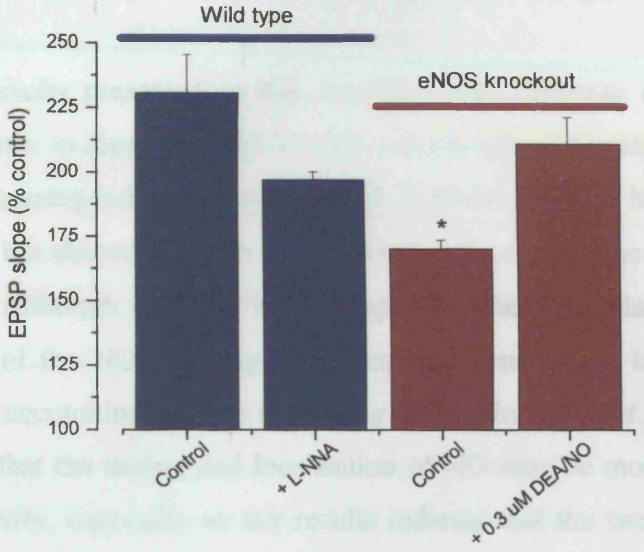

Figure 6.13: Effect of eNOS knockout on EPSP slope immediately following tetanus. *LTP was induced by three trains of 100 Hz; 0.1 s; 20 s intertrain interval at 0.033 Hz basal stimulation frequency (n = 4 – 5). *P < 0.05 vs. wild type control EPSP slope; one-way ANOVA with Tukey's post-hoc test.*

Given the similar deficits in LTP in both the presence of L-NNA, and in eNOS knockout animals, it would be predicted that nNOS would play little or no contribution towards LTP. However, contrary to expectations, selective inhibition of nNOS by either 1400W or L-VNIO produced a gradually decaying potentiation comparable to findings in the presence of L-NNA. That is, similar to findings with L-NNA (Boulton *et al.,* 1995; Lu *et al.,* 1999; Bon & Garthwaite, 2003), nNOS inhibition primarily appears to affect the late-phase LTP. This result supports the growing body of evidence that NO, acting postsynaptically via the NO/cGMP/cGK pathway, contributes to CREB phosphorylation and late-phase LTP (Lu *et al.,* 1999; Lu & Hawkins, 2002; Kleppisch *et al.,* 2003). At first glance the involvement of nNOS in hippocampal LTP found in our work may appear at odds with the previous reports of normal LTP in nNOS -/- mice (O'Dell *et al.,* 1994; Son *et al.,* 1996). However, disruption of the nNOS gene only eliminates 95 - 98 % of nNOS activity (Huang *et al.,* 1993). Two alternatively spliced isoforms of NOS, nNOSβ and nNOSγ, continue to be expressed in nNOS mutant mice (Putzke *et al.,* 2000), and both have recently been identified in hippocampal pyramidal cells as well as in interneurons (Blackshaw *et al.,* 2003). Given that one of these alternatively spliced isoforms (nNOSβ) has been found to be catalytically active *in vivo* (Eliasson *et al.,* 1997), it is feasible that these alternative isoforms may provide an important physiological source

of NO capable of compensating, at least in part, for the lack of nNOSα in mutant animals.

The results presented in this chapter clearly indicate that both eNOS and nNOS contribute to hippocampal LTP and, surprisingly, it appears that the absence of either isoform independently is sufficient to produce a deficit in LTP comparable to that found in the absence of both isoforms (as is the case in the presence of L-NNA; figure 6.14). Although this may initially appear to be a surprising conclusion given that ~ 98 % of the NOS activity in the hippocampus is due to nNOS, with eNOS activity only accounting for the remaining 2 % (Huang *et al.*, 1993). However, it seems likely that the timing and localisation of NO may be more important than the net NOS activity, especially as our results indicate that the two NOS isoforms may possess distinct roles regarding their influence in either the early or late phase of LTP. One study examining the role of NO in cerebellar LTD has shown that LTD is only induced when Ca^{2+} transients coincide precisely with a rise in NO levels in the same Purkinje cell; LTD induction only permits a gap of < 10 ms between these two signals (Lev-Ram *et al.*, 1997). It is very possible that a similar arrangement exists in the hippocampus which may govern the action of NO in LTP; that is selectively inhibiting only one NOS isoform could prevent the NO-dependent component of LTP to occur.

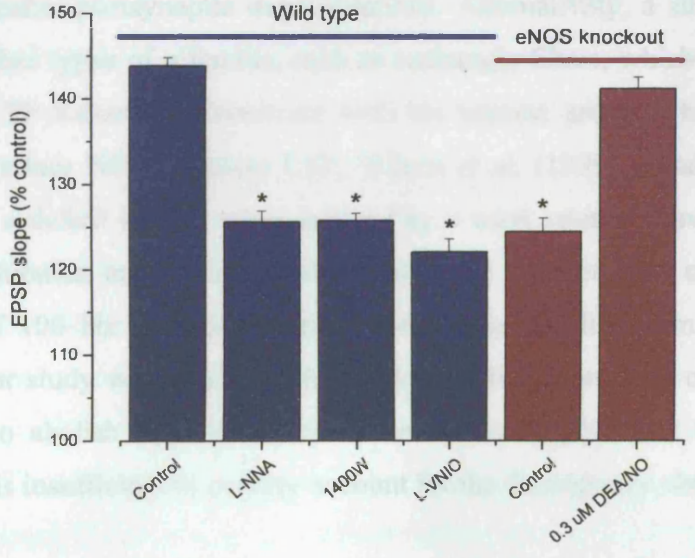

Figure 6.14: Effect of NOS inhibition on EPSP slope measured 80 min post tetanus. *LTP was induced by three trains of 100 Hz; 0.1 s; 20 s intertrain interval at 0.033 Hz baseline frequency (n = 4 - 5). *P < 0.05 vs wild type control EPSP slope; one-way ANOVA with Tukey's post-hoc test.*

The second issue we addressed was whether the strength of the tetanus could account for the discrepant results observed with regards to the degree of LTP in eNOS-deficient mice. A direct comparison between LTP studies is often hindered by the use of widely varying protocols to induce LTP; for example Son *et al.* (1996) used a tetanus of two trains of 100 Hz frequency with 1s duration, whereas Wilson *et al.* (1999) used three trains of 100 Hz frequency with 0.1 s duration. In our experiments we found that although mice deficient in eNOS exhibited a pronounced deficit in LTP, a significant degree of LTP remained. However, no further reduction in LTP was observed in the presence of L-NNA, indicating that the residual component is NO-independent. We are uncertain why our results differ from both Wilson *et al.* (1999) and Son *et al.* (1996), especially since eNOS -/- mice in each case were constructed using the same mouse strains (129SV and C57BL/6), by the same strategy of targeting a mutation to the NADPH binding site of eNOS, and all mice were tested at roughly the same age (8 - 12 weeks). One possible explanation lies in the different tetanus protocols used, since weak tetanus protocols tend to favour NO-dependent forms of LTP whereas stronger stimulations induce NO-independent forms of LTP. Why a stronger stimulation is able to bypass the requirement for NO is not yet clear. Stronger stimulation intensities presumably activate more fibres; by recruiting a larger number of glutamatergic afferents, a strong tetanus could depolarise the postsynaptic cell to a greater degree and thereby engage biochemical pathways which are not activated by weaker postsynaptic depolarisations. Alternatively, a stronger stimulus could recruit other types of afferents, such as aminergic fibres, which may lower the threshold for LTP induction. Consistent with the tetanus protocol being of utmost importance to induce NO-dependent LTP, Wilson *et al.* (1999) found that eNOS -/- mice displayed a deficit in LTP when induced by a weak tetanus (three trains of 100 Hz with 0.1s duration at baseline stimulus intensity) but not by a stronger tetanus (three trains of 100 Hz with 0.1s duration at double baseline stimulus intensity). However, in our study we found that the weak stimulation protocol of Wilson *et al.* (1999) failed to abolish LTP in eNOS animals. This implies that the stimulation protocol alone is insufficient to entirely account for the discrepancy observed between groups.

A second possibility is that since our population of eNOS knockout mice contain a slightly different background to those used in previous studies (i.e. a greater degree of similarity to the C57BL/6 strain in our eNOS knockout) that this may

indicate different expression levels of nNOS, and thereby lead to varying degrees of NO-dependent LTP in the mutant mice. This supposition stems from the recent observation by Blackshaw *et al.,* (2003) that nNOS expression is substantially higher in C57BL/6 than 129SV mice in the CA1 region of the hippocampus, although nNOS levels were indistinguishable between strains in all other regions tested.

Additionally, it is also worth noting that a difference in LTP was observed between the two tetanus protocols (1 train of 100 Hz, 1 s as opposed to 3 trains of 100 Hz, 0.1 s) following NOS inhibition. Both early- and late-phase LTP was found to be reduced following NOS inhibition in the weaker stimulation protocol, whereas no difference in the early-phase was noted when a stronger tetanus was utilised. The most plausible explanation for this finding is that LTP induced by 100 Hz, 1 s may be less NO-dependent than LTP resulting from the weaker protocol. If this was the case, the stronger tetanus may mask the inhibition of the early-phase of LTP observed following weak tetanic stimulation in the absence of NOS activity.

The third issue we addressed was whether the deficit in NO-dependent LTP observed in eNOS -/- animals could be explained simply by the loss of NO generated from eNOS, the assumption being that eNOS is responsible for tonic NO production in the hippocampus (chapter 4). If this was the case, then pairing a low exogenous concentration of DEA/NO that restores basal NO levels should "rescue" the LTP deficit in eNOS knockout slices. Accordingly, 0.3 μM DEA/NO restored LTP in eNOS knockout animals when paired with a weak tetanus, indicating that tonic NOS activity is required for LTP. This finding is in agreement with previous reports which found that LTP could be inhibited by general NOS inhibition for $\leq$ 15 min post tetanus (Haley *et al.,* 1992; Bon & Garthwaite, 2003). It must be noted however that although the degree of LTP observed in the "rescued" eNOS knockout slices did not significantly differ from that in the wild type, the initial transient phase of LTP was not fully restored (figure 5.12). The finding that the initial transient phase of LTP cannot be fully restored by the application of exogenous NO indicates that there may be an NO-independent component to the initial deficit in LTP observed in eNOS-deficient mice. The most likely explanation for this is that compensation mechanisms or structural changes have evolved in eNOS-deficient mice to make up for the lack of eNOS throughout embryonic development.

Similar to the "rescue" of LTP observed in eNOS knockout mice, we then tested whether it was possible to "rescue" the deficit in LTP observed following

nNOS inhibition by pairing a low exogenous concentration of DEA/NO with tetanic stimulation. However, in contrast to the "rescue" of LTP observed in eNOS knockout mice, 0.3 μM DEA/NO resulted in only a partial "rescue" of LTP. This result is not completely unexpected, given that nNOS would typically generate a higher NO concentration following tetanic stimulation than is required to maintain tonic NO at active levels (Chetkovich *et al.*, 1993). Therefore, application of a low exogenous NO concentration (reflective of basal NO levels) would not be expected to substitute for the burst of NO produced as a consequence of NMDA receptor activation at the time of tetanic stimulation. In accordance with this, 3 μM DEA/NO restored LTP in 1400W-treated hippocampal slices when paired with a weak tetanus: a concentration thought to result in NO levels similar to those produced as a consequence of NMDA receptor activation (Bon & Garthwaite, 2003). Interestingly, the initial transient phase of LTP was also fully restored, indicating that the deficit in LTP observed in the presence of 1400W is likely to be explained simply by an insufficient level of NO being present at the time of LTP induction.

The final issue we addressed was whether there is a frequency dependence of the NOS-sensitive component of LTP. It is widely becoming realised that the frequency at which electrophysiological experiments are undertaken is of great importance, especially given the recent report by Bon & Garthwaite (2001b) that stimulation frequencies as low as 0.2 Hz may trigger long lasting plastic changes in central synapses in normal animals that do not occur at 0.033 Hz. In this study NO triggered a long-lasting enhancement of excitatory synaptic transmission that occluded LTP at 0.2 Hz, but not at 0.033 Hz. Furthermore, this NO-triggered potentiation appears to share mechanisms in common with normal HFS-induced LTP; LTP was progressively occluded in proportion with the degree of prior NO-triggered potentiation, and the NO-triggered potentiation could be inhibited by NMDA receptor antagonists, similar to HFS-induced LTP (Bon & Garthwaite, 2001a). One possibility which has been put forward to explain this is that synapses could become "primed" at frequencies as low as 0.2 Hz, possibly as a consequence of the partial loss of GABA-mediated inhibition resulting from $GABA_B$ autoreceptor activation (Davies & Collingridge, 1993). However, in contrast to the robust rebound potentiation observed by Bon & Garthwaite, the depression was followed by only minimal rebound potentiation. Subsequent tetanus-induced LTP (one train of 100 Hz; 1s) was found to be normal. The explanation for this discrepancy is also unclear. The same frequency

of synaptic transmission (0.2 Hz), the same strength of presynaptic stimulation (~ 30 % of maximum fEPSP slope), and the same source of DEA/NO (Alexis Biochemicals), were used in both the current study and in previous reports. Similar observations were also made in both the rat and the mouse hippocampus. Furthermore, various experiments carried out on the same electrophysiological set-up used to obtain the previous findings again resulted in only minimal rebound potentiation.

Given the fact that different groups use widely varying frequencies by which to stimulate baseline fEPSPs, the highest of which being 0.2 Hz (Böhme *et al.*, 1991, 1993), this "priming" may go some way towards explaining the conflicting results regarding the NO dependence of LTP. However, in our experiments we found that there was no difference in the deficit in LTP observed in eNOS knockout animals between 0.2 Hz and at 0.033 Hz. This result therefore indicates that there is little or no frequency dependence to the NOS-sensitive component of LTP at the stimulation frequencies tested.

Overall our findings provide good support for the hypothesis that NO serves as an important messenger in hippocampal LTP, and present evidence for a contribution from both constitutive forms of NOS. The results also propose the interesting possibility that the different isoforms of NOS may possess distinct roles in the modulation of synaptic events; that is eNOS appears to be important for the early phase of LTP, whereas nNOS seems to exert a greater influence on the late phase. However, given the observation that the initial transient phase of LTP remains reduced following the "rescue" of LTP in eNOS-deficient mice, an indication that there may be an NO-independent component to this initial deficit in LTP, the possibility that eNOS and nNOS may carry out the same role cannot be ruled out. We postulate that the previously reported observations of normal LTP in the absence of nNOS (O'Dell *et al.*, 1994; Son *et al.*, 1996) may be explained by either the LTP induction protocol, or more likely, by the activity of alternatively spliced isoforms of nNOS that remain in the nNOS knockout (Eliasson *et al.*, 1997) providing a physiological source of NO capable of potentially compensating for the absence of nNOSα in these animals. Therefore acute inhibition of nNOS in wild type mice, as carried out in the present study, is likely to provide a more accurate portrayal of the contribution that nNOS plays in synaptic transmission.

Chapter 7

General Discussion and Conclusion

7.1 General Discussion

The aim of my research was to investigate and further characterise the role that NO plays in synaptic plasticity in the hippocampus. Given that hippocampal LTP is critically dependent on post-synaptic activation of the NMDA receptor (Bliss & Collingridge, 1993), I initially set out to test some of the primary predictions of the hypothesis that NO regulates NMDA receptor function in central synapses. In chapter 3 the role of endogenous and exogenous NO in synaptic function was investigated on native or cloned NMDA receptors, in acute rat hippocampal slices and HEK-293 cells respectively, and found to have no observable effect on NMDA receptor function. Importantly, these results also indicate that previously reported observations of synaptic NMDA receptor block by NO (Murphy *et al.*, 1994; Murphy & Bliss, 1999) may be artifactual: examination utilising transfected cells demonstrated that NO itself was not responsible for inhibition of NMDA receptor currents, but the combination of NO and UV light. Further inspection revealed the previous indirect evidence that NO affects NMDA receptor function to be questionable, and this, together with the additional direct evidence presented in the current study, places the hypothesis that NO regulates the functioning of synaptic NMDA receptors in serious doubt.

Given the importance of the NO/cGMP pathway in hippocampal LTP, I then went on to investigate the isoform of NOS which mediates the involvement of NO in LTP in chapters 4 and 5. Collectively these results provide good support for the hypothesis that hippocampal LTP requires both a tonic NO level, and a phasic NO signal arising from tetanic stimulation (Bon & Garthwaite, 2003). I additionally present evidence that both eNOS and nNOS contribute to this phenomenon, since a deficit in LTP was observed in both eNOS-deficient mice, and in wild type mice subjected to selective nNOS inhibition. Furthermore, the results propose the interesting possibility that the different isoforms of NOS (nNOS and eNOS) may possess distinct roles in the modulation of synaptic events.

With respect to the tonic component, we found that eNOS is most likely responsible for basal NO production in the hippocampus, and that NO generated from this source appears to be important in the early phase of LTP. In particular, the initial phase of LTP is significantly reduced in eNOS -/- slices when compared to their wild type counterparts. However, this reduction in early LTP does not seem to hinder the capacity of the hippocampus to maintain stable LTP, albeit to a lesser degree than in wild type mice. As these early time points in LTP are considered to represent the presynaptic accumulation and rapid release of Ca^{2+} during tetanisation (Stevens *et al.*, 1994; Zucker, 1999), the observation that the initial phase of LTP is reduced in eNOS-deficient mice presents the possibility that eNOS may mediate, at least in part, an action of NO on the presynaptic terminal.

With respect to the phasic component, it is widely recognised that tetanic simulation results in NMDA receptor activation leading to the consequent influx of Ca^{2+} into the postsynaptic cell. Given the physical coupling of NMDA receptors and nNOS, and the absolute requirement of nNOS for Ca^{2+}, it strongly suggests that the increase in intracellular Ca^{2+} following NMDA receptor activation stimulates the production of NO from nNOS. In our experiments we found that, in contrast to a role for eNOS in early LTP, nNOS primarily appears to influence the late-phase of LTP, a phase dependent on protein and mRNA synthesis (Frey *et al.*, 1993; Huang & Kandel, 1994; Krug *et al.*, 1984; Nguyen *et al.*, 1994; Otani & Abraham, 1989). The gradual decay in potentiation resulting from nNOS inhibition (figure 5.9) is comparable to that observed in the presence of protein synthesis inhibitors. That is, the initial phase of LTP was normal, but there was a deficit that only became apparent ~ 60 min post tetanus.

The mechanism by which NO mediates its effect remains a matter of debate, in part because cGMP and cGK appear to be involved under some circumstances, but not under others (Hawkins *et al.*, 1998). A number of studies indicate that NO contributes to the maintenance of LTP through the stimulation of NO-activated GC and cGK, presumably acting in parallel with the cAMP/PKA pathway to increase phosphorylation of the transcription factor CREB (Lu *et al.*, 1999; Lu & Hawkins, 2002; Kleppisch *et al.*, 2003). Some studies indicate that the protein synthesis most likely occurs in the post-synaptic neuron since late-phase LTP is blocked when the dendrites are surgically separated from the postsynaptic bodies (Frey *et al.*, 1989), whereas both late-phase LTP by tetanic stimulation and late-phase potentiation by NO

or cGMP analogues are normal in slices from which the presynaptic cell bodies have been removed (Lu *et al.*, 1999). Other studies in cultured hippocampal neurons find that intracellular injection of cGK inhibitors into the presynaptic (but not the postsynaptic) neuron blocked LTP. Conversely, cGK injected into the presynaptic (but not the postsynaptic) cell elicited LTP (Arancio *et al.*, 2001).

It is generally accepted that tetanic stimulation produces an increase in postsynaptic Ca^{2+} from a variety of sources. In addition to Ca^{2+} influx through postsynaptic NMDA receptors, two other important Ca^{2+} sources are thought to increase intracellular Ca^{2+} concentration: voltage-dependent Ca^{2+} channels and mGlu receptor-linked IP_3 production with the consequent release of Ca^{2+} from IP_3- and ryanodine-sensitive intracellular stores (Harvey & Collingridge, 1992; Bortollo & Collingridge, 1993; Behnisch & Reymann, 1995; Wilsch *et al.*, 1998). Phosphorylation of IP_3 receptors has been demonstrated in intact aorta in response to elevated cGMP levels, and cGK has been shown to catalyse this phosphorylation in both intact and permeablised cells (Murthy & Makhlouf, 1995; Komalavilas & Lincoln, 1996; Schlossman *et al.*, 2000). NO gas has additionally been found to induce IP_3 phosphorylation (Osct-Gasque *et al.*, 1994), an effect mimicked by analogues of cGMP, but inhibited by inhibitors of NO-activated GC (Vicente *et al.*, 2005). The consequence of cGK activation and IP_3 phosphorylation is the inhibition of IP_3-dependent Ca^{2+}release from intracellular stores (Cavallini *et al.*, 1996; Murthy, 2001).

A second downstream effector of cGK is ADP-ribosyl cyclase, an endogenous modulator of ryanodine receptor Ca^{2+}-releasing channels. Activation of ADP-ribosyl cyclase stimulates the production of cyclic ADP-ribose (cADPR). Enhancement of cADPR formation has been demonstrated in response to NO and cGMP in both rat hippocampal slices (Reyes-Harde *et al.*, 1999) and in homogenates of sea urchin eggs (Galione *et al.*, 1993). Furthermore, blockade of cADPR reduced LTP with a profile similar to protein synthesis inhibition (Reyes-Harde *et al.*, 1999), indicating that the cADPR pathway may be involved in late-phase, as opposed to early-phase, LTP. This pathway is thought to act synergistically with cytoplasmic Ca^{2+} to cause release of Ca^{2+} from ryanodine-sensitive intracellular stores (Galione *et al.*, 1993; Lee, 1993; Lee *et al.*, 1995; Lu *et al.*, 2002), and thereby amplify the Ca^{2+} signal generated from other sources (Alford *et al.*, 1993; Bliss & Collingridge, 1993; Emptage *et al.*, 1999). In agreement with this, Ca^{2+} release from intracellular stores has been implicated in

the induction of LTP in hippocampal slices (Harvey & Collingridge, 1992; Wang *et al.*, 1996). When the Ca^{2+} signal is sufficiently large it would trigger CREB phosphorylation and induction of L-LTP in parallel with PKA (Lu *et al.*, 1999, 2002). Consequently, activation of the NO/cGMP/cGK/ryanodine receptor pathway would lower the stimulation threshold for LTP induction, and inhibiting this pathway would have the opposite effect. The effect of NOS inhibitors is therefore to lower the intracellular Ca^{2+} signal from above to below the threshold for synaptic plasticity for the weaker protocols, but not with the stronger protocols.

In contrast to the cGMP-dependent mechanisms involved in LTP, there are several reports that cGMP analogues or cGK inhibitors have no effect on NO-dependent LTP (Schuman *et al.*, 1994; Selig *et al.*, 1996; Kleppisch *et al.*, 1999). In these cases it has been proposed that NO may induce LTP through an alternative cGMP-independent mechanism, possibly via ADP-ribosylation. In support of this hypothesis, ADP-ribosyl transferase (ADPRT) activity that can be enhanced by NO has been shown in the CA1 region of the hippocampus (Sullivan *et al.*, 1997), but attenuated by inhibition of ADP-ribosylation (Schuman *et al.*, 1994). Although both of these studies utilised SIN-1 and sodium nitroprusside as NO donors (see chapter 3 for problems regarding these compounds), the authors concluded that the enhancement in ADPRT activity was due to NO as ADP ribosylation was not stimulated by non-NO decomposition products, application of a superoxide scavenger did not inhibit ADP-ribosylation, whereas an NO-scavenger (Hb) prevented the enhancement of ADPRT activity (Brüne & Lapentina, 1989; Sullivan *et al.*, 1997; Schuman *et al.*, 1994). Additional evidence supporting a cGMP-independent mechanism comes from the observation that ADP-ribosylation cannot be mimicked by cGMP (Brüne & Lapentina, 1989). Electrophysiological studies also support a role for ADP-ribosylation in LTP: LTP is suppressed in the murine hippocampus by ADPRT inhibitors (at a concentration which does not affect basal excitatory or inhibitory synaptic transmission; Schuman *et al.*, 1994), and a marked reduction in LTP can be observed in cGK-deficient animals following ADPRT inhibition (Kleppisch *et al.*, 1999). The authors in the latter study found that LTP was not reduced in cGKI, cGKII, or double mutant mice when compared to control wild type animals, and that incubation with an NO-activated GC inhibitor also had no effect. Furthermore, NOS inhibitors and NMDA receptor antagonists produced a marked decrease in LTP which was not restored by exogenous cGMP, indicating that LTP is

NO-dependent but cGMP and cGK independent. This therefore challenges the view that expression of LTP involves a cGK-dependent step, and strengthens the hypothesis that NO may act, at least in part, via ADP-ribosylation.

All the evidence points toward the conclusion that NO is capable of influencing both pre- and postsynaptic protein synthesis events. In keeping with this, LTP has been recently demonstrated to involve the rapid formation of clusters or puncta of presynaptic, as well as of postsynaptic, proteins (Wang *et al.*, 2005), both of which are blocked by NMDA receptor antagonists. Because the maintenance of LTP is also thought to involve the growth of new synapses (Luscher *et al.*, 2000; Bozdagi *et al.*, 2000), the rapid formation ($\leq$ 2 min) of new clusters or puncta may represent a very early step in this process. Early stages in LTP are also accompanied by the enlargement of existing postsynaptic spines (Matsukaki *et al.*, 2004), in addition to the formation of new presynaptic filopodia which has been found to involve NO (Nikonenko *et al.*, 2003). These results therefore propose a sequence in that NMDA receptor activation triggers postsynaptic NO production from nNOS, which could then play some role in the formation of new presynaptic filopodia. Accordingly, the new presynaptic filopodia could then influence the formation of new postsynaptic spines and morphologically mature synapses that occurs at around 30 - 60 min post tetanus (Engert & Bonhoeffer, 1999; Maletic-Savatic *et al.*, 1999; Toni *et al.*, 1999; Nikonenko *et al.*, 2003). The time scale for these morphological changes is consistent with our finding of a gradually decaying potentiation following selective nNOS inhibition which only becomes apparent at ~ 60 min post tetanus. Any of these early structural changes could represent the short-lasting (< 3 h) protein synthesis-independent synaptic "tag" proposed by Frey and Morris (1997) which enables the specific targeting of newly synthesized proteins crucial for late-phase LTP to the synapses that are stimulated during LTP induction.

NO and learning behaviour

As mentioned previously, synaptic plasticity is commonly considered to be the cellular correlate to learning and memory. However, despite the well-described involvement of NO in hippocampal synaptic plasticity, inhibition of NOS has generated conflicting results. General NOS inhibition has been reported to slow down (Chapman *et al.*, 1992), as well as to accelerate (Du & Harvey, 1996), classical conditioning. Application of NO donors either improved or impaired avoidance learning, depending on the dose applied (Huang & Lee, 1995). Furthermore, in the Morris water maze systemic NOS inhibition had detrimental effects in some studies (Chapman *et al.*, 1992; Estall *et al.*, 1993; Yamada *et al.*, 1995), whereas other groups demonstrate no effect of either systemic or intrahippocampal inhibition of NO synthesis (Bannerman *et al.*, 1994; Blokland *et al.*, 1999).

Attempts to clear up this issue by means of genetic manipulations have also proved unsuccessful. Given the LTP deficits observed in the absence of eNOS and/or nNOS (Doyle *et al.*, 1996; Kantor *et al.*, 1996; Son *et al.*, 1996; Wilson *et al.*, 1997), and the traditional view of a positive functional relationship between LTP and learning capacity, it would be predicted that disruption of either eNOS or nNOS would result in an impaired learning capacity. However, contrary to the expected learning deficit, various studies indicate that eNOS -/- mice may in fact display improved learning and memory capabilities. Frisch *et al.* (2000) reported that eNOS knockout mice performed better in the Morris water maze than control animals, whereas a more recent study by Reif *et al.* (2004) found that eNOS-deficient mice were less helpless in a learned helplessness paradigm. In contrast, nNOS-deficient mice have been found to exhibit impaired spatial performance in the Morris water maze (Kirchner *et al.*, 2004).

Behavioural assessment of anxiety and activity-related traits also revealed various differences; aggressive behaviour was diminished in eNOS-deficient mice, whereas it was increased in nNOS-deficient animals (Demas *et al.*, 1999). Additionally, eNOS knockout mice were found to be less active than wild-type controls (Firsch et al., 2000), as opposed to nNOS -/- mice which exhibited slightly increased locomotive activity (Kirchner *et al.*, 2004). No other prominent differences were observed between knockout and wild type animals in alternative behavioural paradigms (Demas *et al.*, 1999; Dere *et al.*, 2001; Reif *et al.*, 2004).

The fact that eNOS-deficient mice displayed superior water maze performance whilst exhibiting a deficit in LTP challenges the widely held assumption that LTP represents the molecular basis for memory storage processes. However, it is feasible that the behavioural effects of eNOS inactivation may be due to effects not directly relating to learning and memory, but instead depend on factors such as anxiety predisposition (Frisch *et al.*, 2000), changes in cerebral and peripheral blood flow (Endres *et al.*, 1998; Gödecke *et al.*, 1998), body temperature control (Steiner *et al.*, 1998), or muscular oxygen supply during exercise (Nakane *et al.*, 1993; Shen *et al.*, 1995).

7.2 General Conclusion

Overall our findings provide good support for the hypothesis that NO serves as an important messenger in hippocampal LTP, and presents evidence for a contribution from both nNOS and eNOS. The results also propose the interesting possibility that the different isoforms of NOS may possess distinct roles in the modulation of synaptic events; that is eNOS appears to be important for the early phase of LTP, whereas nNOS seems to exert a greater influence on late phase LTP. Since the majority of studies report hippocampal eNOS expression to be restricted to the vascular endothelium, and the finding from the present work that eNOS is likely to be responsible for tonic NO production in the hippocampus, I hypothesise that the role of eNOS may be to keep the synapse in a state of 'relaxation' capable of allowing plasticity to occur, possibly acting via the NO/cGMP/cGK/ryanodine pathway to lower the threshold required for LTP. In contrast, I propose that NO generated from nNOS can be viewed as a mediator of LTP which acts both presynaptically (as a retrograde messenger) and postsynaptically to influence synaptic "tagging" and transcriptional/translational events.

Chapter 8

References

Abel, T., Nguyen, P.V., Barad, M., Deuel, T.A., Kandel, E.R., Bourtchouladze, R. Genetic demonstration of a role for PKA in the late phase of LTP and in hippocampus-based long-term memory. *Cell* **88**; 615 - 626 (1997).

Adak, S., Ghosh, S., Abu-Soud, H.M., Stuehr, D.J. Role of reductase domain cluster 1 acidic residues in neuronal nitric-oxide synthase. *J. Biol. Chem.* **274**; 22313 – 22320 (1999).

Ahern, G.P., Hsu, S.F., Jackson, M.B. Direct actions of nitric oxide on rat neurohypophysial K^+ channels. *J. Physiol.* **520**; 165- 176 (1999).

Ahern, G.P., Kylachko, V.A., Jackson, M.B. cGMP and *S*-nitrosylation: two routes for modulation of neuronal excitability by NO. *Trends Neurosci.* **25**; 510 - 517 (2002).

Aizenman, E., Potthoff, W.K. Lack of interaction between nitric oxide and the redox modulatory site of the NMDA receptor. *Br. J. Pharmacol.* **126**; 296 – 300 (1999).

Albina, J.E., Mills, C.D., Henry, W.L., Caldwell, M.D. Regulation of macrophage physiology by L-arginine: role of the oxidative L-arginine deiminase pathway. *J. Immunol.* **143**; 3641 - 3646 (1989).

Albina, J.E., Cui, S., Mateo, R.B., Reichner, J.S. Nitric oxide-mediated apoptosis in murine peritoneal macrophages. *J. Immunol.* **150**; 5080 - 5085 (1993).

Alderton, W.K., Cooper, C.E., Knowles, R.G. Nitric oxide synthases: structure, function and inhibition. *J. Biochem.* **357**; 593 – 615 (2001).

Alzheimer, C., Kargl, L., ten Bruggencate, G. Adenosinergic inhibition in hippocampus is mediated by adenosine A1 receptors very similar to those of peripheral tissues. *Eur. J. Pharmacol.* **196**; 313 - 317 (1991).

Andreeva, S.G., Dikkes, P., Epstein, P.M., Rosenberg, P.A. Expression of cGMP-specific phosphodiesterase 9A mRNA in the rat brain. *J. Neurosci.* **21**; 9068 - 9076 (2001).

Aoki, C., Rhee, J., Lubin, M., Dawson, T.M. NMDA-R1 subunit of the cerebral cortex co-localises with neuronal nitric oxide synthase at pre- and postsynaptic sites and in spines. *Brain Res.* **750**; 25 – 40 (1997).

Arancio, O., Antonova, I., Gambaryan, S., Lohmann, S.M., Wood, J.S., Lawrence, D.S., Hawkins, R.D. Presynaptic role of cGMP-dependent protein kinase during long-lasting potentiation. *J. Neurosci.* **21**; 143 - 149 (2001).

Aravind, L., Ponting, C.P. The GAF domain: an evolutionary link between diverse phototransducing proteins. *Trends Biochem. Sci.* **22**; 458 – 459 (1997).

Arnhold, S., Fassbender, A., Klinz, F.J., Kruttwig, K., Lohnig, B., Andressen, C., Addicks, K. NOS-II is involved in early differentiation of murine cortical, retinal and ES cell-derived neurons-an immunocytochemical and functional approach. *Int. J. Dev. Neurosci.* **20**; 83 - 92 (2002).

Arnold, W.P., Mittal, C.K., Katsuki, S., Murad, F. Nitric oxide activates guanylate cyclase and increases guanosine 3':5'-cyclic monophosphate levels in various tissue preparations. *Proc. Natl. Acad. Sci. U.S.A.* **74**; 3203 – 3207 (1977).

Babu, B.R., Griffith, O.W. N-(1-Imino-3-butenyl)-L-ornithine. *J. Biol. Chem.* **273**; 8882 – 8889 (1998).

Bader, C.R., Macleish, P.R., Schwartz, E.A. A voltage-clamp study of the light response in solitary rods of the tiger salamander. *J. Physiol.* **296**; 1 - 26 (1979).

Baltrons, M.A., Saadoun, S., Agullo, L., Garcia, A. Regulation by calcium of the nitric oxide/cyclic GMP system in cerebellar granule cells and astroglia in culture. *J. Neurosci. Res.* **49**; 333 – 341 (1997).

Bannerman, D.M., Chapman, P.F., Kelly, P.A., Butcher, S.P., Morris, R.G. Inhibition of nitric oxide synthase does not prevent the induction of long-term potentiation in vivo. *J. Neurosci.* **14**; 7415-25 (1994).

Barnstable, C.J., Wei, J.Y., Han, M.H. Modulation of synaptic function by cGMP and cGMP-gated cation channels. *Neurochem. Int.* **45**; 875 - 884 (2004).

Barsacchi, R., Perrotta, C., Bulotta, S., Moncada, S., Borgese, N., Clementi, E. Activation of endothelial nitric-oxide synthase by tumor necrosis factor-alpha: a novel pathway involving sequential activation of neutral sphingomyelinase, phosphatidylinositol-3' kinase, and Akt. *Mol. Pharmacol.* **63**; 886 - 895 (2003).

Batchelor, A.M., Garthwaite, J. Frequency detection and temporally dispersed synaptic signal association through a metabotropic glutamate receptor pathway. *Nature* **385**; 74 - 77 (1997).

Beavo, J.A. Multiple isozymes of cyclic nucleotide phosphodiesterase. *Adv. Second Messenger Phosphoprotein Res.* **22**; 1 – 38 (1988).

Beavo, J.A. Cyclic nucleotide phosphodiesterases: functional implications of multiple isoforms. *Physiol. Rev.* **75**; 725 - 748 (1995).

Bec, N., Gorren, A.C.F., Voelker, C., Mayer, B., Lange, R. Reaction of neuronal nitric oxide synthase with oxygen at low temperature. *J. Biol. Chem.* **273**; 13502 – 13508 (1998).

Becker, E.M., Schmidt, P., Schramm, M., Schroder, H., Walter, U., Hoenicka, M., Gerzer, R., Stasch, J.P. The vasodilator-stimulated phosphoprotein (VASP): target of YC-1 and nitric oxide effects in human and rat platelets. *J. Cardiovasc. Pharmacol.* **35**; 390 - 397 (2000).

Becker, E.M., Alonso-Alija, C., Apeler, H., Gerzer, R., Minuth, T., Pleiβ, U., Schmidt, P., Schramm, M., Schröder, H., Schroeder, W., Steinke, W., Straub, A., Stasch, J-P. NO-independent regulatory site of direct sGC stimulators like YC-1 and BAY 41-2272. *BMC Pharmacology* **1**; 13 (2001).

Beckman, J.S., Koppenol, W.H. Nitric Oxide, superoxide, and peroxynitrite: the good, the bad, and ugly. *Am. J. Physiol.* **271**; C1424 – C1437 (1996).

Behrends, S., Vehse, K. The beta(2) subunit of soluble guanylyl cyclase contains a human-specific frameshift and is expressed in gastric carcinoma. *Biochem. Biophys. Res. Commun.* **271**; 64 - 69 (2000).

Bellamy, T.C., Wood, J., Goodwin, D.A., Garthwaite, J. Rapid desensitization of the nitric oxide receptor, soluble guanylyl cyclase, underlies diversity of cellular cGMP responses. *Proc. Natl. Acad. Sci. U.S.A.* **97**; 2928 - 2933 (2000).

Bellamy, T.C., Garthwaite, J. Sub-second kinetics of the nitric oxide receptor, soluble guanylyl cyclase, in intact cerebellar cells. *J. Biol. Chem.* **276**; 4287 - 4292 (2001).

Bellamy, T.C., Wood, J., Garthwaite, J. On the activation of soluble guanylyl cyclase by nitric oxide. *Proc. Natl. Acad. Sci. U.S.A.* **99**; 507 – 510 (2002).

Bezprozvanny, I., Tsien, R.W. Voltage-dependent blockade of diverse types of voltage-gated Ca^{2+} channels expressed in Xenopus oocytes by the Ca2+ channel antagonist mibefradil (Ro 40-5967). *Mol. Pharmacol.* **48**; 540 - 549 (1995).

Biel, M., Zong, X., Ludwig, A., Sautter, A., Hofmann, F. Molecular cloning and expression of the Modulatory subunit of the cyclic nucleotide-gated cation channel. *J. Biol. Chem.* **271**; 6349 - 6355 (1996).

Biel, M., Zong, X., Ludwig, A., Sautter, A., Hofmann, F. Structure and function of cyclic nucleotide-gated channels. *Rev. Physiol. Biochem. Pharmacol.* **135**; 151 - 171 (1999).

Bielefeldt, K., Whiteis, C.A., Chapleau, M.W., Abboud, F.M. Nitric oxide enhances slow inactivation of voltage-dependent sodium currents in rat nodose neurons. *Neurosci. Lett.* **271**; 159 - 162 (1999).

Biffl, W.L., Moore, E.E., Moore, F.A., Barnett, C. Nitric oxide reduces endothelial expression of intercellular adhesion molecule (ICAM)-1. *J. Surg. Res.* **63**; 328 – 332 (1996).

Blackshaw, S., Eliasson, M.J., Sawa, A., Watkins, C.C., Krug, D., Gupta, A., Arai, T., Ferrante, R.J., Synder, S.H. Species, strain and development variations in hippocampal neuronal and endothelial nitric oxide synthase clarity discrepancies in nitric oxide-dependent synaptic plasticity. *Neuroscience* **119**; 979 – 990 (2003).

Blake, J.F., Yates, R.G., Brown, M.W., Collingridge, G.L. 6-Cyano-7-nitroquinoxaline-2,3-dione as an excitatory amino acid antagonist in area CA1 of rat hippocampus. *Br. J. Pharmacol.* **97**; 71 - 76 (1989).

Bliss, T.V.P., Lømo, T. Long-lasting potentiation of synaptic transmission in the dentate area of the anaesthetized rabbit following stimulation of the perforant path. *J. Physiol. (Lond.)* **232**; 331 – 356 (1973).

Bliss, T.V., Collingridge, G.L. A synaptic model of memory: long-term potentiation in the hippocampus. *Nature* **361**; 31 - 39 (1993).

Blokland, A., de Vente, J., Prickaerts, J., Honig, W., Markerink-van Ittersum, M., Steinbusch, H. Local inhibition of hippocampal nitric oxide synthase does not impair place learning in the Morris water escape task in rats. *Eur. J. Neurosci.* **11**; 223 - 232 (1999).

Bloom, T.J., Beavo, J.A. Identification and tissue-specific expression of PDE7 phosphodiesterase splice variants. *Proc. Natl. Acad. Sci. U.S.A.* **93**; 14188 - 14192 (1996).

Boer, R., Ulrich, W.R., Klein, T., Mirau, B., Haas, S., Baur, I. The inhibitory potency and selectivity of arginine substrate site nitric-oxide synthase inhibitors is solely determined by their affinity toward the different isoenzymes. *Mol. Pharmacol.* **58**; 1026 - 1034 (2000).

Boess, F.G., Hendrix, M., van der Staay, F.J., Erb, C., Schreiber, R., van Staveren, W., de Vente, J., Prickaerts, J., Blokland, A., Koenig, G. Inhibition of phosphodiesterase 2 increases neuronal cGMP, synaptic plasticity and memory performance. *Neuropharmacology* **47**; 1081 - 1092 (2004).

Bogers, J.J., Pelckmans, P.A., Boeckxstaens, G.E., De Man, J.G., Herman, A.G., Van Maercke, Y.M. The role of nitric oxide in serotonin-induced relaxations in the canine terminal ileum and ileocolonic junction. *Naunyn Schmiedebergs Arch. Pharmacol.* **344**; 716 - 719 (1991).

Böhme, G.A., Bon, C., Stutzman, J-M., Doble, A., Blanchard, J-C. Possible involvement of NO in LTP. *Eur. J. Pharmacol.* **199**; 379 – 381 (1991).

Böhme, G.A., Bon, C., Lemaire, M., Reibaud, M., Piot, O., Stutzmann, J.M., Doble, A., Blanchard, J.C. Altered synaptic plasticity and memory formation in nitric oxide synthase inhibitor-treated rats. *Proc. Natl. Acad. Sci. U.S.A.* **90**; 9191 - 9194 (1993).

Bolger, G.B., Erdogan, S., Jones, R.E., Loughney, K., Scotland, G., Hoffmann, R., Wilkinson, I., Farrell, C., Houslay, M.D. Characterization of five different proteins produced by alternatively spliced mRNAs from the human cAMP-specific phosphodiesterase PDE4D gene. *Biochem. J.* **328**; 539 - 548 (1997).

Bon, C., Böhme, G.A., Doble, A., Stutzman, J-M., Blanchard, J-C. A role for NO in LTP. *Eur. J. Neurosci.* **4**; 420 – 424 (1992).

Bon, C.L.M., Garthwaite, J. Exogenous nitric oxide causes potentiation of hippocampal synaptic transmission during low-frequency stimulation via endogenous nitric oxide-cGMP pathway. *Eur. J. Neurosci.* **14**; 585 – 594 (2001a).

Bon, C.L.M., Garthwaite, J. Nitric oxide-induced potentiation of CA1 hippocampal synaptic transmission during baseline stimulation is strictly frequency-dependent. *Neuropharmacol.* **40**; 501 – 507 (2001b)

Bon, C.L., Garthwaite, J. Adenosine acting on A1 receptors protects NO-triggered rebound potentiation and LTP in rat hippocampal slices. *J. Neurophysiol.* **87**; 1781 - 1789 (2002).

Bon, C.L.M., Garthwaite, J. NO and hippocampal synaptic plasticity. *J. Neurosci.* **23**; 1 – 8 (2003).

Bönigk, W., Altenhofen, W., Muller, F., Dose, A., Illing, M., Molday, R.S., Kaupp, U.B. Rod and cone photoreceptor cells express distinct genes for cGMP-gated channels. *Neuron* **10**; 865 - 877 (1993).

Bortolotto, Z.A., Anderson, W.W., Isaac, J.T.R., Collingridge, G.L. Synaptic plasticity in the hippocampal slice preparation. *Current protocols in Neurosci.* 6.13.1 – 6.13.23 (2001).

Bossu, J.L., Feltz, A., Rodeau, J.L., Tanzi, F. Voltage-dependent transient calcium currents in freshly dissociated capillary endothelial cells. *FEBS Lett.* **255**; 377 - 380 (1989).

Boulton, C.L., Irving, A.J., Southam, E., Potier, B., Garthwaite, J., Collingridge, G.L. The nitric oxide-cyclic cGMP pathway and synaptic depression in rat hippocampal slices. *Eur. J. Neurosci.* **6**; 1528 – 1535 (1994).

Boulton, C.L., Southam, E., Garthwaite, J. NO-dependent LTP is blocked by a specific inhibitor of soluble guanylyl cyclase. *Neuroscience* **57**; 699 – 703 (1995).

Bozdagi, O., Shan, W., Tanaka, H., Benson, D.L., Huntley, G.W. Increasing numbers of synaptic puncta during late-phase LTP: N-cadherin is synthesized, recruited to synaptic sites, and required for potentiation. *Neuron* **28**; 245 – 259 (2000).

Bradley, J., Li, J., Davidson, N., Lester, H.A., Zinn, K. Heteromeric olfactory cyclic nucleotide-gated channels: a subunit that confers increased sensitivity to cAMP. *Proc. Natl. Acad. Sci. U.S.A.* **91**; 8890 - 8894 (1994).

Bradley, J., Zhang, Y., Bakin, R., Lester, H.A., Ronnett, G.V., Zinn, K. Functional expression of the heteromeric "olfactory" cyclic nucleotide-gated channel in the hippocampus: a potential effector of synaptic plasticity in brain neurons. *J. Neurosci.* **17**; 1993 - 2005 (1997).

Brandes, R.P., Kim, D., Schmitz-Winnenthal, F.H., Amidi, M., Godecke, A., Mulsch, A., Busse, R. Increased nitrovasodilator sensitivity in endothelial nitric oxide synthase knockout mice: role of soluble guanylyl cyclase. *Hypertension* **35**; 231 - 236 (2000).

Bredt, D.S., Snyder, S.H. Nitric oxide mediates glutamate-linked enhancement of cGMP levels in the cerebellum. *Proc. Natl. Acad. Sci. U.S.A.* **86**; 9030 – 9033 (1989).

Bredt, D.S., Huang, P.M., Glatt, C.E., Lowenstein, C., Reed, R.R., Snyder, S. Cloned and expressed nitric oxide synthase structurally resembles cytochrome P-450 reductase. *Nature* **351**; 714 – 718 (1991).

Bredt, D.S., Ferris, C.D., Snyder, S.H. Nitric oxide synthase regulatory sites. Phosphorylation by cyclic AMP-dependent protein kinase, protein kinase C, and calcium/calmodulin protein kinase; identification of flavin and calmodulin binding sites. *J. Biol. Chem.* **267**; 10976 – 10981 (1992).

Brenman, J.E., Chao, D.S., Gee, S.H., McGee, A.W., Craven, S.E., Santillano, D.R., Wu, Z., Huang, F., Xia, H., Peters, M.F., Froehner, S.C., Bredt, D.S. Interaction of nitric oxide synthase with the postsynaptic density protein PSD-95 and α1-syntrophin mediated by PDZ domains. *Cell* **84**; 757 – 767 (1996a).

Brenman, J.E., Christopherson, K.S., Craven, S.E., McGee, A.W., Bredt, D.S. Cloning and characterization of postsynaptic density 93, a nitric oxide synthase interacting protein. *J. Neurosci.* **16**; 7407 - 7415 (1996b).

Broome, M.R., Collingridge, G.L., Irving, A.J. Activation of the NO-cGMP signalling pathway depresses hippocampal synaptic transmission through an adenosine receptor-dependent mechanism. *Neuropharmacology* **33**; 1511 – 1513 (1994).

Brown, G.C. Nitric oxide and mitochondrial respiration. *Biocim. Biophys. Acta* **1411**; 351 – 369 (1999).

Brune, B., Lapetina, E.G. Phosphorylation of nitric oxide synthase by protein kinase A. *Biochem. Biophys. Res. Commun.* **181**; 921 - 926 (1991).

Brunton, T.L. Use of nitrate of amyl in angina pectoris. *Lancet* **185711**; 561 (1867).

Budworth, J., Meillerais, S., Charles, I., Powell, K. Tissue distribution of the human soluble guanylate cyclases. *Biochem. Biophys. Res. Commun.* **263**; 696 - 701 (1999).

Buhl, E.H., Szilagyi, T., Halasy, K., Somogyi, P. Physiological properties of anatomically identified basket and bistatified cells in the CA1 area of the rat hippocampus in vitro. *Hippocampus* **6**; 294 – 305 (1996).

Burette, A., Zabel, U., Weinberg, R.J., Schmidt, H.H.H.W., Valtschanoff, J.G. Synaptic localisation of nitric oxide synthase and soluble guanylyl cyclase in the hippocampus. *J.Neurosci.* **22**; 8961 – 8970 (2002).

Burgunder, J.M., Cheung, P.T. Expression of soluble guanylyl cyclase gene in adult rat brain. *Eur. J. Neurosci.* **6**; 211 - 217 (1994).

Busconi, L., Michel, T. Endothelial nitric oxide synthase. N-terminal myristoylation determines subcellular localization. *J. Biol. Chem.* **268**; 8410 - 8413 (1993).

Butt, E., Bernhardt, M., Smolenski, A., Kotsonis, P., Frohlich, L.G., Sickmann, A., Meyer, H.E., Lohmann, S.M., Schmidt, H.H.H.W. Endothelial nitric-oxide synthase (type III) is activated and becomes calcium independent upon phosphorylation by cyclic nucleotide-dependent protein kinases. *J. Biol. Chem.* **275**; 5179 – 5187 (2000).

Cabin, D.E., Shimazu, K., Murphy, D., Cole, N.B., Gottschalk, W., McIlwain, K.L., Orrison, B., Chen, A., Ellis, C.E., Paylor, R., Lu, B., Nussbaum, R.L. Synaptic vesicle depletion correlates with attenuated synaptic responses to prolonged repetitive stimulation in mice lacking alpha-synuclein. *J.Neurosci.* **22**; 8797 - 8807 (2002).

Campello-Costa, P., Fosse, A.M., Ribeiro, J.C., Paes-De-Carvalho, R., Serfaty, C.A. Acute blockade of nitric oxide synthesis induces disorganization and amplifies lesion-induced plasticity in the rat retinotectal projection. *J. Neurobiol.* **44**; 371 - 381 (2000).

Casado, M., Isope, P., Ascher, P. Involvement of presynaptic N-methyl-D-aspartate receptors in cerebellar long-term depression. *Neuron* **33**; 123 – 130 (2002).

Centonze, D., Gubellini, P., Bernardi, G., Calabresi, P. Permissive role of interneurones in corticostriatal synaptic plasticity. *Brain Res. Brain Res. Rev.* **31**; 1 - 5 (1999).

Chapman, P.F., Atkins, C.M., Allen, M.T., Haley, J.E., Steinmetz, J.E. Inhibition of nitric oxide synthesis impairs two different forms of learning. *Neuroreport* **3**; 567 - 570 (1992).

Charbonneau, H., Prusti, R.K., LeTrong, H., Sonnenburg, W.K., Mullaney, P.J., Walsh, K.A., Beavo, J.A. Identification of a noncatalytic cGMP-binding domain conserved in both the cGMP-stimulated and photoreceptor cyclic nucleotide phosphodiesterases. *Proc. Natl. Acad. Sci. U.S.A.* **87**; 288 - 292 (1990).

Chen, Z.P., Mitchelhill, K.I., Stapleton, D., Rodriguez-Crespo, I., Witters, L.A., Power, D.A., Ortiz de Montellano, P.R., Kemp, B.E. AMP-activated protein kinase phosphorylation of endothelial NO synthase. *FEBS letters* **443**; 285 – 289 (1999).

Chen, C.C., Lamping, K.G., Nuno, D.W., Barresi, R., Prouty, S.J., Lavoie, J.L., Cribbs, L.L., England, S.K., Sigmund, C.D., Weiss, R.M., Williamson, R.A., Hill, J.A., Campbell, K.P. Abnormal coronary function in mice deficient in alpha1H T-type Ca^{2+} channels. *Science* **302**; 1416 - 1418 (2003).

Cheng, A., Wang, S., Cai, J., Rao, M.S., Mattson, M.P. Nitric oxide acts in a positive feedback loop with BDNF to regulate neural progenitor cell proliferation and differentiation in the mammalian brain. *Dev. Biol.* **258**; 319 - 333 (2003).

Chetkovich, D.M., Klan, E., Sweatt, J.D. NOS-independent LTP in area CA1 of hippocampus. *Neuroreport* **4**; 919 – 922 (1993).

Chevaleyre, V., Castillo, P.E. Endocannabinoid-mediated metaplasticity in the hippocampus. *Neuron* **43**; 871 - 881 (2004).

Chittajallu, R., Alford, S., Collingridge, G.L. Ca^{2+} and synaptic plasticity. *Cell Calcium* **24**; 377 - 385 (1998).

Choi, D. Glutamate neurotoxicity and diseases of the nervous system. *Neuron* **1**; 623 – 634 (1988).

Choi, O.H., Shamim, M.T., Padgett, W.L., Daly, J.W. Caffeine and theophylline analogues: correlation of behavioral effects with activity as adenosine receptor antagonists and as phosphodiesterase inhibitors. *Life Sci.* **43**; 387 – 398 (1988).

Choi, Y-B., Tenneti, L., Le, D.A., Ortiz, J., Bai, G., Chen, H-S.V., Lipton, S.A. Molecular basis of NMDA receptor-coupled ion channel modulation by *S*-nitrosylation. *Nature Neurosci.* **3**; 15 - 21 (2000).

Chrisman, T.D., Garbers, D.L., Parks, M.A., Hardman, J.G. Characterisation of particulate and soluble guanylate cyclases from rat lung. *J. Biol. Chem.* **250**; 374 – 381 (1975).

Christopherson, K.S., Hillier, B.J., Lim, W.A., Bredt, D.S. PSD-95 assembles a ternary complex with the N-methyl-D-aspartic acid receptor and a bivalent neuronal NO synthase PDZ domain. *J. Biol. Chem.* **274**; 27467 – 27473 (1999).

Clementi, E., Meldolesi, J. The cross-talk between nitric oxide and Ca^{2+}: a story with a complex past and a promising future. *Trends Pharmacol. Sci.* **18**; 266 - 269 (1997).

Clutton-Brock, J. Two cases of poisoning by contamination of nitrous oxide with higher oxides of nitrogen during anaesthesia. *Br. J. Anaesth.* **39**; 388 – 392 (1967).

Cohen, C.J., McCarthy, R.T., Barrett, P.Q., Rasmussen, H. Ca channels in adrenal glomerulosa cells: K+ and angiotensin II increase T-type Ca channel current. *Proc. Natl. Acad. Sci. U.S.A.* **85**; 2412 - 2416 (1988).

Colasanti, M., Venturini, G., Merante, A., Musci, G., Lauro, G.M. Nitric oxide involvement in Hydra vulgaris very primitive olfactory-like system. *J. Neurosci.* **17**; 493 - 499 (1997).

Collingridge, G.L., Bliss, T.V.P. Memories of NMDA receptors and LTP. *Trends Neurosci.* **18**; 54 - 56 (1995).

Contestabile, A. Roles of NMDA receptor activity and nitric oxide production in brain development. *Brain Res. Brain Res. Rev.* **32**; 476 - 509 (2000).

Cooper, G.R., Mialkowski, K., Wolff, D.J. Cellular and enzymatic studies of N(omega)-propyl-L-arginine and *S*-ethyl-N-[4-(trifluoromethyl)phenyl]isothiourea as reversible, slowly dissociating inhibitors selective for the neuronal nitric oxide synthase isoform. *Arch. Biochem. Biophys.* **375**; 183 - 194 (2000).

Corbin, J.D., Turko, I.V., Beasley, A., Francis, S.H. Phosphorylation of phosphodiesterase-5 by cyclic nucleotide-dependent protein kinase alters its catalytic and allosteric cGMP-binding activities. *Eur. J. Biochem.* **267**; 2760 - 2767 (2000).

Corbin, J.D., Francis, S.H., Webb, D.J. Phosphodiesterase type 5 as a pharmacologic target in erectile dysfunction. *Urology* **60**; 4 – 11 (2002).

Cowart, M., Kowaluk, E.A., Daanen, J.F., Kohlhaas, K.L., Alexander, K.M., Wagenaar, F.L., Kerwin, J.F. Jr. Nitroaromatic amino acids as inhibitors of neuronal nitric oxide synthase. *J. Med. Chem.* **41**; 2636 - 2642 (1998).

Crane, B.R., Arvai, A.S., Gachhui, R., Wu C., Ghosh, D.K., Getzoff, E.D., Stuehr D.J., Tainer, J.A. The structure of nitric oxide synthase oxygenase domain and inhibitor complexes. *Science* **278**; 425 - 431 (1997).

Crane, B.R., Arvai, A.S., Ghosh, D.K., Wu, C., Getzoff, E.D., Stuehr, D.J., Tainer, J.A. Structure of nitric oxide synthase oxygenase dimer with pterin and substrate. *Science* **279**; 2121 – 2126 (1998).

Creba, J.A., Karobath, M. The effect of dihydropyridine calcium agonists and antagonists on neuronal voltage sensitive calcium channels. *Biochem. Biophys. Res. Commun.* 134; 1038 - 1047 (1986).

Crepel, F., Jaillard, D. Protein kinases, nitric oxide and long-term depression of synapses in the cerebellum. *Neuroreport* **1**; 133 – 136 (1990).

Cronberg, T., Rytter, A., Asztely, F., Soder, A., Wieloch, T. Glucose but not lactate in combination with acidosis aggravates ischemic neuronal death in vitro. *Stroke* **35**; 753 - 757 (2004).

Cudeiro, J., Rivadulla, C. Sight and insight - on the physiological role of nitric oxide in the visual system. *Trends Neurosci.* **22**; 109 - 116 (1999).

Cummings, J.A., Nicola, S.M., Malenka, R.C. Induction in the rat hippocampus of LTP and LTD in the presence of a NOS inhibitor. *Neurosci. Letters* **176**; 110 – 114 (1994).

Curtis, D.R., Phillis, J.W., Watkins, J.C. Chemical excitation of spinal neurones. *Nature* **183**; 611 – 612 (1959).

Cuttle, M.F., Rusznak, Z., Wong, A.Y., Owens, S., Forsythe, I.D. Modulation of a presynaptic hyperpolarization-activated cationic current (I_h) at an excitatory synaptic terminal in the rat auditory brainstem. *J. Physiol.* **534**; 733 - 744 (2001).

Daff, S., Sagami, I., Shimizu, T. The 42-amino acid insert in the FMN domain of neuronal nitric-oxides exerts control over Ca^{2+}/Calmodulin-dependent electron transfer. *J. Biol. Chem.* **274**; 30589 – 30595 (1999).

Daniel, H., Hemart, N., Jaillard, D., Crepel, F. Long-term depression requires nitric oxide and guanosine 3':5' cyclic monophosphate production in rat cerebellar Purkinje cell. *Eur. J. Neurosci.* **5**; 1079 – 1082 (1993).

Daniel, H., Levenes, C., Crepel, F. Cellular mechanisms of cerebellar LTD. *Trends Neurosci.* **21**; 401 – 407 (1998).

Davies, C.H., Collingridge, G.L. The physiological regulation of synaptic inhibition by GABAB autoreceptors in rat hippocampus. *J. Physiol.* **472**; 245 - 265 (1993).

Davies, C.H., Clarke, V.R., Jane, D.E., Collingridge, G.L. Pharmacology of postsynaptic metabotropic glutamate receptors in rat hippocampal CA1 pyramidal neurones. *Br. J. Pharmacol.* **116**; 1859 - 1869 (1995).

Davy, H. *Researches Chemical and Philosophical, Chiefly Concerning Nitrous Oxide or Dephlogisticated Nitrous Air.* London: J Johnson (1800).

Degerman, E., Belfrage, P., Manganiello, V.C. Structure, localization, and regulation of cGMP-inhibited phosphodiesterase (PDE3). *J. Biol. Chem.* **272**; 6823 - 6826 (1997).

Delpiano, M.A., Altura, B.M. Modulatory effect of extracellular Mg^{2+} ions on K^+ and Ca^{2+} currents of capillary endothelial cells from rat brain. *FEBS Lett.* **394**; 335 - 339 (1996).

Demas, G.E., Kriegsfeld, L.J., Blackshaw, S., Huang, P., Gammie, S.C., Nelson, R.J., Snyder, S.H. Elimination of aggressive behavior in male mice lacking endothelial nitric oxide synthase. *J. Neurosci.* **19**; RC30 (1999).

Denninger, J.W., Marletta, M.A. Guanylate cyclase and the NO/cGMP signalling pathway. *Biochim. Biophys. Acta* **1411**; 334 – 350 (1999).

Dere, E., Frisch, C., De Souza Silva, M.A., Godecke, A., Schrader, J., Huston, J.P. Unaltered radial maze performance and brain acetylcholine of the endothelial nitric oxide synthase knockout mouse. *Neuroscience* **107**; 561 – 570 (2001).

De Zeeuw, C.I., Hansel, C., Bian, F., Koekkoek, S.K., van Alphen, A.M., Linden, D.J., Oberdick, J. Expression of a protein kinase C inhibitor in Purkinje cells blocks cerebellar LTD and adaptation of the vestibule-ocular reflex. *Neuron* **20**; 495 – 508 (1998).

Dhallan, R.S., Yau, K.W., Schrader, K.A., Reed, R.R. Primary structure and functional expression of a cyclic nucleotide-activated channel from olfactory neurons. *Nature* **347**; 184 – 187 (1990).

Dierks, E.A, Burstyn, J.N. Nitric oxide (NO), the only nitrogen monoxide redox form capable of activating soluble guanylyl cyclase. *Biochem. Pharmacol.* **51**; 1593 - 1600 (1996).

Dillon, J., Ortwerth, B.J., Chignell, C.F., Reszka, K.J. Electron paramagnetic resonance and spin trapping investigations of the photoreactivity of human lens proteins. *Photochem. Photobiol.* **69**; 259 – 264 (1999).

Dimmeler, S., Fleming, I., Fisslthaler, B., Hermann, C., Busse, R., Zeiher, A.M. Activation of nitric oxide synthase in endothelial cells by Akt-dependent phosphorylation. *Nature* **399**; 601 – 605 (1999).

Dinerman, J.L., Dawson, T.M., Schell, M.J., Snowman, A., Snyder, S.H. Endothelial nitric oxide synthase localized to hippocampal pyramidial cells: Implications for synaptic plasticity. *Proc. Natl. Acad. Sci. USA* **91**; 4214 – 4218 (1994a).

Dinerman, J.L., Steiner, J.P., Dawson, T.M., Dawson, V., Snyder, S.H. Cyclic nucleotide dependent phosphorylation of neuronal nitric oxide synthase inhibits catalytic activity. *Neuropharmacology* **33**; 1245 – 1251 (1994b).

Ding, J.D., Burette, A., Nedvetsky, P.I., Schmidt, H.H., Weinberg, R.J. Distribution of soluble guanylyl cyclase in the rat brain. *J. Comp. Neurol.* **472**: 437 - 448 (2004).

Dingledine, R., Borges, K., Bowie, D., Traynelis, S.F. The glutamate receptor ion channels. *Pharmacol Rev.* **51**; 7 – 61 (1999).

Dolmetsch, R.E., Pajvani, U., Fife, K., Spotts, J.M., Greenberg, M.E. Signaling to the nucleus by an L-type calcium channel-calmodulin complex through the MAP kinase pathway. *Science* **294**; 333 – 339 (2001).

Dolphin, A.C., Errington, M.L., Bliss, T.V. Long-term potentiation of the perforant path in vivo is associated with increased glutamate release. *Nature* **297**; 496 - 498 (1982).

Doyle, C., Hölscher, C., Rowan, M.J., Anwyl, R. The selective neuronal NO synthase inhibitor 7-nitro-indazole blocks both long-term potentiation and depotentiation of field EPSPs in rat hippocampal CA1 in vivo. *J. Neurosci.* **16**; 418 - 424 (1996).

Doyle, C., Slater, P. Localisation of neuronal and endothelial nitric oxide synthase isoforms in human hippocampus. *Neurosci.* **76**; 387 – 395 (1997).

Drapier, J.C., Hibbs, J.B. Murine cytotoxic activated macrophages inhibit aconitase in tumor cells. Inhibition involves the iron-sulfur prosthetic group and is reversible. *J. Clin. Invest.* **78**; 790 – 797 (1986).

Du, W., Harvey, J.A. The nitric oxide synthesis inhibitor L-NAME facilitates associative learning. *Prog. Neuropsychopharmacol. Biol. Psychiatry* **20**; 1183 - 1195 (1996).

Dumuis, A., Sebben, M., Haynes, L., Pin, J.P., Bockaert, J. NMDA receptors activate the arachidonic acid cascade system in striatal neurons. *Nature* **336**; 68 - 70 (1988).

Dunwiddie, T.V., Perez-Reyes, E., Rice, K.C., Palmer, M.R. Stereoselectivity of opiate antagonists in rat hippocampus and neocortex: responses to (+) and (-) isomers of naloxone. *Neuroscience* 7; 1691 - 1702 (1982).

Dunwiddie, T.V., Fredholm, B.B. Adenosine A1 receptors inhibit adenylate cyclase activity and neurotransmitter release and hyperpolarize pyramidal neurons in rat hippocampus. *J. Pharmacol. Exp. Ther.* **249**; 31 - 37 (1989).

Durner, J., Gow, A..J., Stamler, J.S., Glazebrook, J. Ancient origins of nitric oxide signalling in biological systems. *Proc. Natl. Acad. Sci. U.S.A.* **96**; 14206 - 14207 (1999).

East, S.J., Garthwaite, J. NMDA receptor activation in rat hippocampus induces cyclic GMP formation through the L-arginine-nitric oxide pathway. *Neurosci. Letters* **123**, 17 - 19 (1991).

Edwards, F.A. LTP - a structural model to explain the inconsistencies. *Trends Neurosci.* **18**; 250 – 255 (1995).

Eissa, N.T., Strauss, A.J., Haggerty, C.M., Choo, E.K., Chu, S.C., Moss, J. Alternative splicing of human inducible nitric-oxide synthase mRNA. Tissue specific regulation and induction by cytokines. *J. Biol. Chem.* **271**; 27184 – 21787 (1996).

Eliasson, M.J., Blackshaw, S., Schell, M.J., Snyder, S.H. Neuronal nitric oxide synthase alternatively spliced isoforms: prominent functional localisations in the brain. *Proc. Natl. Acad. Sci. USA* **94**; 3396 – 3401 (1997).

Eller, P., Berjukov, S., Wanner, S., Huber, I., Hering, S., Knaus, H.G., Toth, G., Kimball, S.D., Striessnig, J. High affinity interaction of mibefradil with voltage-gated calcium and sodium channels. *Br. J. Pharmacol.* **130**; 669 - 677 (2000).

Endo, S., Suzuki, M., Sumi, M., Nairn, A.C., Morita, R., Yamakawa, K., Greengard, P., Ito, M. Molecular identification of human G-substrate, a possible downstream component of the cGMP-dependent protein kinase cascade in cerebellar Purkinje cells. *Proc. Natl. Acad. Sci. U.S.A.* **96**; 2467 - 2472 (1999).

Endoh, M., Maiese, K., Wagner, J.A. Expression of the neural form of nitric oxide synthase by CA1 hippocampal neurons and other central nervous system neurons. *Neuroscience* **63**; 679 – 689 (1994)

Endres, M., Laufs, U., Huang, Z., Nakamura, T., Huang, P., Moskowitz, M.A., Liao, J.K. Stroke protection by 3-hydroxy-3-methylglutaryl (HMG)-CoA reductase

inhibitors mediated by endothelial nitric oxide synthase. *Proc. Natl. Acad. Sci. U.S.A.* **95**; 8880 - 8885 (1998).

Engert, F., Bonhoeffer, T. Dendritic spine changes associated with hippocampal long-term synaptic plasticity. *Nature* **399**; 66 – 70 (1999).

Ertel, E.A., Campbell, K.P., Harpold, M.M., Hofmann, F., Mori, Y., Perez-Reyes, E., Schwartz, A., Snutch, T.P., Tanabe, T., Birnbaumer, L., Tsien, R.W., Catterall, W.A. Nomenclature of voltage-gated calcium channels. *Neuron* **25**; 533 - 535 (2000).

Estall, L.B., Grant, S.J., Cicala, G.A. Inhibition of nitric oxide (NO) production selectively impairs learning and memory in the rat. *Pharmacol. Biochem. Behav.* **46**; 959 – 962 (1993).

Faber-Zuschratter, H., Seidenbecher, T., Reymann, K., Wolf, G. Ultrastructural distribution of NADPH-diaphorase in the normal hippocampus and after long-term potentiation. *J. Neural Transm.* **103**; 807 – 817 (1996).

Fagni, L., Olivier, M., Lafon-Cazal, M., Bockaert, J. Involvement of divalent ions in the nitric oxide-induced blockade of N-methyl-D-aspartate receptors in cerebellar granule cells. *Mol. Pharmacol.* **47**; 1239 – 1247 (1995).

Fawcett, L., Baxendale, R., Stacey, P., McGrouther, C., Harrow, I., Soderling, S., Hetman, J., Beavo, J.A., Phillips, S.C. Molecular cloning and characterization of a distinct human phosphodiesterase gene family: PDE11A. *Proc. Natl. Acad. Sci. U.S.A.* **97**; 3702 - 3707 (2000).

Feelisch, M., Ostrowski, J., Noack, E. On the mechanism of NO release from synonimines. *J. Cardiovasc. Pharmacol.* **14**; S13 – S22 (1989).

Feelisch, M. The use of nitric oxide donors in pharmacological studies. *Naunyn-Schmiedeberg's Arch. Pharmacol.* **358**, 113 - 122 (1998).

Feil, R., Hartmann, J., Luo, C., Wolfsgruber, W., Schilling, K., Feil, S., Barski, J.J., Meyer, M., Konnerth, A., De Zeeuw, C.I., Hofmann, F. Impairment of LTD and cerebellar learning by Purkinje cell-specific ablation of cGMP-dependent protein kinase I. *J. Cell Biol.* **163**; 295 - 302 (2003).

Feron, O., Dessy, C., Moniotte, S., Desager, J-P., Balligand, J-L. Hypocholesterolemia decreases nitric oxide production by promoting the interaction of caveolin and endothelial nitric oxide synthase. *J. Clin. Invest.* **103**; 897 – 905 (1999).

Ferrendelli, J.A., Chang, M.M., Kinscherf, D.A. Elevation of cyclic GMP levels in central nervous system by excitatory and inhibitory amino acids. *J. Neurochem.* **22**; 535 – 540 (1974).

Fesenko, E.E., Kolesnikov, S.S., Lyubarsky, A.L. Induction by cyclic GMP of cationic conductance in plasma membrane of retinal rod outer segment. *Nature* **313**; 310 - 313 (1985).

Figtree, G.A., Lu, Y., Webb, C.M., Collins, P. Raloxifene acutely relaxes rabbit coronary arteries in vitro by an estrogen receptor-dependent and nitric oxide-dependent mechanism. *Circulation* **100**; 1095 – 1101 (1999).

Finn, J.T., Grunwald, M.E., Yau, K.W. Cyclic nucleotide-gated ion channels: an extended family with diverse functions. *Annu. Rev. Physiol.* **58**; 395 – 426 (1996).

Fischmann, T.O., Hruzal, A., Niu, X.D., Fossetta, J.D., Lunn, C.A., Dolphin, E., Prongay, A.J, Reichert, P., Lundell, D.J., Narula, S.K., Weber, P.C. Structural characterization of nitric oxide synthase isoforms reveals striking active-site conservation. *Nature structural biology* **6**; 233 – 242 (1999).

Fisher, D.A., Smith, J.F., Pillar, J.S., St Denis, S.H., Cheng, J.B. Isolation and characterization of PDE9A, a novel human cGMP-specific phosphodiesterase. *J. Biol. Chem.* **273**; 15559 – 15564 (1998a).

Fisher, D.A., Smith, J.F., Pillar, J.S., St Denis, S.H., Cheng, J.B. Isolation and characterization of PDE8A, a novel human cAMP-specific phosphodiesterase. *Biochem. Biophys. Res. Commun* **246**; 570 – 577 (1998b).

Fleming, I., Fisslthaler, B., Dimmeler, S., Kemp, B.E., Busse, R. Phosphorylation of Thr(495) regulates Ca^{2+}/calmodulin-dependent endothelial nitric oxide synthase activity. *Circ. Res.* **88**; E68 – E75 (2001).

Foerster, J., Harteneck, C., Malkewitz, J., Schultz, G., Koesling, D. A functional heme-binding site of soluble guanylyl cyclase requires intact N-termini of alpha 1 and beta 1 subunits. *Eur. J. Biochem.* **240**; 380 - 386 (1996).

Ford, E., Hughes, M.N., Wardman, P. Kinetics of the reactions of nitrogen dioxide with glutathione, cysteine, and uric acid at physiological pH. *Free Radic. Med.* **32**; 1314 – 1323 (2002).

Fowler, J.C., Gervitz, L., Partridge, L.D. Hydroxylamine blocks pre- but not postsynaptic adenosine A(1) receptor-mediated actions in rat hippocampus. *Brain Res.* **837**; 309 – 313 (1999).

Francis, S.H., Bessay, E.P., Kotera, J., Grimes, K.A., Liu, L., Thompson, W.J., Corbin, J.D. Phosphorylation of isolated human phosphodiesterase-5 regulatory domain induces an apparent conformational change and increases cGMP binding affinity. *J. Biol. Chem.* **277**; 47581 - 47587 (2002).

Freichel, M., Suh, S.H., Pfeifer, A., Schweig, U., Trost, C., Weissgerber, P., Biel, M., Philipp, S., Freise, D., Droogmans, G., Hofmann, F., Flockerzi, V., Nilius, B. Lack of an endothelial store-operated Ca^{2+} current impairs agonist-dependent vasorelaxation in TRP4-/- mice. *Nat. Cell Biol.* **3**; 121 - 127 (2001).

Frenguelli, B.G., Potier, B., Slater, N.T., Alford, S., Collingridge, G.L. Metabotropic glutamate receptors and calcium signalling in dendrites of hippocampal CA1 neurones. *Neuropharmacology* **32**; 1229 - 1237 (1993).

Frey, U., Krug, M., Brodemann, R., Reymann, K., Matthies, H. Long-term potentiation induced in dendrites separated from rat's CA1 pyramidal somata does not establish a late phase. *Neurosci. Lett.* **97**; 135 – 139 (1989).

Frey, U., Huang, Y.Y., Kandel, E.R. Effects of cAMP simulate a late stage of LTP in hippocampal CA1 neurons. *Science* **260**; 1661 – 1664 (1993).

Frey, U., Morris, R.G. Synaptic tagging and long-term potentiation. *Nature* **385**; 533 – 536 (1997).

Friebe, A., Wedel, B., Harteneck, C., Foerster, J., Schultz, G., Koesling, D. Functions of conserved cysteines of soluble guanylyl cyclase. *Biochemistry* **36**; 1194 - 1198 (1997).

Friebe, A., Mullershausen, F., Smolenski, A., Walter, U., Schultz, G., Koesling, D. YC-1 potentiates nitric oxide- and carbon monoxide-induced cyclic GMP effects in human platelets. *Mol. Pharmacol.* **54**; 962 – 967 (1998).

Friebe, A., Koesling, D. Regulation of the nitric oxide-sensitive guanylyl cyclase. *Circ. Res.* **93**; 96 – 105 (2003).

Frings, S., Seifert, R., Godde, M., Kaupp, U.B. Profoundly different calcium permeation and blockage determine the specific function of distinct cyclic nucleotide-gated channels. *Neuron* **15**; 169 - 179 (1995).

Frisch, C., Dere, E., Silva, M.A., Godecke, A., Schrader, J., Huston, J.P. Superior water maze performance and increase in fear-related behavior in the endothelial nitric oxide synthase-deficient mouse together with monoamine changes in cerebellum and ventral striatum. *J. Neurosci.* **20**; 6694 – 6700 (2000).

Fujishige, K., Kotera, J., Michibata, H., Yuasa, K., Takebayashi, S., Okumura, K., Omori, K. Cloning and characterization of a novel human phosphodiesterase that hydrolyzes both cAMP and cGMP (PDE10A). *J. Biol. Chem.* **274**; 18438 - 18445 (1999a).

Fujishige, K., Kotera, J., Omori, K. Striatum- and testis-specific phosphodiesterase PDE10A isolation and characterization of a rat PDE10A. *Eur. J. Biochem.* **266**; 1118 – 1127 (1999b).

Fulton, D., Gratton, J.P., McCabe, T.J., Fontana, J., Fujio, Y., Walsh, K., Franke, T.F., Papapetropoulos, A., Sessa, W.C. Regulation of endothelium-derived nitric oxide production by the perotein kinase Akt. *Nature* **399**; 597 – 601 (1999).

Furchgott, R.F., Zawadzki, J.V. The obligatory role of endothelial cells in the relaxation of arterial smooth muscle by acetylcholine. *Nature* **288**; 373 - 376 (1980).

Furuyama, T., Iwahashi, Y., Tano, Y., Takagi, H., Inagaki, S. Localization of 63-kDa calmodulin-stimulated phosphodiesterase mRNA in the rat brain by in situ hybridization histochemistry. *Brain Res. Mol. Brain Res.* **26**; 331 - 336 (1994).

Gallis, B., Corthals, G.L., Goodlett, D.R., Ubea, H., Kim, F., Presnell, S.R., Figeys, D., Harrison, D.G., Berk, B.C., Aebersold, R., Corsonj, M.A. Identification of flow-dependent endothelial nitric-oxide synthase phosphorylation sites by mass spectrometry and regulation of phosphorylation and nitric oxide production by the phosphatidylinositol 3-kinase inhibitor LY294002. *J. Biol. Chem.* **274**; 30101 – 30108 (1999).

Gallo, G., Ernst, A.F., McLoon, S.C., Letourneau, P.C. Transient PKA activity is required for initiation but not maintenance of BDNF-mediated protection from nitric oxide-induced growth-cone collapse. *J. Neurosci.* **22**; 5016 - 5023 (2002).

Gally, J.A., Montague, P.R., Reeke, G.N.,Jr., Edelman, G.M. The NO hypothesis: possible effects of a short-lived, rapidly diffusible signal in the development and function of the nervous system. *Proc. Natl. Acad. Sci. USA* **87**; 3547 - 3551 (1990).

Gambaryan, S., Palmetshofer, A., Glazova, M., Smolenski, A., Kristjansson, G.I., Zimmer, M., Lohmann, S.M. Inhibition of cGMP-dependent protein kinase II by its own splice isoform. *Biochem. Biophys. Res. Commun.* **293**; 1438 - 1444 (2002).

Garbers, D.L., Gray, J.P. Guanylate cyclase from sperm of the sea urchin, *Stronglyocentrolus purpuratus. Methods Enzymol.* **38**; 196 – 199 (1974).

Garthwaite. J., Balazs, R. Excitatory amino acid-induced changes in cyclic GMP levels in slices and cell suspensions from the cerebellum. *Adv. Biochem. Psychopharmacol.* **27**; 317 – 326 (1981).

Garthwaite, J., Garthwaite, G. Cellular origins of cyclic GMP responses to excitatory amino acid receptor agonists in rat cerebellum in vitro. *J. Neurochem.* **48**; 29 - 39 (1987).

Garthwaite, J., Charles, S.L., Chess-Williams, R. Endothelium-derived relaxing factor release on activation of NMDA receptors suggests role as intercellular messenger in the brain. *Nature* **336**; 385 - 388 (1988).

Garthwaite, J., Boulton, C.L. Nitric oxide signalling in the central nervous system. *Annu. Rev. Physiol.* **57**; 683 – 706 (1995a).

Garthwaite, J., Southam, E., Boulton, C.L., Nielsen, E.B., Schmidt, K., Mayer, B. Potent and selective inhibition of nitric oxide-sensitive guanylyl cyclase by 1H-[1,2,4]oxadiazolo[4,3-a]quinoxalin-1-one. *Mol. Pharmacol.* **48**; 184 - 188 (1995b).

Garvey, E.P., Oplinger, J.A., Furfine, E.S., Kiff, R.J., Laszlo, F., Whittle, B.J.R., Knowles, R.G. 1400W is a slow, tight binding, and highly selective inhibitor of inducible nitric-oxide synthase *in vitro* and *in vivo*. *J. Biol. Chem.* **272**; 4959 – 4963 (1997).

Gatley, S.J., Gifford, A.N., Volkow, N.D., Lan, R., Makriyannis, A. 123I-labeled AM251: a radioiodinated ligand which binds in vivo to mouse brain cannabinoid CB1 receptors. *Eur. J. Pharmacol.* **307**; 331 - 338 (1996).

Gbadegesin, M., Vicini, S., Hewett, S.J., Wink, D.A., Espey, M., Pluta, R.M., Colton, C.A. Hypoxia modulates nitric oxide-induced regulation of NMDA receptor currents and neuronal cell death. *Am. J. Physiol.* **277**; C673 – C683 (1999).

Ge, J., Barnes, N.M. 5-HT4 receptor-mediated modulation of 5-HT release in the rat hippocampus in vivo. *Br. J. Pharmacol.* **117**; 1475 - 1480 (1996).

Gerstner, A., Zong, X., Hofmann, F., Biel, M. Molecular cloning and functional characterization of a new modulatory cyclic nucleotide-gated channel subunit from mouse retina. *J. Neurosci.* **20**; 1324 - 1332 (2000).

Gerzer, R., Bohme, E., Hofmann, F., Schultz, G. Soluble guanylate cyclase purified from bovine lung contains heme and copper. *FEBS Lett.* **132**; 71 – 74 (1981).

Gibb, B.J., Garthwaite, J. Subunits of the nitric oxide receptor, soluble guanylyl cyclase, expressed in rat brain. *Eur. J. Neurosci.* **13**; 539 - 544 (2001).

Gifford, A.N., Johnson, K.M. A pharmacological analysis of the effects of (+)-AJ 76 and (+)-UH 232 at release regulating pre- and postsynaptic dopamine receptors. *Eur. J. Pharmacol.* **237**; 169 - 175 (1993).

Giovine, M., Pozzolini, M., Favre, A., Bavestrello, G., Cerrano, C., Ottaviani, F., Chiarantini, L., Cerasi, A., Cangiotti, M., Zocchi, E., Scarfi, S., Sara, M., Benatti, U. Heat stress-activated, calcium-dependent nitric oxide synthase in sponges. *Nitric Oxide* **5**; 427 - 431 (2001).

Giuili, G., Scholl, U., Bulle, F., Guellaen, G. Molecular cloning of the cDNAs coding for the two subunits of soluble guanylyl cyclase from human brain. *FEBS Lett.* **304**; 83 – 88 (1992).

Gödecke, A., Decking, U.K.M., Ding, Z., Hirchenhain, J., Bidmon, H.J., Gödecke, S., Schrader, J. Coronary hemodynamics in endothelial NO synthase knockout mice. *Circ. Res.* **82**; 186 - 194 (1998).

Goldberg, N.D., Dietz, S.B., O'Toole, A.G. Cyclic guanosine 3',5'-monophosphate in mammalian tissues and urine. *J. Biol. Chem.* **244**; 4458 – 4466 (1969).

Golderer, G., Werner, E.R., Leitner, S., Grobner, P., Werner-Felmayer, G. Nitric oxide synthase is induced in sporulation of Physarum polycephalum. *Genes Dev.* **15**; 1299 - 1309 (2001).

Goldstein, J.M., Litwin, L.C. NBQX is a selective non-NMDA receptor antagonist in rat hippocampal slice. *Mol. Chem. Neuropathol.* **18**; 145 - 152 (1993).

Golovina, V.A., Platoshyn, O., Bailey, C.L., Wang, J., Limsuwan, A., Sweeney, M., Rubin, L.J., Yuan, J.X. Upregulated TRP and enhanced capacitative $Ca^{(2+)}$ entry in human pulmonary artery myocytes during proliferation. *Am. J. Physiol. Heart Circ. Physiol.* **280**; H746 - 755 (2001).

Göthert, M., Molderings, G.J. Mibefradil- and omega-conotoxin GVIA-induced inhibition of noradrenaline release from the sympathetic nerves of the human heart. *Naunyn Schmiedebergs Arch. Pharmacol.* **356**; 860 - 863 (1997).

Gowda, C., Toomayan, G.A., Qi, W-N., Chen, L-E., Cai, Y., Allen, D.M., Seaber, A.V., Urbaniak, J.R. The effects of N-propyl-L-arginine on reperfusion injury of skeletal muscle. *Nitric Oxide* **11**; 17-24 (2004).

Granger, D.L., Taintor, R.R., Cook, J.L., Hibbs, J.B. Injury of neoplastic cells by murine macrophages leads to inhibition of mitochondrial respiration. *J. Clin. Invest.* **65**; 357 - 370 (1980).

Granger, D.L., Lehninger, A.L. Sites of inhibition of mitochondrial electron transport in macrophage-injured neoplastic cells. *J. Cell. Biol.* **95**; 527 - 535 (1982).

Green, L.C., Ruiz de Luzuriaga, K., Wagner, D.A., Rand, W., Istfan, N., Young, V.R., Tannenbaum, S.R. Nitrate biosynthesis in man. *Proc. Natl. Acad. Sci. U.S.A.* **78**; 7764 - 7768 (1981a).

Green, L.C., Tannenbaum, S.R., Goldman, P. Nitrate synthesis in the germfree and conventional rat. *Science* **212**; 56 – 58 (1981b).

Greene, R.W., Haas, H.L. The electrophysiology of adenosine in the mammalian central nervous system. *Prog. Neurobiol.* **36**; 329 - 341 (1991).

Gribkoff, V.K., Lum-Ragan, J.T. Evidence for NOS inhibitor-sensitive and insensitive hippocampal synaptic potentiation. *J. Neurophysiol.* **68**; 639 – 642 (1992).

Griffiths, C., Garthwaite, J. The shaping of the nitric oxide signals by a cellular sink. *J. Physiol. (London)* **536**; 855 – 862 (2001).

Griffiths, C., Garthwaite, G., Goodwin, D.A., Garthwaite, J. Dynamics of nitric oxide during simulated ischaemia-reperfusion in rat striatal slices measured using an intrinsic biosensor, soluble guanylyl cyclase. *Eur. J. Neurosci.* **15**; 962 – 968 (2002).

Grover, L.M., Teyler, T.J. Two components of long-term potentiation induced by different patterns of afferent activation. *Nature* **347**; 477 - 479 (1990).

Grunwald, M.E., Yu, W.P., Yu, H.H., Yau, K.W. Identification of a domain on the beta-subunit of the rod cGMP-gated cation channel that mediates inhibition by calcium-calmodulin. *J. Biol. Chem.* **273**; 9148 - 9157 (1998).

Güler, A.D., Lee, H., Iida, T., Shimizu, I., Tominaga, M., Caterina, M. Heat-evoked activation of the ion channel, TRPV4. *J. Neurosci.* **22**; 6408 – 6414 (2002).

Gyurko, R., Kuhlencordt, P., Fishman, M.C., Huang, P.L. Modulation of mouse cardiac function in vivo by eNOS and ANP. *Am. J. Physiol. Heart Circ. Physiol.* **278**; H971 - 981 (2000).

Hada, J., Kaku, T., Jiang, M.H., Morimoto, K., Hayashi, Y. Inhibition of high K^+-evoked gamma-aminobutyric acid release by sodium nitroprusside in rat hippocampus. *Eur. J. Pharmacol.* **467**; 119 - 123 (2003).

Hagen, T.J., Bergmanis, A.A., Kramer, S.W., Fok, K.F., Schmelzer, A.E., Pitzele, B.S., Swenton, L., Jerome, G.M., Kornmeier, C.M., Moore, W.M., Branson, L.F., Connor, J.R., Manning, P.T., Currie, M.G., Hallinan, E.A. 2-Iminopyrrolidines as potent and selective inhibitors of human inducible nitric oxide synthase. *J. Med. Chem.* **41**; 3675 - 3683 (1998).

Hagiwara, N., Irisawa, H., Kameyama, M. Contribution of two types of calcium currents to the pacemaker potentials of rabbit sino-atrial node cells. *J. Physiol.* **395**; 233 - 253 (1988).

Halasy, K., Buhl, E.H., Lorinczi, Z., Tamas, G., Somogyi, P. Synaptic target selectivity and input of GABAergic basket and bistrtified interneurons in the CA1 area of the rat hippocampus. *Hippocampus* **6**; 306 – 329 (1996).

Haley, J.E., Wilcox, G.L., Chapman. P.F. The role of nitric oxide in hippocampal long-term potentiation. *Neuron* **8**; 211 - 216 (1992).

Haley, J.E., Malen, P.L., Chapman, P.L. NOS inhibitors block LTP induced by weak but not strong titanic stimulation at physiological brain temperatures in rat hippocampal slices. *Neurosci. Letters* **160**; 85 – 88 (1993).

Halliwell, J.V., Adams, P.R. Voltage-clamp analysis of muscarinic excitation in hippocampal neurons. *Brain Res.* **250**; 71 - 92 (1982).

Hanbauer, I., Wink, D., Osawa, Y., Edelman, G.M., Gally, J.A. Role of nitric oxide in NMDA-evoked release of [3H]-dopamine from striatal slices. *Neuroreport* **3**; 409 – 412 (1992).

Hanson, J.E., Smith, Y. Subcellular distribution of high-voltage-activated calcium channel subtypes in rat globus pallidus neurons. *J. Comp. Neurol.* **442**; 89 - 98 (2002).

Hardman, J.G., Sutherland, E.W. Guanyl cyclase, an enzyme catalysing the formation of guanosine 3'5'-monophosphate from guanosine triphosphate. *J. Biol. Chem.* **244**; 6363 – 6370 (1969).

Harris, M.B., Ju, H., Venema, V.J., Liang, H., Zou, R., Michell, B.J., Chen, Z-P., Kemp, B.E., Venema, R.C. Reciprocal phosphorylation and regulation of endothelial nitric-oxide synthase in response to bradykinin stimulation. *J. Biol. Chem.* **276**; 16587 – 16591 (2001).

Harteneck, C., Wedel, B., Koesling, D., Malkewitz, J., Bohme, E., Schultz, G. Molecular cloning and expression of a new alpha-subunit of soluble guanylyl cyclase. Interchangeability of the alpha-subunits of the enzyme. *FEBS Lett.* **292**; 217 - 222 (1991).

Hashimoto, Y., Sharma, R.K., Soderling, T.R. Regulation of Ca2+/calmodulin-dependent cyclic nucleotide phosphodiesterase by the autophosphorylated form of Ca^{2+}/calmodulin-dependent protein kinase II. *J. Biol. Chem.* **264**; 10884 - 10887 (1989).

Hawkins, R.D., Son, H., Arancio, O. Nitric oxide as a retrograde messenger during long-term potentiation in hippocampus. *Prog. Brain Res.* **118**; 155 - 172 (1998).

Hayahashi, M., Matsushima, K., Chashi, H., Tsunoda, H., Murase, S., Kawarada, Y., Tanaka, T. Molecular cloning and characterisation of human PDE8, a novel thyroid-specific isozyme of 3',5'-cyclic nucleotide phosphodiesterase. *Biochem. Biophys. Res. Commun.* **250**; 751 – 756 (1998).

Hayashi, T. Effects of sodium glutamate on the nervous system. *Keio J. Med.* **3**; 183 - 195 (1954).

Hayashi, Y., Nishio, M., Naito, Y., Yokokura, H., Nimura, Y., Hidaka, H., Watanabe, Y. Regulation of neuronal nitric-oxide synthase by calmodulin kinases. *J. Biol. Chem.* **274**; 20597 - 20602 (1999).

He, Y., Yu, W., Baas, P.W. Microtubule reconfiguration during axonal retraction induced by nitric oxide. *J. Neurosci.* **22**; 5982 - 5991 (2002).

Hedlund, P., Aszodi, A., Pfeifer, A., Alm, P., Hofmann, F., Ahmad, M., Fassler, R., Andersson, K.E. Erectile dysfunction in cyclic GMP-dependent kinase I-deficient mice. *Proc. Natl. Acad. Sci. U.S.A.* **97**; 2349 - 2354 (2000).

Hegesh, E., Shiloah, J. Blood nitrates and infantile methemoglobinemia. *Clin. Chim. Acta.* **125**; 107 - 115 (1982).

Heitz, C., Descombes, J.J., Miller, R.C., Stoclet, J.C. Alpha-adrenoceptor antagonistic and calcium antagonistic effects of nicergoline in the rat isolated aorta. *Eur. J. Pharmacol.* **123**; 279 - 285 (1986).

Hell, J.W., Westenbroek, R.E., Warner, C., Ahlijanian, M.K., Prystay, W., Gilbert, M.M., Snutch, T.P., Catterall, W.A. Identification and differential subcellular localization of the neuronal class C and class D L-type calcium channel alpha 1 subunits. *J. Cell Biol.* **123**; 949 - 962 (1993).

Hemmens, B., Goessler, W., Schmidt, K. and Mayer, B. Role of bound zinc in dimer stabilization but not enzyme activity of neuronal nitric-oxide synthase. *J. Biol. Chem.* **275**, 35786 – 35791 (2000).

Hevel, J.M., White, K.A., Marletta, M.A. Purification of the inducible murine macrophage nitric oxide synthase. Identification as a flavoprotein. *J. Biol. Chem.* **266**; 22789 – 22791 (1991).

Hibbs, J.B., Taintor, R.R., Vavrin, Z. Macrophage cytotoxicity: role for L-arginine deiminase and imino nitrogen oxidation to nitrite. *Science* **235**; 473 - 476 (1987).

Hibbs, J.B., Taintor, R.R., Vavrin, Z., Rachlin, E.M. Nitric oxide: a cytotoxic activated macrophage effector molecule. *Biochem. Biophys. Res. Commun.* **157**; 87 - 94 (1988).

Hirsch, D.B., Steiner, J.P., Dawson, T.M., Mammen, A., Hayek, E., Snyder, S.H. Neurotransmitter release regulated by nitric oxide in PC-12 cells and brain synaptosomes. *Curr. Biol.* **3**; 749 - 754 (1993).

Hobbs, A.J. Soluble guanylate cyclase: the forgotten sibling. *Trends. Pharmacol. Sci.* **18**: 484 - 491 (1997).

Hoenicka, M., Becker, E.M., Apeler, H., Sirichoke, T., Schroder, H., Gerzer, R., Stasch, J.P. Purified soluble guanylyl cyclase expressed in a baculovirus/Sf9 system: stimulation by YC-1, nitric oxide, and carbon monoxide. *J. Mol. Med.* **77**; 14 - 23 (1999).

Hogg, N. The biochemistry and physiology of *S*-nitrosothiols. *Annu. Rev. Pharmacol. Toxicol.* **42**; 585 – 600 (2002).

Hölscher, C. Nitric oxide, the enigmatic neuronal neuronal messenger: its role in synaptic plasticity. *Trends Neurosci.* **20**; 298 – 303 (1997).

Hölscher, C. Nitric oxide is required for expression of LTP that is induced by stimulation phase-locked with theta rhythm. *Eur. J. Neurosci.* **11**; 335 - 343 (1999).

Hölscher, C. Different strains of rat show different sensitivities to long-term potentiation by nitric oxide synthase inhibitors. *Eur. J. Pharmacol.* **457**; 99 – 106 (2002).

Hoyt, K.R., Tang, L.H., Aizenman, E., Reynolds, I.J. Nitric oxide modulates NMDA-induced increases in intracellular Ca^{2+} in cultured rat forebrain neurons. *Brain Res.* **592**; 310-316 (1992).

Huang, P.L., Dawson, T.M., Bredt, D.S., Snyder, S.H., Fishman, M.C. Targeted disruption of the neuronal nitric oxide synthase gene. *Cell* **75**; 1273 – 1286 (1993).

Huang, Y.Y., Kandel, E.R. Recruitment of long-lasting and protein kinase A-dependent long-term potentiation in the CA1 region of hippocampus requires repeated tetanization. *Learn. Mem.* **1**; 74 – 82 (1994).

Huang, A.M., Lee, E.H. Role of hippocampal nitric oxide in memory retention in rats. *Pharmacol. Biochem. Behav.* **50**; 327 – 332 (1995).

Huang, P.L., Huang, Z., Mashimo, H., Bloch, K.D., Moskowitz, M.A., Bevan, J.A., Fishman, M.C. Hypertension in mice lacking the gene for endothelial nitric oxide synthase. *Nature* **377**; 239 - 242 (1995).

Huang, C.C., Chan, S.H., Hsu, K.S. cGMP/protein kinase G-dependent potentiation of glutamatergic transmission induced by nitric oxide in immature rat rostral ventrolateral medulla neurons in vitro. *Mol. Pharmacol.* **64**; 521 - 532 (2003).

Huang, C.C., Hsu, K.S. Reexamination of the role of hyperpolarization-activated cation channels in short- and long-term plasticity at hippocampal mossy fiber synapses. *Neuropharmacology* **44**; 968 - 981 (2003).

Hughes, S.W., Cope, D.W., Toth, T.I., Williams, S.R., Crunelli, V. All thalamocortical neurones possess a T-type Ca^{2+} 'window' current that enables the expression of bistability-mediated activities. *J. Physiol.* **517**; 805 - 815 (1999).

Humbert, P., Niroomand, F., Fischer, G., Mayer, B., Koesling, D., Hinsch, K.D., Gausepohl, H., Frank, R., Schultzm, G., Bohme, E. Purification of soluble guanylyl cyclase from bovine lung by a new immunoaffinity chromatographic method. *Eur. J. Biochem.* **190**; 273 - 278 (1990).

Hussain, M.B., MacAllister, R.J., Hobbs, A.J. Reciprocal regulation of cGMP-mediated vasorelaxation by soluble and particulate guanylate cyclases. *Am. J. Physiol. Heart Circ. Physiol.* **280**; H1151 - 1159 (2001).

Iga, Y., Yoshioka, M., Togashi, H. Saito, H. Inhibitory action of N omega-nitro-L-arginine methyl ester on in vivo long-term potentiation in the rat dentate gyrus." *Eur. J. Pharmacol.* **238**; 395 - 398 (1993).

Igarashi, J., Michel., T. Agonist-modulated targeting of the EDG-1 receptor to plasmalemmal caveolae. eNOS activation by sphingosine 1-phosphate and the role of caveolin-1 in sphingolipid signal transduction. *J. Biol. Chem.* **275**; 32363 – 32370 (2000).

Ignarro, L.J., Lippton, H., Edwards, J.C., Baricos, W.H., Hyman, A.L., Kadowitz, P.J., Gruetter, C.A. Mechanism of vascular smooth muscle relaxation by organic nitrates, nitrites, nitroprusside and nitric oxide: evidence for the involvement of *S*-nitrosothiols as active intermediates. *J. Pharmacol. Exp. Ther.* **218**; 739 - 749 (1981).

Ignarro, L.J., Wood, K.S., Wolin, M.S. Activation of purified soluble guanylate cyclase by protoporphyrin IX. *Proc. Natl. Acad. Sci. U.S.A.* **79**; 2870 – 2873 (1982).

Ignarro, L.J., Adams, J.B., Horwitz, P.M., Wood, K.S. Activation of soluble guanylate cyclase by NO-hemoproteins involves NO-heme exchange. Comparison of heme-containing and heme-deficient enzyme forms. *J. Biol. Chem.* **261**; 4997 - 5002 (1986).

Ignarro, L.J., Buga, G.M., Wood, K.S., Byrns, R.E., Chaudhuri, G. Endothelium-deriving relaxing factor from pulmonary artery and vein possesses pharmacological and chemical properties that are identical to those of nitric oxide radical. *Circ. Res.* **61**; 866 - 879 (1987).

Imbrogno, S., Cerra, M.C., Tota, B. Angiotensin II-induced inotropism requires an endocardial endothelium-nitric oxide mechanism in the in-vitro heart of Anguilla anguilla. *J. Exp. Biol.* **206**; 2675 - 2684 (2003).

Inglis, F.M., Furia, F., Zuckerman, K.E., Strittmatter, S.M., Kalb, R.G. The role of nitric oxide and NMDA receptors in the development of motor neuron dendrites. *J. Neurosci.* **18**; 10493 - 10501 (1998).

Ingram, S.L., Williams, J.T. Modulation of the hyperpolarization-activated current (I_h) by cyclic nucleotides in guinea-pig primary afferent neurons. *J. Physiol.* **492**; 97 – 106 (1996).

Isenovic, E., Walsh, M.F., Muniyappa, R., Bard, M., Diglio, C.A., Sowers, J.R. Phosphatidylinositol 3-kinase may mediate isoproterenol-induced vascular relaxation in part through nitric oxide production. *Metabolism* **51**: 380 – 386 (2002).

Ishikawa, E., Ishikawa, S., Davis, J.W., Sutherlans, E.W. Determination of guanosine 3',5'-monophosphate in tissues and of guanyl cyclase in rat intestine. *J. Biol. Chem.* **244**; 6371 – 6376 (1969).

Ito, M., Karachot, L. Messengers mdiating long-term desensitization in cerebellar Purkinje cells. *Neuroreport* **1**; 129 – 132 (1990).

Iwai, A., Masliah, E., Yoshimoto, M., Ge, N., Flanagan, L., de Silva, H.A., Kittel, A., Saitoh, T. The precursor protein of non-A beta component of Alzheimer's disease amyloid is a presynaptic protein of the central nervous system. *Neuron* **14**; 467 – 475 (1995).

Jacoby, S., Sims, R.E., Hartell, N.A. Nitric oxide is required for the induction and heterosynaptic spread of long-term potentiation in rat cerebellar slices. *J. Physiol.* **535**; 825 - 839 (2001).

Jaffrey, S.R., Erdjument-Bromage, H., Ferris, C.D., Tempst, P., Synder, S.H. Protein *S*-nitrosylation: a physiological signal for neuronal nitric oxide. *Nature Cell Biology* **3**; 193 - 197 (2001).

Jayaraman, T., Ondrias, K., Ondriasova, E., Marks, A.R. Regulation of the inositol 1,4,5-trisphosphate receptor by tyrosine phosphorylation. *Science* **272**; 1492 - 1494 (1996).

Jefferys, J.G., Traub, R.D., Whittingham, M.A. Neuronal networks for induced '40 Hz' rhythms. *Trends Neurosci.* **19**; 202 – 208 (1996).

Jin. S.L., Bushnik, T., Lan, L., Conti, M. Subcellular localization of rolipram-sensitive, cAMP-specific phosphodiesterases. Differential targeting and activation of the splicing variants derived from the PDE4D gene. *J. Biol. Chem.* **273**; 19672 – 19678 (1998).

Jin, S.L., Richard, F.J., Kuo, W.P., D'Ercole, A.J., Conti, M. Impaired growth and fertility of cAMP-specific phosphodiesterase PDE4D-deficient mice. *Proc. Natl. Acad. Sci. U.S.A.* **96**; 11998 - 12003 (1999).

Johnston, D., Amaral, D.G. Hippocampus. The synaptic organisation of the brain 4th Edition. Oxford University Press (1998).

Jones, S.W. Calcium channels: unanswered questions. *J. Bioenerg. Biomembr.* **35**; 461 - 475 (2003).

Ju, H., Zou, R., Venema, V.J., Venema, R.C. Direct interaction of endothelial nitric-oxide synthase and caveolin-1 inhibits synthase activity. *J. Biol. Chem.* **272**; 18522 - 18525 (1997).

Juilfs, D.M., Soderling, S., Burns, F., Beavo, J.A. Cyclic GMP as substrate and regulator of cyclic nucleotide phosphodiesterases (PDEs). *Rev. Physiol. Biochem. Pharmacol.* **135**; 67 – 104 (1999).

Kakkar, R., Raju, R.V., Sharma, R.K. Calmodulin-dependent cyclic nucleotide phosphodiesterase (PDE1). *Cell Mol. Life Sci.* **55**; 1164 – 1186 (1999).

Kaneda, M., Oyama, Y., Ikemoto, Y., Akaike, N. Blockade of the voltage-dependent sodium current in isolated rat hippocampal neurons by tetrodotoxin and lidocaine. *Brain Res.* **484**; 348 - 351 (1989).

Kantor, D.B., Lanzrein, M., Stary, S.J., Sandoval, G.M., Smith, W.B., Sullivan, B.M., Davidson, N., Schuman, E.M. A role for endothelial NO synthase in LTP revealed by adenovirus-mediated inhibition and rescue. *Science* **274**; 1744 – 1748 (1996).

Kato, H., Kogure, K., Liu, Y., Araki, T., Itoyama, Y. Induction of NADPH-diaphorase activity in the hippocampus in a rat model of cerebral ischemia and ischemic tolerance. *Brain Res.* **652**; 71-75 (1994).

Katsuki, S., Arnold, W.P., Murad, F. Effects of sodium nitroprusside, nitroglycerin, and sodium azide on levels of cyclic nucleotides and mechanical activity of various tissues. *J. Cyclic Nucleotide Res.* **3**; 239 – 247 (1977).

Kaupp, U.B., Niidome, T., Tanabe, T., Terada, S., Bonigk, W., Stuhmer, W., Cook, N.J., Kangawa, K., Matsuo, H., Hirose, T. Primary structure and functional expression from complementary DNA of the rod photoreceptor cyclic GMP-gated channel. *Nature* **342**; 762 – 766 (1989).

Kaupp, U.B. Family of cyclic nucleotide gated ion channels. *Curr. Opin. Neurobiol.* **5**; 434 – 442 (1995).

Kazerounian, S., Pitari, G.M., Ruiz-Stewart, I., Schulz, S., Waldman, S.A. Nitric oxide activation of soluble guanylyl cyclase reveals high and low affinity sites that mediate allosteric inhibition by calcium. *Biochemistry* **41**; 3396 - 3404 (2002).

Keefer, L.K., Nims, R.W., Davies, K.M., Wink, D.A. 'NO-NOates' (1 – substituted diazen-1-ium-1,2-diolates) as nitric oxide donors: Convenient nitric oxide dosage forms. *Meth. Enzymol.* **268**; 281 – 293 (1996).

Kharitonov, V.G., Sharma, V.S., Magde, D., Koesling, D. Kinetics of nitric oxide dissociation from five- and six-coordinate nitrosyl hemes and heme proteins, including soluble guanylate cyclase. *Biochemistry* **36**; 6814 - 6818 (1997a).

Kharitonov, V.G., Russwurm, M., Magde, D., Sharma, V.S., Koesling, D. Dissociation of nitric oxide from soluble guanylate cyclase. *Biochem. Biophys. Res. Commun.* **239**; 284 - 286 (1997b).

Kharitonov, V.G., Sharma, V.S., Magde, D., Koesling, D. Kinetics and equilibria of soluble guanylate cyclase ligation by CO: effect of YC-1. *Biochemistry* **38**; 10699 - 10706 (1999).

Kimura, H., Murad, F. Evidence for two different forms of guanylate cyclase in rat heart. *J. Biol. Chem.* **249**; 6910 – 6916 (1974).

Kingston, P.A., Zufall, F., Barnstable, C.J. Rat hippocampal neurons express genes for both rod retinal and olfactory cyclic nucleotide-gated channels: novel targets for cAMP/cGMP function. *Proc. Natl. Acad. Sci. U.S.A.* **93**; 10440 – 10445 (1996).

Kirchner, L., Weitzdoerfer, R., Hoeger, H., Url, A., Schmidt, P., Engelmann, M., Villar, S.R., Fountoulakis, M., Lubec, G., Lubec, B. Impaired cognitive performance in neuronal nitric oxide synthase knockout mice is associated with hippocampal protein derangements. *Nitric Oxide* **11**; 316 - 330 (2004).

Kiss, P.J. Role of nitric oxide in the regulation of monoaminergic neurotransmission. *Brain research Bulletin* **6**; 459 – 466 (2000).

Kitamura, T., Kitamura, Y., Kuroda, S., Hino, Y., Ando, M., Kotani, K., Konishi, H., Matsuzaki, H., Kikkawa, U., Ogawa, W., Kasuga, M. Insulin-induced phosphorylation and activation of cyclic nucleotide phosphodiesterase 3B by the serine-threonine kinase Akt. *Mol. Cell. Biol.* **19**; 6286 – 6296 (1999).

Kitayama, J., Kitazono, T., Ibayashi, S., Wakisaka, M., Watanabe, Y., Kamouchi, M., Nagao, T., Fujishima, M. Role of phosphatidylinositol-3-kinase in acetylcholine-induced dilation of rat basilar artery. *Stroke* **31**; 2487 – 2493 (2000).

Kitazono, T., Ibayashi, S., Nagao, T., Fujii, K., Kagiyama, T., Fujishima, M. Role of tyrosine kinase in dilator responses of rat basilar artery in vivo. *Hypertension* **31**; 861 - 865 (1998).

Klatt, P., Schmidt, K., Lehner, D., Glatter, O., Bachinger, H.P., Mayer, B. Structural analysis of porcine brain nitric oxide synthase reveals a role for tetrahydrobiopterin and L-arginine in the formation of an SDS-resistant dimer. *EMBO J.* **14**; 3687 – 3695 (1995).

Klatt, P., Pfeiffer S., List B.M., Lehner, D., Glatter, O., Bächinger, H.P., Werner, E.R., Schmidt, K., Mayer, B. Characterisation of heme-deficient neuronal nitric oxide synthase reveals a role for heme in subunit dimerisation and binding of the amino acid substrate and tetrahydrobiopterin. *J. Biol. Chem.* **271**; 7336 – 7342 (1996).

Kleppisch, T., Pfeifer, A., Klatt, P., Ruth, P., Montkowski, A., Fassler, R., Hofmann, F. Long-term potentiation in the hippocampal CA1 region of mice lacking cGMP-dependent kinases is normal and susceptible to inhibition of nitric oxide synthase. *J Neurosci.* **19**; 48 – 55 (1999).

Kleppisch, T., Wolfsgruber, W., Feil, S., Allmann, R., Wotjak, C.T., Goebbels, S., Nave, K.A., Hofmann, F., Feil, R. Hippocampal cGMP-dependent protein kinase I supports an age- and protein synthesis-dependent component of long-term

potentiation but is not essential for spatial reference and contextual memory. *J. Neurosci.* **23**; 6005 – 6012 (2003).

Knowles, R.G., Salter, M. Measurement of NOS activity by conversion of radiolabeled arginine to citrulline using ion-exchange separation. *Methods Mol. Biol.* **100**; 67 - 73 (1998).

Ko, F.N., Wu, C.C., Kuo, S.C., Lee, F.Y., Teng, C.M.. YC-1, a novel activator of platelet guanylate cyclase. *Blood* **84**; 4226 - 4233 (1994).

Ko, G.Y., Kelly, P.T. Nitric oxide acts as a postsynaptic signalling molecule in calcium/calmodulin-induced synaptic potentiation in hippocampal CA1 pyramidial neurones. *J. Neurosci.* **19**; 6784 – 6794 (1999).

Kobayashi, T., Taguchi, J.K., Yasuhiro, T., Matsumoto, T., Kamata, K. Impairment of PI3-K/Akt pathway underlies attenuated endothelial function in aorta of type 2 diabetic mouse model. *Hypertension* **44**; 956 – 962 (2004).

Koesling, D., Herz, J., Gausepohl, H., Niroomand, F., Hinsch, K.D., Mulsch, A., Bohme, E., Schultz, G., Frank, R. The primary structure of the 70 kDa subunit of bovine soluble guanylate cyclase. *FEBS Lett.* **239**; 29 - 34 (1988).

Koesling, D., Harteneck, C., Humbert, P., Bosserhoff, A., Frank, R., Schultz, G., Bohme, E. The primary structure of the larger subunit of soluble guanylyl cyclase from bovine lung. Homology between the two subunits of the enzyme. *FEBS Lett.* **266**; 128 - 132 (1990).

Koglin, M., Behrends, S. A functional domain of the alpha1 subunit of soluble guanylyl cyclase is necessary for activation of the enzyme by nitric oxide and YC-1 but is not involved in heme binding. *J. Biol. Chem.* **278**; 12590 - 12597 (2003).

Köhr, G., De Koninck, Y., Mody, I. Properties of NMDA receptor channels in neurons acutely isolated from epileptic (kindled) rats. *J. Neurosci.* **13**; 3612 – 3627 (1993).

Komeima, K., Hayashi, Y., Naito, Y., Watanabe, Y. Inhibition of neuronal nitric-oxide synthase by calcium/ calmodulin-dependent protein kinase IIalpha through Ser847 phosphorylation in NG108-15 neuronal cells. *J. Biol. Chem.* **275**; 28139 – 28143 (2000).

Komeima, K., Watanabe, Y. Dephosphorylation of nNOS at Ser(847) by protein phosphatase 2A. FEBS Lett. 497; 65 – 66 (2001).

Kononenko, N.I., Shao, L.R., Dudek, F.E. Riluzole-sensitive slowly inactivating sodium current in rat suprachiasmatic nucleus neurons. *J. Neurophysiol.* **91**; 710 - 718 (2004).

Koppenol, W.H. NO nomenclature? *Nitric Oxide* **6**; 96 – 98 (2002).

Kornau, H.C., Schenker, L.T., Kennedy, M.B., Seeburg, P.H. Domain interaction between NMDA receptor subunits and the postsynaptic density protein PSD-95. *Science* **269**; 1737 - 1740 (1995).

Körschen, H.G., Illing, M., Seifert, R., Sesti, F., Williams, A., Gotzes, S., Colville, C., Muller, F., Dose, A., Godde, M. A 240 kDa protein represents the complete beta subunit of the cyclic nucleotide-gated channel from rod photoreceptor. *Neuron* **15**; 627 – 636 (1995).

Koshland, D.E. The molecule of the year. *Science* **258**; 1861 (1992).

Krug, M., Lossner, B., Ott, T. Anisomycin blocks the late phase of long-term potentiation in the dentate gyrus of freely moving rats. *Brain Res. Bull.* **13**; 39 - 42 (1984).

Kubes, P. Nitric oxide affects microvascular permeability in the intact and inflamed vasculature. *Microcirculation* **2**; 235 – 244 (1995).

Kuo, J.F., Greengard, P. Cyclic nucleotide-dependent protein kinases. VI. Isolation and partial purification of a protein kinase activated by guanosine 3',5'-monophosphate. *J. Biol. Chem.* **245**; 2493 - 2498 (1970).

Kuzin, B., Roberts, I., Peunova, N., Enikolopov, G. Nitric oxide regulates cell proliferation during Drosophila development. *Cell* **87**; 639 - 649 (1996).

Kuzin, B., Regulski, M., Stasiv, Y., Scheinker, V., Tully, T., Enikolopov, G. Nitric oxide interacts with the retinoblastoma pathway to control eye development in Drosophila. *Curr. Biol.* **10**; 459 - 462 (2000).

Lacza, Z., Snipes, J.A., Zhang, J., Horvath, E.M., Figueroa, J.P., Szabo, C., Busija, D.W. Mitochondrial nitric oxide synthase is not eNOS, nNOS or iNOS. *Free Radic. Biol. Med.* **35**; 1217 - 1228 (2003).

Lancaster, J.R. A tutorial on the diffusibility and reactivity of free nitric oxide. *Nitric Oxide* **1**; 18 - 30 (1997).

Lapcha, P.A., Araujo, D.M., Collier, B. Regulation of endogenous acetylcholine release from mammalian brain slices by opiate receptors: hippocampus, striatum and cerebral cortex of guinea-pig and rat. *Neuroscience* **31**; 313 - 325 (1989).

Larkman, A.U., Jack, J.J. Synaptic plasticity: hippocampal LTP. *Curr. Opin. Neurobiol.* **5**; 324 – 334 (1995).

Lauer, T., Preik, M., Rassaf, T., Strauer, B.E., Deussen, A., Feelisch, M., Kelm, M. Plasma nitrite rather than nitrate reflects regional endothelial nitric oxide synthase activity but lacks intrinsic vasodilator action. *Proc. Natl. Acad. Sci. U.S.A.* **98**; 12814 – 12819 (2001).

Lawson, D.M., Stevenson, C.E., Andrew, C.R., Eady, R.R. Unprecedented proximal binding of nitric oxide to heme: implications for guanylate cyclase. *EMBO J.* **19**; 5661 – 5671 (2000).

Lawson, D.M., Stevenson, C.E., Andrew, C.R., George, S.J., Eady, R.R. A two-faced molecule offers NO explanation: the proximal binding of nitric oxide to haem. *Biochem. Soc. Trans.* **31**: 553 – 557 (2003).

Lei, S.Z., Pan, Z.H., Aggarwal, S.K., Chen, H.S., Hartman, J., Sucher, N.J., Lipton, S.A. Effect of nitric oxide production on the redox modulatory site of the NMDA receptor-channel complex. *Neuron* **8**; 1087 - 1099 (1992).

Leinders-Zufall, T., Zufall, F. Block of cyclic nucleotide-gated channels in salamander olfactory receptor neurons by the guanylyl cyclase inhibitor LY83583. *J. Neurophysiol.* **74**; 2759 - 2762 (1995a).

Leinders-Zufall, T., Rosenboom, H., Barnstable, C.J., Shepherd, G.M., Zufall, F. A calcium-permeable cGMP-activated cation conductance in hippocampal neurons. *Neuroreport* **6**; 1761 - 1765 (1995b).

Lev-Ram, V., Makings, L.R., Keitz, P.F., Kao, J.P., Tsien, R.Y. Long-term depression in cerebellar Purkinje neurons results from coincidence of nitric oxide and depolariation-induced Ca^{2+} transients. *Neuron* **15**; 407 – 15 (1995).

Lev-Ram, V., Jiang, T., Wood, J., Lawrence, D.S., Tsien, R.Y. Synergies and coincidence requirements between NO, cGMP, and Ca2+ in the induction of cerebellar long-term depression. *Neuron* **18**; 1025 – 1038 (1997).

Lev-Ram, V., Wong, S.T., Storm, D.R., Tsien, R.Y. A new form of cerebellar long-term potentiation is postsynaptic and depends on nitric oxide but not cAMP. *Proc. Natl. Acad. Sci. U.S.A.* **99**; 8389 - 8393 (2002)

Lewko, B., Wendt, U., Szczepanska-Konkelm, M., Stepinski, J., Drewnowska, K., Angielski, S. Inhibition of endogenous nitric oxide synthesis activates particulate guanylyl cyclase in the rat renal glomeruli. *Kidney Int.* **52**; 654 - 659 (1997).

Li, H., Raman, C.S., Glaser, C.B., Blasko, E., Young, T.A., Parkinsoni, J.F, Whitlow, M., Poulos, T.L. Crystal structures of zinc-free and -bound heme domain of human inducible nitric-oxide synthase. *J. Biol. Chem.* **274**; 21276 – 21284 (1999a).

Li, L., Yee, C., Beavo, J.A. CD3- and CD28-dependent induction of PDE7 required for T cell activation. *Science* **283**; 848 – 851 (1999).

Li, D., Laubach, V.E., Johns, R.A. Upregulation of lung soluble guanylate cyclase during chronic hypoxia is prevented by deletion of eNOS. *Am. J. Physiol. Lung Cell. Mol. Physiol.* **281**; L369 - 376 (2001).

Li, D.P., Chen, S.R., Pan, H.L. Nitric oxide inhibits spinally projecting paraventricular neurons through potentiation of presynaptic GABA release. *J. Neurophysiol.* 88; 2664 - 2674 (2002).

Liman, E.R., Buck, L.B. A second subunit of the olfactory cyclic nucleotide-gated channel confers high sensitivity to cAMP. *Neuron* **13**; 611 - 621 (1994).

Lin, S.Z., Chiou, A.L., Wang, Y. Ketamine antagonizes nitric oxide release from cerebral cortex after middle cerebral artery ligation in rats. *Stroke* **27**; 747 – 752 (1996).

Linden, D.J., Connor, J.A. Long-term depression of glutamate currents in cultured cerebellar Purkinje neurons does not require nitric oxide signalling. *Eur. J. Neurosci.* **4**; 10 – 15 (1992).

Linden, D.J., Smeyne, M., Connor, J.A. Induction of cerebellar long-term depression in culture requires postsynaptic action of sodium ions. *Neuron* **11**; 1093 - 1100 (1993).

Linden, D.J., Dawson, T.M., Dawson, V.L. An evaluation of the nitric oxide/cGMP/cGMP-dependent protein kinase cascade in the induction of cerebellar long-term depression in culture. *J. Neurosci.* **15**; 5098 – 5105 (1995).

Lipton, S.A., Choi, Y-B., Takahashi, H., Zhang, D., Li, W., Godzik, A., Bankston, L.A. Cysteine regulation of protein function – as exemplified by NMDA-receptor modulation. *Trends Neurosci.* **25**; 474 - 480 (2002).

Liu, J., Garcia-Cardena, G., Sessa, W.C. Biosynthesis and palmitoylation of endothelial nitric oxide synthase: mutagenesis of palmitoylation sites, cysteines-15 and/or -26, argues against depalmitoylation-induced translocation of the enzyme. *Biochemistry* **34**; 12333 - 12340 (1995).

Liu, L., Hausladen, A., Zeng, M., Que, L., Heitman, J., Stamler, J.S. A metabolic enzyme for *S*-nitrosothiol conserved from bacteria to humans. *Nature* **410**; 490 – 494 (2001).

Liu, S., Ninan, I., Antonova, I., Battaglia, F., Trinchese, F., Narasanna, A., Kolodilov, N., Dauer, W., Hawkins, R.D., Arancio, O. alpha-Synuclein produces a long-lasting increase in neurotransmitter release. *EMBO J.* **23**; 4506 - 4516 (2004).

Lobban, M., Shakur, Y., Beattie, J., Houslay, M.D. Identification of two splice variant forms of type-IVB cyclic AMP phosphodiesterase, DPD (rPDE-IVB1) and PDE-4 (rPDE-IVB2) in brain: selective localization in membrane and cytosolic compartments and differential expression in various brain regions. *Biochem. J.* **304**; 399 – 406 (1994).

Loesch, A. Belai, A., Burnstock, G. An ultrastructural study of NADPH-diaphorase and nitric oxide synthase in the perivascular nerves and vascular endothelium of the rat basilar artery. *J Neurocytol.* **23**; 49 – 59 (1994).

Lohmann, S.M., Vaandrager, A.B., Smolenski, A., Walter, U., De Jonge, H.R. Distinct and specific functions of cGMP-dependent protein kinases. *Trends Biochem. Sci.* **22**; 307 – 312 (1997).

Loughney, K., Snyder, P.B., Uher, L., Rosman, G.J., Ferguson, K., Florio, V.A. Isolation and characterization of PDE10A, a novel human 3', 5'-cyclic nucleotide phosphodiesterase. *Gene* **234**; 109 – 117 (1999).

Lu, Y.F., Kandel, E.R., Hawkins, R.D. Nitric oxide signalling contributes to late-phase LTP and CREB phosphorylation in the hippocampus. *J. Neurosci.* **19**; 10250 – 10261 (1999).

Lu, Y.F., Hawkins, R.D. Ryanodine receptors contribute to cGMP-induced late-phase LTP and CREB phosphorylation in the hippocampus. *J. Neurophysiol.* **88**; 1270 - 1278 (2002).

Lu, Y., Li, Y., Herin, G.A., Aizenman, E., Epstein, P.M., Rosenberg, P.A. Elevation of intracellular cAMP evokes activity-dependent release of adenosine in cultured rat forebrain neurons. *Eur. J. Neurosci.* 19; 2669 – 2681 (2004).

Lucas, K.A., Pitari, G.M., Kazerounian, S., Ruiz-Stewart, I., Park, J., Schultz, S., Chepenik, K.P., Waldman, S.A. Guanylyl cyclases and signalling by cyclic GMP. *Pharmacol. Rev.* **52**; 375 – 413 (2000).

Ludvig, N., Burmeister, V., Jobe, P.C., Kincaid, R.L. Electron microscopic immunocytochemical evidence that the calmodulin-dependent cyclic nucleotide phosphodiesterase is localized predominantly at postsynaptic sites in the rat brain. *Neuroscience* **44**; 491-500 (1991).

Ludwig, A., Zong, X., Jeglitsch, M., Hofmann, F., Biel, M. A family of hyperpolarization-activated mammalian cation channels. *Nature* **393**; 587 – 591 (1998).

Lumme, A., Soinila, S., Sadeniemi, M., Halonen, T., Vanhatalo, S. Nitric oxide synthase immunoreactivity in the rat hippocampus after status epilepticus induced by perforant pathway stimulation. *Brain Res.* **871**; 303 – 310 (2000).

Lum-Ragan, J.T., Gribkoff, V.K. The sensitivity of hippocampal long-term potentiation to nitric oxide synthase inhibitors is dependent upon the pattern of conditioning stimulation. *Neuroscience* **57**; 973 – 983 (1993).

Luscher, C., Nicoll, R.A., Malenka, R.C., Muller, D. Synaptic plasticity and dynamic modulation of the postsynaptic membrane. *Nat. Neurosci.* **3**; 545 – 550 (2000).

MacMicking, J., Xie, Q.W., Nathan, C. Nitric oxide and macrophage function. *Annu. Rev. Immunol.* **15**; 323 - 350 (1997).

Madison, D.V., Malenka, R.C., Nicoll, R.A. Mechanisms underlying long-term potentiation of synaptic transmission. *Annu. Rev. Neurosci.* **14**; 379 – 397 (1991).

Magee, T., Fuentes, A.M., Garban, H., Rajavashisth, T., Marquez, D., Rodriguez, J.A., Rajfer, J., Gonzalez-Cadavid, N.F. Cloning of a novel neuronal nitric oxide synthase expressed in penis and lower urinary tract. *Biochem. Biophys. Res. Commun.* **226**; 145 – 151 (1996).

Magee, J.C., Johnston, D. A synaptically controlled, associative signal for Hebbian plasticity in hippocampal neurons. *Science* **275**; 209 - 213 (1997).

Majocha, R., Baldessarini, R.J. Increased muscarinic receptor binding in rat forebrain after scopolamine. *Eur. J. Pharmacol.* **67**; 327 - 328 (1980).

Makino, R., Matsuda, H., Obayashi, E., Shiro, Y., Iizuka, T., Hori, H. EPR characterization of axial bond in metal center of native and cobalt-substituted guanylate cyclase. *J. Biol. Chem.* **274**; 7714 - 7723 (1999).

Malen, P.L., Chapman, P.F. Nitric oxide facilitates long-term potentiation, but not long-term depression. *J. Neurosci.* **17**; 2645 - 2651 (1997).

Malenka, R.C. The role of postsynaptic calcium in the induction of long-term potentiation. *Mol. Neurobiol.* **5**; 289 - 295 (1991).

Maletic-Savatic, M., Malinow, R., Svoboda, K. Rapid dendritic morphogenesis in CA1 hippocampal dendrites induced by synaptic activity. *Science* **283**; 1923 - 1927 (1999).

Manganiello, V.C., Degerman, E. Cyclic nucleotide phosphodiesterases (PDEs): diverse regulators of cyclic nucleotide signals and inviting molecular targets for novel therapeutic agents. *Thromb. Haemost.* **82**; 407 – 411 (1999).

Manzoni, O., Prezeau, L., Marin, P., Deshager, S., Bockaert, J., Fagni, L. Nitric oxide-induced blockade of NMDA receptors. *Neuron* **8**; 653 - 662 (1992).

Margulis, A., Sitaramayya, A. Rate of deactivation of nitric oxide-stimulated soluble guanylate cyclase: influence of nitric oxide scavengers and calcium. *Biochemistry* **39**; 1034 - 1039 (2000).

Martin, R.L., Lee, J.H., Cribbs, L.L., Perez-Reyes, E., Hanck, D.A. Mibefradil block of cloned T-type calcium channels. *J. Pharmacol. Exp. Ther.* **295**; 302 - 308 (2000).

Martin, S.J., Grimwood, P.D., Morris, R.G. Synaptic plasticity and memory: an evaluation of the hypothesis. *Annu. Rev. Neurosci.* **23**: 649 - 711 (2000).

Martinez, S.E., Beavo, J.A., Hol, W.G. GAF Domains: Two-Billion-Year-Old Molecular Switches that Bind Cyclic Nucleotides. *Mol. Interv.* **2**; 317 - 323 (2002).

Martins, T.J., Mumby, M.C., Beavo, J.A. Purification and characterization of a cyclic GMP-stimulated cyclic nucleotide phosphodiesterase from bovine tissues. *J. Biol. Chem.* **257**; 1973 - 1979 (1982).

Massie, B.M. Mibefradil: a selective T-type calcium antagonist. *Am. J. Cardiol.* **80**; 23I - 32I (1997).

Masters, B.S., McMillan, K., Sheta, E.A., Nishimura, J.S., Roman, L.J., Martasek, P. Neuronal nitric oxide synthase, a modular enzyme formed by convergent evolution:

structure studies of a cysteine thiolate-liganded heme protein that hydroxylates L-arginine to produce NO as a cellular signal. *FASEB J.* **10**; 552 - 528 (1996).

Matsuda, H., Iyanagi, T. Calmodulin activates intramolecular electron transfer between the two flavins of neuronal nitric oxide synthase flavin domain. *Biochimica et Biophysica Acta* **1473**; 345 – 355 (1999).

Matsuoka, I., Giuili, G., Poyard, M., Stengel, D., Parma, J., Guellaen, G., Hanoune, J. Localization of adenylyl and guanylyl cyclase in rat brain by in situ hybridization: comparison with calmodulin mRNA distribution. *J. Neurosci.* **12**; 3350 - 3360 (1992).

Matsuzaki, M., Honkura, N., Ellis-Davies, G.C., Kasai, H. Structural basis of long-term potentiation in single dendritic spines. *Nature* **429**; 761 – 766 (2004).

Mayer, B., Brunner, F., Schmidt, K. Inhibition of nitric oxide synthesis by methylene blue. *Biochem. Pharmacol.* **45**; 367 - 374 (1993a).

Mayer, B., Koesling, D., Bohme, E. Characterization of nitric oxide synthase, soluble guanylyl cyclase, and Ca^{2+}/calmodulin-stimulated cGMP phosphodiesterase as components of neuronal signal transduction. *Adv. Second Messenger Phosphoprotein Res.* **28**; 111 – 119 (1993b).

McCabe, T.J., Fulton, D., Roman, L.J., Sessa, W.C. Enhanced electron flux and reduced calmodulin dissociation may explain "calcium-independent" eNOS activation by phosphorylation. *J. Biol. Chem.* **275**; 6123 – 6128 (2000).

Meldrum, B., Garthwaite, J. Excitatory amino acid neurotoxicity and neurodegenerative disease. *Trends Pharmacol Sci.* **11**; 379 – 387 (1990).

Mergia, E., Russwurm, M., Zoidl, G., Koesling, D. Major occurrence of the new alpha2beta1 isoform of NO-sensitive guanylyl cyclase in brain. *Cell Signal.* **15**; 189 – 195 (2003).

Michel, J.B., Feron, O., Sacks, D., Michel, T. Reciprocal regulation of endothelial nitric-oxide synthase by Ca2+-calmodulin and caveolin. *J. Biol. Chem.* **272**; 15583 – 15586 (1997a).

Michel, J.B., Feron, O., Sase, K., Prabhakar, P., Michel, T. Caveolin versus calmodulin. Counterbalancing allosteric modulators of endothelial nitric oxide synthase. *J Biol Chem.* **272**; 25907 – 25912 (1997b).

Michell, B.J., Chen, Z-P., Tiganis, T., Stapleton, D., Katsis, F., Power, D.A., Sim, A.T., Kemp, B.E. Coordinated control of endothelial nitric-oxide synthase phosphorylation by protein kinase C and the cAMP-dependent protein kinase. *J. Biol. Chem.* **276**; 17625 – 17628 (2001).

Michell, B.J., Harris, M.B., Chen, Z-P., Ju, H., Venema, V.J., Blackstone, M.A., Huang, W., Venema, R.C., Kemp, B.E. Identification of regulatory sites of phosphorylation of the bovine endothelial nitric-oxide synthase at Serine 617 and Serine 635. *J. Biol. Chem.* **277**; 42344 – 42351 (2002).

Mitchell, H.H., Shonle, H.A., Grindley, H.S. The origin of the nitrates in the urine. *J. Biol. Chem.* **24**; 461 – 490 (1916).

Mitchell, J.B., Lupica, C.R., Dunwiddie, T.V. Activity-dependent release of endogenous adenosine modulates synaptic responses in the rat hippocampus. *J. Neurosci.* **13**; 3439 - 3447 (1993).

Mitchell, D., Tyml, K. Nitric oxide release in rat skeletal muscle capillary. *Am J. Physiol.* **270**; H1696 – H1703 (1996).

Monaghan, D.T., Yao, D., Olverman, H.J., Watkins, J.C., Cotman, C.W. Autoradiography of D-2-[3H]amino-5-phosphonopentanoate binding sites in rat brain. *Neurosci. Lett.* **52**; 253 – 258 (1984).

Montague, P.R., Gancayco, C.D., Winn, M.J., Marchase, R.B., Friedlander, M.J. Role of NO production in NMDA receptor-mediated neurotransmitter release in cerebral cortex. *Science* **263**; 973 - 977 (1994).

Moreno-Lopez, B., Noval, J.A., Gonzalez-Bonet, L.G., Estrada, C. Morphological bases for a role of nitric oxide in adult neurogenesis. *Brain Res.* **869**; 244 - 250 (2000).

Moreno-Lopez, B., Romero-Grimaldi, C., Noval, J.A., Murillo-Carretero, M., Matarredona, E.R., Estrada, C. Nitric oxide is a physiological inhibitor of neurogenesis in the adult mouse subventricular zone and olfactory bulb. *J. Neurosci.* **24**; 85 - 95 (2004).

Mülsch, A., Bauersachs, J., Schafer, A., Stasch, J.P., Kast, R., Busse, R. Effect of YC-1, an NO-independent, superoxide-sensitive stimulator of soluble guanylyl cyclase, on smooth muscle responsiveness to nitrovasodilators. *Br. J. Pharmacol.* **120**; 681 - 689 (1997).

Muradov, H., Boyd, K.K., Artemyev, N.O. Structural determinants of the PDE6 GAF A domain for binding the inhibitory gamma-subunit and noncatalytic cGMP. *Vision Res.* **44**; 2437 – 2444 (2004).

Murphy, S., Simmons, M.L., Agullo, L., Garcia, A., Feinstein, D.L., Galea, E., Reis, D.J., Minc-Golomb, D., Schwartz, J.P. Synthesis of nitric oxide in CNS glial cells. *Trends Neurosci.* **16**; 323 – 328 (1993).

Murphy, K.P.S.J., Williams, J.H., Bettache, N., Bliss, T.V.P. Photolytic release of nitric oxide modulates NMJDA receptor-mediated transmission but does not induce long-term potentiation at hippocampal slices. *Neuropharmacol.* **33**; 1375 - 1385 (1994).

Murphy, K.P.S.J., Bliss, T.V.P. Photolytically released nitric oxide produces a delayed but persistent suppression of LTP in area CA1 of the rat hippocampal slice. *J. Physiol.* **515**; 453 - 462 (1999).

Musleh, W.Y., Shahi, K., Baudry, M. Further studies concerning the role of nitric oxide in LTP induction and maintenance. *Synapse* **13**; 370 - 375 (1993).

Nagao, S., Ito, M. Subdural application of hemoglobin to the cerebellum blocks vestibuloocular reflex adaptation. *Neuroreport* **2**; 193 - 196 (1991).

Nahum-Levy, R., Lipinski, D., Shavit, S., Benveniste, M. Desensitisation of NMDA receptor channels is modulated by glutamate agonists. *Biophysical Journal* **80**; 2152 – 2166 (2001).

Nakamura, T., Gold, G.H. A cyclic nucleotide-gated conductance in olfactory receptor cilia. *Nature* **325**; 442 – 444 (1987).

Nakane, M., Saheki, S., Kuno, T., Ishii, K., Murad, F. Molecular cloning of a cDNA coding for 70 kilodalton subunit of soluble guanylate cyclase from rat lung. *Biochem. Biophys. Res. Commun.* **157**; 1139 - 1147 (1988).

Nakane, M., Arai, K., Saheki, S., Kuno, T., Buechler, W., Murad, F. Molecular cloning and expression of cDNAs coding for soluble guanylate cyclase from rat lung. *Biol. Chem.* **265**; 16841 – 16845 (1990).

Nakane, M., Mitchell, J., Forstermann, U., Murad, F. Phosphorylation by calcium calmodulin-dependent protein kinase II and protein kinase C modulates the activity of nitric oxide synthase. *Biochem. Biophys. Res. Commun.* **180**; 1396 - 1402 (1991).

Nakane, M., Schmidt, H.H., Pollock, J.S., Forstermann, U., Murad, F. Cloned human brain nitric oxide synthase is highly expressed in skeletal muscle. *FEBS Lett.* **316**; 175 - 180 (1993).

Nakane, M., Klinghofer, V., Kuk, J.E., Donnelly, J.L., Budzik, G.P., Pollock, J.S., Basha, F., Carter, G.W. Novel potent and selective inhibitors of inducible nitric oxide synthase. *Mol. Pharmacol.* **47**; 831 - 834 (1995).

Nelson, R.J., Kriegsfeld, L.J., Dawson, V.L., Dawson, T.M. Effects of nitric oxide on neuroendocrine function and behavior. *Front. Neuroendocrinol.* **18**; 463 - 491 (1997).

Newcomb, R., Szoke, B., Palma, A., Wang, G., Chen, X., Hopkins, W., Cong, R., Miller, J., Urge, L., Tarczy-Hornoch, K., Loo, J.A., Dooley, D.J., Nadasdi, L., Tsien, R.W., Lemos, J., Miljanich, G. Selective peptide antagonist of the class E calcium channel from the venom of the tarantula Hysterocrates gigas. *Biochemistry* **37**; 15353 - 15362 (1998).

Nguyen, P.V., Abel, T., Kandel, E.R. Requirement of a critical period of transcription for induction of a late phase of LTP. *Science* **265**; 1104 – 1107 (1994).

Nikonenko, I., Jourdain, P., Muller, D. Presynaptic remodeling contributes to activity-dependent synaptogenesis. *J. Neurosci.* **23**; 8498 - 8505 (2003).

Nilius, B., Hess, P., Lansman, J.B., Tsien, R.W. A novel type of cardiac calcium channel in ventricular cells. *Biomed. Biochim. Acta* **45**; S167 - 170 (1986).

Nilius, B., Watanabe, H., Vriens, J. The TRPV4 channel: structure-function relationship and promiscuous gating behaviour. *Pflugers Arch.* **446**; 298-303 (2003).

Nishida, C., Ortiz de Montellano, P.R. Autoinhibition of endothelial nitric-oxide synthase. *J. Biol. Chem.* **274**; 14692 – 14698 (1999).

Noma, A., Irisawa, H. A time- and voltage-dependent potassium current in the rabbit sinoatrial node cell. *Pflugers Arch.* **366**; 251 - 258 (1976).

Notomi, T., Shigemoto, R. Immunohistochemical localization of I_h channel subunits, HCN1-4, in the rat brain. *J. Comp. Neurol.* **471**; 241 - 276 (2004).

Ny, L., Pfeifer, A., Aszodi, A., Ahmad, M., Alm, P., Hedlund, P., Fassler, R., Andersson, K.E. Impaired relaxation of stomach smooth muscle in mice lacking cyclic GMP-dependent protein kinase I. *Br. J. Pharmacol.* **129**; 395 – 401 (2000).

O'Dell, T.J., Hawkins, R.D., Kandel, E.R., Arancio, O. Tests of the roles of two diffusible substances in long-term potentiation: evidence for nitric oxide as a possible early retrograde messenger. *Proc. Natl. Acad. Sci. USA* **88**; 11285-89 (1991).

O'Dell, T.J., Huang, P.L., Dawson, T.M., Dinerman, J.L., Snyder, S.H., Kandel, E.R., Fishman, M.C. Endothelial NOS and the blockade of LTP by NOS inhibitors in mice lacking neuronal NOS. *Science* **265**; 542 – 546 (1994).

Ogura, T., Yokoyama, T., Fujisawa, H., Kurashima, Y., Esumi, H. Structural diversity of neuronal nitric oxide synthase mRNA in the nervous system. *Biochem. Biophys. Res. Commun.* **193**; 1014 – 1022 (1993).

Okada, M., Osumi, Y., Okuma, Y., Ueno, H. Nitric oxide inhibits the release of acetylcholine in the isolated retina. *Graefes. Arch. Clin. Exp. Ophthalmol.* **239**; 217 – 221 (2001).

Olearczyk, J.J., Ellsworth, M.L., Stephenson, A.H., Lonigro, A.J., Sprague, R.S. Nitric oxide inhibits ATP release from erythrocytes. *J. Pharmacol. Exp. Ther.* **309**; 1079 - 1084 (2004).

Otani, S., Abraham, W.C. Inhibition of protein synthesis in the dentate gyrus, but not the entorhinal cortex, blocks maintenance of long-term potentiation in rats. *Neurosci. Lett.* **106**; 175 – 180 (1989).

Packer, M.A., Stasiv, Y., Benraiss, A., Chmielnicki, E., Grinberg, A., Westphal, H., Goldman, S.A., Enikolopov, G. Nitric oxide negatively regulates mammalian adult neurogenesis. *Proc. Natl. Acad. Sci. U.S.A.* **100**; 9566 - 9571 (2003).

Palmer, R.M., Ferrige, A.G., Moncada, S. Nitric Oxide release accounts for the biological activity of endothelium-derived relaxing factor. *Nature* **327**; 524 - 526 (1987).

Palmer, R.M.J., Moncado, S. A novel citrulline-forming enzyme implicated in the formation of nitric oxide by vascular endothelial cells. *Biophys. Res. Commun.* **158**; 348 – 352 (1989).

Palumbo, A., Di Cosmo, A., Gesualdo, I., d'Ischia, M. A calcium-dependent nitric oxide synthase and NMDA R1 glutamate receptor in the ink gland of Sepia officinalis: a hint to a regulatory role of nitric oxide in melanogenesis? *Biochem. Biophys. Res. Commun.* **235**; 429 - 432 (1997).

Panda, K., Ghosh, S., Stuehr, D.J. Calmodulin activates intersubunit electron transfer in the neuronal nitric-oxide synthase dimer. *J. Biol. Chem.* **276**; 23349 - 23356

Pape, H.C., Mager, R. Nitric oxide controls oscillatory activity in thalamocortical neurons. *Neuron* **9**; 441 - 448 (1992).

Pape, H.C. Queer current and pacemaker: the hyperpolarization-activated cation current in neurons. *Annu. Rev. Physiol.* **58**; 299 - 327 (1996).

Paton, J.F., Kasparov, S., Paterson, D.J. Nitric oxide and autonomic control of heart rate: a question of specificity. *Trends Neurosci.* **25**; 626 - 631 (2002).

Pereira, E.F., Reinhardt-Maelicke, S., Schrattenholz, A., Maelicke, A., Albuquerque, E.X. Identification and functional characterization of a new agonist site on nicotinic acetylcholine receptors of cultured hippocampal neurons. *J. Pharmacol. Exp. Ther.* **265**; 1474 - 1491 (1993).

Perez-Reyes, E. Molecular physiology of low-voltage-activated t-type calcium channels. *Physiol. Rev.* **83**; 117 - 161 (2003).

Persson, C.G.A. On the medical history of xanthines and other remedies for asthma: a tribute to HH Salter. *Thorax* **40**; 881 – 886 (1985).

Petros, A., Bennett, D., Vallance, P. Effect of nitric oxide synthase inhibitors on hypotension in patients with septic shock. *Lancet* **338**; 1557 – 1558 (1991).

Peunova, N., Enikolopov, G. Nitric oxide triggers a switch to growth arrest during differentiation of neuronal cells. *Nature* **375**; 68 - 73 (1995).

Pfeifer, A., Aszodi, A., Seidler, U., Ruth, P., Hofmann, F., Fassler, R. Intestinal secretory defects and dwarfism in mice lacking cGMP-dependent protein kinase II. *Science* **274**; 2082 - 2086 (1996).

Pfeifer, A., Klatt, P., Massberg, S., Ny, L., Sausbier, M., Hirneiss, C., Wang, G.X., Korth, M., Aszodi, A., Andersson, K.E., Krombach, F., Mayerhofer, A., Ruth, P., Fassler, R., Hofmann, F. Defective smooth muscle regulation in cGMP kinase I-deficient mice. *EMBO J.* **17**; 3045 - 3051 (1998).

Pfeifer, A., Ruth, P., Dostmann, W., Sausbier, M., Klatt, P., Hofmann, F. Structure and function of cGMP-dependent protein kinases. *Rev. Physiol. Biochem. Pharmacol.* **135**; 105 – 149 (1999).

Phung, Y.T., Bekker, J.M., Hallmark, O.G., Black, S.M. Both neuronal NO synthase and nitric oxide are required for PC12 cell differentiation: a cGMP independent pathway. *Brain Res. Mol. Brain Res.* **64**; 165 - 178 (1999).

Powis, G., Bonjouklian, R., Berggren, M.M., Gallegos, A., Abraham, R., Ashendel, C., Zalkow, L., Matter, W.F., Dodge, J., Grindey, G. Wortmannin, a potent and selective inhibitor of phosphatidylinositol-3-kinase. *Cancer Res.* **54**; 2419 - 2423 (1994).

Prast, H., Philippu, A. Nitric oxide as modulator of neuronal function. *Prog. Neurobiol.* **64**; 51 - 68 (2001).

Putzke, J., Seidel, B., Huang, P.L., Wolf, G. Differential expression of alternatively spliced isoforms of neuronal nitric oxide synthase (nNOS) and N-methyl-D-aspartate receptors (NMDAR) in knockout mice deficient in nNOSα (nNOSα $^{\Delta/\Delta}$ mice). *Molecular Brain Research* **85**; 13 – 23 (2000).

Raman, C.S., Li, H., Martâsek, P., Král, V., Masters, B.S.S., Poulos, TL. Crystal structure of constitutive endothelial nitric oxide synthase: A paradigm for pterin function involving a novel metal center. *Cell* **95**; 939 – 950 (1998).
Randall, A.D., Tsien, R.W. Contrasting biophysical and pharmacological properties of T-type and R-type calcium channels. *Neuropharmacology* **36**; 879 - 893 (1997).

Regulski, M., Tully, T. Molecular and biochemical characterization of dNOS: a Drosophila Ca2+/calmodulin-dependent nitric oxide synthase. *Proc. Natl. Acad. Sci. U.S.A.* **92**; 9072 – 9076 (1995).

Reif, A., Schmitt, A., Fritzen, S., Chourbaji, S., Bartsch, C., Urani, A., Wycislo, M., Mossner, R., Sommer, C., Gass, P., Lesch, K.P. Differential effect of endothelial nitric oxide synthase (NOS-III) on the regulation of adult neurogenesis and behaviour. *Eur. J. Neurosci.* **20**; 885 – 895 (2004).

Reinhardt, R.R., Bondy, C.A. Differential cellular pattern of gene expression for two distinct cGMP-inhibited cyclic nucleotide phosphodiesterases in developing and mature rat brain. *Neuroscience* **72**; 567 - 578 (1996).

Repaske, D.R., Corbin, J.G., Conti, M., Goy, M.F. A cyclic GMP-stimulated cyclic nucleotide phosphodiesterase gene is highly expressed in the limbic system of the rat brain. *Neuroscience* **56**; 673 - 686 (1993).

Rialas, C.M., Nomizu, M., Patterson, M., Kleinman, H.K., Weston, C.A., Weeks, B.S. Nitric oxide mediates laminin-induced neurite outgrowth in PC12 cells. *Exp. Cell. Res.* **260**; 268 - 276 (2000).

Ribak, C.E., Seress, L., Five types of basket cell in the hippocampus dentate gyrus: a combined Golgi and electron microscopic study. *J. Neurocytol.* **12**; 577 – 597 (1983).

Ribeiro, J.M., Nussenzveig, R.H. Nitric oxide synthase activity from a hematophagous insect salivary gland. *FEBS Lett.* **330**; 165 - 168 (1993).

Robinson, R.B., Siegelbaum, S.A. Hyperpolarization-activated cation currents: from molecules to physiological function. *Annu. Rev. Physiol.* **65**; 453 – 480 (2003).

Rudic, R.D., Shesely, E.G., Maeda, N., Smithies, O., Segal, S.S., Sessa, W.C. Direct evidence for the importance of endothelium-derived nitric oxide in vascular remodeling. *J. Clin. Invest.* **101**; 731 - 736 (1998).

Russwurm, M., Behrends, S., Harteneck, C., Koesling, D. Functional properties of a naturally occurring isoform of soluble guanylyl cyclase. *Biochem J.* **335**; 125 - 130 (1998).

Russwurm, M., Wittau, N., Koesling, D., Guanylyl cyclase/PSD-95 interaction: targeting of the nitric oxide-sensitive alpha2beta1 guanylyl cyclase to synaptic membranes. *J. Biol. Chem.* **276**; 44647 - 44652 (2001).

Russwurm, M., Koesling, D. Isoforms of NO-sensitive guanylyl cyclase. *Mol. Cell. Biochem.* **230**; 159 - 164 (2002).

Saeij, J.P., Stet, R.J., Groeneveld, A., Verburg-van Kemenade, L.B., van Muiswinkel, W.B., Wiegertjes, G.F. Molecular and functional characterization of a fish inducible-type nitric oxide synthase. *Immunogenetics* **51**; 339 – 346 (2000).

Salerno, J.C., Harris, D.E., Irizarry, K., Patel, B., Morales, A.J., Smith, S.M., Martasek, P., Roman, L.J., Masters, B.S., Jones, C.L., Weissman, B.A., Lane, P., Liu, Q., Gross, S.S. An autoinhibitory control element defines calcium-regulated isoforms of nitric oxide synthase. *J. Biol. Chem.* **272**; 29769 - 29777 (1997).

Santoro, B., Liu, D.T., Yao, H., Bartsch ,D., Kandel, E.R., Siegelbaum, S.A., Tibbs, G.R. Identification of a gene encoding a hyperpolarization-activated pacemaker channel of brain. *Cell* **93**; 717 – 729 (1998).

Satoh, S., Kimura, T., Toda, M., Miyazaki, H., Ono, S., Narita, H., Murayama, T., Nomura, Y. NO donors stimulate noradrenaline release from rat hippocampus in a calmodulin-dependent manner in the presence of L-cysteine. *J. Cell. Physiol.* **169**; 87 – 96 (1996).

Sattin, A., Rall, T.W. The effect of adenosine and adenine nucleotides on the cyclic adenosine 3', 5'-phosphate content of guinea pig cerebral cortex slices. *Mol. Pharmacol.* **6**; 13 - 23 (1970).

Sautter, A., Zong, X., Hofmann, F., Biel, M. An isoform of the rod photoreceptor cyclic nucleotide-gated channel beta subunit expressed in olfactory neurons. *Proc. Natl. Acad. Sci. U.S.A.* **95**; 4696 – 4701 (1998).

Schmidt, K., Desch, W., Klatt, P., Kukovertz, W.R., Mayer, B. Release of nitric oxide from donors with known half-life: a mathematical model of calculating nitric oxide

concentrations in aerobic solutions. *Naunyn Schmiedebergs Arch. Pharmacol.* **335**; 457 – 462 (1997).

Schmidt, H., Werner, M., Heppenstall, P.A., Henning, M., More, M.I., Kuhbandner, S., Lewin, G.R., Hofmann, F., Feil, R., Rathjen, F.G. cGMP-mediated signalling via cGKIalpha is required for the guidance and connectivity of sensory axons. *J. Cell. Biol.* **159**; 489 - 498 (2002).

Schultz, G., Böhme, E., Munske, K. Guanyl cyclase: determination of enzyme activity. *Life Sci.* **8**; 1323 – 1332 (1969).

Schuman, E.M., Madison, D.V. A requirement for the intercellular messenger nitric oxide in long-term potentiation. *Science* **254**; 1503 - 1506 (1991).

Schuman, E.M., Meffert, M.K., Schulman, H., Madison, D.V. An ADP-ribosyltransferase as a potential target for nitric oxide action in hippocampal long-term potentiation. *Proc. Natl. Acad. Sci. U.S.A.* **91**; 11958 – 11962 (1994).

Schrammel, A., Behrends, S., Schmidt, K., Koesling, D., Mayer, B. Characterization of 1H-[1,2,4]oxadiazolo[4,3-a]quinoxalin-1-one as a heme-site inhibitor of nitric oxide-sensitive guanylyl cyclase. *Mol. Pharmacol.* **50**; 1 - 5 (1996).

Scoville, W.B., Milner, B. Loss of recent memory after bilateral hippocampal lesions. *J. Neurochem.* **20**; 11 - 21 (1957).

Segovia, G., Porras, A., Mora, F. Effects of a nitric oxide donor on glutamate and GABA release in striatum and hippocampus of the conscious rat. *Neuroreport* **5**; 1937 - 1940 (1994).

Seidel, B., Stanarius, A., Wolf, G. Differential expression of neuronal and endothelial nitric oxide synthase in blood vessels of the rat brain. *Neurosci. Lett.* **239**; 109 – 112 (1997).

Selig, D.K., Segal, M.R., Liao, D., Malenka, R.C., Malinow, R., Nicoll, R.A., Lisman, J.E. Examination of the role of cGMP in long-term potentiation in the CA1 region of the hippocampus. *Learn. Mem.* **3**; 42 – 48 (1996).

Senter, P.D., Eckstein, F., Mulsch, A., Bohme, E. The stereochemical course of the reaction catalyzed by soluble bovine lung guanylate cyclase. *J. Biol. Chem.* **258**; 6741 – 6745 (1983).

Seress, L., Abraham, H., Lin, H., Totterdell, S. Nitric oxide-containing pyramidal neurons of the subiculum innervate the CA1 area. *Exp. Brain Res.* **147**; 38 – 44 (2002).

Shakur, Y., Takeda, K., Kenan, Y., Yu, Z.X., Rena, G., Brandt, D., Houslay, M.D., Degerman, E., Ferrans, V.J., Manganiello, V.C. Membrane localization of cyclic nucleotide phosphodiesterase 3 (PDE3). Two N-terminal domains are required for the efficient targeting to, and association of, PDE3 with endoplasmic reticulum. *J. Biol. Chem.* **275**; 38749 – 38761 (2000).

Sharma, V.S., Magde, D. Activation of soluble guanylate cyclase by carbon monoxide and nitric oxide: a mechanistic model. *Methods* **19**; 494 – 505 (1999).

Sharma, R.K., Wang, J.H. Calmodulin and Ca^{2+}-dependent phosphorylation and dephosphorylation and dephosphorylation of 63 kDa subunit-containing bovine brain calmodulin-stimulated cyclic nucleotide phosphodiesterase isoenzyme. J. Biol. Chem. 261; 1322 – 1328 (1986).

Shen, W., Zhang, X., Zhao, G., Wolin, M.S., Sessa, W., Hintze, T.H. Nitric oxide production and NO synthase gene expression contribute to vascular regulation during exercise. *Med. Sci. Sports Exerc.* **27**; 1125 - 1134 (1995).

Shibata, S., Kodama, K., Tominaga, K., Tanaka, T., Watanabe, S. Effect of muscarinic cholinergic drugs on ischemia-induced decreases in glucose uptake and CA1 field potentials in rat hippocampus slices. *Eur. J. Pharmacol.* **221**; 113 - 119 (1992).

Shibuki, K., Okada, D. Endogenous nitric oxide release required for long-term synaptic depression in the cerebellum. *Nature* **349**; 326 – 328 (1991).

Shinoura, H., Tsujimoto, G., Teranishi, Y., Tsuru, H. Antagonistic effects of antimuscarinic drugs on alpha 1-adrenoceptors. *Naunyn Schmiedebergs Arch. Pharmacol.* **366**; 368 - 371 (2002).

Shukula, A., Dikshit, M., Srimal, R.C. Nitric oxide-dependent blood-brain barrier permeability alteration in the rat brain. *Experientia* **52**; 136 – 140 (1996).

Siddhanta, U., Presta, A., Fan, B., Wolan, D., Rousseau, D.L., Stuehr, D.J. Domain swapping in inducible nitric-oxide synthase. Electron transfer occurs between flavin and heme groups located on adjacent subunits in the dimer. *J. Biol. Chem.* **273**; 18950 - 18958 (1998).

Silvagno, F., Xia, H., Bredt, D.S. Neuronal nitric oxide synthase-mu, an alternatively spliced isoform expressed in differentiated skeletal muscle. *J. Biol. Chem.* **271**; 11204 – 11208 (1996).

Simoncini, T., Genazzani, A.R. Raloxifene acutely stimulates nitric oxide release from human endothelial cells via an activation of endothelial nitric oxide synthase. *The journal of clinical endocrinology & metabolism* **85**; 2966 – 2969 (2000).

Simoncini, T., Genazzani, A.R., Liao, J.K. Nongenomic mechanisms of endothelial nitric oxide synthase activation by the selective estrogen receptor modulator raloxifene. *Circulation* **105**; 1368 - 1373 (2002a).

Simoncini, T., Varone, G., Fornari, L., Mannella, P., Luisi, M., Labrie, F., Genazzani, A.R. Genomic and nongenomic mechanisms of nitric oxide synthesis induction in human endothelial cells by a fourth-generation selective estrogen receptor modulator. *Endocrinology* **143**; 2052 – 2061 (2002b).

Smith, S.L., Otis, T.S. Persistent changes in spontaneous firing of Purkinje neurons triggered by the nitric oxide signaling cascade. *J. Neurosci.* **23**; 367 - 372 (2003).

Soderling, S.H., Bayuga, S.J., Beavo, J.A. Identification and characterization of a novel family of cyclic nucleotide phosphodiesterases. *J. Biol. Chem.* **273**; 15553 – 15558 (1998a).

Soderling, S.H., Bayuga, S.J., Beavo, J.A. Cloning and characterization of a cAMP-specific cyclic nucleotide phosphodiesterase. *Proc. Natl. Acad. Sci. U.S.A.* **95**; 8991 – 8996 (1998b).

Soderling, S.H., Bayuga, S.J., Beavo, J.A. Isolation and characterization of a dual-substrate phosphodiesterase gene family: PDE10A. *Proc. Natl. Acad. Sci. U.S.A.* **96**; 7071 – 7076 (1999).

Soderling, S.H., Beavo, J.A. Regulation of cAMP and cGMP signaling: new phosphodiesterases and new functions. *Curr. Opin. Cell. Biol.* **12**; 174 – 179 (2000).

Soong, T.W., Stea, A., Hodson, C.D., Dubel, S.J., Vincent, S.R., Snutch, T.P. Structure and functional expression of a member of the low voltage-activated calcium channel family. *Science* **260**; 1133 – 1136 (1993).

Son, H., Hawkins, R.D., Martin, K., Kiebler, M., Huang, P.L., Fishman, M.C., Kandel, E.R. Long-term potentiation is reduced in mice that are doubly mutant in endothelial and neuronal nitric oxide synthase. *Cell* **87**; 1015 – 1023 (1996).

Song, T., Hatano, N., Horii, M., Tokumitsu, H., Yamaguchi, F., Tokuda, M., Watanabe, Y. Calcium/calmodulin-dependent protein kinase I inhibits neuronal nitric-oxide synthase activity through serine 741 phosphorylation. *FEBS Lett.* **570**; 133 – 137 (2004).

Southam, E., Garthwaite, J. The nitric oxide-cyclic GMP signalling pathway in rat brain. *Neuropharmacology* **32**; 1267 - 1277 (1993).

Specht, C.G., Schoepfer, R. Deletion of the alpha-synuclein locus in a subpopulation of C57BL/6J inbred mice. *B.M.C. Neurosci.* **2**; 11 (2001).

Stamler, J.S., Lamas, S., Fang, F.C. Nitrosylation: The prototypic redox-based signalling mechanism. *Cell* **106**; 675 - 683 (2001).

Stanarius, A., Topel, I., Schulz, S., Noack, H., Wolf, G. Immunocytochemistry of endothelial nitric oxide synthase in the rat brain: a light and electron microscopical study using the tyramide signal amplification technique. *Acta Histochem.* **99**; 411 – 429 (1997).

Stasch, J-P., Becker, E.M., Alonso-Alija, C., Apeler, H., Dembowsky, K., Feurer, A., Gerzer, R., Minuth, T., Perzborn, E., Pleiβ, U., Schröder, H., Schroeder, W., Stahl, E., Steinke, W., Straub, A., Schramm, M. NO-independent regulatory site on soluble guanylate cyclase. *Nature* **410**; 212 –215 (2001).

Steigerwald, F., Schulz, T.W., Schenker, L.T., Kennedy, M.B., Seeburg, P.H., Köhr, G. C-Terminal truncation of NR2A subunits impairs synaptic but not extra synaptic localization of NMDA receptors. *J. Neurosci.* **20**; 4573 - 4581 (2000).

Steinbach, K., Volkmer, H., Schlosshauer, B. Semaphorin 3E/collapsin-5 inhibits growing retinal axons. *Exp. Cell. Res.* **279**; 52 - 61 (2002).

Steiner, A.A., Carnio, E.C., Antunes-Rodrigues, J., Branco, L.G. Role of nitric oxide in systemic vasopressin-induced hypothermia. *Am. J. Physiol.* **275**; R937 - R941 (1998).

Stern, J.E., Li, Y., Zhang, W. Nitric oxide: a local signalling molecule controlling the activity of pre-autonomic neurones in the paraventricular nucleus of the hypothalamus. *Acta Physiol. Scand.* **177**; 37 - 42 (2003).

Stevens, C.F., Tonegawa, S., Wang, Y. The role of calcium-calmodulin kinase II in three forms of synaptic plasticity. *Curr. Biol.* **4**; 687 - 693 (1994).

Stevens-Truss, R., Marletta, M.A., Interaction of calmodulin with the inducible murine macrophage nitric oxide synthase. *Biochem.* **34**; 15638 – 15645 (1995).

Stone, J.R., Marletta, M.A. Soluble guanylate cyclase from bovine lung: activation with nitric oxide and carbon monoxide and spectral characterization of the ferrous and ferric states. *Biochemistry* **33**; 5636 - 5640 (1994).

Straub, A., Stasch, J-P., Alonso-Alija, C., Benet-Buchholz, J., Ducke, B., Feurer, A., Fürstner, C. NO-independent stimulators of soluble guanylate cyclase. *Bioorganic & Medicinal Chemistry letters* **11**; 781 – 784 (2001).

Stuehr, D.J., Marletta, M.A. Mammalian nitrate biosynthesis: mouse macrophages produce nitrite and nitrate in response to Escherichia coli lipopolysaccharide. *Proc. Natl. Acad. Sci. U.S.A.* **82**; 7738 - 7742 (1985).

Stuehr, D.J., Nathan, C.F. Nitric oxide. A macrophage product responsible for cytostasis and respiratory inhibition in tumor target cells. *J. Exp. Med.* **169**; 1543 - 1555 (1989).

Stuehr, D.J. Structure-function aspects in the nitric oxide synthases. *Annu. Rev. Pharmacol. Toxicol.* **37**; 339 - 359 (1997).

Sunahara, R.K., Beuve, A., Tesmer, J.J., Sprang, S.R., Garbers, D.L., Gilman, A.G. Exchange of substrate and inhibitor specificities between adenylyl and guanylyl cyclases. *J. Biol. Chem.* **273**; 16332 - 16338 (1998).

Sutherland, E.W., Rall, T.W. The properties of an adenosine ribonucleotide produced with cellular particles, ATP, Mg^{++} and epinephrine or glucagon. *J. Am. Chem. Soc.* **79**; 3608 (1957).

Sutherland, E.W., Rall, T.W. Fractionation and characterization of a cyclic adenine ribonucleotide formed by tissue particles. *J. Biol. Chem.* **232**; 1077 - 1091 (1958).

Suvarna, N.U., O'Donnell, J.M. Hydrolysis of N-methyl-D-aspartate receptor-stimulated cAMP and cGMP by PDE4 and PDE2 phosphodiesterases in primary neuronal cultures of rat cerebral cortex and hippocampus. *J. Pharmacol. Exp. Ther.* **302**; 249 - 256 (2002).

Takahashi, K., Akaike, N. Nicergoline inhibits T-type Ca^{2+} channels in rat isolated hippocampal CA1 pyramidal neurones. *Br. J. Pharmacol.* **100**; 705 - 710 (1990).

Takahashi, M., Ikeda, U., Masuyama, J., Funayama, H., Kano, S., Shimada, K. Nitric oxide attenuates adhesion molecule expression in human endothelial cells. *Cytokine* **8**; 817 – 821 (1996).

Talley, E.M., Cribbs, L.L., Lee, J.H., Daud, A., Perez-Reyes, E., Bayliss, D.A. Differential distribution of three members of a gene family encoding low voltage-activated (T-type) calcium channels. *J. Neurosci.* **19**; 1895 – 1911 (1999).

Tanaka, T., Saito, H., Matsuki, N. Endogenous nitric oxide inhibits NMDA- and kainate- responses by a negative feedback system in rat hippocampal neurons. *Brain Res.* **631**; 72 - 76 (1993).

Thomas, M.K., Francis, S.H., Corbin, J.D. Substrate- and kinase-directed regulation of phosphorylation of a cGMP-binding phosphodiesterase by cGMP. *J. Biol. Chem.* **265**; 14971 - 14978 (1990).

Toni, N., Buchs, P.A., Nikonenko, I., Bron, C.R., Muller, D. LTP promotes formation of multiple spine synapses between a single axon terminal and a dendrite. *Nature* **402**; 421 - 425 (1999).

Töpel, I., Stanarius, A., Wolf, G. Distribution of the endothelial constitutive nitric oxide synthase in the developing rat brain: an immunohistochemical study. *Brain Res.* **788**; 43 – 48 (1998).

Tottene, A., Moretti, A., Pietrobon, D. Functional diversity of P-type and R-type calcium channels in rat cerebellar neurons. *J. Neurosci.* **16**; 6353 - 6363 (1996).

Trimmer, B.A., Aprille, J.R., Dudzinski, D.M., Lagace, C.J., Lewis, S.M., Michel, T., Qazi, S., Zayas, R.M. Nitric oxide and the control of firefly flashing. *Science* **292**; 2486 – 2488 (2001).

Tsikas, D., Denker, K., Frolich, J.C. Artifactual-free analysis of *S*-nitrosoglutathione and *S*-nitroglutathione by neutral-pH, anion-pairing, high-performance liquid chromatography. Study on peroxynitrite-mediated *S*-nitration of glutathione under physiological conditions. *J. Chromatogr. A* **916**; 107 – 116 (2001).

Tsou, K., Snyder, G.L., Greengard, P. Nitric oxide/cGMP pathway stimulates phosphorylation of DARPP-32, a dopamine- and cAMP-regulated phosphoprotein, in the substantia nigra. *Proc. Natl. Acad. Sci. U.S.A.* **90**; 3462 - 3465 (1993).

Tucker, C.L., Hurley, J.H., Miller, T.R., Hurley, J.B. Two amino acid substitutions convert a guanylyl cyclase, RetGC-1, into an adenylyl cyclase. *Proc. Natl. Acad. Sci. U.S.A.* **95**; 5993 - 5997 (1998).

Tuladhar, B.R., Costall, B., Naylor, R.J. Pharmacological characterization of the 5-hydroxytryptamine receptor mediating relaxation in the rat isolated ileum. *Br. J. Pharmacol.* **119**; 303 - 310 (1996).

Turko, I.V., Francis, S.H., Corbin, J.D. Binding of cGMP to both allosteric sites of cGMP-binding cGMP-specific phosphodiesterase (PDE5) is required for its phosphorylation. *Biochem. J.* **329**; 505 - 510 (1998).

Turko, I.V., Ballard, S.A., Francis, S.H., Corbin, J.D. Inhibition of cyclic GMP-specific phosphodiesterase (Type 5) by sildenafil and related compounds. *Mol. Pharmacol.* **56**; 124 – 130 (1999).

Tyrell, R.M.. Keyse, S.M. New trends in photobiology. The interaction of UVA radiation with cultured cells. *J. Photochem. Photobiol. B* **4**; 349 – 361 (1990).

Ulens, C., Tytgat, J. Functional heteromerization of HCN1 and HCN2 pacemaker channels. *J. Biol. Chem.* **276**; 6069 – 6072 (2001).

Umans, J.G., Levi, R. Nitric oxide in the regulation of blood flow and arterial pressure. *Annu. Rev. Physiol.* **57**; 771 – 790 (1995).

Vaandrager, A.B., Smolenski, A., Tilly, B.C., Houtsmuller, A.B., Ehlert, E.M., Bot, A.G., Edixhoven, M., Boomaars, W.E., Lohmann, S.M., de Jonge, H.R. Membrane targeting of cGMP-dependent protein kinase is required for cystic fibrosis transmembrane conductance regulator Cl^- channel activation. *Proc. Natl. Acad. Sci. U.S.A.* **95**; 1466 – 1471 (1998).

Vaandrager, A.B., Bot, A.G., Ruth, P., Pfeifer, A., Hofmann, F., De Jonge, H.R. Differential role of cyclic GMP-dependent protein kinase II in ion transport in murine small intestine and colon. *Gastroenterology* **118**; 108 – 114 (2000).

Valentino, R.J., Dingledine, R. Presynaptic inhibitory effect of acetylcholine in the hippocampus. *J. Neurosci.* **1**; 784 - 792 (1981).

Valtschanoff, J.G., Weinberg, R.J., Kharazia, V.N., Nakane, M., Schmidt, H.H. Neurons in rat hippocampus that synthesise nitric oxide. *J. Comp. Neurol.* **331**; 111 – 121 (1993).

Valtschanoff, J.G., Weinberg, R.J. Laminar organisation of the NMDA receptor complex with the postsynaptic density. *J. Neurosci.* **21**; 1211 – 1217 (2001).

Van der Lee, R., Pfaffendorf, M., De Mey, J.G., van Zwieten, P.A. Inhibitory effect of mibefradil on contractions induced by sympathetic neurotransmitter release in the rat tail artery. *Naunyn Schmiedebergs Arch. Pharmacol.* **361**; 74 - 79 (2000).

Van Staveren, W.C., Markerink-van Ittersum, M., Steinbusch, H.W., de Vente, J. The effects of phosphodiesterase inhibition on cyclic GMP and cyclic AMP accumulation in the hippocampus of the rat. *Brain Res.* **888**; 275 - 286 (2001).

Van Staveren, W.C., Steinbusch, H.W., Markerink-van Ittersum, M., Behrends, S., de Vente J. Species differences in the localization of cGMP-producing and NO-responsive elements in the mouse and rat hippocampus using cGMP immunocytochemistry. *Eur. J. Neurosci.* **19**; 2155 - 2168 (2004).

Venema, R.C., Sayegh, H.S., Kent, J.D., Harrison, D.G. Identification, characterization, and comparison of the calmodulin-binding domains of the endothelial and inducible nitric oxide synthases. *J. Biol. Chem.* **271**; 6435 - 6440. (1996).

Venema, R.C., Ju, H., Zou, R., Ryan, J.W., Venema, V.J. Subunit interactions of endothelial nitric oxide synthase. *J. Biol. Chem.* **272**; 1276 – 1282 (1997).

De Vente, J., Steinbusch, H.W. On the stimulation of soluble and particulate guanylate cyclase in the rat brain and the involvement of nitric oxide as studied by cGMP immunocytochemistry. *Acta Histochem.* **92**; 13 – 38 (1992).

De Vente, J., Hopkins, D.A., Markerink-Van Ittersum, M., Emson, P.C., Schmidt, H.H., Steinbusch, H.W. Distribution of nitric oxide synthase and nitric oxide-receptive, cyclic GMP-producing structures in the rat brain. *Neuroscience* **87**; 207 - 241 (1998).

De Vente, J., Asan, E., Gambaryan, S., Markerink-van Ittersum, M., Axer, H., Gallatz, K., Lohmann, S.M., Palkovits, M. Localization of cGMP-dependent protein kinase type II in rat brain. *Neuroscience* **108**; 27 - 49 (2001).

Vigne, P., Lund, L., Frelin, C. Cross talk among cyclic AMP, cyclic GMP, and Ca^{2+}-dependent intracellular signalling mechanisms in brain capillary endothelial cells. *J. Neurochem.* **62**; 2269 – 2274 (1994).

Vinet, R., Vargas, F.F. L- and T-type voltage-gated Ca^{2+} currents in adrenal medulla endothelial cells. *Am. J. Physiol.* **276**; H1313 - 1322 (1999).

Vlahos, C.J., Matter, W.F., Hui, K.Y., Brown, R.F. A specific inhibitor of phosphatidylinositol 3-kinase, 2-(4-morpholinyl)-8-phenyl-4H-1-benzopyran-4-one (LY294002). *J. Biol. Chem.* **269**; 5241 - 5248 (1994).

Wagner, D.A., Young, V.R., Tannenbaum, S.R., Schultz, D.S, Deen W.M. Mammalian nitrate biochemistry: metabolism and endogenous synthesis. *I.A.R.C. Sci. Publ.* **57**; 247 – 253 (1984).

Wagner, C., Pfeifer, A., Ruth, P., Hofmann, F., Kurtz, A. Role of cGMP-kinase II in the control of renin secretion and renin expression. *J. Clin. Invest.* **102**; 1576 – 1582 (1998).

Wall, M.J. Endogenous nitric oxide modulates GABAergic transmission to granule cells in adult rat cerebellum. *Eur. J. Neurosci.* **18**; 869 - 878 (2003a).

Wall, M.E., Francis, S.H., Corbin, J.D., Grimes, K., Richie-Jannetta, R., Kotera, J., Macdonald, B.A., Gibson, R.R., Trewhella, J. Mechanisms associated with cGMP binding and activation of cGMP-dependent protein kinase. *Proc. Natl. Acad. Sci. U.S.A.* **100**; 2380 – 2385 (2003b).

Wang, Y., Goligorsky, M.S., Lin, M., Wilcox, J.N., Marsden, P.A. A novel, testis-specific mRNA transcript encoding an NH2-terminal truncated nitric oxide synthase. *J. Biol. Chem.* **272**; 11392 – 11401 (1997).

Wang, H.G., Lu, F.M., Jin, I., Udo, H., Kandel, E.R., de Vente, J., Walter, U., Lohmann, S.M., Hawkins, R.D., Antonova, I. Presynaptic and postsynaptic roles of NO, cGK, and RhoA in long-lasting potentiation and aggregation of synaptic proteins. *Neuron* **45**; 389 – 403 (2005).

Wassmann, S., Laufs, U., Stamenkovic, D., Linz, W., Stasch, J.P., Ahlbory, K., Rosen, R., Bohm, M., Nickenig, G. Raloxifene improves endothelial dysfunction in hypertension by reduced oxidative stress and enhanced nitric oxide production. *Circulation* **105**; 2083 - 2091 (2002).

Watkins, J.C. L-glutamate as a central neurotransmitter: looking back. *Biochem. Soc. Trans.* **28**; 297 – 309 (2000).

Wedel, B., Humbert, P., Harteneck, C., Foerster, J., Malkewitz, J., Bohme, E., Schultz, G., Koesling, D. Mutation of His-105 in the beta 1 subunit yields a nitric oxide-insensitive form of soluble guanylyl cyclase. *Proc .Natl. Acad. Sci. U.S.A.* **91**; 2592 - 2596 (1994).

Wedel, B., Harteneck, C., Foerster, J., Friebe, A., Schultz, G., Koesling, D. Functional domains of soluble guanylyl cyclase. *J. Biol. Chem.* **270**; 24871 - 24875 (1995).

Weitz, D., Zoche, M., Muller, F., Beyermann, M., Korschen, H.G., Kaupp, U.B., Koch, K.W. Calmodulin controls the rod photoreceptor CNG channel through an unconventional binding site in the N-terminus of the beta-subunit. *EMBO J.* **17**; 2273 – 2284 (1998).

Wendland, B., Schweizer, F.E., Ryan, T.A., Nakane, M., Murad, F., Scheller, R.H., Tsein, R.W. Existence of nitric oxide synthase in rat hippocampal pyramidial cells. *Proc. Natl. Acad. Sci. USA* **91**; 2151 – 2155 (1994).

Westenbroek, R.E., Hell, J.W., Warner, C., Dubel, S.J., Snutch, T.P., Catterall, W.A. Biochemical properties and subcellular distribution of an N-type calcium channel alpha 1 subunit. *Neuron* **9**; 1099 – 1115 (1992).

Westenbroek, R.E., Sakurai, T., Elliott, E.M., Hell, J.W., Starr, T.V., Snutch, T.P., Catterall, W.A. Immunochemical identification and subcellular distribution of the alpha 1A subunits of brain calcium channels. *J. Neurosci.* **15**; 6403 - 6418 (1995).

Wheeler, D.B., Randall, A., Tsien, R.W. Roles of N-type and Q-type Ca2+ channels in supporting hippocampal synaptic transmission. *Science* **264**; 107 - 111 (1994).

White, A.A., Aurbach, G.D. Detection of guanyl cyclase in mammalian tissues. *Biochim. Biophys. Acta.* **191**; 686 – 697 (1969).

White, R.E. Cyclic GMP and ion channel regulation. *Adv. Second Messenger Phosphoprotein Res.* **33**; 251 – 277 (1999).

Williams, J.H., Errington, M.L., Lynch, M.A., Bliss, T.V.P. Arachidonic acid induces a long-term activity-dependent enhancement of synaptic transmission in the hippocampus. *Nature* **341**; 739 - 742 (1989).

Williams, J.H., Li, Y-G., Nayak, A., Errington, M.L., Murphy, K.P.S.J., Bliss, T.V.P. The suppression of long-term potentiation in rat hippocampus by inhibitors of nitric oxide synthase is temperature- and age-dependent. *Neuron* **11**; 877 – 884 (1993a).

Williams, J.H., Errington, M.L., Li, Y-G., Lynch, M.A., Bliss, T.V.P. The search for retrograde messengers in LTP. *Seminars in the Neurosciences* **5**; 149 – 158 (1993b).

Wilson, R.I., Yanovsky, J., Godecke, A., Stevens, D.R., Schrader, J., Haas, H.L. Endothelial nitric oxide synthase and LTP. *Nature* **386**; 338 (1997).

Wilson, R.I., Godecke, A., Brown, R.E., Schrader, J., Haas, H.L. Mice deficient in endothelial nitric oxide synthase exhibit a selective deficit in hippocampal long-term potentiation. *Neurosci.* **90**; 1157 – 1165 (1999).

Wingrove, J.A., O'Farrell, P.H. Nitric oxide contributes to behavioral, cellular, and developmental responses to low oxygen in Drosophila. *Cell* **98**; 105 - 114 (1999).

Wissenbach, U., Bodding, M., Freichel, M., Flockerzi, V. Trp12, a novel Trp related protein from kidney. *FEBS Lett.* **485**; 127 – 134 (2000).

Wolf, G. Nitric oxide and nitric oxide synthase: biology, pathology, localisation. *Histol. Histopathol.* **12**; 251 – 261 (1997).

Wolff, D.J., Lubeskie, A., Gauld, D.S., Neulander, M.J. Inactivation of nitric oxide synthases and cellular nitric oxide formation by N6-iminoethyl-L-lysine and N5-iminoethyl-L-ornithine. *Eur. J. Pharmacol.* **350**; 325 – 334 (1998).

Wood, J., Garthwaite, J. Models of the diffusional spread of nitric oxide: implications for neural nitric oxide signalling and its pharmacological properties. *Neuropharmacology* **33**; 1235 - 1244 (1994).

Wu, L.G., Saggau, P. Adenosine inhibits evoked synaptic transmission primarily by reducing presynaptic calcium influx in area CA1 of hippocampus. *Neuron* **12**; 1139 – 1148 (1994).

Wu, C.C., Ko, F.N., Kuo, S.C., Lee, F.Y., Teng, C.M. YC-1 inhibited human platelet aggregation through NO-independent activation of soluble guanylate cyclase. *Br. J. Pharmacol.* **116**; 1973 – 1978 (1995).

Wu, C.C., Ko, F.N., Teng, C.M. Inhibition of platelet adhesion to collagen by cGMP-elevating agents. *Biochem. Biophys. Res. Commun.* **231**; 412 – 416 (1997).

Wu, H.H., Cork, R.J., Huang, P.L., Shuman, D.L., Mize, R.R. Refinement of the ipsilateral retinocollicular projection is disrupted in double endothelial and neuronal nitric oxide synthase gene knockout mice. *Brain Res. Dev. Brain Res.* **120**; 105 - 111 (2000).

Wu, H.H., Selski, D.J., El-Fakahany, E.E., McLoon, S.C. The role of nitric oxide in development of topographic precision in the retinotectal projection of chick. *J. Neurosci.* **21**; 4318 - 4325 (2001).

Yamada, K.A., Dubinsky, J.M., Rothman, S.M. Quantitative physiological characterization of a quinoxalinedione non-NMDA receptor antagonist. *J. Neurosci.* **9**; 3230 - 3236 (1989).

Yamada, K., Noda, Y., Nakayama, S., Komori, Y., Sugihara, H., Hasegawa, T., Nabeshima, T. Role of nitric oxide in learning and memory and in monoamine metabolism in the rat brain. *Br. J. Pharmacol.* **115**; 852 - 858 (1995).

Yamazaki, M., Chiba, K., Mohri, T., Hatanaka, H. Activation of the mitogen-activated protein kinase cascade through nitric oxide synthesis as a mechanism of neuritogenic effect of genipin in PC12h cells. *J. Neurochem.* 79; 45 - 54 (2001).

Yeoman, M.S., Parish, D.C., Benjamin, P.R. A cholinergic modulatory interneuron in the feeding system of the snail, Lymnaea. *J. Neurophysiol.* **70**; 37 - 50 (1993).

Young, R.J., Beams, R.M., Carter, K., Clark, H.A., Coe, D.M., Chambers, C.L., Davies, P.I., Dawson, J., Drysdale, M.J., Franzman, K.W., French, C., Hodgson, S.T., Hodson, H.F., Kleanthous, S., Rider, P., Sanders, D., Sawyer, D.A., Scott, K.J., Shearer, B.G., Stocker, R., Smith, S., Tackley, M.C., Knowles, R.G. Inhibition of inducible nitric oxide synthase by acetamidine derivatives of hetero-substituted lysine and homolysine. *Bioorg. Med. Chem. Lett.* **10**; 597 – 600 (2000).

Yuen, P.S., Potter, L.R., Garbers, D.L. A new form of guanylyl cyclase is preferentially expressed in rat kidney. *Biochemistry* **29**; 10872 - 10878 (1990).

Zabel, U., Weeger, M., La, M., Schmidt, H.H. Human soluble guanylate cyclase: functional expression and revised isoenzyme family. *Biochem. J.* **335**; 51 - 57 (1998).

Zagotta, W.N., Siegelbaum, S.A. Structure and function of cyclic nucleotide-gated channels. *Annu. Rev. Neurosci.* **19**; 235 – 263 (1996).

Zagotta, W.N., Olivier, N.B., Black, K.D., Young, E.C., Olson, R., Gouaux, E. Structural basis for modulation and agonist specificity of HCN pacemaker channels. *Nature* **425**; 200 – 205 (2003).

Zamponi, G.W., Bourinet, E., Snutch, T.P. Nickel block of a family of neuronal calcium channels: subtype- and subunit-dependent action at multiple sites. *J. Membr. Biol.* **151**; 77 – 90 (1996).

Zhang, H.Q., Fast, W., Marletta, M.A., Martasek, P., Silverman, R.B. Potent and selective inhibition of neuronal nitric oxide synthase by N-omega-propyl-L-arginine. *J. Med. Chem.* **40**; 3869 – 3870 (1997).

Zhao, Y., Marletta, M.A. Localization of the heme binding region in soluble guanylate cyclase. *Biochemistry* **36**; 15959 - 15964 (1997).

Zhao, Y., Schelvis, J.P., Babcock, G.T., Marletta, M.A. Identification of histidine 105 in the beta1 subunit of soluble guanylate cyclase as the heme proximal ligand. *Biochemistry* **37**; 4502 – 4509 (1998a).

Zhao, Y., Hoganson, C., Babcock, G.T., Marletta, M.A. Structural changes in the heme proximal pocket induced by nitric oxide binding to soluble guanylate cyclase. *Biochemistry* **37**; 12458 - 12464 (1998b).

Zhao, Y., Brandish, P.E., Ballou, D.P., Marletta, M.A. A molecular basis for nitric oxide sensing by soluble guanylate cyclase. *Proc. Natl. Acad. Sci. U.S.A.* **96**; 14753 – 14758 (1999).

Zhao, Y., Brandish, P.E., DiValentin, M., Schelvis, J.P., Babcock, G.T., Marletta, M.A. Inhibition of soluble guanylate cyclase by ODQ. *Biochemistry* **39**; 10848 - 10854 (2000).

Zhong H., Molday, L.L., Molday, R.S., Yau, K.W. The heteromeric cyclic nucleotide-gated channel adopts a 3A:1B stoichiometry. *Nature* **420**; 193 – 198 (2002).

Zhuo, M., Small, S.A., Kandel, E.R., Hawkins, R.D. Nitric oxide and carbon monoxide produce activity-dependent long-term synaptic enhancement in hippocampus. *Science* **260**; 1946 - 1950 (1993).

Zhuo, M., Hu, Y., Schultz, C., Kandel, E.R., Hawkins, R.D. Role of guanylyl cyclase and cGMP-dependent protein kinase in long-term potentiation. *Nature* **368**; 635 - 639 (1994).

Zhuo, M., Laitinen, J.T., Li, X.C., Hawkins, R.D. On the respective roles of nitric oxide and carbon monoxide in long-term potentiation in the hippocampus. *Learn. Mem.* **6**; 63 – 76 (1999).

Zucker, R.S. Calcium- and activity-dependent synaptic plasticity. *Curr. Opin. Neurobiol.* **9**; 305 – 313 (1999).

Zufall, F., Firestein, S., Shepherd GM. Cyclic nucleotide-gated ion channels and sensory transduction in olfactory receptor neurons. *Annu. Rev. Biophys. Biomol. Struct.* **23**; 577 – 607 (1994).

Zufall, F., Shepherd, G.M., Barnstable, C.J. Cyclic nucleotide gated channels as regulators of CNS development and plasticity. *Curr. Opin. Neurobiol.* **7**; 404 – 412 (1997).

Zweifach, A., Lewis, R.S. Mitogen-regulated Ca^{2+} current of T lymphocytes is activated by depletion of intracellular Ca^{2+} stores. *Proc. Natl. Acad. Sci. U.S.A.* **90**; 6295 - 6299 (1993).

Zweifach, A., Lewis, R.S. Calcium-dependent potentiation of store-operated calcium channels in T lymphocytes. *J. Gen. Physiol.* **107**; 597 - 610 (1996).

Appendix:

Publications

Hopper, R., Garthwaite, J. Does nitric oxide regulate the NMDA receptor? *J. Physiol. (Lond)* **547P**; C35 (2003).

Wolfson Institute for Biomedical Research, University College London, Gower Street, London, WC1E 6BT, UK

Nitric oxide (NO) functions as a messenger throughout the central nervous system, where many of its actions are exerted through guanylyl cyclase activation, leading to cGMP formation. A putative alternative transduction pathway is the modification of protein function by nitrosation of thiol groups (Ahern *et al.*, 2002). A prototypic protein considered to be regulated in this way is the NMDA receptor but, despite extensive research, there is little direct evidence that NO performs this function. To address this issue, we have investigated the effect of NO on native or cloned NMDA receptors (NMDARs) in hippocampal slices and HEK-293 cells respectively.

Field EPSPs were recorded from the CA1 stratum radiatum of hippocampal slices obtained from 6- to 8-week-old rats killed humanely according to Home Office regulations (Bon and Garthwaite, 2001). EPSPs mediated through NMDARs were isolated pharmacologically. The responses were not significantly changed by bath application of the NO synthase substrate, L-arginine (100 μM), nor by inhibition of NO synthase using L-nitroarginine (100 μM). Diethylamine NO adduct (DEA/NO) was used to supply NO exogenously. Whilst DEA/NO at a concentration of 10 μM caused maximal cGMP accumulation in hippocampal slices, concentrations up to 30-fold higher produced no detectable change in the NMDAR-mediated synaptic responses. However, in accordance with a previous study (Murphy *et al.*, 1994), photolysis of a caged NO derivative using a flash of UV light depressed NMDAR-mediated EPSPs by 94 ± 3 % (mean ± S.E.M; n = 4).

As a further test, whole-cell membrane currents in response to 100 ms pulses of 100 μM glutamate were recorded at –60 mV from HEK-293 cells transfected with NMDAR subunits NR1 and NR2A (Köhr and Seeburg, 1996). Similar to findings in the slices, photolysis of the caged compound by UV light depressed the NMDAR currents by 55 ± 3 % (n = 5), whereas 100 μM DEA/NO had no significant effect on the NMDAR current alone, but depressed the NMDAR currents by 35 ± 7 % (n = 4) when in combination with UV light. Perfusion of 100 nM DEA/NO had no effect on NMDAR function.

The results suggest that NO released endogenously, or exogenous NO in concentrations well in excess of those needed to activate guanylyl cyclase, does not modify NMDAR function. It is possible that other factors, such as UV light, may have contributed to the inhibition of NMDAR responses observed previously (Murphy *et al.*, 1994).

Ahern, G.P., Kylachko, V.A., Jackson, M.B. (2002) *Trends Neurosci.* **25**: 510-517.
Bon, C.L.M., Garthwaite, J. (2001). *Eur. J. Neurosci.* **14**; 585-594.
Köhr, G., Seeburg, P.H. (1996). *J. Physiol.* **492**, 445-452.
Murphy, K.P.S.J., Williams, J.H., Bettache, N., Bliss, T.V.P. (1994). *Neuropharmacol.* **33**, 1375-1385.

Supported by a BBSRC CASE studentship with Merck Sharp and Dohme (Harlow, UK) and The Wellcome Trust. We thank Dr. B. Lancaster for expert advice.

European Journal of Neuroscience, Vol. 19, pp. 1675–1682, 2004

On the regulation of NMDA receptors by nitric oxide

Rachel Hopper, Barrie Lancaster and John Garthwaite

doi:10.1111/j.1460-9568.2004.03306.x

Materials and methods

Tissue preparation

Hippocampal slices were prepared from 6 to 8-week-old male Sprague–Dawley rats. The animals were killed by stunning followed by cervical dislocation and decapitation. The brain was rapidly removed and the hippocampus dissected out and placed in cold (0–4 °C) artificial cerebrospinal fluid (ACSF) of the following composition (in mM): NaCl 124, KCl 3, NaH_2PO_4 1.25, $MgSO_4$ 1, $NaHCO_3$ 26, $CaCl_2$ 2, D-glucose 10, equilibrated with 95% O_2 and 5% CO_2. Transverse slices (400 μm thick) were cut and maintained in an interface holding chamber containing ACSF at room temperature.

Electrophysiological recording from hippocampal slices

Extracellular recordings of field excitatory postsynaptic potentials (fEPSPs) were made at room temperature (22–24 °C) from the stratum radiatum of the CA1 area following electrical stimulation (baseline frequency = 0.033 Hz) of the Schaffer collateral-commissural pathway. NMDA receptor-mediated responses were isolated pharmacologically using nominally Mg^{2+}-free ACSF containing 10 μM 6-cyano-7-nitroquinoxaline-2,3-dione (CNQX) to block AMPA receptors. D(−)-2-amino-5-phosphonopentanoate (D-AP5) was added to confirm that the responses were NMDA receptor-mediated. AMPA receptor-mediated responses were obtained in normal ACSF. Photolysis of caged NO (potassium pentachloronitrosylruthenate, $K_2Ru(NO)Cl_5$; Alfa Aesar, Karlsruhe, Germany) was performed using the 1 ms discharge from a xenon arc bulb (Zeiss) transmitted through a fibre optic, and filtered with a UG11 filter (270–370 nm). Stock solutions of the NONOate NO donor, diethylamine/NO adduct (DEA/NO) were made up in 10 mM NaOH and diluted at least 1 : 100 into the ACSF solution. Separate slices were used for each DEA/NO concentration tested. Slope measurements were made during the initial linear phase of each evoked potential (20–50% of the peak) and the values were normalized relative to the mean values obtained within the first 10 or 15 min of recording in the absence of any treatment.

Whole-cell current-clamp recordings were made from CA1 hippocampal cells at room temperature using an Axoclamp 2A (Axon Instrument, Foster city, CA). Typical pipette resistance was 2–4 MΩ. Pipette solutions contained (in mM): $KMeSO_4$ 150, KCl 10, HEPES 10, NaCl 4, Mg_2ATP 4. The pH was adjusted to 7.4 and the osmolarity to 280–290 mOsm/L. NMDA receptor-mediated responses were isolated using ACSF containing 10 μM CNQX and 50 μM picrotoxin. Some experiments ($n = 2$) were carried out in the nominal absence of extracellular Mg^{2+} with the membrane potential being held at −80 mV by current injection through the recording electrode; in others ($n = 2$) normal extracellular Mg^{2+} was used and the membrane potential was held at −60 mV. A short current pulse was included in every trace to ensure correct adjustment of bridge balance. Slope measurements were made during the initial linear phase (20–50%) of each evoked potential and the values were normalized relative to the mean values obtained within the first 10 min of recording in the absence of any treatment.

All data are presented as the means ± SEM.

Measurement of cGMP

Determination of cGMP levels was carried out as described previously (Boulton *et al.*, 1995). Briefly, hippocampal slices were allowed to recover for 1–2 h in gassed ACSF maintained in a shaking water bath at 22.5 °C (the average temperature in the electrophysiological experiments). The slices were then transferred to a fresh solution containing the phosphodiesterase inhibitor 3-isobutyl-1-methylxanthine (1 mM) for 15 min, before being exposed to the NO donor, diethylamine/NO adduct (DEA/NO) for 2 min. At the end of the exposure the slices were removed, inactivated by immersion in boiling hypotonic buffer, and homogenized by sonication. The protein content was determined using the bicinchoninic acid method (Pierce Rockford, IL, USA) with bovine serum albumin as standard. Following centrifugation, the cGMP content of the supernatant was determined by radioimmunoassay. Results are expressed as mean cGMP content/mg protein ± SEM.

Cell culture

Human embryonic kidney 293 cells (HEK-293 cells; European Collection of Cell Cultures, CAMR, Salisbury, ECACC no. 85120602) were grown in DMEM containing 10% fetal bovine serum (FBS) and 100 U/mL of both penicillin and streptomycin, at 37 °C in a 5% CO_2 incubator. Exponentially growing cells were plated onto 9 mm diameter coverslips 24 h prior to transfection. HEK-293 cells were transfected with a mixture of plasmids containing the NR1 (provided by Dr R. Shoepfer, University College London, UK) and NR2a (from Dr P. Seeburg, Heidelberg, Germany) subunits of the NMDA receptor, and green fluorescent protein (Clontech, USA) to allow visualization of the transfected cells. Transfections were performed using Effectene Transfection Reagent (Qiagen UK, Ltd) following the manufacturer's instructions. Approximately 76% of cells expressing green fluorescent protein also expressed functional NMDA receptors. Following transfection, 500 μM ketamine was added to the DMEM culture medium to reduce glutamate-mediated cell toxicity. Studies on the recombinantly expressed receptors were performed two days after transfection, which gave optimal transient expression of the proteins.

Whole-cell electrophysiology

Transfected HEK-293 cells were studied at room temperature. The recording chamber was mounted on an inverted microscope (Zeiss), and was continuously perfused with extracellular solution containing (in mM): NaCl 135, KCl 5.4, $CaCl_2$ 1.8, glycine 0.01, HEPES 5. The pH was adjusted to 7.25 with NaOH and osmolarity was maintained at 280–300 mOsm/L with sucrose. Whole-cell voltage clamp recordings were made from green fluorescent protein-positive cells using an Axopatch 1D (Axon Instrument, Foster city, CA) after capacitance and series resistance compensation. Typical pipette resistance was 3–6 MΩ. Patch pipette solutions contained (in mM): CsCl 140, $MgCl_2$ 1, EGTA 10, HEPES 10, Mg-ATP 4, pH 7.25 (CsOH) and osmolarity 280–300 mOsm/L (adjusted with sucrose).

Immediately after establishing the whole-cell configuration, short (100 ms) pressure pulses of glutamate (100 μM dissolved in external solution) were applied with a Picospritzer (Picospritzer IID, General Valve Corporation; New Jersey, USA) every 20 s. Photolysis of caged NO was performed by illuminating an ≈100 μm diameter circle surrounding the cell of interest using a mercury vapour 50 W bulb (Osram, UK) filtered with the UG11 filter used in the slice experiments (see above). Data acquisition and analysis were with pClamp6 or pClamp8 (Axon Instruments, CA, USA).

Measurement of NO

NO concentrations were measured using an electrochemical probe (ISO-NO; World Precision Instruments, Stevenage, UK) under the same experimental conditions used to record currents from the HEK-293 cells.

Results

Effect of endogenous NO on NMDA receptor-mediated synaptic transmission

Electrophysiological recordings of pharmacologically isolated NMDA receptor-mediated fEPSPs were made from the CA1 region of adult rat